Detection and quantification of chronic wasting disease prions

by

Anthony Maurice Ness

A thesis submitted in partial fulfillment of the requirements for the degree of

Doctor of Philosophy

in
Molecular Biology and Genetics

Department of Biological Sciences
University of Alberta

Abstract

Chronic wasting disease (CWD), a neurodegenerative prion disease of cervids, is geographically spreading across North America and Northern Europe. Wild cervids are infected by CWD disproportionately by species and sex. The precise mechanisms and animal behaviours that contribute to the patterns in CWD prevalence are poorly understood. CWD prions are shed from preclinically and clinically infected animals in body fluids, excretions, and from carcasses. Shed CWD prions contaminate the environment – providing a source for indirect disease transmission. Deer have a variety of skin scent glands used for social communication could be exposed to- or shed prions. Involvement of these skin glands was hypothesized to be involved in CWD transmission and was investigated. Cellular prion protein presence in six skin glands and two other exocrine gland-containing tissues of mule deer and white-tailed deer were surveyed and quantified. The presence of cellular prion protein expression within glandular structures suggests that the tissues may be capable of replicating infectious prions. Disease-associated CWD prions were identified within interdigital glands in the feet of mule deer. CWD prions were observed in or near glandular structures of the interdigital glands, as well as within soil found in the hoof of an infected mule deer. The results suggest that prions may be secreted from the feet of infected deer. Cervid behaviours that could contribute to CWD transmission are reviewed. CWD prions entering the environment contaminate soils and surfaces for years. A method was developed to detect and quantify adsorbed prion inactivation by anti-prion compounds – with a focus on humic substances. Insights into the use of humic substances for the inactivation of prions is discussed.

Preface

A version of Appendix 1 will be submitted to the peer-reviewed journal as:

> Ness, Anthony; Judd, Aiken; McKenzie, Debbie. Presence of sheep scrapie and deer rabies in England prior to 1800.

While researching the history of prion diseases for the introduction of this thesis, I stumbled upon a historical reference to scrapie that predated those previously known to the prion literature. From there, the introduction spun-off into an entire new chapter regarding the history of scrapie in 18th century England. The chapter did not fit with the theme of the thesis and was ultimately sequestered to the appendix. One historical English writer, well known to the prion literature, had noted that a scrapie-like disease existed in deer. I had initially been excited that the writer may have been referring to chronic wasting disease existing in England during the 18th century. A dive into historical accounts led me to discover that the cause of the disease in deer was not chronic wasting disease, but rabies. Appendix 1 further details the 18th century distribution of sheep scrapie and deer rabies in England. Dr. Judd Aiken and Dr. Debbie McKenzie assisted with edits and revisions to the manuscript that sprouted from the introduction of this thesis.

A manuscript from Chapter 1 will be submitted as a review to a peer-reviewed journal as:

> Ness, Anthony; Saboraki, Kelsey; Aiken, Judd; Lingle, Susan; McKenzie, Debbie. The potential for cervid scent glands and behaviour to influence CWD exposure and prevalence.

During the SARS-CoV-2 'COVID-19' pandemic, there were several months where laboratory access was restricted. During that time, I spent numerous hours reviewing the literature to assess

the feasibility of cervid gland involvement in CWD transmission. The manuscript snowballed into an in-depth review on how cervid behaviours may influence CWD transmission. I thank Dr. Susan Lingle and Kelsey Saboraki for their incredible patience and assistance in editing and revising the work using their expert knowledge on deer behaviour. Dr. Judd Aiken and Dr. Debbie McKenzie assisted with edits and revisions to the manuscript. We plan to submit this review to a peer-reviewed journal to further the understandings of the numerous links between cervid behaviours and CWD transmission. To confirm the presence of osmetrichia in mule deer tarsal glands, I developed a novel methodology to examine surface and internal hair structures using confocal fluorescence microscopy. This methodology became redundant for my needs when I obtained access to a scanning electron microscope. Although images from the methodology will not be included in the intended publication, I have included the methodology in this thesis (Appendix 2).

A version of Chapter 2 has been published in the journal Prion as:

> Ness, Anthony; Jacob, Aradhana; Saboraki, Kelsey; Otero, Alicia; Gushue, Danielle; Martinez Moreno, Diana; de Peña, Melanie; Tang, Xinli; Aiken, Judd; Lingle, Susan; McKenzie, Debbie (2022). Cellular prion protein distribution in the vomeronasal organ, parotid, and scent glands of white-tailed deer and mule deer.

Chapter 2 contains additional data not included in the published paper or in the supplementary data. My contribution to this paper included data generation for the bicinchoninic acid assays, western blots, capillary electrophoresis immunoassays, enzyme-linked immunosorbent assays, data analysis, statistics, and histology analysis. I wrote the manuscript first draft, led the

revisions and editing. Aradhana Jacob processed and analyzed the histological sections and with assistance from Dr. Alicia Otero Garcia. Kelsey Saboraki and Melanie de Peña collected samples under Dr. Susan Lingle's instruction. Dr. Lingle helped conceptualize the project and was of great assistance with revisions, cervid knowledge, and statistics. Danielle Gushue helped establish the gland homogenization protocols and Diana Martinez Moreno assisted with running the dozens of western blots. Dr. Xinli (Lili) Tang, who taught me how to create and use custom enzyme-linked immunosorbent assays, produced the N5 antibody for the assays in-house. Dr. Andrew Castle taught me how to use capillary immunoassay system. Dr. Judd Aiken and Dr. Debbie McKenzie conceptualized the project with Dr. Susan Lingle and assisted with edits and revisions to the manuscript.

A version of Chapter 3 is published in PLOS ONE as:

> Ness, Anthony; Zeng, Doris; Kuznetsova, Alsu; Otero, Alicia; Kim, Chiye; Saboraki, Kelsey; Lingle, Susan; Pybus, Margo; Aiken, Judd; Gilch, Sabine; McKenzie, Debbie. Presence and evidence of chronic wasting disease prion secretion from the hoof interdigital glands of mule deer.

Dr. Alicia Otero Garcia was the first to identify PrP^{CWD} in histological slides of a mule deer interdigital gland. She tested blinded interdigital gland homogenates by sPMCA. Upon Dr. Otero Garcia's departure from the lab, I took the lead on the project. Dr. Otero Garcia continued to assist with trouble shooting histological protocols and identifying structures. For the manuscript, I extracted and homogenized interdigital glands for sPMCA and RT-QuIC. I analyzed the histological slides to identify PrP^{CWD}. I wrote the first draft of the manuscript and led the edits

and revisions. Doris Zeng tested blinded samples using RT-QuIC under the supervision of Dr. Sabine Gilch. While preparing a CWD-infected hoof for gland extraction, I discovered that some soil had been lodged between the cleft hooves. Dr. Alsu Kuznetsova, our soil specialist, tested this soil sample with sPMCA. Chiye Kim sequenced the PrP genotypes. Kelsey Saboraki and Drs. Lingle and Pybus provided samples used for this study. Dr. Duque Velásquez suggested switching the histology chromogen from DAB to AEC for better image contrast – a fruitful suggestion. Dr. Judd Aiken and Dr. Debbie McKenzie assisted with experimental design, edits, and revisions to the manuscript. We are thankful to Dr. Nick Nation who confirmed that I had correctly identified a PrP^{CWD}-containing structure to be an acrosyringium. Histological slides were prepared by Nathalie Daude and Trang Nguyen from the Centre for Prions and Protein Folding Diseases histological core services.

Data from Chapter 4 has been included in a manuscript submitted to Chemosphere as:

> Ness, Anthony; Dzhabrailov, Isa; Kuznetsova, Alsu; Martinez Moreno, Diana; Tang, Xinli; Aiken, Judd; McKenzie, Debbie. Quantification of prion inactivation by humic acid using enzyme-linked immunosorbent assay.

The Aiken and McKenzie labs have been investigating the anti-prion effects of humic acids for several years now with the majority of the work undertaken by Dr. Alsu Kuznetsova. The precise mechanism of action for prion inactivation by humic substances is not clear. Most of the previous inactivation experiments involved infectious brain homogenates mixed with humic acid in solution. These experiments, however, do not represent environmental prion contamination where the infectious agent is bound to solid surfaces. I sought to examine inactivation of prions

in a context that simulated environmentally-bound prions instead of in an aqueous state. The resulting assay I developed was an enzyme-linked immunoassay-based system to expose adsorbed prions to anti-prion agents. The infectious prions to be adsorbed for the experiment required me to develop a prion purification scheme derived from a publication of the Wadsworth laboratory (2015). I wrote the manuscript first draft and led the edits and revisions. Diana Martinez Moreno assisted by testing hundreds of deer brains for relative PrP^{CWD} levels. Isa Dzhabrailov assisted with the prion purifications and some of the assays. Dr. Xinli (Lili) Tang provided antibodies for custom ELISAs. Dr. Alsu Kuznetsova assisted with humic acid analysis, trouble shooting, and cross-validation with western blots not included in this manuscript. Dr. Judd Aiken and Dr. Debbie McKenzie oversaw the project and assisted with conceptualization, troubleshooting, and manuscript edits and revisions. Using the prion inactivation assay, I formulated an enhanced anti-prion humic acid mixture that will soon be tested on soil-bound prions.

I conclude this preface with a desire for the future of academia. Throughout my studies I was fortunate enough to have a financially supportive mother and fiancé. I am now 30 years old and, accounting for hours worked, I have spent many years earning less than minimum wage. I hope for a future society where the work of graduate students is valued more than, at the very least, some jobs.

> Here, then, I say is what the student has to undergo; first of all poverty: not that all are poor, but to put the case as strongly as possible: and when I have said that he endures poverty, I think nothing more need be said about his hard fortune, for he who is poor has no share of the good things of life.
>
> Miguel de Cervantes
> Don Quixote, 1605

Dedication

This thesis is dedicated to my father,

ROBERT GORDON NESS (1949-2007)

I wish you were here to see the man that I have become

Acknowledgements

I thank my supervisors, Dr. Debbie McKenzie and Dr. Judd Aiken, for supporting my work and progress in science. They both took a risk by giving me free reins to pursue my multiple interests and avenues of research – some fruitful, some not, and others ongoing. Dr. Satyabrata Kar has been a guiding and supporting committee member at the centre. Dr. Susan Lingle has been of immense help with her contributions, insights, and corrections to the writings on cervid behaviours. The numerous coworkers and associates at the Centre for Prions and Protein Folding Diseases see and know the daily struggle. I thank my mother and Jennifer, my soon to be wife, for their financial and emotional support throughout all these years. My good friends Dave Keeler and Connor Davidiuk helped keep me questionably sane.

Multiple research projects, grants, and collaborators have contributed to this multifaceted thesis. Funders that made this work possible include the Alberta Prion Research Institute (part of Alberta Innovates), the Alberta Conservation Association, Genome Canada and Genome Alberta, and the Government of Canada New Frontiers in Research Fund. Collaborations who provided samples, analysis, and manuscript contributions include Dr. Susan Lingle (University of Winnipeg), Dr. Margo Pybus (Alberta Fish and Wildlife), and Dr. Sabine Gilch (University of Calgary). The current and former lab members of the Aiken and McKenzie labs have assisted with experimentation, training, and brainstorming – many of whom have been noted in the preface for their contributions

Table of Contents

List of Tables:

List of Figures:

List of Abbreviations:

AEBSF	4-(2-aminoethyl)benzenesulfonyl fluoride hydrochloride
AEC	3-Amino-9-ethylcarbazole
AGH	Anterior grey horn
ANOVA	Analysis of variance
AOB	Accessory olfactory bulb
APM	Arrector pili muscle
b. abt.	Born about
BCA	Bicinchoninic acid
BH	Brain homogenate
Bis-Tris	Bis-tris methane (2-[Bis(2-hydroxyethyl)amino]-2-(hydroxymethyl)propane-1,3-diol)
BNAOT	Bed nucleus of the accessory olfactory tract
BNST	Bed nucleus of the stria terminalis
BSA	Bovine serum albumin
BSE	Bovine spongiform encephalopathy
$CaCl_2$	Calcium chloride
Carb/Bicarb	Carbonate-bicarbonate buffer
CC	Charged clusters
CFB	Canadian Forces Base
C_γ	Immunoglobulin gamma heavy chain conserved domain
CJD	Creutzfeldt-Jakob disease
C_L	Immunoglobulin light chain conserved domain
CN IX	Cranial nerve IX (glossopharyngeal nerve)
CNS	Central nervous system
CN V	Cranial nerve V (trigeminal nerve)
CN VII	Cranial nerve VII (facial nerve)
CNN	Caudal nasal nerve
CSA	Conformational stability assay

CWD	Chronic wasting disease
DAB	3,3′-Diaminobenzidine
DMNV	Dorsal motor nucleus of the vagus nerve
DPX	Distyrene, plasticizer, xylene
E	Epidermis
ECN	External carotid nerve
EDTA	Ethylenediaminetetraacetic acid
ELISA	Enzyme-linked immunosorbent assay
Fab	Fragment antigen-binding region
Fapp	Apparent fractional change
FC	Follicular canal
Fc	Fragment crystallizable region
FH	Forehead gland
GdnHCl	Guanidine hydrochloride
GPI	Glycosylphosphatidylinositol
H_2SO_4	Sulfuric acid
H&E	Hematoxylin and eosin
HA	Humic acid
HCl	Hydrochloride
HRP	Horseradish peroxidase
HS	Hair shaft
ICN	Internal carotid nerve
ID	Interdigital gland
IgG	Immunoglobulin G
IgG1	Immunoglobulin G subclass 1
IMN	Intermediolateral nucleus
IRN	Intermediate reticular nucleus
kDa	Kilodaltons
L (Chapter 1)	Lymphatic vessel
L (Chapter 2)	Leukocytic infiltrates

L (Chapter 2)	Standard protein ladder
M	Skeletal muscle
MD	Mule deer
MET	Metatarsal gland
MOPS	3-(N-Morpholino)propane sulfonic acid
N	Normality
n	Sample number
N-terminal	amino-terminus
$Na_2HPO_4 \cdot 7H_2O$	Sodium phosphate dibasic heptahydrate
NaCl	Sodium chloride
$NaH_2PO_4 \cdot 1H_2O$	Sodium phosphate monobasic monohydrate
NaOH	Sodium hydroxide
Neg Soil	Negative control soil
NG	Nasal gland (integumentary)
NHS	Nucleated region of the hair shaft
Nor98	Atypical scrapie
PAGE	Polyacrylamide gel electrophoresis
PAR	Parotid gland
PBS	Phosphate-buffered saline
PCR	Polymerase chain reaction
PE	Pronase E
PE-PTA-Filter	Prions enriched by sequential pronase E digestion, PTA precipitation, and 0.45µm filtration
PK	Proteinase K
PK-PTA-Filter	Prions enriched by sequential proteinase K digestion, PTA precipitation, and 0.45µm filtration
PMCA	Protein misfolding cyclic amplification
PO	Preorbital gland
PRNP	Prion protein encoding gene
PrP	Prion protein

PrP^{C}	Cellular prion protein
PrP^{CWD}	Chronic wasting disease-associated prion protein
PrP^{Res}	Disease-associated proteinase-resistant prion protein
PrP^{Sc}	Disease-associated prion protein
PTA	Phosphotungstic acid hydrate
PVDF	Polyvinylidene fluoride
QuIC	Quake-induced conversion
RFU	Relative fluorescence units
RIPA	Radioimmunoprecipitation assay
ROI	Regions of interest
RPLN	Retropharyngeal lymph nodes
RS	Follicular root sheath
RT	Room temperature
RT-QuIC	Real-time quake-induced conversion
SA	Serous acini
SAF	Scrapie-associated fibril
SARS-CoV-2	Severe acute respiratory syndrome coronavirus 2
SCG	Superior cervical ganglia
sCJD	sporadic Creutzfeldt-Jakob Disease
SD	Striated ducts
SDS	Sodium dodecyl sulfate
SE	Sebaceous glands
SM	Submucosa
SOFIA	Surround optical fiber immunoassay
sPMCA	Serial protein misfolding cyclic amplification
Su	Sudoriferous glands
TBS-T	Tris-buffered saline with Tween-20
TG	Tarsal gland
TM	Transmembrane region
TMB	3,3',5,5'-tetramethylbenzidine

Tris	Trisaminomethane
Tris-HCl	Trisaminomethane hydrochloride
TSE	Transmissible spongiform encephalopathy
USA	United States of America
vCJD	Variant Creutzfeldt-Jakob disease
VDL	Vomeronasal duct lumen
V_H	Immunoglobulin heavy chain variable domain
V_L	Immunoglobulin light chain variable domain
VL	Vomeronasal lumen
VNO	Vomeronasal organ
VRE	Vomeronasal respiratory epithelium
VTS	Vomeronasal tubular serous glands
v/v	Volume by volume
WMU	Wildlife management unit
WMZ	Wildlife management zone
w/v	Weight by volume
WT	White-tailed deer

Chapter 1 Prion diseases and transmission of scrapie and chronic wasting disease

A portion of this chapter will be submitted as a review manuscript:

Ness, Anthony; Saboraki, Kelsey; Aiken, Judd; Lingle, Susan; McKenzie, Debbie. The potential for cervid scent glands and behaviour to influence CWD exposure and prevalence.

1.1 Introduction

1.1.1 Prion diseases

Transmissible spongiform encephalopathies (TSEs) are a unique class of diseases that can be inherited, spontaneously occurring, or pathologically acquired. TSEs are fatal neurodegenerative disorders caused by prions – disease-associated misfolded proteins that replicate their structural isoforms using host proteins [1-4]. TSEs of humans include sporadic Creutzfeldt-Jakob disease (sCJD), variant Creutzfeldt-Jakob disease (vCJD), Gerstmann-Sträussler-Scheinker syndrome, Kuru, and the fatal insomnias [5-6]. The best-known TSE is likely bovine spongiform encephalopathy (BSE or mad cow disease) in cattle [7-9]. Scrapie, which infects sheep and goats, and chronic wasting disease (CWD) affecting cervids are TSEs noted for being contagious among susceptible animals [10-12]. Scrapie, the oldest known prion disease, has long been thought to have been first reported in 1750, but an earlier historical reference has been found which dates scrapie to between 1693 and 1706 (Appendix 1). The most recently discovered prion disease, camel prion disease in Algeria and Tunisia, is also likely to be contagious [13-14].

The etiological agent of prion diseases is a misfolded protein. The cellular prion protein (PrP^{C}) (**Figure 1.1**) – encoded by the prion protein gene *PRNP* – contacts the disease-associated proteinaceous isoform (PrP^{Sc}) and is converted into PrP^{Sc} through a template-like mechanism [1-4, 15-17]. Individual PrP^{Sc} monomers aggregate in a parallel in-register intermolecular β-sheet (PIRIBS) multimeric structure [18-22]. Prion diseases are typically characterized by long incubation periods followed by rapid clinical onset, decline, and death [5, 23]. The neuropathology of prion disease is characterized by PrP^{Sc} deposition in the brain (either in the form of plaques or diffuse deposition), vacuolation (spongiform change) caused by neuropil axonal and dendritic dilation, gliosis, and neuronal loss [23-25].

Prion diseases are inevitably fatal, there are no existing cures or effective treatments [26-29]. Infectious prions are remarkably difficult to inactivate when exposed to heat, ionizing radiation, chemical agents, and proteases [30-32]. Consequently, human prions pose significant iatrogenic transmission risks while scrapie and CWD can persist in the environment of endemic regions [32-35].

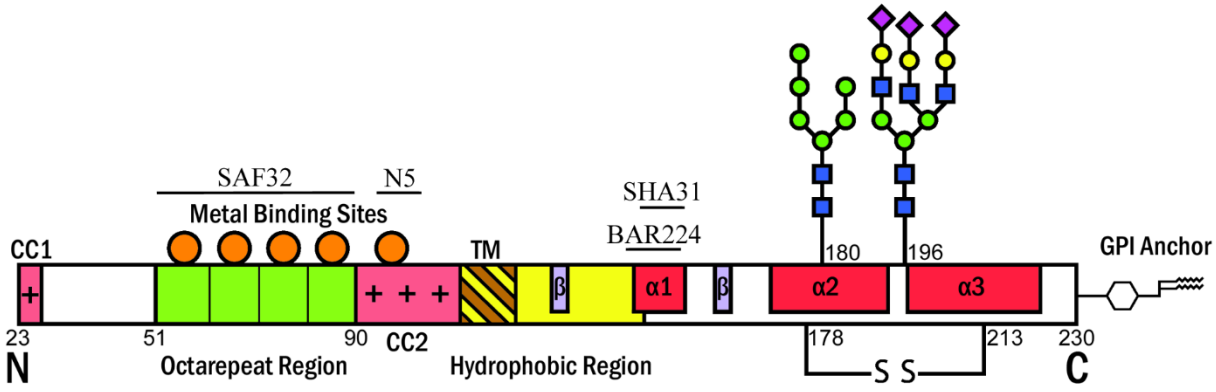

Figure 1.1. Linear structural representation of the mature mouse PrP^C protein and locations of anti-PrP monoclonal antibody epitopes used in this thesis. Regions contributing to secondary protein structure beta sheets (β) and alpha helices (α) are shown. Features include two N-terminal charged clusters (CC), metal binding site-containing octapeptide repeat region, hydrophobic domain, and transmembrane region (TM). Post-translational modifications include one disulfide bridge (S S), two N-linked glycosylation sites, and a C-terminal glycosylphosphatidylinositol (GPI) anchor.

1.2 Chronic wasting disease

1.2.1 North American and European species affected

Chronic wasting disease (CWD) is a contagious prion disease of free-ranging and captive cervids. Clinical signs of CWD are initially subtle behavioural changes with later stage clinical signs including inanition (exhaustion, weakness, and wasting from lack of nutrition), polydipsia (excessive thirst), polyuria (excessive urination), sialorrhea (hypersalivation), incoordination, and ultimately death [36-37]. Infected cervids replicate and shed infectious prions in secreta

including saliva, feces, and urine [38-45]. Although cervids acquire infectious prions through direct or indirect contact [45-46], the specific mechanisms underlying the natural transmission of CWD remains understudied. The most accepted route of indirect CWD exposure is the oral-nasal uptake of PrP^{CWD} from environmental fomites including soil particles, vegetation, and salt licks [46-51].

1.2.2 Geographic distribution and spread of CWD

The first known cases of CWD appeared in mule deer (*Odocoileus hemionus*) at a Colorado, United States captive wildlife facility in 1967 although the disease was likely already present in the state, outside the facility [36, 52]. Elk/wapiti (*Cervus canadensis*) that used the same pens as the infected mule deer were diagnosed with CWD in 1979 [53]. Samples collected in Colorado between 1981 and 1995 identified CWD in wild mule deer, elk, and white-tailed deer (*Odocoileus virginianus*) [54]. The first known international transport of CWD occurred when two Colorado mule deer purchased by the Toronto Zoo (Ontario, Canada) in 1974 developed clinical signs of CWD by 1975 [55]. The Toronto Zoo cases have not been linked to any other cases of CWD in Canada. CWD in a captive mule deer was identified in a second state, Wyoming, in 1978 [56]. In 1996, an elk was diagnosed with CWD in Saskatchewan Canada [57]. The animal had been imported from South Dakota in 1989 – a suspected source of the disease [57]. The disease is believed to have hopped continents when a CWD-infected elk was transported from Saskatchewan, Canada to South Korea in 1997 [58]. Once in South Korea, the disease infected sika deer (*Cervus nippon*), red deer (*Cervus elaphus*), and hybrids of the two species with new outbreaks being reported as recent as 2016 [59-60]. Alberta, Canada identified its first case of CWD in a captive elk deer in 2002 [61-62]. As of early 2022, the distribution of CWD in North America includes 30 American states and 4 Canadian provinces (Alberta,

Saskatchewan, Manitoba, and Quebec). The rapid spread of CWD is best demonstrated by geographical tracking of CWD (**Figure 1.2**) [63].

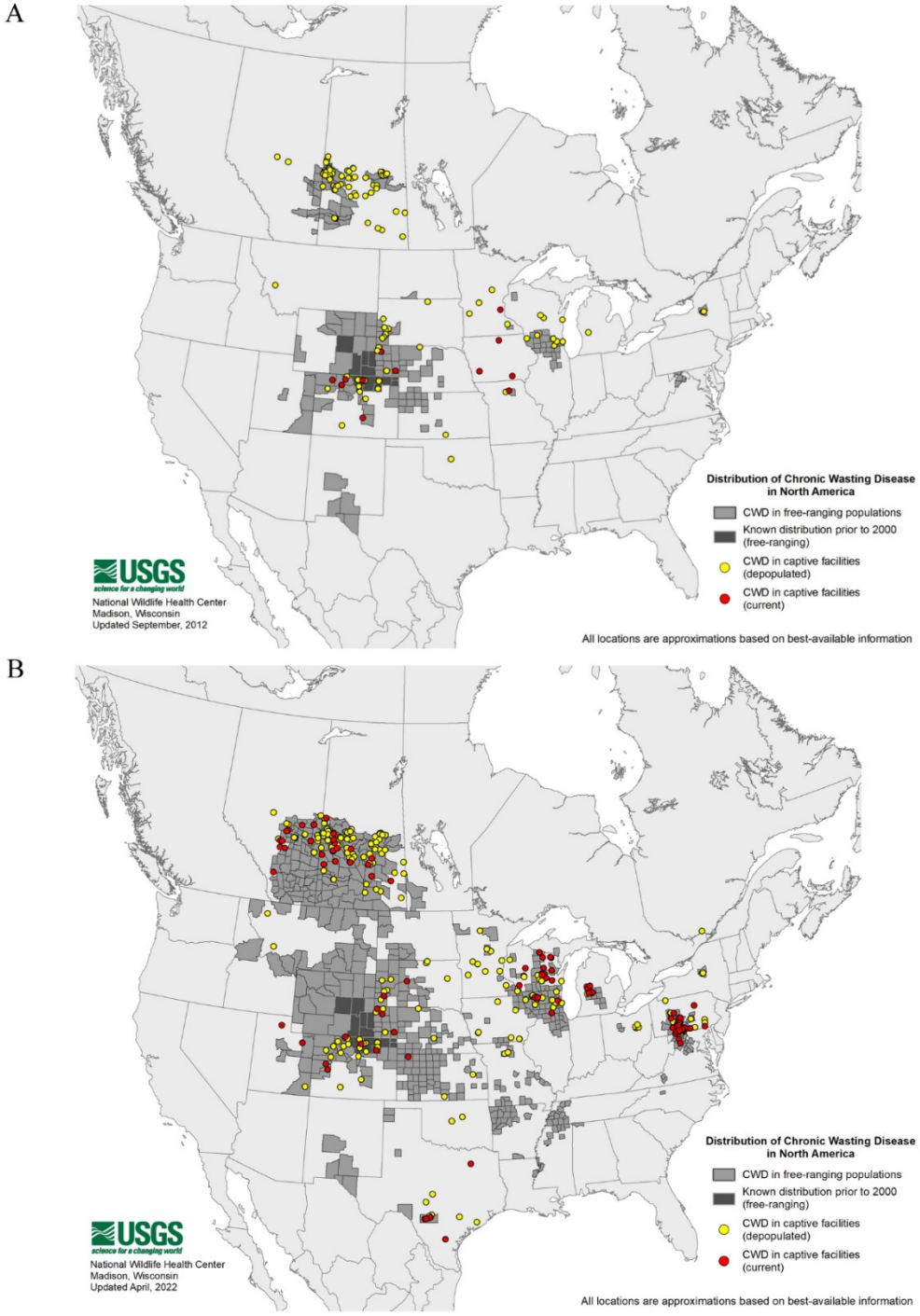

Figure 1.2. North American distribution of chronic wasting disease in captive and free-ranging cervid populations in A) September of 2012, and B) April of 2022. Attribution: Byran Richards, United States Geological Survey.

Canadian boreal woodland caribou (*Rangifer tarandus*) in Alberta and Saskatchewan are currently at risk of being infected by CWD (**Figure 1.3**). In Alberta, CWD is closest to the Cold Lake caribou population in the east of the province. CWD was reported in wildlife management unit (WMU) 501 in 2018 – immediately south of the southernmost range of the Cold Lake caribou [64-65]. Between 2018, when CWD was reported in WMU 501, and 2022, the probability that CWD is now overlapping with the Cold Lake caribou range is likely. In Saskatchewan, CWD is nearly at the Cold Lake caribou range (as with Alberta) but is now overlapping the caribou population range further east. CWD is present in Saskatchewan wildlife management zones (WMZ) 59 and 63 where the southern woodland Caribou range extends [66-67]. Although cases of CWD in wild North American caribou has yet to be reported, it inevitably will be. To the south of the continent, CWD has been endemic for more than a decade in free-ranging deer populations in state regions of New Mexico and Texas that border with Mexico – suggesting that the disease is present, but unreported, in northern Mexico (**Figure 1.2**).

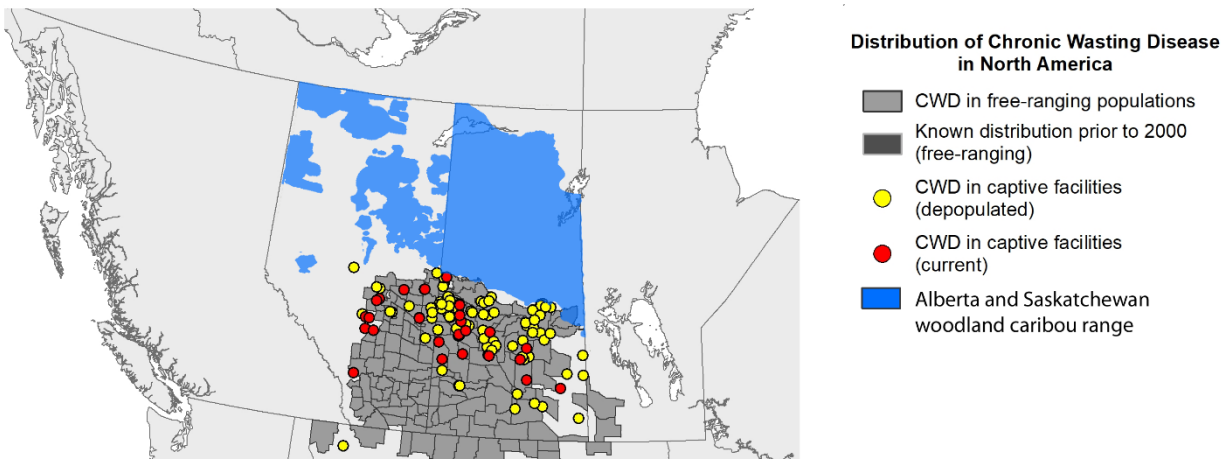

Figure 1.3. Overlay of geographical CWD and boreal woodland caribou range in Alberta and Saskatchewan, Canada. Maps modified from Byran Richards, United States Geological Survey, and Environment Canada.

All cases of CWD were linked, or presumed to be linked, to the original Colorado outbreak until seemingly unrelated cases were identified in Norwegian reindeer in 2016 [68]. Norwegian moose infected with what is now known as atypical moose CWD were also sampled in 2016 [69]. The anticipation of CWD spreading rapidly through large reindeer herds led to the pre-emptive culling of more than 2,000 animals in Norway between 2017 and 2018 [70]. Norway identified the first European case of wild red deer (*Cervus elaphus*) CWD in 2017 [71]. Atypical moose CWD has since been identified in Finland (2018) and Sweden (2019) [72-73]. Increased CWD surveillance in Fennoscandia has discovered a large geographical distribution of CWD cases (**Figure 1.4**). Atypical moose CWD has been identified in eastern Finland within kilometers of the border with the Republic of Karelia, Russia (**Figure 1.4**) suggesting the disease is likely present, but unreported, in Russia. The broad geographic range suggests CWD has been present for years prior to 2016. Roe deer (*Capreolus capreolus*) and fallow deer (*Dama dama*) are present in Fennoscandia and are at risk of CWD. Interestingly, white-tailed deer are at risk of CWD infection in Finland. In 1934, five white-tailed deer calves were imported from Minnesota, United States to a private estate in Finland [74]. Six more calves were imported from the United States in 1948 [74]. The Finnish white-tailed deer population is concentrated in the southwest of the country and was estimated to number 48,000 in the mid-2000's and 60,000 by 2018 [75-76].

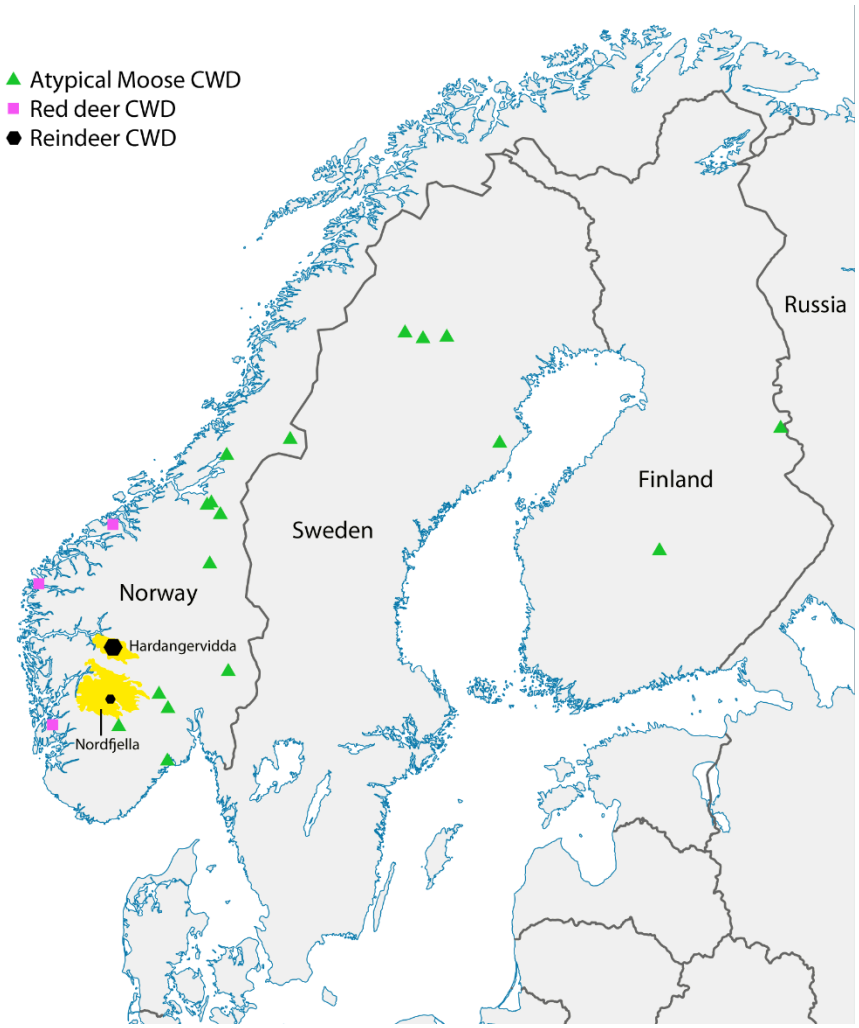

Figure 1.4. Distribution of detected cases of CWD in Fennoscandia as of June 21, 2022. CWD case locations from the Norwegian Institute for Nature Research.

Whether atypical moose CWD is spontaneous or acquired is unknown. Available surveillance data suggests that Fennoscandian moose have a prion disease incidence higher than sporadic prion diseases in humans, cattle, and caprids, and is more in line with acquired prion diseases (**Table 1.1**). The incidence of atypical moose CWD in Sweden and Finland is comparable to classical moose CWD in Alberta, Canada [73, 77]. The incidence and distribution of atypical moose CWD is, in my opinion, suggestive that the disease is an acquired prion disease – similar

to classical moose CWD in North America. The mechanisms of disease transmission are anticipated to differ between North American moose CWD and Fennoscandian atypical moose CWD due to differences in lymphotropism [72-73].

Table 1.1. Incidence of prion diseases.

Prion Disease	Species	Incidence (per million)	Location	Positive Cases	Sample Size	Time Period	Reference
Moose CWD (North America)	Moose (*Alces alces*)	1,981.5	Alberta, Canada	6	1,514	2012-2022	Government of Alberta
Atypical Moose CWD (Northern Europe)		274.5 2,324.2 2,445.0	Norway Sweden Finland	8 4 2	29,143 1,721 818	2002-2021 2007-2021 2006-2020	Tranulis, 2021
Reindeer CWD	Reindeer (*Rangifer tarandus*)	328.3 0.0 0.0	Norway Sweden Finland	20 0 0	60,928 3,101 1,719	2002-2021 2007-2021 2006-2020	Tranulis, 2021
sCJD*	Human (*Homo sapiens*)	0.6 - 1.7	22 Countries Reviewed				Uttley, 2020
Kuru		25,701.3	Papua New Guinea	896	34,862	1957-1960	Gajdusek, 1961
Classical BSE	Cattle (*Bos taurus*)	496.4 - 8,322.0	United Kingdom			1988-1992	Kimberlin, 1994
Atypical BSE*		6.1	European Union	7	1,150,388	2019	European Food Safety Authority, 2020
Classical Scrapie	Sheep (*Ovis aries*)	2,694.5		911	338,098		
	Goat (*Capris hircus*)	2,640.6		379	143,529		
Atypical Scrapie*†	Sheep (*Ovis aries*)	254.4		86	338,098		
	Goat (*Capris hircus*)	76.6		11	143,529		
Camel Prion Disease‡	Dromedary camel (*Camelus dromedarius*)	31,429.8	Algeria	71§	2,259	2015-2016	Babelhadj, 2018

* Sporadic prion diseases
† Low rates of transmissibility
‡ Unknown transmission route.
§ Clinically suspected cases.

Evidence of CWD disease presence in Northern Europe before 2016 will likely be brought to light from archival samples as exemplified by retrospective analysis of other prion diseases. Atypical scrapie (Nor98) was first reported in 2003 with samples as old as 1998 [78]. Archival samples from the United Kingdom have identified atypical scrapie in sheep from a flock tested in 1988 and in an experimentally infected sheep that died in 1972 [79]. Likewise, human archived appendix studies identified abnormal prion protein in samples collected between 1977 and 1979

– suggesting that human exposure to cattle BSE likely occurred before the first confirmed case of BSE in 1986 [80-82].

1.2.3 Zoonotic potential of CWD

Whether humans are susceptible to CWD is hotly debated. Scrapie and BSE offer diametric examples of what largescale human exposure to CWD can amount to. Scrapie represents the best-case scenario for human CWD exposure. Human exposure to scrapie dates back at least 250 years. Thomas Comber reported in 1772 that flocks of scrapie-infected sheep were sold off to butchers [83]. Modern epidemiological studies of human CJD risk factors have failed to provide evidence of scrapie transmission to humans [84-86]. The species barrier between sheep scrapie and humans is likely complete or sufficiently strong enough that any transmissions are subclinical or infrequent enough to be lost in the noise of sporadic Creutzfeldt-Jakob disease (sCJD) statistics. Unlike scrapie, exposure of humans to meat from BSE-infected cattle has been linked to more than 200 cases of variant Creutzfeldt-Jakob disease (vCJD) in humans [23, 87-89]. Cases of vCJD lagged those of the BSE epizootic. Cases of BSE in cattle reached their apex in 1992, the first symptoms of human patients with vCJD appeared in 1995 with human case numbers peaking in 2000 [89-90]. The species barrier limiting the transmission between BSE and humans was formidable. An estimated 1-3 million BSE-infected cattle are estimated to have entered the food chain in the United Kingdom with fewer than 200 Britons developing vCJD [23, 82]. Subclinical infections from BSE exposure have been demonstrated by retrospective examinations of human appendices. Two appendix surveys estimated the incidence of vCJD subclinical infections in Britain to be 237 and 493 per million persons [80, 91-92]. Human appendices positive for abnormal PrP are temporally linked to the BSE epizootic [80]. Whether those with vCJD subclinical infections will develop disease is unknown but is theoretically

possible as exemplified by the last cases of human Kuru which had incubation periods of more than 50 years [93].

Transgenic mice expressing the human prion protein (tgHu mice) have been used to assess prion species barriers. TgHu mice challenged with BSE develop prion disease with biochemical similarities to tgHu mice challenged with CJD isolates [94-97]. Although epidemiological evidence of scrapie transmission to humans is lacking, scrapie isolates do cause disease in tgHu mice, but only after two passages (animal transmissions), providing further evidence of a strong scrapie to human species barrier [98-99]. TgHu mice are resistant to challenges with North American CWD, Norwegian reindeer and Norwegian moose CWD isolates suggesting that the species barrier between cervid CWD and humans is stronger than that of cattle BSE and humans [100-105]. Concerningly, RT-QuIC has identified possible transmission of CWD isolates into tgHu mice following long incubation times (greater than 650 days post exposure) [106-107]. Hannaoui *et al*., intracerebrally challenged tgHu mice with CWD isolates resulting in positive clinical disease and a small number of animals presenting with positive RT-QuIC and one mouse with prion biochemical properties (detected by western blot) resembling the less common sporadic human prion diseases Gerstmann-Sträussler-Scheinker syndrome and variably protease-sensitive prionopathy [107-108]. More transmission experiments are required to confirm the findings.

Non-human primates offer an alternative model for assessing interspecies transmission of prion diseases to humans. Squirrel monkeys (*Saimiri sciureus*) challenged by co-intracerebral and intraperitoneal exposure to classical BSE developed clinical disease 29-95 months post exposure, interestingly with additional tau and α-synuclein pathology [109]. Intracerebral CWD challenge experiments of squirrel monkeys resulted in the comparable development of terminal prion

disease 31-75 months post exposure with all challenged animals succumbing to disease [110-112]. Squirrel monkeys orally exposed to CWD developed disease 59-107 months post infection with a 92% attack rate [112] and squirrel monkeys challenged with sheep scrapie developed disease by 33 months [113]. The relative ease at which sheep scrapie transmits to squirrel monkeys relative to BSE signals that squirrel monkeys are not a suitable model for assessing the potential of CWD interspecies transmission to humans.

Cynomolgus macaques (*Macaca fascicularis*) are, arguably, a better model for representing interspecies prion disease to humans. Outcomes of macaque studies have demonstrated species barriers that are more reminiscent of understood human species barriers. Macaques challenged with classical BSE develop clinical disease between 2-8 years (depending on the exposure route and dose) [114-116]. Intracerebral inoculation of cynomolgus macaques with sheep scrapie failed to transmit disease in one experiment (although scrapie first passaged into rodents did transmit disease to macaques) [117], but resulted in one animal developing clinical disease after 9 years in a longer experiment [116]. The stronger species barrier between sheep scrapie and macaques relative to BSE suggests that macaques are a better model for assessing prion species barriers to humans relative to squirrel monkeys. Transmission of CWD to macaques have provided conflicting results. In one study, 14 macaques challenged with CWD orally or intracerebrally failed to develop disease or evidence of subclinical infection up to 13 years post exposure [118]. An ongoing transmission study using intracerebral steel wire and oral challenges of macaques suggests that CWD may transmit as early as 4.5 years post exposure [119]. The macaque studies would suggest that a stronger species barrier stands between humans and CWD relative to BSE.

An appreciable amount of PrP^{CWD} is now being consumed by humans. CWD-infected animals accumulate PrP^{CWD} is found in a wide variety of tissues including skeletal muscle [41, 120-125]. By contrast, prion distribution of classical BSE is almost entirely restricted to the central nervous system [126-129]. Humans ingesting venison of CWD-infected animals are likely exposed to more prion infectivity than individuals consuming beef from cattle infected with classical BSE. Between 7,000-15,000 CWD-infected animals were estimated to have been consumed by hunters, their families, and other individuals in 2017 with the number expected to increase by 20% per annum [130]. When a CWD-infected farmed or wild deer is killed, 13% of total carcass infectivity is estimated to enter the food chain for human consumption unless the entire carcass is disposed [131]. Human prion disease cases have not been linked to CWD exposure and epidemiological studies have yet to demonstrate increased CJD cases in regions with high CWD exposure [132-136], but if CWD does prove to infect humans, the first cases would be expected to appear in the coming years as CWD-exposed human population approaches the millions – a consequence of the expanding geographical range and increasing cervid incidence of CWD.

Human prion protein genetics influence the species barrier. All but one case of clinical vCJD occurred in people with the *PRNP* 129MM genotype [137-138]. A single vCJD patient with the 129MV genotype died in 2016 although an earlier suspected vCJD patient of the same genotype died in 2009, but no autopsy was performed to confirm the disease [139-140]. The dominance of the 129MM genotype in vCJD cases is highlighted by the United Kingdom population having 129MM and 129 MV genotypes frequencies of 42% and 47% respectively [141]. Retrospective examination of human appendices in the United Kingdom found abnormal PrP in people with all 129 genotypes suggests that although BSE can infect any genotype, the genotype influences neuroinvasion and disease progression [80, 92, 137, 142]. If cases of zoonotic CWD become

evident, human *PRNP* genetics will likely influence human susceptibility as seen with the BSE-linked vCJD epidemic.

1.3 Environmental contamination and transmission by scrapie and CWD

1.3.1 Early theories on the indirect transmission of prions

Recognition of CWD transmission routes was influenced by prior knowledge and research of the scrapie in sheep and goats. Theories of indirect scrapie transmission appeared very shortly after the disease was identified. Johann George Leopoldt, who first reported scrapie in mainland Europe, forewarned (correctly) in 1750 that '*trab*' (scrapie) was contagious – a theory that would be heavily debated for more than two centuries but largely dismissed in favor of hereditary transmission theories [143-144,p.348]. The extent of Leopoldt's knowledge regarding the symptoms and speculated transmission route of scrapie is indicative of a well-established disease at the time in the Lordship of Sorau, the Holy Roman Empire (today in western Poland).

Andreas Karl Samuel von Richthofen (1762-1836) [145,p.636] noted theories involving indirect transmission. Regarding a theory of contagious transmission, he wrote in 1827:

> … if one drives one's otherwise good, clean rams or ewes to such places to graze or keeps them overnight in a stall during a cattle transport, for example, where a scrapie-infected herd used to be grazed or stabled. For since the white or greenish mucus left behind by the latter and any sick animals that were among them, the white or greenish mucous left on the pasture and storage places was always regarded as very capable of infection…
>
> … wenn man seine sonst guten reinen Sprungböcke oder Mutterschaafe auf solche Orte zur Weide getrieben oder in einem Stalle über Nacht während eins Viehtransportes etwan gehalten, wo früher Trabervieh geweidet oder eingestallt gewesen war. Denn da der von leßteren und den mit darunter befindlich etwan gewesenen kranken Thieren, der au den Weide- und Lagerorten zurückgelassene weiße oder grünliche Schleim immer als der Ansteckung sehr wohl fähig erachtet worden war… [146,p.102-103]

Between 1912 and 1914, John Pool M'Gowan (1879?-1961) [147-148] interviewed and gathered the opinions of farmers and shepherds in scrapie endemic areas to assess the epizootiology of scrapie in Scotland [149,p.102]. M'Gowan ultimately rejected the following transmission theory of those interviewed, but included their thoughts in his work:

> One view of the infection which I have heard canvassed is that it is "on the ground," and the lambs pick it up. [149,p.102]

Scrapie transmissibility would finally and conclusively be demonstrated by Jean Cuillé and Paul-Louis Chelle in 1936 when they intraocularly infected sheep and waited more than a year for clinical signs to appear [150]. Greig reported, in 1940, of experimental indirect transmission of scrapie by exposing imported sheep lacking any history of scrapie to pastures contaminated by scrapie-infected sheep [151]

1.3.2 Prion environmental contamination

Multiple mechanisms of scrapie transmission are now recognized. Sources of scrapie PrP^{Sc} prions include urine, feces, saliva, milk, and possibly skin [40, 152-159]. Lambing is believed to be the largest contributor to scrapie transmission [12, 160-161]. Vertical transmission from ewes to offspring occurs [162-164] and early co-housing experiments demonstrated that horizontal transmission was possible [165-166]. Oral transmission is the predominant route of exposure as evidenced by PrP^{Sc} accumulation in the cranial and gut-associated lymphoid tissues (from the tonsils and retropharyngeal lymph nodes to the Peyer's patches) of young lambs prior to accumulation in the central nervous system [167-168]. Direct or indirect transmission can occur when animals contact infectious placenta and birthing matter [169-171]. Direct oral transmission from ewes to lambs can occur via colostrum or milk suckling [152, 156, 172-175]. Exposure of sheep to contaminated fomites including water troughs, fences, and scratching posts resulted in

successful indirect transmission of scrapie [153]. PrP^{Sc} has been reported to accumulate in the skin of scrapie-infected sheep [154] and the positive indirect transmission experiment with scratching posts suggests that skin is a source of infectivity.

Indirect transmission of CWD by contaminated soils was theorized as early as 1992 [56]. Similar to scrapie, CWD prions are shed in urine, feces, and saliva, but in free-ranging populations deer blood and carcasses are recognized as additional sources of environmental prion contamination [38-41, 44-46, 176-177]. The primary route of CWD transmission is believed to be primarily through oral exposure. Early accumulation of PrP^{CWD} is found in the cranial and gut-associated lymphoid tissues of naturally and orally infected deer prior to detectable presence in the central nervous system [122, 178-180].

Studies directly comparing scrapie and CWD prion shedding in body fluids are limited in number. Comparison of deer CWD and sheep scrapie prion detection in urine using surround optical fiber immunoassay (SOFIA) of serial protein misfolding cyclic amplification (sPMCA) products found comparable levels of prions between the species [40]. Bioassay comparison of saliva from scrapie-infected sheep and CWD-infected deer indicated that sheep saliva may have a higher prionemia than deer saliva, although different mouse models were (justifiably) used for each disease [44]. Further studies are required to compare shedding of prions in body fluids and excretions between deer and sheep. Differing body sizes of caprids and cervids must also be considered when comparing prion shedding.

Prions are notoriously difficult to destroy, remaining infectious in the environment for years to decades – contributing to horizontal disease transmission [35, 181-183]. Environmental contamination of caprid or cervid farms by scrapie or CWD renders the farms prone to newly introduced, naïve animals becoming infected [35, 37, 46, 184]. Shed prions bind to soil,

vegetation, and other fomites including soils, vegetation, salt licks, and feeding sites that provide reservoirs for naïve animal exposure [37, 46-51, 185].

The expanding geographical range of CWD may be placing other species at risk of prion diseases. As local environments become heavily contaminated by PrP^{CWD}, sympatric species are exposed to CWD prions. Experiments using intracerebrally-challenged transgenic mice expressing the beaver (*Castor* sp.) prion protein suggest that beavers in North American and Europe are susceptible to CWD prions [186]. Five species of North American rodents that share geographic range with CWD-endemic areas are experimentally susceptible to CWD [186-187]. Meadow voles (*Microtus pennsylvanicus*), red-backed voles (*Myodes gapperi*), white-footed mice (*Peromyscus leucopus*), and deer mice (*Peromyscus maniculatus*) were experimentally infected with CWD by intracerebral inoculation [187]. Raccoons (*Procyon lotor*) are also susceptible to intracerebral CWD challenge and oral dose experiments are underway to determine elucidate whether raccoons can be naturally infected [188-189].

1.4 CWD prevalence

Striking differences in CWD prevalence exist amongst wild cervid species and between the sexes. CWD in free-ranging populations is more prevalent in males than females of mule deer, white-tailed deer, and reindeer even though the species differ in grouping patterns, social behaviours, and habitat use. CWD is more prevalent in male deer than female deer of the same species in Alberta, Colorado, Montana, Wisconsin, and Wyoming [77, 190-196]. Although still at an early stage of epidemic, 2016-2018 CWD prevalence in tested Norwegian reindeer was significantly higher in males (1.5%) than females (0.5%) [197]. South Converse County, Wyoming is a known exception to the sex-associated disparity of deer CWD prevalence [198-199]. Higher female CWD prevalence relative to male white-tailed deer of South Converse

County has been attributed to locally small female deer home ranges (more philopatric) resulting in concentrated environmental contamination and loss of typical sex-based prevalence patterns [199]. State-wide, male deer have a higher CWD prevalence than females in Wyoming [190]. Sex-based differences in CWD prevalence are anticipated to narrow in areas of prolonged environmental prion contamination [200]. In such locations, indirect acquisition of prions through feeding and other daily activities is expected to surpass direct social contacts as the predominant exposure source [200].

Prevalence of CWD differs between cervid species. The 2019 surveillance results from Alberta, Canada show that CWD prevalence was highest in mule deer (17.5%), then white-tailed deer (3.9%), elk (1.3%), and moose (0.9%) [77]. In Alberta and Wyoming, where the two deer species are sympatric, mule deer are more likely to be infected with CWD than white-tailed deer [77, 190-191]. Montana, still in an early epidemic stage, reported its first detected case of sylvatic CWD in a mule deer male in 2017 [201]. In contrast, white-tailed deer of two hunting districts of Montana (2017-2021) had significantly higher CWD prevalence relative to sympatric mule deer [192]. Future analysis of prevalence rates will provide a more appropriate view of species prevalence rates as the disease distribution and prevalence expands.

Increased risk of mule deer and white-tailed males to infectious disease is not unique to CWD. Male white-tailed deer are more likely than females to be infected by *Mycobacterium bovis*, *Toxoplasma gondii*, viral cutaneous fibromas, viral keratoconjunctivitis, *Trueperella pyogenes* associated abscesses, and SARS-CoV-2 [202-213]. Unlike CWD, age-specific incidence of sporadic CJD, variant CJD, and scrapie do not produce definitive or consistent sex-based patterns [34, 138, 214-218].

Deer and reindeer disease incidence increases with age, but falls in the oldest animals [191, 193-194, 197, 220-222]. Similar age-related modal incidence patterns are found with other prion diseases including classical scrapie, bovine spongiform encephalopathy, sporadic CJD, and variant CJD despite a myriad of different factors driving each disease [34, 214, 219, 223-227]. CWD sex and age associated prevalence patterns are presumably heavily influenced by behaviours of sexually mature cervids.

The prevalence of CWD in endemic regions increases with time. Albertan male mule deer prevalence has increased from 1.1% in 2005 to 22.1% in 2021 (**Figure 1.5**) [77, 191]. Eastern Alberta had 13 wildlife management units in 2019 where male mule deer prevalence ranges from 31-55% [77]. Adult male white-tailed deer prevalence in Iowa County, Wisconsin have risen from near 0% in 2005 to more than 40% in 2020 [195]. The increasing abundance of CWD within endemic areas is a concern for animal populations and the possible zoonotic implications from increased human consumption of infected animals.

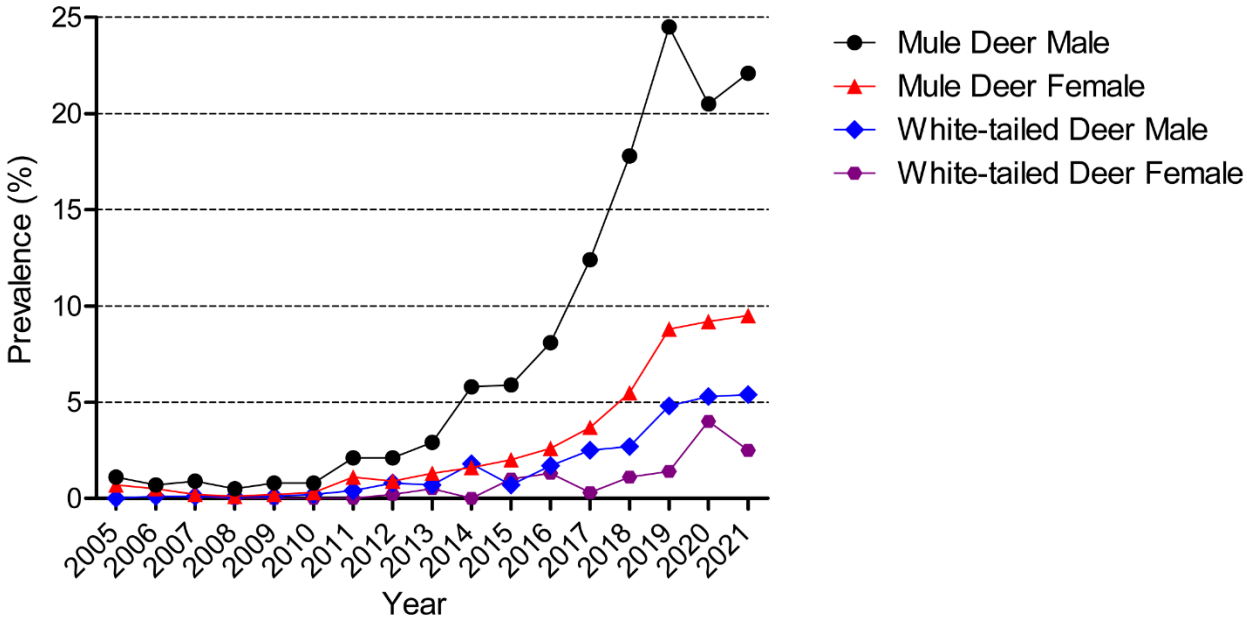

Figure 1.5. Alberta mule deer and white-tailed deer CWD prevalence from 2005-2021. Data from Smolko, *et al*., 2021, and the Government of Alberta.

While many mechanisms of CWD transmission have been suggested (e.g., excretion and secretion of PrP^{CWD}, contaminated cervid carcasses, environmental persistence, oral and intranasal exposure, or vertical transmission), none adequately explain the differences in prevalence of CWD with respect to species and sex. Cervid behaviours have long been proposed to explain the differences in CWD prevalence, but specific animal behaviours have yet to be concretely married with PrP^{CWD} transmission mechanisms [193, 220, 228-229]. Sex-associated CWD prevalence patterns generally break down in cervid farm outbreaks [56, 230-232]. Reasons for more uniform CWD prevalence in captive herds may be explained by increased animal concentration (with the associated increase in physical contact frequencies), concentration of PrP^{CWD} shed into the captive area, and contamination of shared feeding and drinking sources [230-232].

Less data is available for CWD prevalence in wild cervids other than mule deer and white-tailed deer. CWD can reach very high prevalence rates in captive elk herds, but prevalence in free-ranging elk is lower than in sympatric mule deer and white-tailed deer despite elk typically forming larger herds [54, 77, 190, 233-237]. CWD may be more prevalent in wild female elk than in male elk in Colorado (45% of 53 female versus 16% of 25 male carcasses tested) [238] and Alberta (0.65% of 1075 female versus 0.45% of 2477 male wild elk tested from 2011 to early 2022) (M Pybus, personal communication; email, 2022), although the sample sizes needed to confirm sex differences in wild populations of elk are limited. No evidence of sex or age-based differences was found in South Dakota elk [239]. Elk CWD prevalence patterns may change as the disease becomes more prevalent in affected populations. The rarity of moose CWD in North America prevents sex-based prevalence analysis [77, 240]. Most cases of atypical moose CWD in Fennoscandia have been in females (13 females, 1 male), but data is insufficient to assess age-specific sex differences in prevalence [73]. The low prevalence of CWD in moose is attributed to low animal density and group numbers [241-242]. The relative solitariness of moose is contrasted by the gregariousness of caribou and reindeer which can be found in herds consisting of hundreds of animals. Norwegian reindeer in the Nordfjella region, still at an early epidemic stage of CWD, had a CWD prevalence of 1.5% in males and 0.5% in females for animals tested between 2016 and 2018 [197]. The anticipation of CWD spreading rapidly through large reindeer herds has led to the pre-emptive culling of more than 2,000 animals in Norway [70].

PrP^{CWD} shedding during the long preclinical phase of CWD [37] is likely critical for CWD transmission. During the preclinical stage of disease, deer shed PrP^{CWD} in saliva as early as 3 months post infection, and in the urine and feces by at least 6 months [243-246]. Real-time

quake-induced conversion (RT-QuIC) methods detected prion seeding activity in elk feces as early as 14 days post oral CWD exposure, prion seeding activity in feces 8 and 9 days post oral challenge was attributed to the initial inocula [247]. Differences in CWD pathophysiology between species may also factor into disease transmission. The relative transmissibility of prion diseases is understood to be correlated with the degree of prion lymphotropism, i.e., the ability to replicate in lymphoreticular structures [12, 248-250]. The tonsils and retropharyngeal lymph nodes of CWD-infected deer at various stages of disease contain higher levels of proteinase K-resistant PrP^{CWD} than elk at the clinical stage of disease - suggesting that elk may shed less PrP^{CWD} into the environment than deer [251]. RT-QuIC analysis and bioassay of CWD-infected white-tailed deer and elk retropharyngeal lymph nodes identified similar levels of infectivity, suggesting no difference in CWD transmission potential between white-tailed deer and elk [250]. Proteinase K digestion of samples in the former study may not represent infectivity present in the lymphatic structures as accurately as RT-QuIC and bioassay due to the enzymatic digestion step. Preclinical elk, mule deer, and white-tailed deer all shed PrP^{CWD} in feces by 6 months and in urine by 18 months post oral challenge - suggesting that the species have similar capacities to shed PrP^{CWD} [245].

1.5 Cervid peripheral exocrine glands

Exocrine glands are points of entry for bacterial and viral pathogens [252-258]. As exocrine glands are innervated by the sympathetic nervous system, they are possible sites of neuroinvasion by PrP^{CWD}. Exocrine glands are often paired with lymphoid tissues for immune surveillance; immune cells at these sites may traffic PrP^{CWD} from glands to secondary lymphatic structures for later neuroinvasion. PrP^{CWD} in salivary glands of CWD infected deer [41, 123, 243], and high levels of PrP^{C} in mammary glands of healthy animals [259] suggest that PrP^{C} and

the capacity for conversion into PrP^{CWD} will be high in other peripheral exocrine glands. The parotid gland has attracted attention in CWD research due to their immediate proximity to the oral cavity that would permit the gland and its periglandular lymph nodes to contact orally ingested PrP^{CWD} and produce infectious saliva [39, 41, 49, 123, 179-180, 232, 260-262].

Outside of carefully controlled experimental conditions, identification of direct and indirect pathogen transmission routes between wild animals is, unsurprisingly, difficult to establish, but has precedence for cutaneous gland secretions. Transmission of *Mycobacterium mungi* between banded mongooses (*Mungos mungu*) and transmission of *Trypanosoma cruzi* between *Didelphis* and *Philander* opossums occur by contaminated anal gland secretions [263-267]. Gut bacteria transfer between groups of Verreaux's sifaka (*Propithecus verreauxi*) is linked to sternal gland and anogenital gland scent-marking behaviours [268-269]. Banded mongoose and Verreaux's sifaka investigating scent signposts and overmarking - the deposition of secretions overtop of a pre-scented site - are suspected routes of indirect disease and bacteria transmission [263, 268].

Cervids have numerous scent glands (specialized exocrine glands of the integumentary system) on their face and legs (**Figure 1.6**) [252, 270-273]. The presence and morphology of these glands vary across North American cervid species, but are most comprehensively present in mule deer and white-tailed deer (**Table 1.2**). The mammary gland is the only skin gland thoroughly investigated for prion shedding. Sheep scrapie-associated PrP^{Sc} has been identified in the lymphoid follicles adjacent to mammary gland ducts and within mammary gland ducts and acini [152, 173-175]. Ewes experimentally infected simultaneously with scrapie and a mastitis-causing virus transmit PrP^{Sc} via infected milk [175]. Mastitis is not required for secretion of PrP^{Sc} into milk of scrapie-infected ewes [152, 156], the inflammation-associated dense concentrations of infiltrating immune cells increases the likelihood of observing PrP^{Sc}-containing immune cells by

immunohistochemistry. Investigations into CWD-infected cervid mammary glands have been limited, but PrP^{CWD} has been reported in gland homogenates [274-275].

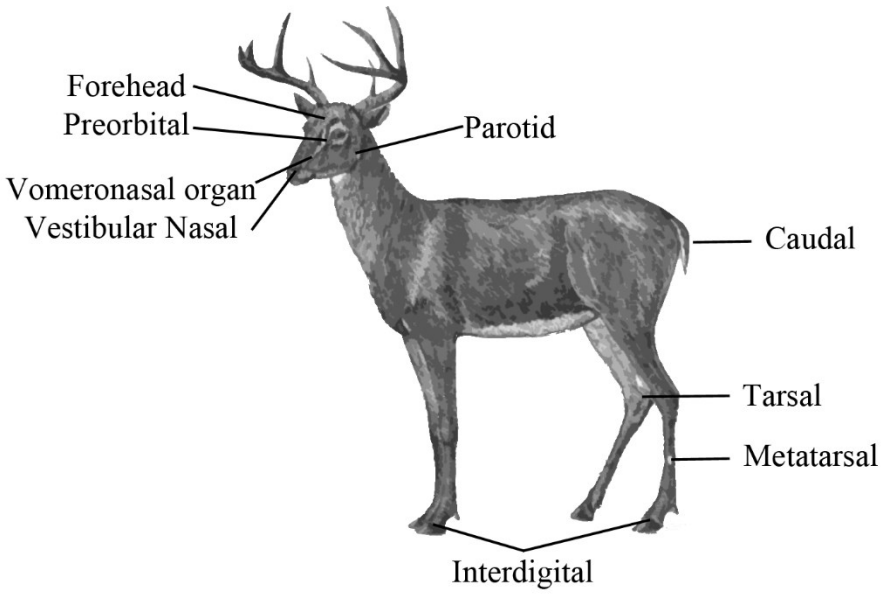

Figure 1.6. Locations of select exocrine glands and the vomeronasal organ in Odocoileus sp.

Table 1.2. Presence of select integumentary exocrine glands in cervids of North America.

Species	Peripheral Exocrine Glands						Notes
	Forehead	Preorbital	Nasal	Tarsal	Metatarsal	Interdigital	
White-tailed Deer (*Odocoileus virginianus*)	+	+	+	+	+	+	• White-tailed deer have very actively secreting interdigital glands. • Males possess penile preputial glands.
Mule Deer (*Odocoileus hemionus*)	+	+	+	+	+	+	• Mule deer have the largest metatarsal glands. • Larger preorbital glands than white-tailed deer. • Interdigital gland immune cell infiltrates are common.
Elk/Wapiti (*Cervus canadensis*)	-	+	-	-	+	-	• Elk can still develop interdigital infections despite a lack of interdigital glands.
Caribou/Reindeer (*Rangifer tarandus*)	-	+	+	+	-	+	• The forefoot interdigital glands are underedeveloped. • Possess ventral vestibular nasal glands instead of lateral vestibular glands of the other listed cervids.
Moose (*Alces alces*)	None described	+/-	+	+	+/-	+	• Forehead glands are predicted to be present in moose. • Preorbital glands are absent in Newfoundland moose, but are present in European and Alaskan moose.

1.6 Cervid behaviors with CWD transmission potential

1.6.1 Grouping patterns and habitat use among cervids

Considerable differences in behaviour and grouping patterns occur between white-tailed deer and mule deer, between males and females, and between older and younger individuals. The behavioural differences influence the level of direct and indirect contact between deer and, therefore, the implied risk of prion transmission [229, 276]. Deer behaviours and grouping patterns that concentrate animal density – including winter concentration, the formation of pre-rut male bachelor groups, and movement during the breeding season – have been proposed as key factors resulting in the observed patterns of CWD prevalence [46, 220, 277-282]. Hypotheses to explain the higher prevalence of CWD in males include more numerous male contacts with environmental contaminants (through increased nutritional requirements and larger home ranges) [193, 229, 283-284], female to male transmission during the mating season [193, 229, 276, 283-284], and physical contact between males (such as sparring and grooming) when they form bachelor groups [193, 220, 222, 229, 280-281].

The type and size of groups formed by white-tailed deer and mule deer vary substantially across seasons. Social interactions occurring within groups may influence CWD exposure risk. During summer, most females are relatively isolated as they rear neonatal fawns. Matrilineal groups of female deer are typically more philopatric (preferring to stay in an area) than males, especially mule deer, which may contribute to the higher prevalence of CWD infection among genetically related individuals as smaller home ranges become more contaminated [193, 283, 285-289]. Males of both species form bachelor groups throughout summer and the early autumn pre-rut period, and affiliative male-male social interactions (e.g., sparring) [290-294] within these groups may contribute to sex differences in prevalence [193, 220, 222, 229, 280-281]. Bachelor

groups are of interest to CWD transmission dynamics, but it is important to note that the average male-only group sizes are typically smaller than either female-only or mixed-sex groups (the largest) [291, 294, 295-302,p.177-182]. Mule deer females and males have more frequent and prolonged physical contact than white-tailed pairs during courtship, increasing the potential for mule deer to exchange saliva, urine, and glandular secretions [276]. The risk of repeat exposure appears higher for older males, because they are more likely to engage in marking activities and courtship [291, 293, 303-305]. Notably, mule deer tend to move to new areas single file along trails [302,p.133].

Mixed sex groups increase in frequency during fall and are the most common and largest type of mule deer group throughout winter [292, 296, 303]. Deer group size increases over winter for both white-tailed deer and mule deer [291-292, 296], and mule deer groups become increasingly cohesive as winter progresses [296]. In colder regions, deer habitat use and grouping behaviour is also affected by snow depth. White-tailed deer are well known for yarding behaviour, which refers to concentrations of deer occupying specific areas, where they form networks of trails that enable deer to conserve energy and reduce predation [306-309]. Mule deer form larger, more cohesive groups than white-tailed deer from fall throughout winter, and they have stronger interindividual associations and coordinated antipredator defences throughout the year [296, 310-313]. White-tailed deer also form mixed sex groups during winter when living in relatively open habitats [291, 296], but these groups are less common and smaller than mixed sex groups of mule deer [296]. Concentration of deer may increase CWD exposure risk by direct conspecific contact, or indirectly via soil or vegetation contaminated by body fluids, excretions, and possibly gland secretions. Reports of winter concentration of moose are variable and cannot be generalized for the species [314].

Localized foci of cervid concentration occurs because of human influences and natural geology. During harsh winters, elk concentrate their populations in winter ranges which may have artificial winter feedgrounds to support the population [315-316]. Increased animal densities at winter yards and supplemental elk feedgrounds are intra- and interspecies transmission factors for non-prion pathogens including *Brucella abortus* and the parasitic worm *Parelaphostrongylus tenuis* in the cervids [315, 317-320]. Concentration of deer and elk at feedgrounds and grain sources likely contributes to CWD transmission [37, 51, 185, 321]. Mineral licks (natural and artificial) also attract and concentrate cervids - even moose - to mineral sources [322-326]. PrP^{CWD} has been identified in soil samples of natural mineral licks - suggesting that mineral licks do act as reservoirs for CWD [51].

1.6.2 Allogrooming

Social grooming (allogrooming) of conspecifics may contribute to CWD horizontal transmission. Allogrooming is a suspected route of disease transmission for other species including the transmission of *Mycobacterium bovis* between meerkats (*Suricata suricatta*) and various parasites transmitting between brown spider monkeys (*Ateles hybridus*) and Japanese macaques (*Macaca fuscata yakui*) [327-329]. Allogrooming in white-tailed deer and mule deer often involves animals thoroughly licking the ears, face, neck, chest, and shoulders of their social partner – areas individuals cannot groom themselves [302,p.147-149, 330-336]. Facial grooming behaviours may result in the deposition of saliva onto the nose, mouth, and facial integumentary glands (forehead, preorbital, and possibly the vestibular nasal glands) of the social partner, while contacting and consuming secretions from these glands. Yearling (1-2 years old) and adult allogrooming in wild mule deer and white-tailed deer populations is most common between females [276, 291, 332]. Female white-tailed deer and mule deer engage in relatively high levels

of mutual grooming year-round, except during the fawning season when females are more dispersed [276, 291, 332]. Mule deer females do not allogroom more often than white-tailed females during the breeding season, as might be expected from the mule deer's more cohesive groups [276]. Allogrooming involving male deer is less frequent than between females. Male white-tailed deer engage in male-male grooming during spring and summer when antlers are in velvet [291], but not during the breeding season [276, 291, 303]. Descriptions of allogrooming between mule deer males are either absent [302] or very rare [332]. Allogrooming between individuals appears to be exaggerated in frequency, season, and partner type in penned deer compared to wild populations [333, 337]. Increased frequencies of allogrooming in penned deer may contribute to very high CWD prevalence rates seen in some captive deer herds.

Allogrooming is primarily restricted to female elk. Elk females will groom the face, ears, and neck of social partners - usually their offspring or other females [338-339]. Oral-gland interactions have been experimentally demonstrated by a tracer experiment involving 6 captive elk fed hay mixed with ink-adsorbed montmorillonite for 3 days. All elk were observed with stains around the mouth, nostrils, eyes (including preorbital glands), perineum, and one animal with stains on the teats [340]. Mutual grooming is absent in caribou and reindeer - individuals will sniff and lick conspecifics unidirectionally [341-343].

1.6.3 Sparring and antler fights.

Sparring and fighting between males are behaviours that could contribute to CWD transmission [220, 229, 276, 284]. Sparring typically begins after the antlers are stripped of velvet and is a gentle form of antler wrestling. Overarching similarities in sparring and fighting behaviours exist between the North American cervids. Sparring in all North American cervids is most common in smaller, younger males in the leadup to the peak rut with sparring partners typically differing in

size [291, 293, 303, 343, 344-352]. Sparring of deer increases again after the peak rut [291, 293, 303]. Female caribou, who have antlers, will spar, but at a much lower frequency than males [343, 353]. Captive female caribou spar more frequently than those in the wild [343]. Antler fights are infrequent, typically occurring between large, similarly sized males during peak breeding season - antler fights are the last resort after a series of dominance displays have failed to settle a match [291, 293, 303, 338, 343, 345, 350, 353-355].

Sparring may contribute to *T. pyogenes*, bovine tuberculosis, and SARS-CoV-2 transmission between cervids [202, 210-211]. Although aerosols are assumed to contribute to bovine tuberculosis and SARS-CoV-2 transmission between deer, more research is required to determine whether CWD is transmitted naturally by aerosols, including during sparring and fighting. CWD has been transmitted by aerosols under experimental conditions, but the dose used (~5mg of brain) is 16.7 times more than the minimum dose estimated to establish an oral infection (0.3mg of brain) [356-357]. If aerosol transmission is a natural route of CWD transmission, then male sparring and fighting may present opportunities for aerosol exposure.

1.6.4 Rubs, scrapes, and wallows

Indirect transmission of CWD could occur during the rut when males create three classes of scenting behaviours - rubs, scrapes, and wallows. These scent signposts are visited by conspecifics and are possible sites of indirect disease transmission.

Mule deer, white-tailed deer, and elk make scent signposts called ‘rubs’ or ‘rub sites’ by marking trees and vegetation with their forehead, preorbital, and possibly the vestibular nasal glands, interspersed by licking the rubbed vegetation, and antler thrashing (horning) [272, 291, 293, 303, 358-359]. Other individuals visit these scented sites, sniffing and licking deposited secretions

while adding their own facial secretions (overmarking) [293, 302,p.505-506, 337, 351, 360-363]. Mature, larger, dominant mule deer, white-tailed deer, and elk males are more likely to create scent marks [351, 364-366,p.293]. Mule deer males may scent mark vegetation (primarily by antler thrashing) more frequently, intensely, and for a longer period of time than white-tailed deer [354, 358, 366,p.293], but further interspecies analysis is required. Mule deer were attracted to rods artificially marked with forehead and preorbital gland secretions [367]. Experimentally, male mule deer sniff and lick rods marked with preorbital or forehead gland secretions more frequently than control rods. Female deer sniffed the secretion-marked rods more than controls but did not lick or rub marked rods any more than controls.

Despite variation in the presence of facial skin glands (**Table 1.2**), both sexes of elk and moose scent mark vegetation using their foreheads and preorbital gland regions with additional licking of the vegetation similar to white-tailed deer and mule deer rubbing [351, 360, 368-370]. As with deer, larger, older elk males are more likely to make scent marks by licking and rubbing their forehead and face on trees [351, 371]. Caribou and reindeer of both sexes rub their foreheads and orbital regions on vegetation with both sexes sniffing and licking the rubbed vegetation [342, 372-374]. Antler thrashing of vegetation is more common in larger caribou males [343]. Both sexes of moose routinely make and interact with rub sites during the rutting season [369, 375]. Moose bite and mouth trees or shrubs, rub the vegetation with the forehead and sides of their face, and occasionally lick the sites [369]. Males will antler thrash the sites and females may strip the bark of scent-marked trees with their teeth [355, 369].

The feasibility of rub sites as a source of CWD transmission is supported by other transmissible deer diseases that have prevalence characteristics similar to CWD. Adult white-tailed males are also more prone to abscesses attributed to opportunistic *Trueperella pyogenes* bacterial

infections than females [208-211]. Transmission of *T. Pyogenes* has is likely via rubbing and sparring [208, 210-211]. The commensal bacteria is present in cervid microflora and requires broken or abraded skin to establish opportunistic infections commonly found in the antler pedicle, and orbit [209, 211]. During the rut, deer rub and antler thrash vegetation vigorously enough to strip bark from trees [291, 358, 376]. The propensity for white-tailed deer males to present with *T. pyogenes*-associated infections in the forehead and orbit may have an underlying behavioural cause including male antler rubbing, traumatic antler casting, sparring, and social grooming [210-211, 377-378]. *T. pyogenes* may be transmitted indirectly at rubbing sites; however, attempts to culture bacteria from rub sites failed; the investigators noted that culturing conditions were not optimized [211]. Regardless, *T. pyogenes* was found more frequently in forehead swabs of white-tailed deer males than in swabs from females, suggesting behaviour-associated horizontal transmission [209-210].

Adult male mule deer were predominantly infected in two Wyoming outbreaks of infectious viral keratoconjunctivitis [206-207]. Muñoz Gutiérrez *et al*. speculated that rut-associated rubbing behaviour was responsible for the male prevalence and the winter timing of the ocular infection [207]. Male predominance of a spring 1943 keratoconjunctivitis outbreak was attributed to male bachelor groups [206]. The similar sex-related prevalence of ocular keratoconjuctivitis outbreaks and CWD lends credence to facial gland-related behaviours being involved in CWD transmission.

Rutting-associated ‘scrapes’ are made by white-tailed deer (but not mule deer) by pawing at the ground, likely depositing interdigital gland secretions, with additional mouthing and rubbing behaviour on an overhead branch [291, 359, 362, 376, 379-383,p.103-104]. White-tailed deer scraping behaviours with overhead branches were first recorded in 1887 by Tony Alexander (b.

Abt. 1862), then later in 1954 by Pruitt [379, 383,p.103-104]. Similar to scent rubs, white-tailed deer of both sexes visit and physically interact with scrapes. Scraping behaviours correlate better with peak breeding season relative to isolated rubbing [364, 376]. As with rubbing, larger white-tailed deer males are more likely to create scrapes [364-365].

Hypotheses linking scent rub sites and scrapes to indirect CWD transmission and sex-associated risk date back to at least 2006 [193, 228, 359]. At or near scrape sites, deer urinate on their tarsal glands while rubbing the glands together in so-called 'rub-urination' (see section 1.7.5 Tarsal glands) [291, 358-359, 384] which may deposit and concentrate PrP^{CWD} at the rub sites and scrapes. Male white-tailed deer may smell and lick female deer urine at scrapes during the rut (see section 1.7.4 on the flehmen response) [333, 335-336, 359]. During these complex behaviours, deer would be exposed to soil-bound and urine-containing PrP^{CWD} via the interdigital glands, facial glands, and the alimentary tract. Female white-tailed deer visit scrapes more frequently; however, males are more likely to physically interact with scrapes [359, 380] - disproportionately exposing them to PrP^{CWD}. Although the observation of white-tailed deer at scrapes correlates with white-tailed deer male and female CWD prevalence, it does not explain why mule deer have higher CWD prevalence rates despite mule deer lacking scraping behaviours [303, 354, 366,p.294].

During the rutting season, elk males use their antlers and hooves to create wallows (rutting pits) in marshy or moist ground [338, 351, 371, 385]. The males scent themselves and the wallows with urine and rub their neck, chest, belly, legs, and the side of the face with mud in the wallow. Rutting wallows are visited by multiple males and thus may be an indirect source for CWD transmission [338, 385]. Nasal-oral contact of individuals with wallow sites has been recorded for elk making wallows, but also of elk, mule deer, and moose inspecting the sites [385].

Although only elk males make wallows, elk of both sexes visit the sites in approximately equal numbers [385]. VerCauteren *et al*. concluded that elk wallows likely play a small role in CWD transmission based on the short period of time that elk males wallow during the rut and a low frequency of wallows being reused by other males [385]. Male moose create wallows in a similar manner to elk (including marking wallows with urine) but, unlike elk, female moose will also use wallows made by males [348, 355, 386-390].

1.7 Involvement of peripheral tissues in cervid behaviors

1.7.1 Forehead and orbital glands

Observations of North American deer scent marking vegetation by forehead rubbing led to the discovery of forehead glands in mule deer and white-tailed deer [252, 272]. The size of the forehead gland secretory epithelia changes seasonally. White-tailed deer forehead glands are thicker in males year-round although both sexes experience increases in secretory epithelia thickness and glandular activity during the rut [272] - similar to observations of roe deer forehead glands [391]. Quay and Müller-Schwarze found no differences in forehead gland thickness between mule deer sexes in samples collected within a two day span at the beginning of the rutting season [252]. Whether seasonal changes in glandular size and activity impact susceptibility to CWD infection has not been investigated for mule deer or white-tailed deer. Although moose are predicted to have forehead glands, they have not yet been reported [388].

The preorbital gland (infraorbital sinus, suborbital gland, preocular gland) is a sac-like structure of smooth skin anterior to the inner canthus of the eye of many cervids [252, 392-393,p.238-280]. Preorbital glands have been described in all North American cervid species except moose where the presence of the gland is variable. Moose in Newfoundland, Canada lack preorbital glands [394] while the glands are present in Alaskan and European moose [395-397]. Mule deer

have larger preorbital glands than white-tailed deer [398-400]. Preorbital glands of reindeer become enlarged and actively secrete during the rut [341, 401]. Elk, mule deer, and white-tailed deer can open their preorbital gland slits widely - especially during aggressive displays or when elk are bugling [271,p.162, 371, 402].

The preorbital gland can contain caseous masses that accumulate primarily from local secretions and from orbital drainage of the lacrimal glands and the nictitating membrane (third eyelid)-associated Harderian gland which lies in the inner canthus of the orbit [302,p.107, 392, 403]. The caseous masses have been found to carry dirt and plant fragments in white-tailed deer, and small arthropod ectoparasites in white-tailed deer and mule deer [404-405]. The presence of foreign material inside the preorbital sac is indicative of broad orbital exposures to materials potentially contaminated with PrP^{CWD}. During the rut, elk males lie down and rub the side of their face in the dirt and mud of urine-scented wallows such that preorbital gland secretions could be deposited on the wallows [338, 351]. The forehead and preorbital glands are most likely to encounter or deposit PrP^{CWD} during allogrooming, rubbing, and wallowing (Sections 1.6.2 and 1.6.4). Forehead exposure could also occur during sparring as theorized with *T. Pyogenes* transmission [208, 210-211].

1.7.2 Antler velvet and osteophagy

Antler velvet is a modified sebaceous gland-rich skin that is well innervated and vascularized [406-410]. Weeks to months before the peak rut, males of all North American cervid species strip antler velvet by thrashing and scraping their antlers against vegetation - behaviour distinct from scent rubbing during the rut [302,p.498-506, 341, 344-345, 349, 355, 358, 376, 386, 411-414]. Velvet and hairs can be found on vegetation where cervids have cleaned their antlers of velvet [355, 358, 376, 415]. Concern regarding possible PrP^{CWD} presence in antler velvet was

raised as early as 2002 [37, 58, 416]. Angers *et al*. confirmed the presence of PrP^{CWD} in elk antler velvet in 2009 using bioassay and PMCA and suggested that antler velvet could contribute to environmental contamination [417]. The presence of CWD infectivity in elk antler velvet supports rub sites as possible sites of indirect disease transmission [417]. Antlered cervids are observed consuming their own shed antler velvet, but reports of velvet being eaten by conspecifics are rare enough to cast doubt on CWD transmission [355, 372, 418].

Mysterud *et al*. recently proposed that reindeer consumption of cast antlers and also the uncast antlers of live individuals may be a source of CWD transmission [419]. CWD infectivity in antler velvet and sporadic Creutzfeldt-Jakob disease prion infectivity in human bone marrow was identified as supporting evidence [417, 420]. Presence of PrP^{CWD} within the hard antlers after ossification has not yet been demonstrated. Osteophagy - the consumption of antlers or bone - in cervids is a dietary source of phosphate and calcium [421]. Adult caribou and reindeer are the most avid consumers of cast antlers - with individuals reported to chew on antlers for up to 20 minutes [341, 345, 412, 419, 422-424]. Caribou and reindeer also gnaw on the unshed antlers of conspecifics, sometimes before the velvet is shed [345, 419, 425]. Multiple caribou have been observed consuming parts of individual cast antlers – suggesting possible transfer of saliva-derived PrP^{CWD} [345]. Other skeletal bones are chewed, but not as frequently as antlers [423]. Female caribou and reindeer more frequently consume cast antlers (most often in spring) and are more likely to have their own antlers gnawed on [341, 419, 425-426,p.321]. In one Norwegian reindeer herd all antlered individuals (mostly female at the time) demonstrated evidence of their antlers being gnawed on with 24.4% of the individuals having at least one antler gnawed to the antler base [419]. Osteophagy may permit indirect CWD transmission by exposure to PrP^{CWD} originating from the antlers or from the saliva of individuals consuming the antlers.

Osteophagy is less commonly observed in other cervids. Male elk have been observed consuming antlers and bones more frequently than female elk [427-428]. The behaviour is rarely observed in mule deer, white-tailed deer, and moose [429-433]. Despite few recorded direct observations of North American deer osteophagy, two studies of collected cast antlers concluded that 38.8% of mule deer and 15.5% of white-tailed deer antlers displayed evidence of chewing by their respective species [302,p.29-31, 430].

Although osteophagy is observed in all North American cervid species, it is a recurring and established behaviour in caribou and reindeer that could be a mechanism of direct and indirect CWD spread. Caution must be taken if considering osteophagy in CWD transmission models. Cervid osteophagy varies based on regional mineral availability and seasonal intake [421]. Variable frequency of osteophagy is exemplified by reindeer of the Nordfjella region of Norway. Mysterud *et al*. determined the prevalence of antler gnawing varied between 1984 and 2018 by examining photographs of reindeer in the region [419]. The frequency of reindeer with little or no signs of antler gnawing decreased from 92.3% in 1984 to 27.6% in 2009, and to 3.4% in 2018.

1.7.3 Vestibular Nasal Glands

Vestibular nasal glands are among the least studied cervid integumentary glands. Anatoly Ivanovich Akaevsky (1893-1983) described the vestibular nasal glands of reindeer in 1939 - terming the structures *sinus vestibuli nasi* [434,p.159-160;315]. The vestibular nasal glands of cervids were previously thought to have been first discovered in South American marsh deer (*Blastocerus dichotomus*) in 1976 [435]. The lateral vestibular nasal glands are pocket-like structures found in white-tailed deer and mule deer, but are absent in elk [273]. Newfoundland moose possess lateral nasal glands midway in the nasal cavity - a feature attributed to the greatly

enlarged nasal vestibule of moose [394]. It is unlikely that behavioural interactions resulting in direct physical contact of the nasal gland between moose would occur due to the deep positioning of the lateral vestibular nasal glands inside the nasal cavity. Reindeer lack the lateral nasal glands; instead possessing analogous ventral vestibular nasal glands characterized by structural folds instead of lateral vestibular nasal gland pocket-like invaginations [273, 434,p.159-160].

The function of the cervid vestibular nasal glands is unknown. The glands are solely sebaceous in nature, accumulating low-volatility, waxy secreta within the gross glandular structures of white-tailed deer and reindeer [273, 434,p.315]. The proportion of the waxy vestibular nasal gland secretions that end up in mucous leaving the nose is unknown. These accumulations have not been described in mule deer or moose [273]. Vestibular nasal glands are hypothesized to be used for scent-marking vegetation during scraping behaviours [270, 273]. When white-tailed deer males mark vegetation, they rub the side of their nose on the branch (or grass), then lick it in 'nasal-oral' marking [276] although this may be analogous to white-tailed deer rubbing (section 1.6.4). These glands and their secretions may also be associated with a social behaviour termed naso-nasal testing [436]. White-tailed deer adults briefly touch noses with other adults or fawns during social interactions [291, 437]. Mule deer naso-nasal testing occurs between deer that know each other, can result in mutual grooming, and appears to be seasonally independent [321, 335]. Countering the involvement of vestibular nasal gland with naso-nasal testing is the observation of the behaviour in elk despite elk not possessing these glands [273, 339, 438]. Naso-nasal testing of moose involves mutual muzzle sniffing [348, 355, 387]. The deep-set moose vestibular nasal gland is anatomically inaccessible between partners. Licking of one's own nose during aggressive behaviours has been noted in penned male mule deer, but not in

white-tailed deer [402, 439]. Whether the vestibular nasal gland is involved in the aggressive behaviour is unclear. Deer naso-naso contact would be at risk for PrP^{CWD} exposure originating from nasal secretions, saliva, or possibly the vestibular nasal glands.

1.7.4 Vomeronasal organ and the flehmen response

The vomeronasal organ (Jacobson's organ) is a paired tubular structure that lies along the base of the nasal septum, dorsal to the hard palate. The organ is the sensory element of a specialized accessory olfactory system associated with the flehmen (lip-curling) response primarily involved in chemical signal detection [440-444]. Fluids from either the nasal or oral cavities pass through the cervid nasopalatine ducts to enter the sensory epithelium-containing vomeronasal lumen [440, 445-447]. In cervids, exocrine vomeronasal serous glands are associated with the organ lamina propria and the vomeronasal respiratory epithelium [446-447]. During courtship, the flehmen response and vomeronasal organ assists males with detecting female estrous [354, 441, 448].

Deer and moose of both sexes exhibit the flehmen; however, males are most likely to exhibit the flehmen response, primarily when coming into contact with urine or vaginal secretions during the rutting season [276, 291, 354, 371, 401, 449-452]. Male mule deer begin sampling female urine (with the flehmen response) by 3 months of age; however, fawns sampling urine is rare (Lingle S, personal communication) [361]. Mule deer and white-tailed males travel through female groups, trying to sample female urine during the breeding season, either as the female urinates or by sampling urine from the ground [354]. Flehmen in mule deer is more common with direct contact with urine - direct contact was 6 times more likely to yield the flehmen response than simply sniffing urine on the ground [450, 453]. No significant difference was observed in the frequency or duration of male urine sampling and flehmen of sympatric mule

deer and white-tailed deer [276]. During advanced courtship, male mule deer and white-tailed deer may inspect and lick the perineum or vulva of the female being tended [276, 291, 293, 298, 303].

Urine-induced flehmen response in males has been reported in all North American cervids except elk [291, 293, 303, 348, 354, 401, 448-449, 454]. The flehmen response in elk is less described but is associated with the rutting season when elk males inspect the vulva and perineum of females [338, 371, 413]. Direct urine sampling by elk males has not been reported but is presumed to occur [371]. The flehmen response in moose has been observed after males inspect female genitalia, sampling urine being voided by females, or when sniffing or licking urine on the ground [339, 348, 355, 366,p.96]. Sexually receptive moose females are attracted to male urine – interacting with urine-soaked wallows, rubbing onto urine-soaked males, and sometimes placing their nose into the stream of male urine [389-390]. Moose (presumably males) have been observed to inspect and sip voided urine from the ground [388]. Relative exposure of males and female moose to urine of the other sex is unknown. Caribou and reindeer males flehmen after investigating or licking a female's urine or vulva during the rutting season [341-343, 374, 401]. Interestingly, caribou males ingest voided female urine; the stomach of one Newfoundland caribou male contained approximately 64g of gravel from eating urine-soaked dirt [343, 401]. Plants urinated on by females during the rutting season are selectively consumed by caribou males [343].

1.7.5 Tarsal glands

Tarsal glands on the inside of the hind leg hocks are regularly used by mule deer and white-tailed deer for rub-urination, whereby a deer urinates on the paired glands while rubbing the hind legs

and tarsal glands together. White-tailed deer and mule deer of all age groups and both sexes engage in rub-urination - often during normal urination unaffiliated with scent marking behaviours [302,p.113-116, 354, 361, 455]. Mule deer and white-tailed deer males are more likely to rub-urinate during the rutting season with larger, more dominant males rub-urinating most frequently [293, 302,p.110, 303, 354, 456-457]. Mule deer are reported to rub-urinate more frequently than white-tailed deer; however, quantitative confirmation is required [458]. Moose in British Columbia were reported to rarely rub-urinate, but 32% of observed Quebec moose urination events were reported as rub-urinations [323, 348]. Caribou and reindeer rarely rub-urinate, but mature males will engage in an analogous 'tramping' behaviour that is similar to rub-urination. Caribou and reindeer tramping involves standing and stamping in a single spot, hunching over to urinate on the lower hind legs [341-342, 373, 401, 459]. The behaviour in elk - who lack tarsal glands [271,p.82] - that is analogous to rub-urination is antler thrashing of soil and vegetation with copious urination [351].

Deer smell and lick the leg tarsal glands of social partners [276, 354, 361, 366,p.66, 460]. Licking and sniffing of tarsal glands is associated with individual recognition - occurring between mule deer, white-tailed deer, and occasionally tarsal gland sniffing (but not licking) between caribou and reindeer [342, 366,p.66, 361, 460-461]. PrP^{CWD} could be deposited onto the tarsal gland and its hairs of infected animals during rub-urination, then acquired by social partners licking the contaminated tarsal glands [276, 359]. The opposite scenario could occur when the tarsal gland of an uninfected animal is exposed to PrP^{CWD} when an infected animal licks the tarsal gland. The tarsal glands of the uninfected individual could be the site of the initial infection, or the animal could be orally infected when later licking their own tarsal glands.

Mule deer may be more prone to tarsal gland-mediated CWD transmission than white-tailed deer due to a unique hair feature. The tarsal gland hairs of mule deer are structurally specialized for scent-dispersion [462], possessing smaller cuticular scales with a strobilus-like appearance that trap and retain sebum, lipids, and other materials (**Figure 1.7 and Figure 1.8**). These specialized hairs - termed 'osmetrichia' - assist with tarsal gland-associated rub-urination scent dispersion. Müller-Schwarze *et al*. reported that osmetrichia are present in male and female mule deer tarsal glands but are absent in white-tailed deer [462]. The tarsal gland hairs of white-tailed deer have cuticular scales that are acutely angled outwards which capture materials similar to the osmetrichia Müller-Schwarze described in mule deer [463], observations we confirm. The smaller-scaled, more strobilus-like tarsal gland hairs of mule deer (**Figure 1.7B**) appear more likely to capture and retain material relative to the larger scales of white-tailed tarsal gland hairs (**Figure 1.7D**).

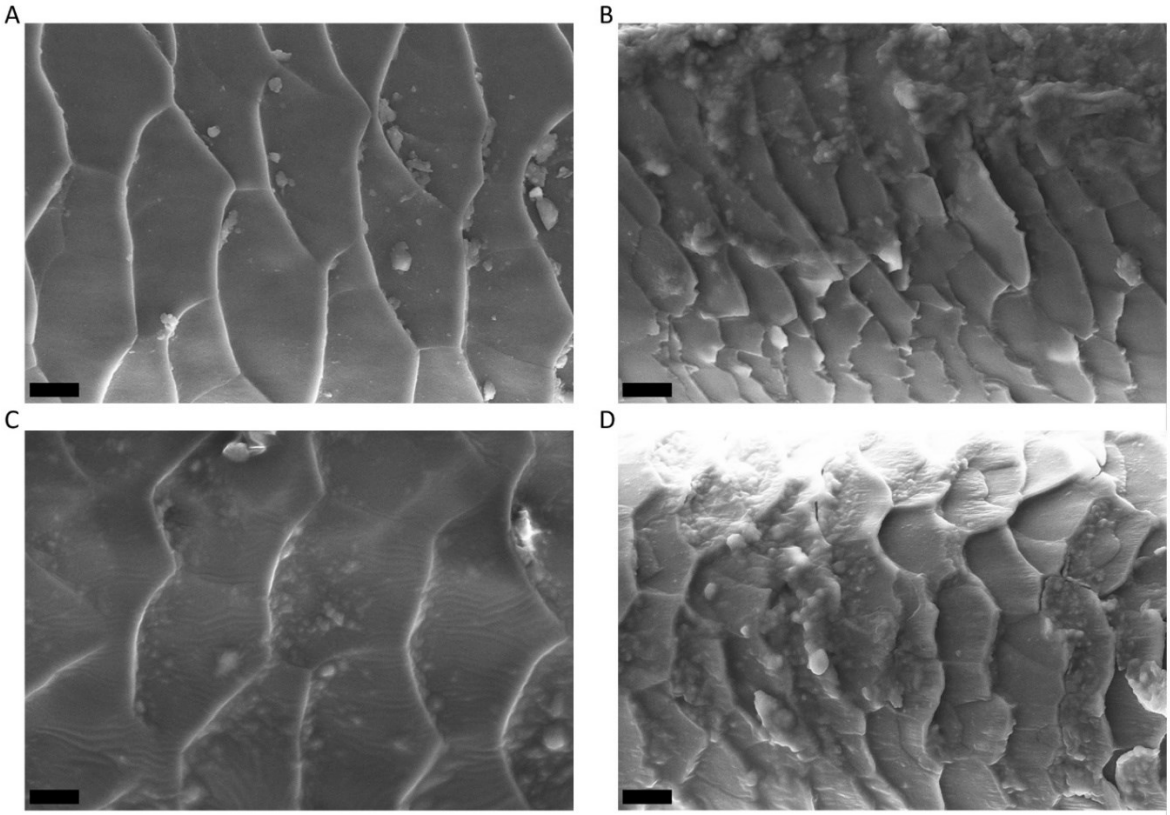

Figure 1.7. Scanning electron micrographs of deer normal skin guard hairs and tarsal gland hairs. A-B) Mule deer male and C-D) white-tailed deer male A, C) unmodified skin guard hairs, and B, D) tarsal gland tuft hairs. Scale bar represents 10µm with an image magnification of 1,000x. See Appendix 2 for methodology.

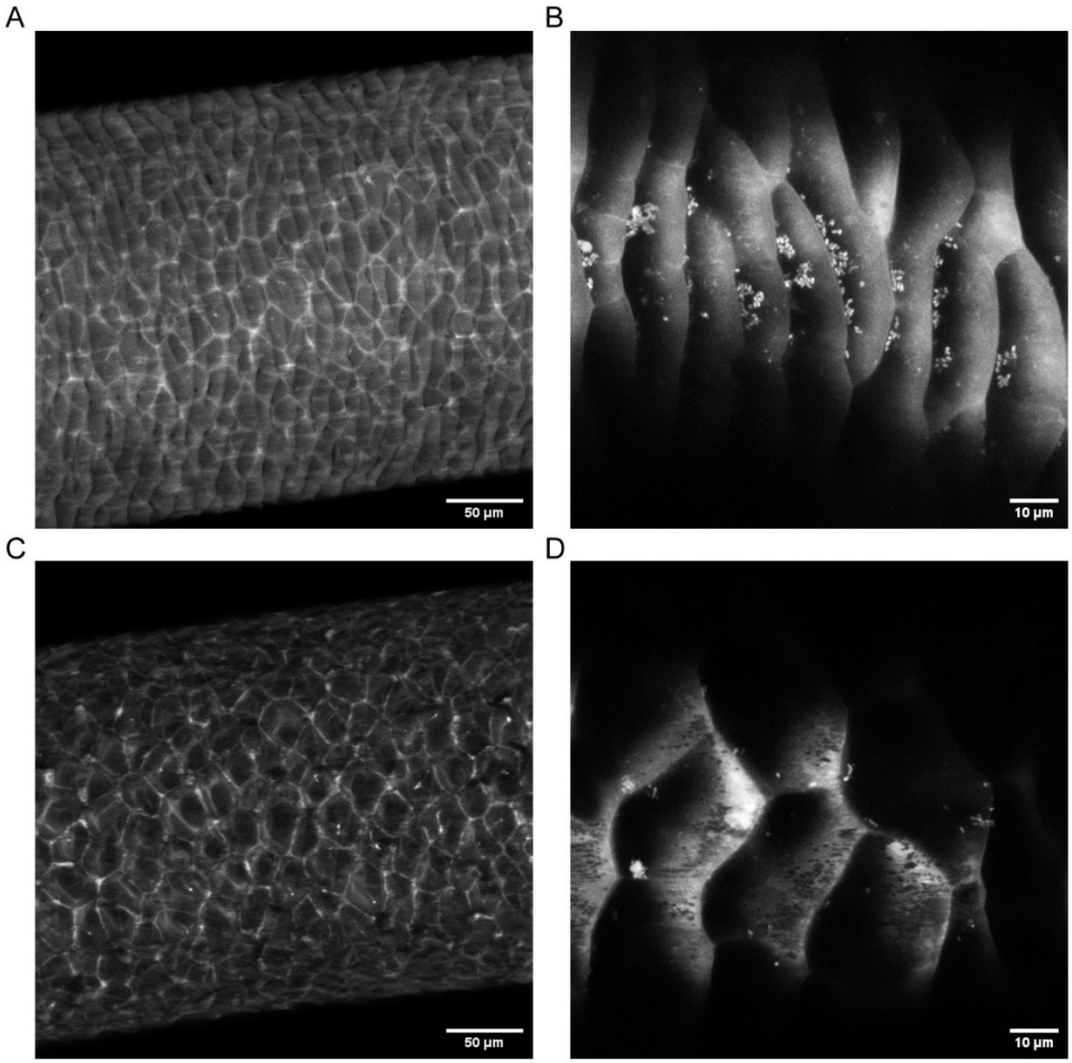

Figure 1.8. Mule deer tarsal gland hair osmetrichia and normal skin guard hair structure. Male mule deer A-B) tarsal gland specialized hair osmetrichia and C-D) normal skin hair. A, C) 20x magnification confocal fluorescence Z-projections of internal and external structures. B, D) 63x magnification Z-projections of the surface cuticular scale architecture. Hair fluorescence was induced by glutaraldehyde fixation and visualized by fluorescent confocal microscopy Z-stack projections. See Appendix 2 for methodology.

We suggest that the particle-trapping abilities of mule deer tarsal gland osmetrichia may enhance the risk of CWD transmission relative to the less specialized tarsal gland hairs of white-tailed deer. A CWD-infected animal may contaminate their tarsal glands with prion-containing urine

via rub-urination followed by transmission to a naïve animal through social tarsal gland licking. Indirect experimental testing of tarsal gland involvement in CWD transmission can be undertaken by assaying tarsal gland hairs for urine or saliva-derived PrP^{CWD} by serial protein misfolding cyclic amplification (sPMCA) or real-time quake-induced conversion (RT-QuIC). Complex chemical gland secretions and bacterial flora bound to the tarsal gland hairs [461, 464-467] could inhibit detection by PMCA or RT-QuIC. Such a methodology would be anticipated to yield the best surveillance results for adults during the rutting season when rub-urination is most common [293, 361, 384].

1.7.6 Metatarsal Glands

The metatarsal glands exist on the outside of the hindfeet and are composed of sudoriferous and sebaceous glands with a central keratinized ridge [252, 468]. Mule deer hind legs have well-developed tarsal and interdigital glands but also the largest known metatarsal glands [271,p.257-258, 335]. The gross morphology of mule deer and white-tailed deer tarsal and metatarsal gland sizes is not sexually dimorphic [404, 468-470]. Moose metatarsal glands are either small or entirely absent [395, 467, 471,p.971]. Variable presence of moose preorbital and metatarsal glands can be attributed to genetic and morphological diversity of moose across geographies and subspecies [472-473]. Metatarsal glands are highly innervated structures that become active in mule deer when stressed, fleeing, or alarmed to produce aerial alarm chemical signal [252, 468, 470]. An alarm function of metatarsal glands has not been observed in white-tailed deer which possess smaller, less developed metatarsal glands. However, the tarsal gland hairs of alarmed white-tailed deer will similarly erect and aerate tarsal gland scent [271,p.266, 302,p.112-113, 458, 474]. The function of the metatarsal glands has been hypothesized as a means of marking

bedding areas although this has not been tested [302,p.109-110, 471,p.974]. Observations of conspecifics interacting with the metatarsal glands of social partners are lacking for both species. Linsdale and Tomich noted that mule deer do not focus attention on grooming the metatarsal gland region [302,p.110]. From a behavioural standpoint, the role of the metatarsal gland in horizontal CWD transmission is considered unlikely. If so, the metatarsal gland presents as an excellent glandular control for centrifugal prion spread.

1.7.7 Interdigital Glands

The interdigital glands of cervids are anteriorly-facing pocket-like structures between the two first phalangeal bones of the fore and hind feet. Interdigital glands are more actively secreting in white-tailed deer than in mule deer [271,p.264]. The sebaceous and sudoriferous glandular layers of mule deer interdigital glands thicken with age [404]. Structurally, the interdigital glands of mule deer, white-tailed deer, caribou, and reindeer are not sexually dimorphic [404, 474, 475-476]. No sexual or seasonal differences in caribou and reindeer interdigital gland structure have been observed [475-476]. There are conflicting reports on seasonal changes in moose interdigital gland size [396, 477-478].

Caribou and reindeer have large interdigital glands in the hind feet, but lack the typical interdigital gland sac in the forefeet [271,p.265, 471,p.960, 475, 479]. The forefoot interdigital glands instead possess a layer of less developed sebaceous and sudoriferous glands reminiscent of unmodified skin [475]. Reindeer rarely lick or groom their own fur with the exception of their fore and hind interdigital glands [342, 374, 480-481]. Penned reindeer sniffed or licked their own interdigital glands in a seasonal manner - most frequently in September (2.6 times per hour and individual) versus a nadir in July (0.6 times per hour and individual) - but rarely sniff or lick the interdigital region of conspecifics [342]. The frequency of interdigital gland licking in wild

populations is not known. Interdigital gland licking, particularly in reindeer, may present an opportunity for soil- or gland secretion-bound PrP^{CWD} to be ingested by cervids. The spread of interdigital gland secretions in reindeer was demonstrated by injecting rhodanine tracer into the pocket structure of the hind interdigital glands of reindeer [481]. Tracer was identified, hours later, on interdigital hair tufts, hairs between the digits, nose, antler tips, and in fresh tracks in the snow, suggesting a route for PrP^{CWD} dissemination. An example of disease transmission via this route is necrobacillosis in reindeer. Necrobacillosis is an opportunistic infection caused by the soil bacteria *Fusobacterium necrophorum* invading broken or abraded skin or mucous membranes. Infection of the digits (digital necrobacillosis or footrot) is the most common form of this infection in reindeer, but foot licking is thought to contribute to concurrent foot and oral necrobacillosis infections [482-483]. Reminiscent of CWD indirect transmission, reindeer likely obtain oral necrobacillosis infections by grazing from grounds contaminated by infected individuals during outbreaks [483]. It is possible that secretion of PrP^{CWD} from the interdigital glands could result in oral exposure of conspecifics. Unlike caribou, mule deer and white-tailed deer have not been observed licking interdigital glands. Both deer species, however, scratch their noses with their hind feet after sneezing; white-tailed deer then, on rare occasions, lick the hind foot afterwards [302,p.96, 484-485].

CWD transmission associated with the interdigital glands likely involves geophagy - the ingestion of soils and minerals. Contamination of soils by interdigital gland secretions could be subsequently ingested by naïve animals. Indirect transmission of CWD likely occurs via contaminated soils [46, 56, 228, 486]. Soils and low vegetation contaminated by CWD prions are ingested by naïve deer. Deer consume tens of grams of soil and minerals per day - partly from soil attached to roots of vegetation [324, 487-488]. Quantification of mule deer fecal titanium

was used to estimate soil consumption to range from 7.7-29.6g/day with significantly more soil being consumed in the spring versus summer or fall [487]. Behaviours that concentrate deer and prion shedding, could therefore, be expected to enhance geophagy-associated CWD transmission. Males are also expected to be at a higher risk of prion exposure based on their larger body masses and caloric demands relative to females.

Mule deer, white-tailed deer, caribou, and reindeer smell and track trails scented by interdigital gland secretions [302,p.107, 341-342, 458, 489]. Under experimental conditions, male reindeer more frequently investigate interdigital gland secretions of other males, while females more frequently investigate the secretions of other females [489]. Moose are not thought to track scent trails based on their tall stature and small necks introducing physical difficulty in smelling trails [478].

Elk are the only North American cervids lacking interdigital glands [271,p.78, 411]. The absence of interdigital glands in elk does not exclude the possibility of prion infection at the site of the hoof. Prion invasion by environmentally contaminating PrP^{CWD} can be conceived when the skin barrier is compromised by physical injury of the hoof and local inflammation if present. Cervids, including elk, can develop infections of the hoof sole and interdigital region [482, 490-492].

1.7.8 C*audal glands and preputial glands*

Mule deer and white-tailed deer have sebaceous-containing caudal glands in the tail [252, 493-494]. The caudal gland acts primarily as an alarm organ in the absence of physical contact by conspecifics – similar to the metatarsal gland discussed earlier [493-494]. Penned white-tailed deer males nibble and nudge a female deer's tail and rump prior to copulation, but it is unclear if this is related to the caudal glands [454]. In reindeer, who lack metatarsal glands, the caudal

gland acts as a combined alarm and recognition organ [493]. Reindeer will smell the caudal glands of conspecifics, but will not lick them [342, 493]. Caudal glands are not described in moose. Elk have caudal glands, but they have not been described histologically [411]. The caudal glands of elk are likely also sebaceous in nature, similar to the closely related European red deer (*Cervus elaphus*) [495]. Overall, the caudal gland is an unlikely contributor to CWD transmission based on limited observations of cervids physically interacting with the caudal gland of conspecifics.

White-tailed deer males have sebaceous gland-containing penile preputial glands [496]. Penned white-tailed deer males have been observed licking their own prepuce immediately after copulation, but the gland function remains poorly understood [454]. Presence of the glands in other North American cervids has not been investigated and potential transmission risk is unknown.

1.8 Anticipated glandular PrP^{CWD} lymphatic accumulation and routes of neuroinvasion

Evidence of horizontal CWD transmission involving integumentary and cranial exocrine glands would require naturally infected deer to have PrP^{CWD} in supplying nerves and/or the efferently draining lymph nodes (**Table 1.3**). Cervid integumentary glands are comprised of sudoriferous, sebaceous, and pilosebaceous glands that are innervated by the sympathetic nervous system [252, 475]. Testing retropharyngeal lymph nodes (RPLN) and the medulla oblongata at the level of the obex is the gold standard for CWD surveillance and is demonstrably the most accurate known tissue for diagnosing animals preclinically infected with CWD [260, 497]. Testing the obex and RPLN from 4430 hunter-harvested white-tailed deer in Wisconsin determined that screening RPLNs was more accurate for detecting CWD [232]. Biologically relevant routes of

prion migration from exocrine glands would be expected to coincide with observations of PrP^{CWD} progression in preclinical animals naturally infected with CWD.

Table 1.3. Expected routes of PrP^{CWD} nerve and lymphatic transport following CWD exposure.

Structure	Nerve Supply	Lymphatic Drainage
Forehead Gland Preorbital Gland Harderian Gland	Sympathetic: Gland → Supraoptic Branch of the Ophthalmic Nerve → CN V → ICN → SCG → ? → IMN / AGH / IRN Parasympathetic: Gland → Pterygopalantine Ganglion → Greater Petrosal Nerve → CN VII / Zygomatic Nerve → CN V	Gland ↓ Parotid lymph nodes ↓ Medial Retropharyngeal lymph nodes ↓ Lateral Retropharyngeal lymph nodes ↓ Tracheal ducts
Parotid Gland	Sympathetic: Gland → ECN → SCG → IMN Parasympathetic: Gland → Otic ganglion → CN IX → Inferior Salivatory Nucleus	
Vestibular Nasal Gland	Sympathetic: Gland → Infraorbital Nerve → Maxillary Nerve → SCG → IMN	Gland ↓ ? ↓ Lateral Retropharyngeal lymph nodes ↓ Tracheal ducts
Vomeronasal Organ	Sympathetic: Gland → CNN → Pterygopalantine Ganglion → Vidian Nerve → SCG → IMN Parasympathetic: Organ → CNN → Pterygopalantine Ganglion → Vidian Nerve → CN V Olfactory: Organ → Vomeronasal Nerve → AOB → BNAOT / BNST / Vomeronasal Amygdala → Hypothalamus	
Fore Interdigital Gland	Sympathetic: Gland → Medial Nerve → Brachial Plexus → IMN	Gland ↓ Axillary or Superficial Cervical Lymph Nodes ↓ Venous Angle and/or Jugular Trunk
Tarsal, Metatarsal, Hind Interdigital Glands	Sympathetic: Gland → Sciatic Nerve → Sacral Plexus → IMN	Gland ↓ Popliteal or Sublumbar Lymph Nodes ↓ Lumbar Trunk

Abbreviations:

AGH	Anterior Grey Horn
AOB	Accessory Olfactory Bulb
BNAOT	Bed Nucleus of the Accessory Olfactory Tract
BNST	Bed Nucleus of the Stria Terminalis
CN V	Cranial Nerve V (Trigeminal Nerve)
CN VII	Cranial Nerve VII (Facial Nerve)
CN IX	Cranial Nerve IX (Glossopharyngeal Nerve)
CNN	Caudal Nasal Nerve
ECN	External Carotid Nerve
ICN	Internal Carotid Nerve
IMN	Intermediolateral Nucleus
IRN	Intermediate Reticular Nucleus
SCG	Superior Cervical Ganglia

1.8.1 Cranial tissue exposure

If preorbital and Harderian glands are exposed to PrP^{CWD} from deer-to-deer social behaviours or indirect transfer during rubbing behaviours, PrP^{CWD} may invade the gland innervations. Interpretation of PrP^{CWD} accumulation in the preorbital glands is complicated by potential infectivity draining from the orbit into the preorbital gland. Harderian glands and the nictitating membrane of cervids offer potential sources of preorbital gland PrP^{CWD}. Prion infectivity within the Harderian gland has been reported in mice intraocularly infected with the ME7 prion strain from 24 hours to 160 days post infection [498]. Sprague Dawley rats infected with a rat-adapted RML prion strain manifest clinical signs of disease including increased Haderian gland secretions (porphyrin-containing chromodacryorrhea) [499]. Infectivity of the gland or its secretions was, however, not tested. Stress-related porphyrin Harderian secretions are rodent-specific and are particularly conspicuous in rats [500].

The Harderian gland duct empties onto the associated nictitating membrane [403, 500]. Deposition of PrP^{Sc} in the lymphoid follicles of nictitating membranes in scrapie-infected sheep is an established antemortem and postmortem tissue used for scrapie surveillance [501-504]. PrP^{CWD} has been identified within the nictitating membranes of preclinical, orally infected white-tailed deer and naturally infected elk [505]. PrP^{CWD} was observed in lymphoid follicles of the nictitating membranes by immunohistochemistry in white-tailed deer 23 months post infection and were, by RT-QuIC, positive at 1 month [505]. PrP^{CWD} in the nictitating membrane could drain into the preorbital gland with lubricating Harderian and lacrimal secretions.

The source of preorbital gland innervation has not been described, but the immediate proximity to the Harderian gland suggests that the two likely share the same source of sympathetic innervations. Unlike the integumentary glands, the Harderian gland contains both sympathetic

and parasympathetic innervations. Sympathetic innervation of the Harderian gland leads from the ophthalmic nerve of the trigeminal nerve (cranial nerve V) to the superior cervical ganglion [506-507]. If Harderian gland parasympathetic nerves are infected, PrP^{CWD} would be expected to be transported to the zygomatic nerve, to the maxillary branch of the trigeminal nerve (cranial nerve V); or, from the parasympathetic pterygopalatine ganglion to the greater petrosal nerve, then to the facial nerve (cranial nerve VII) [507-5-11]. The forehead skin, including that of the forehead glands, and antler pedicles of deer are also innervated by the supraoptic branch of the ophthalmic nerve [408, 512]. Feasibility of prion infectivity being found in the forehead glands of deer is supported by identification of PrP^{CWD} in elk antler velvet [417]. Any PrP^{CWD} entering the sympathetic innervations of the forehead, preorbital, or Harderian glands would, therefore, be expected to migrate through the trigeminal ganglia before being retrogradely transported to the superior cervical ganglion. Unknown specific preganglionic neurons from the superior cervical ganglion most likely project from, in order of likelihood, any of i) the intermediolateral cell column of the T1 to T4 regions, ii) the lamina IX of the anterior gray horn of the C1 to C4 regions, or iii) the intermediate reticular nuclei of the brainstem [513-514].

Investigation of PrP^{CWD} presence in the superior cervical ganglia and the facial regions of the trigeminal nerve are generally lacking. PrP^{CWD} has been identified in the spinal trigeminal nucleus and the dorsal motor nucleus of the vagus nerve (DMNV) of naturally infected moose, elk, and reindeer [58, 68, 233, 242, 515-516]. The presence in these structures mirror that of orally infected white-tailed deer, reindeer, and moose [262, 517-518]. Medullary involvement of the spinal trigeminal nucleus is consistent with proximal, radial PrP^{CWD} spread from the DMNV. Sigurdson *et al*. examined a broad range of neuronal pathways of six captive, naturally infected mule deer with clinical CWD to elucidate routes of prion neuronal trafficking [519]. The same

investigation examined one superior cervical ganglion and one Gasserian (trigeminal) ganglion by immunohistochemistry and found no PrP^{CWD}. The intermediolateral column consistently accumulated PrP^{CWD} which could have originated from almost any organ with sympathetic innervation. Overall, past investigations into the structures that would support CWD neuroinvasion at the sites of the preorbital gland, forehead, or the Harderian gland are limited.

If the superior cervical ganglion accumulated PrP^{CWD}, interpretation would be confounded for the palatine tonsils are sympathetically innervated by the superior cervical ganglion-glossopharyngeal neuronal pathway [520]. PrP^{Sc} accumulates in the superior cervical ganglia of orally, conjunctivally, and intra-tonsillarly infected sheep, albeit at clinical stages of disease [521-523]. The more studied sympathetic innervations of the parotid gland also originate from intermediolateral cell column, projecting to the superior cervical ganglia. Parotid parasympathetic preganglionic innervation originates from the inferior salivatory nucleus in the medulla which transmit through the glossopharyngeal nerve (cranial nerve IX) to the otic ganglion, and finally the parotid gland [524-525]. Postganglionic neurons then project to the parotid gland via the external carotid nerve [525-526]. As such, the presence of PrP^{CWD} in the superior cervical ganglia of wild cervids cannot be confidently differentiated as having originated from either oral or facial gland exposure.

Afferent cervid and caprid lymphatic vessels connect the regions of the forehead, Harderian, preorbital, and parotid glands to the parotid lymph nodes which efferently drain into the medial and lateral retropharyngeal lymph nodes [527-528,p.405-407]. Exposure of any of the facial glands, during rubbing or social grooming behaviours, to PrP^{CWD} would be identified by RPLN-based CWD surveillance. Social grooming between deer, or the licking of rub sites resulting in oral uptake of facial gland secretions could further result in the classical RPLN, tonsillar,

vagosympathetic, and mesenteric hallmarks of an oral CWD transmission. Carefully structured experimental topical PrP^{CWD} exposure of cervid integumentary glands to simulate exposure via rubbing or social behaviour will be required to validate this route of exposure and eliminate the possibility of oral exposure.

1.8.2 Vestibular nasal gland

The nasal vestibule of ruminants is innervated by the infraorbital nerve branch of the maxillary nerve [529]. PrP^{CWD} transport from vestibular nasal gland sympathetic innervations are expected to divert from the maxillary nerve to the superior cervical glanglia before entering the intermediolateral nuclei. The regions of the vestibular nasal glands are drained by the parotid lymph nodes in goats and sheep and a combination of the parotid and submandibular lymph nodes in cattle [528]. As with other ruminant cranial lymph nodes, efferent drainage flows to the lateral retropharyngeal lymph nodes before entering the tracheal ducts.

1.8.3 Vomeronasal organ

Scrapie and CWD was proposed to be horizontally transmitted by prions shed from olfactory and vomeronasal sensory epithelium into mucus or saliva [530]. McFarlane suggested that horizontal CWD transmission occurs when males sample the urine of females; however, the author did not mention or discuss the flehmen response, nor the vomeronasal organ [283]. Prion neuroinvasion of the vomeronasal organ was proposed in 2009 [531-532]. The hypothesis of vomeronasal organ involvement in CWD transmission was expanded by the proposal that the flehmen response may be involved [356, 359, 533]. Male propensity for exhibiting the flehmen response has since been considered for integration into CWD transmission models [534].

Sympathetic and parasympathetic signals to the vomeronasal organ induce intraluminal pressure changes that result in fluid exchanges between the organ and the nasopalatine ducts [535-536]. Flehmen studies in goats presented with tracing dye-laced urine found that small amounts of dye entered the vomeronasal organ passively in control animals that did not flehmen [442, 537]. Using cannulated goats, the flehmen response increased vomeronasal uptake of dyed urine approximately 3-4 fold relative to passive diffusion without flehmen [537]. Flehmen is therefore expected to greatly facilitate prion exposure of the vomeronasal organ but is not required for the vomeronasal organ to be exposed to PrP^{CWD}.

PrP^{Sc} spreads centrifugally to the vomeronasal sensory epithelium in clinical stage hamsters infected with the Hyper prion strain by the intracerebral or intra-olfactory bulb routes [530, 538]. Hamsters inoculated with the 263K prion strain deep into the nasal cavity did not accumulate PrP^{Sc} in the vomeronasal organ until late in the preclinical stage of disease – indicative of centrifugal spread [532]. The intranasal inoculation near the cribriform plate likely did not grant access to the vomeronasal organs via the nasopalatine duct.

The olfactory bulb, nucleus, tubercle, and stria accumulate PrP^{CWD} in naturally acquired CWD [69, 180, 539]. These structures are associated with the main olfactory bulb, not the accessory olfactory bulb and the vomeronasal organ. The olfactory structures are affected by pathology after DMNV and vagal PrP^{CWD} accumulation in mule deer oral infections [179] - suggesting that the olfactory system is affected by early centrifugal spread rather than exposure of olfactory epithelium of the main olfactory bulb. Interestingly, PrP^{CWD} was not observed in the main or accessory olfactory bulbs of transgenic mice expressing the deer prion protein experimentally infected with CWD by intranasal exposure of aerosolized CWD brain homogenate nor in white-tailed deer infected with lyophilized PrP^{CWD} bound to montmorillonite into cervids [49, 533].

PrP^{CWD} was observed in the olfactory epithelium in the white-tailed deer transmission study but did not progress further by 175 days [49].

Support for initiation of CWD infection in the vomeronasal organ was provided by combined intranasal and oral CWD infection of white-tailed deer which resulted in PrP^{CWD} being detected in vomeronasal organ homogenate, by RT-QuIC, 3 months post exposure - prior to detection in the obex [122]. Infectivity in the vomeronasal organ was preceded by infectivity in the retropharyngeal, parotid, mandibular lymph nodes, and the tonsils. The early, unexpected, detection of infectivity in the vomeronasal organ at three months - well before known cerebral infectivity detection - may represent a site of CWD infection independent of the cranial lymph nodes.

If a vomeronasal organ were exposed to PrP^{CWD}, the transport of prions to the CNS would be expected to track the two major organ innervations. Olfactory-associated neurons of the sensory epithelium transmit signals from the caudal-dorsal aspect of the organ, via the vomeronasal nerve, to the accessory olfactory bulb [440, 447, 540-543]. Secondary projections of the accessory olfactory bulb lead to the vomeronasal amygdala (thus linking to the hypothalamus), the bed nucleus of the stria terminalis, and the bed nucleus of the accessory olfactory tract [444, 544-545]. Sympathetic innervations of the mammalian vomeronasal organ (including those of the glands) enter the caudal-ventral aspect of the organ from the caudal nasal nerve, from the pterygopalantine ganglion, from the Vidian nerve - originating from the superior cervical ganglia [440, 536, 542, 546]. Parasympathetic innervations enter the vomeronasal organ from a similar pathway of the caudal nasal nerve via the pterygopalantine ganglion via the vidian nerve, from the trigeminal ganglia [440, 536, 546-547].

Details of vomeronasal organ lymphatics require further anatomical research. Early attempts to trace the lymphatics with injected markers proved difficult in the mid-19th century [548]. Lymphatics have been repeatedly observed in mouse and rats [549-551], but no successful lymphatic tracing of the vomeronasal organ has been completed in mammals. Vomeronasal organ lymphatic vessels have been reported in artiodactyls; however, there is disagreement as to whether these are nasal venous sinuses, or even if there are venous sinuses [541-543, 552]. Lymphatics draining the vomeronasal organ have been reported in giraffe, and both venous sinuses and lymphatic vessels have been observed in reindeer and dromedary camel [445, 553-555]. We observed the distinctive valves of lymphatic vessels in the anterior aspect of the vomeronasal organ lamina propria of mule deer (**Figure 1.9**). The lymphatic drainage of the vomeronasal organs can be inferred by drainage of immediately adjacent structures. The palates, nasal septum, and ventral nasal cavity in cattle, sheep, and goats are drained by a combination of the parotid, submandibular, and medial retropharyngeal lymph nodes [528]. The efferent lymphatic drainage inevitably leads to the lateral retropharyngeal lymph nodes in ruminants.

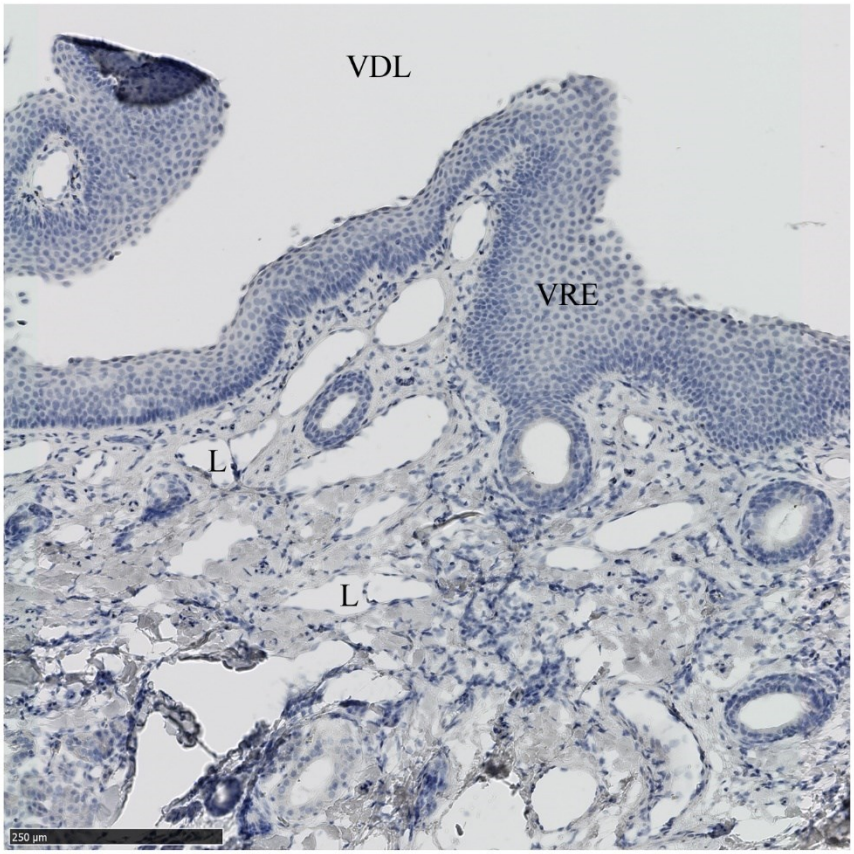

Figure 1.9. Lymphatic vessels in the anterior aspect of an adult mule deer vomeronasal organ haematoxylin. Lymphatic vessels (L) within the lamina propria beneath the vomeronasal respiratory epithelium (VRE) that lines the vomeronasal duct lumen (VDL).

1.8.4 Leg glands

Of the major integumentary exocrine glands of mule deer and, to a lesser extent, white-tailed deer the interdigital glands have the highest densities of leukocytes suggesting that interdigital glands are sites of chronic low-grade inflammation and infection [252, 404]. The interdigital glands of deer feet could, therefore, be expected to be sites of enhanced CWD entry or shedding similar to enhanced prion release in milk by mastitis [173, 175]. Sites of chronic inflammation likely localize prion-trafficking follicular dendritic cells and other immune cells to the sites of glandular inflammation. With respect to origin, centrifugal spread of PrP^{CWD} to the interdigital

glands by immune cells is more appealing than slow intraneuronal transportation from the central nervous system to the most distal aspects of the legs. Innervation of the cervid forefoot interdigital glands likely originates from sympathetic nerves that merge into medial nerve [556] while the nerve supply of the tarsal, metatarsal, and hind interdigital glands join with the sciatic nerves [557]. The fore and hind limb gland sympathetic innervations both reach the intermediolateral cell column via the brachial and sacral plexuses, respectively. PrP^{CWD} localized in the brachial plexus and sciatic nerves of clinical-stage mule deer is sparse to non-existent [180, 519].

Lymphatic drainage of the tarsal, metatarsal, and the interdigital glands of cervids is unknown but can be inferred by the drainage routes in sheep, goats, and cattle. The tarsal, metatarsal, and hind interdigital glands in these species are drained by the popliteal and sublumbar lymph nodes (the tarsal glands of deer may drain directly into the sublumbar lymph nodes) before draining into the lumbar trunk [528, 558-559]. The fore interdigital gland regions drain into either the axillary lymph nodes, then efferently to the venous angle or superficial cervical (prescapular) lymph nodes; or directly to the superficial cervical lymph nodes, and efferently into the jugular trunk and venous angle [528, 559-560].

Following PrP^{CWD} replication in the exposed lymph nodes, typical prion neuroinvasion of the sympathetic fibers that innervate lymph nodes [561-564] would be anticipated for PrP^{CWD} migration to the brainstem via the intermediolateral column of the spinal cord. Connections of the intermediolateral column originate from the pons, hypothalamus, ventral medulla, and medulla caudal raphé [565]. Expected neuronal transport routes of PrP^{CWD} from the leg glands do not overlap with tissues examined in large CWD surveillance programs - the RPLN or DMNV in the medulla obex. CWD lacking RPLN lymphatic accumulation typically manifests

with PrP^{CWD} in the DMNV at the level of the obex – consistent with neuroinvasion from gastrointestinal CWD exposure. An exception is atypical Norwegian moose CWD with PrP^{CWD} deposition in the medulla oblongata, but minimal deposition in the DMNV [69]. One possible route of PrP^{CWD} transport from the legs to the DMNV would require lymphatic transport of PrP^{CWD} to the spleen with subsequent neuroinvasion. Parasympathetic neuroinvasion in the spleen can result in prion accumulation in the DMNV at the level of the obex as seen with intra-splenic prion or viral experimental infections [566-567]. Overall, there is a paucity of evidence to support CWD infection initiation in the legs due to either the intermediolateral column not being examined in most CWD surveillance programs, or due to the extremities not playing a role in naturally acquired CWD pathogenesis.

Rapid centrifugal spread of PrP^{CWD} to lymph nodes in oral exposures complicates inferring whether cervids naturally infected by CWD were exposed by the interdigital glands. PrP^{CWD} was detected in the popliteal and superior cervical lymph nodes as early as 90 days post exposure [179]. Rapid spread of PrP^{CWD} to distant lymph nodes is assumed to result from PrP^{CWD} in the first exposed lymph nodes entering the venous supply [179]. Vertical transmission studies identified PrP^{CWD} within popliteal lymph nodes of elk and white-tailed deer fetal tissues [274-275]. Experimental exposure of cervid leg integumentary glands to CWD will be required to determine the transmission potential of these tissues.

Deer solely infected by CWD exposure of the leg glands would be expected to present with migrating PrP^{CWD} in the intermediolateral column of the spinal cord without vagal, tonsillar, mesenteric, or RPLN involvement. Such early-stage infections may not be detected by typical RPLN and obex-based CWD screening as surveillance programs. CWD histological and ELISA-based testing of the RPLNs and the obex region of the medulla oblongata is the standard method

of CWD surveillance; however, Fennoscandian atypical moose CWD and a minority of naturally infected elk, mule deer, white-tailed deer, and red deer present as RPLN and tonsil negative, but obex positive [69, 71-72, 178, 232, 251, 516]. Animals presenting with PrP^{CWD} in the obex, but not in RPLN or tonsils, typically have IHC staining localized at the DMNV, consistent with splanchnic nerve PrP^{CWD} transport from gastrointestinal CWD exposure. Some or all of the RPLN negative, obex positive CWD cases could still have been exposed orally. Shira's moose experimentally orally exposed to CWD resulted in one of three preclinical moose accumulating PrP^{CWD} in the DMNV, but lacking PrP^{CWD} in the tonsils and lymph nodes [518].

Glandular involvement of CWD uptake in the extremities of elk can be partly excluded due to the absence of tarsal and interdigital glands (**Table 1.2**). Spraker *et al*. found 26% of obex-positive captive elk lacked PrP^{CWD} in the lymphatic tissues and proposed that captive elk fed coarse feed are more likely to have oral abrasions that would facilitate a more direct route of CWD infection [516]. Minor lingual lesions in cervidized mice enhanced susceptibility to oral CWD infection, with PrP^{CWD} accumulation in the obex, but not in non-neuronal tissues [568].

1.8.5 Summary of anticipated exocrine gland PrP^{CWD} trafficking routes

Exposure of exocrine tissues to CWD prions would result in prion trafficking from the tissues to the intermediolateral column of the spinal cord via sympathetic innervations (**Table 1.4**). The intermediolateral column is a known site of PrP^{CWD} accumulation in oral and naturally infected deer [179, 519]. Exposure of any of the described cranial exocrine glands and tissues to CWD prions could result in earlier accumulation of PrP^{CWD} in the RPLN – the most reliable tissue for classical CWD testing and diagnosis. Cervid behaviours that could expose the facial tissues to PrP^{CWD} include allogrooming (section 1.6.2), rubbing and wallowing (section 1.6.4), and vomeronasal-associated urine sampling (section 1.7.4). The most feasible route of leg gland

infection that would result in known PrP^{CWD} deposition patterns is immune cell trafficking of PrP^{CWD} from interdigital glands to the blood and spleen prior to neuroinvasion at the spleen.

1.9. Implications for CWD disease transmission

1.9.1 Conserved behaviours exposing cervids to CWD

Cervid behaviours likely influence CWD transmission and subsequent sex and species-associated disease prevalence rates. Several mechanisms of PrP^{CWD} shedding or exposure are consistent between all of the species discussed (**Figure 1.10** – **Figure 1.13**). All infected cervid species contaminate the environment by shedding PrP^{CWD} in urine, feces, saliva, and nasal secretions. Carcasses and blood also contaminate the landscape. Likewise, all cervids are orally exposed to contaminated soil via geophagy - including consuming soil bound to the roots of vegetation. Males are potentially exposed to PrP^{CWD} during the rut when sampling urine and ingesting urine-soaked dirt. The contribution of CWD spread resulting from transmission between sympatric cervid species is beyond the scope of these models.

1.9.2 Model of CWD transmission in moose

The few cases of CWD in moose and the resulting lack of moose CWD research limits our understanding of how sex affects CWD prevalence and how moose are exposed to PrP^{CWD}. Moose behaviours that could contribute to CWD spread are summarized (**Figure 1.10**). Moose stand out among the cervids of North American with respect to the females frequently interacting with rub sites and wallows made by males [348, 355, 375, 386-388]. Sexually receptive female moose actively sample male urine – unique among North American cervids [389-390]. Both sexes are, therefore, expected to be exposed to male urine in wallows [355, 387]. The sex difference of moose CWD exposure risk by rubbing and wallowing behaviours would be small relative to the other cervids. Interdigital gland involvement in PrP^{CWD} exposure or shedding is

speculative, especially when considering the small group sizes and low population density of moose.

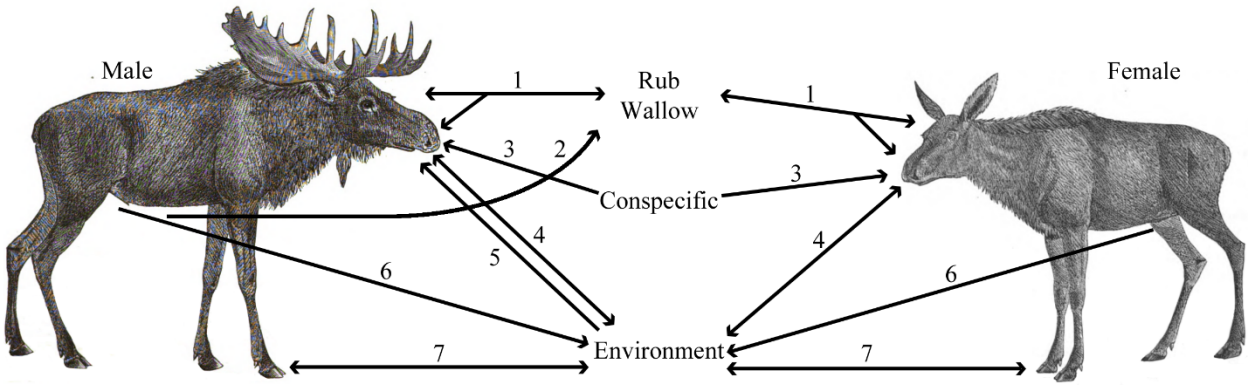

Figure 1.10. Pathway model of moose PrP^{CWD} shedding and exposure. 1) Rub sites and wallows are scent-marked with the facial glands (preorbital and forehead glands if present). Rubs are licked and moose splash themselves with wallow mud. 2) Bulls urinate into wallows. 3) Vomeronasal-associated sampling of urine and investigation of cow genitalia by males and sampling of male urine by estrous females. 4) Geophagy and shedding of CWD infectivity in saliva. 5) Vomeronasal-associated ingestion of urine-soaked dirt. 6) Shedding of infectivity by urination and defecation. 7) Interdigital gland prion shedding and exposure to soil.

1.9.3 Model of CWD transmission in elk

Understanding elk behaviour is likely key for understanding why CWD prevalence rates are generally low in wild elk herds but can be very high rates in captive herds (**Figure 1.11**). Elk males are more likely to interact with rubs and wallows than females; however, the contributions of wallows to CWD transmission is likely minimal due to limited observations of wallows being reused [338, 385]. Conversely, elk females are reported to more frequently groom the faces of conspecifics relative to more aggressive males [338-339]. The lack of interdigital glands in elk may become an important modeling consideration if future experiments determine that the interdigital glands of deer contribute to PrP^{CWD} shedding or exposure.

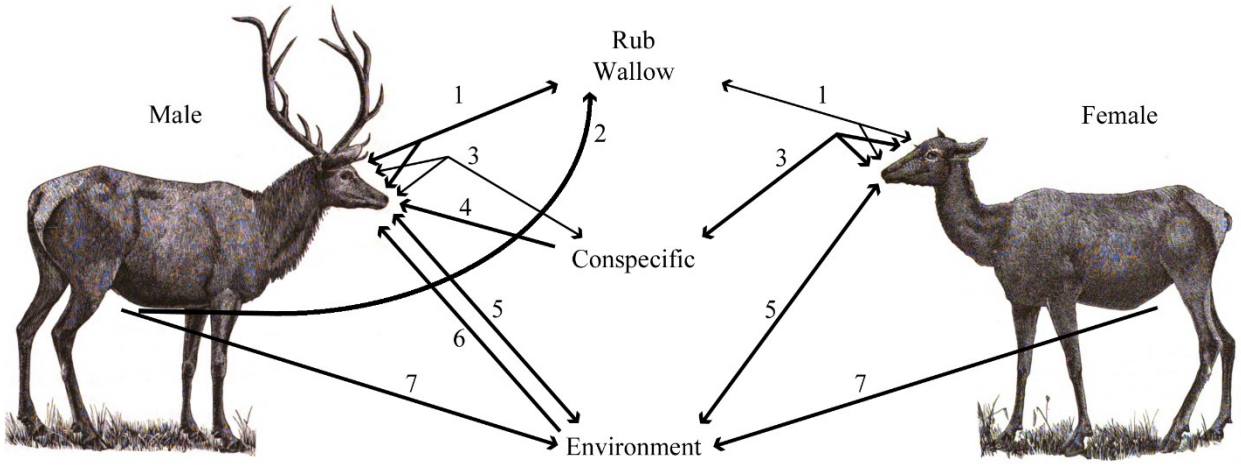

Figure 1.11. Pathway model of elk PrP^{CWD} shedding and exposure. 1) Rub sites and wallows are scent-marked with the facial preorbital glands. Rubs are licked and elk splash themselves with wallow mud. 2) Bulls urinate into wallows. 3) Facial allogrooming. 4) Vomeronasal-associated sampling of urine and investigation of cow genitalia. 5) Geophagy and shedding of CWD infectivity in saliva. 6) Vomeronasal-associated ingestion of urine-soaked dirt. 7) Shedding of infectivity by urination and defecation.

1.9.4 Model of CWD transmission in caribou

Mechanisms of caribou and reindeer PrP^{CWD} exposure and shedding are proposed (**Figure 1.12**). Antler thrashing of vegetation (including reported licking of thrashed vegetation) may facilitate CWD transmission of PrP^{CWD} to and from the oral cavity, nasal cavity, Harderian, and preorbital glands. Male caribou are more likely to antler thrash than females [343], and are, therefore, more at risk to infectious agent exposure by antler thrashing. Osteophagy of cast or existing antlers of conspecifics may contribute to CWD transmission between reindeer [419]. Female reindeer are more likely to gnaw on antlers and have their existing antlers gnawed on [341, 419, 425]. Vomeronasal-associated testing of urine and the ingestion of urine-soaked dirt by males is expected to disproportionately expose the alimentary tract and vomeronasal organ of males to PrP^{CWD}. Reports of males ingesting large amounts of urine-soaked dirt and readily eating plants urinated on by females during the rut is of particular interest [343, 401]. The tendency for reindeer to lick their own interdigital glands could predispose the species to CWD-contaminated

soil oral exposure relative to the other North American cervid species [342]. Frequent interdigital gland licking is not observed in the other cervid species examined. The high density of caribou and reindeer in herds would be expected to amplify the risk of CWD soil-mediated indirect disease transmission.

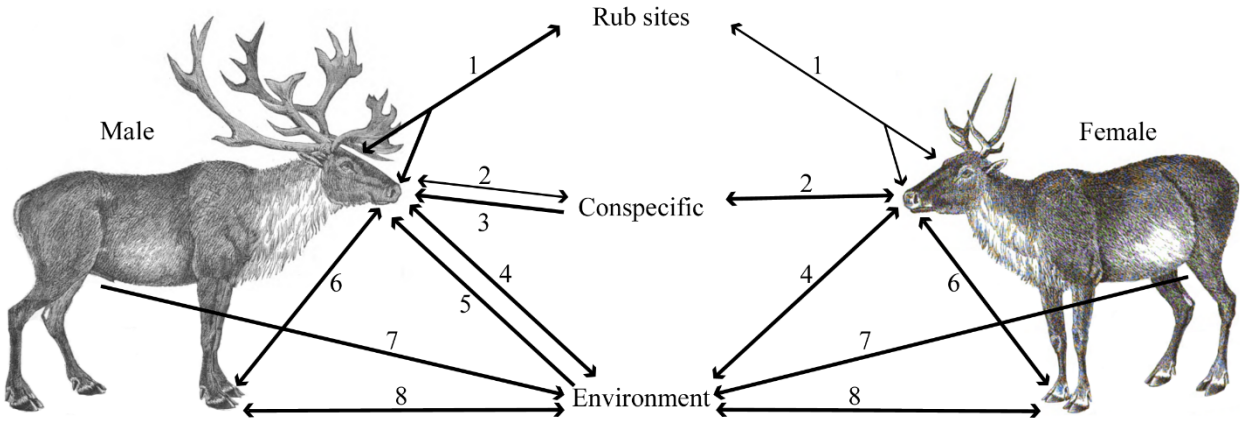

Figure 1.12. Pathway model of caribou and reindeer PrP^{CWD} shedding and exposure. 1) Rub sites scent-marked (bush thrashing) with the facial glands (preorbital and possibly vestibular nasal glands). Rubbed vegetation may be licked. 2) Antler osteophagy. 3) Vomeronasal-associated sampling of urine and investigation of cow genitalia. 4) Geophagy and shedding of CWD infectivity in saliva. 5) Vomeronasal-associated ingestion of urine-soaked dirt. 6) Licking of interdigital glands. 7) Shedding of infectivity by urination and defecation. 8) Interdigital gland prion shedding and exposure.

1.9.5 Model of CWD transmission in Odocoileus sp.

Mule deer and white-tailed deer have the most complex network of behaviours with risks of prion exposure (**Figure 1.13**). Physical interactions with scent-marked scrapes (white-tailed deer only) and rub sites (both species) increases the risk for males more than females. Of the cervids discussed, mule deer and white-tailed deer are also most at risk for direct CWD transmission by facial allogrooming. Wild adult deer allogrooming appears most common between females,

especially between white-tailed deer females [276, 291]. Inspecting and licking rub-urinated tarsal glands of conspecifics - behaviour largely restricted to mule deer and white-tailed deer - could also be a source of orally-obtained horizontal CWD transmission [354, 361, 366,p.66, 460]. Scrapes, uniquely made by white-tailed deer, are potential sites of facial gland exposure, salivary deposition, interdigital gland exposure, and male sampling of urine-soaked dirt [303, 354, 366,p.294].

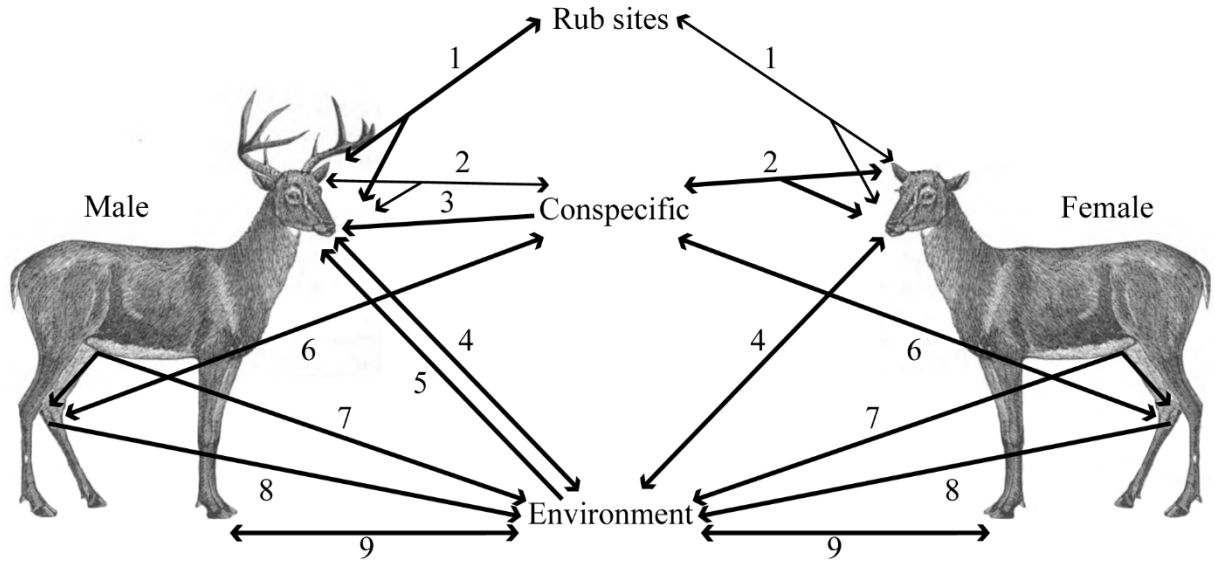

Figure 1.13. Pathway model of mule deer and white-tailed deer PrP^{CWD} shedding and exposure. 1) Rub sites are scent-marked with the facial glands (forehead, preorbital, and possibly vestibular nasal glands) and are licked. 2) Facial allogrooming. 3) Vomeronasal-associated sampling of urine and investigation of doe genitalia. 4) Geophagy and shedding of CWD infectivity in saliva. 5) Vomeronasal-associated ingestion of urine-soaked dirt. 6) Individual recognition involving tarsal gland licking. 7) Shedding of infectivity by urination and defecation. 8) Tarsal-gland associated rub-urination. 9) Interdigital gland prion shedding and exposure.

1.9.6 Implications for understanding CWD transmission

Many behaviours likely contribute to the sex and species-specific CWD prevalence patterns observed in wild cervids. CWD is more prevalent in mule deer, white-tailed deer, and reindeer

males relative to females and is more prevalent in wild mule deer and white-tailed deer relative to the other North American species. Sex-specific behaviours that may contribute to higher male CWD prevalence rates include male-associated scent rubbing, scraping, and flehmen-associated urine sampling behaviours. Many scent gland associated behaviours including scent-rubbing, tarsal gland licking, and allogrooming involve oral exposure. Animal densities, home ranges, group size, group composition, and sex-differences in individual movements between groups are other important factors influencing CWD transmission that interact with the behaviours discussed here. Larger male body size and nutritional requirements also influence contaminated soil, mineral, and vegetation-based exposures to PrP^{CWD}. The insights from the behaviour based PrP^{CWD} exposure models presented here will improve future comprehensive, predictive models of CWD geographical spread with species-specific considerations.

1.10 Remediation of prion-contaminated environments

1.10.1 Challenges facing environmental prion remediation

Remediating CWD- and scrapie-contaminated farms has proven to be a refractory problem. The cost of remediating contaminated farms can be immense and with uncertain outcomes. Past attempts to prevent recurrence of scrapie include disposal of farm tools and equipment and burning existing structures [569]. Repeated applications of sodium hypochlorite to a scrapie-contaminated farm site failed to prevent naïve animal infection - infectious dust being implicated as a possible source of reinfection [570-572].

Mitigating the geographic spread of CWD is a daunting task. Endemic areas span numerous, environments, climates, and soil types (**Figure 1.2**). Policies addressing CWD containment and spread are hampered by public and private lands of multiple countries and jurisdictions being contaminated. Smaller, enclosed research and game farms have and will continue to spearhead attempts to decontaminate prions.

The first serious attempt to remediate CWD-contaminated land was in 1985 at a Colorado research facility [184]. All cervids at the site were euthanized, contaminated paddocks were sprayed with calcium hypochlorite, 30cm of soil removed, and remaining soil treated again with hypochlorite. Possible fomites were removed or cleaned with calcium hypochlorite. Paddocks were left for a year before being repopulated by elk. The decontamination methods failed to prevent CWD infection [184]. A South Korean attempt to eradicate imported CWD by an aggressive protocol involving stripping the top 30cm of soil, multiple 2N sodium hydroxide sprays, and the use of a flamethrower [573]- an expensive and destructive procedure that requires further land reclamation. The results of the South Korean decontamination efforts are pending, but new CWD outbreaks in South Korea have been reported as recently as 2016 [60]. With few exceptions, environments where CWD is endemic are not remediated.

Several methodologies can be employed for assaying the efficacy of environmental prion decontamination. Bioassays with rodents or larger animals provide true biological readouts but are expensive and require long incubation periods [570, 574-575]. Alternatively, prions can be experimentally adsorbed to soils or minerals and exposed to anti-prion compounds followed by detection of remaining prions [576-577]. The prions are typically desorbed from the soils or minerals through heating in detergent-containing buffers, then remaining prions are detected by western blot [51, 576-579]. The desorption-western blot method has a low sensitivity, can be confounded by detection of both desorbed PrP^{C} and PrP^{CWD}, and an inability to distinguish infectious PrP^{CWD} from inactivated, chemically denatured PrP. Protein misfolding cyclic amplification (PMCA) and real-time quake-induced conversion (RT-QuIC) are prion detection methods that can be used on desorbed prions [51, 580-583]. PMCA and RT-QuIC are faster than bioassay and provide ultra-sensitive results, but only indirectly provide lethal dose information

and are subject to inhibition effects by some compounds. A variety of methods have been used to demonstrate soil and mineral inactivation of adsorbed prions using known anti-prion compounds which include hydrochloric acid, LpH®, sodium hydroxide, sodium hypochlorite, and enzymatic mixtures [575-577, 584].

An enzyme-linked immunosorbent assay (ELISA)-based system could be used to assay prion inactivation, but detection by ELISA is less sensitive than PMCA and RT-QuIC. ELISA has been used for assaying relative prion inactivation by enzymes in solution [585], but the use of quantitative ELISA for assaying prion inactivation is lacking. Use of ELISA for prion inactivation assays would be benefited by having standard curve-based calculations of exact prion quantities. I investigated ELISA as a means for quantifying inactivation of adsorbed prions (Chapter 4).

1.10.2 Humic substances as anti-prion compounds

Humic substances are complex organic compounds found in soil organic matter. Humic substances can be divided into three categories of increasing molecular size; fulvic acids, humic acids, and humin [586-587]. The humic substances are formed through the chemical reactions and crosslinking of organic compounds (including carbohydrates, lipids, and peptides) which produce large organic complexes with many chemical moeities [587-591]. Humic substances, including humic acids and fulvic acids, have anti-prion properties that reduces detectable abnormal PrP, by western blot, relative to untreated controls [592-593]. Infectious prion titre is reduced by humic acid as demonstrated by extended incubation periods when challenging hamsters intracranially with humic acid-treated Hyper prions [593] and by transgenic mice expressing elk prion protein intraperitoneally challenged with humic acid-treated CWD [592]. Humic substances have yet to be experimentally tested on prion-contaminated lands but can be

expected to respond differently when the prions are bound to soil and vegetation in contrast to benchtop experimental settings.

1.11 Chronic wasting disease research areas investigated and hypotheses

Cervid skin glands have not been thoroughly investigated for possible involvement in CWD transmission. The only reported investigation into integumentary gland PrP^{CWD} presence of the leg or face was by Spraker *et al*., who observed no PrP^{CWD} by immunohistochemistry in the tarsal glands of free-ranging and captive mule deer with end-stage, naturally acquired CWD [180]. I investigated the hypothesis that white-tailed deer and mule deer integumentary glands express PrP^{C} and that PrP^{CWD} can be found in these tissues. The presence of PrP^{C} in various skin glands and exocrine glands were surveyed and quantified to assess the potential for CWD prion replication in those tissues (Chapter 2). The presence of PrP^{CWD} will be investigated in the tissues with a focus on the interdigital glands (Chapter 3). Finally, methods of quantifying adsorbed prion inactivation using humic acid will be investigated (Chapter 4). I hypothesized that an enzyme-linked immunosorbent assay (ELISA) could be used to quantify PrP^{CWD} inactivation by humic acids. Experimental inactivation of adsorbed prions is intended to simulate environmental prion contamination and set the groundwork for testing soil decontamination by humic acid.

1.12 Chapter Figure acknowledgements

Attribution of Figure 1.6 and Figures 1.10 to Figure 1.13. Cervid illustrations adapted from those of the J. Manz Engraving Company as found in John Caton's The antelope and deer of America, 1877.

Attribution of Figure 1.4 is a derivative of "Scandinavia location map" by NordNordWest, Wikimedia Commons, used under CC BY-SA 3.0.

Chapter 2 Cellular prion protein distribution in cervid integumentary glands

Data in this chapter has been published in Prion as:

Ness, Anthony; Jacob, Aradhana; Saboraki, Kelsey; Otero, Alicia; Gushue, Danielle; Martinez Moreno, Diana; de Peña, Melanie; Tang, Xinli; Aiken, Judd; Lingle, Susan; McKenzie, Debbie (2022). Cellular prion protein distribution in the vomeronasal organ, parotid, and scent glands of white-tailed deer and mule deer.

Prion. 2022;16(1):40-47.

2.1 Abstract

Chronic wasting disease (CWD) is a contagious and fatal transmissible spongiform encephalopathy affecting species of the cervidae family. CWD has an expanding geographic range and complex, poorly understood transmission mechanics. CWD transmission has been hypothesized to be related to animal behaviours that involve deer facial and body exocrine glands. Understanding CWD transmission potential requires a foundational knowledge of the cellular prion protein (PrP^C) in glands associated with cervid behaviours. In this study, we characterized the presence and distribution of PrP^C in 6 integumentary and 2 non-integumentary tissues of hunter-harvested mule deer (*Odocoileus hemionus*) and white-tailed deer (*O. virginianus*). We report that white-tailed deer expressed significantly more PrP^C than their mule deer in the parotid, metatarsal, and interdigital glands. Mule deer and white-tailed deer females expressed more PrP^C than males in the forehead and preorbital glands. The distribution of PrP^C within the integumentary exocrine glands of the face and legs were localized to glandular cells, hair follicles, epidermis, and immune cell infiltrates. All tissues examined expressed sufficient quantities of PrP^C to serve as possible sites of prion initial infection, propagation, and shedding.

2.2 Introduction

Chronic wasting disease (CWD) is a contagious prion disease of free-ranging and captive species of the Cervidae family including mule deer (*Odocoileus hemionus*), white-tailed deer (*Odocoileus virginianus*), Rocky Mountain elk (*Cervus elaphus nelsoni*), reindeer/caribou (*Rangifer tarandus*), and moose (*Alces alces*). CWD, like all prion diseases, is characterized by a long preclinical period followed by a rapid clinical onset and decline leading to death. In a CWD-infected individual infectious prions convert healthy cellular prion protein (PrP^C) into the

CWD-associated isoform (PrP^{CWD}) through a protein template misfolding mechanism [16-17]. Throughout the course of disease, prions propagate in infected cervids and are shed via body fluids and excreta including saliva, feces, and urine [38-41, 44-45, 594]. Although cervids can acquire infectious prions through direct or indirect contact [45-46], the specific mechanisms underlying the transmission of CWD prions in wild and captive populations remains poorly understood. The most accepted route of indirect CWD exposure is the oral-nasal uptake of PrP^{CWD} from environmental fomites including soil particles, vegetation, and salt licks [46-51]. Oral-nasal CWD transmission mechanisms are, however, inadequate for explaining remarkably disproportionate disease prevalence patterns in wild cervid populations whereby males and mule deer are more likely to be infected by CWD than females and white-tailed deer [190-191, 193-194, 197, 595].

Glandular tissues offer an alternative route of CWD transmission that has not been characterized. Cervids have numerous integumentary scent glands on their face and legs [252, 270-272]. Cervid exocrine gland secretory tubules and acini are possible sources of PrP^{CWD} shedding and possible entry points for PrP^{CWD} during direct or indirect pathogen exposure. Integumentary glands are well innervated by the autonomic nervous system including the sympathetic nervous system. These innervations offer possible sites of neuroinvasion by PrP^{CWD}. Similarly, integumentary exocrine glands are points of entry for many pathogens [252-255]. Secondary to neuroinvasion at the glands, immune cells may traffic PrP^{CWD} from glands to secondary lymphatic structures for later neuroinvasion. PrP^{CWD} in salivary glands of CWD infected deer [41, 243], and high levels of PrP^{C} in mammary glands of healthy animals [259] suggest that PrP^{C} and the capacity for conversion into PrP^{CWD} will be high in other integumentary exocrine glands. The parotid gland (and its associated lymph nodes) has been widely investigated for CWD involvement [41, 49,

179-180, 232, 260-262]. The immediate proximity to the oral cavity makes the parotid gland and its paraglandular lymph nodes [527] likely to contact orally ingested PrP^{CWD} and the gland is an intuitive source of CWD infectivity in saliva. Other peripheral cervid glands have been largely neglected in CWD distribution studies. The only reported investigation into integumentary gland PrP^{CWD} presence of the leg or face was by Spraker *et al*., who observed no PrP^{CWD} by immunohistochemistry in the tarsal glands of free-ranging and captive mule deer with end-stage, naturally acquired CWD [180]. A broad range of common deer behaviours, including grooming, sparring, courtship, and dominance interactions bring animals in direct contact with exocrine glands or indirect contact with glandular secretions deposited in the environment [354]. These behaviours also involve contact with known sources of infectious prions (e.g., urine and saliva) and are hypothesized to contribute to CWD transmission and to the increased prevalence of CWD in mule deer and in males of wild populations [193, 220, 229, 276]. If exocrine glands play a role in CWD infection, our understanding of the body sites that serve as routes of infection, and the behavioural contexts in which CWD transmission occurs, may change dramatically.

Scent-marking is one form of indirect contact that may contribute to the sex bias in CWD prevalence [193, 220, 359]. Male white-tailed deer interact with scrapes - scent signposts made by bucks involving pawing the ground and interacting with nearby vegetating - more frequently than does [359], and male mule deer and white-tailed deer, but not females, engage in high levels of advertisement activities including nasal-oral marking, antler thrashing, and scrapes [276] support scent marking as a contributor to sex biased CWD prevalence. Kinsell (2010) further proposed a risk model of CWD prion shedding and exposure via the preorbital, forehead, tarsal, and interdigital glands associated with deer marking and scraping behaviours [359]. As yet,

biochemical characterization to support CWD involvement with exocrine glands is lacking. In this study, we describe the presence and distribution of PrP^{C} within integumentary exocrine glands of mule deer and white-tailed deer to assess the potential for PrP^{CWD} uptake or shedding from these glands and to determine whether sex and species differences in PrP^{C} in these glands correspond to the sex and species skew in CWD prevalence.

2.3 Methods

2.3.1 Tissue collection

Mule deer and white-tailed deer were harvested by hunters on the Canadian Forces Base (CFB) Wainwright in southeastern Alberta, Canada, between November 30, 2017 and December 13, 2017. For this analysis, we collected samples from 15 mule deer (8 male, 7 female), and 16 white-tailed deer (8 of each sex). All animals were ≥1.5 years of age, with a similar distribution in body and antler size (for males) of the two species. More accurate age estimation by cementum annuli analysis was not available. Glandular tissues were extracted at the time the deer were brought to the hunter-check station, 1.3 to 10.1 hours after the animal was killed. Samples for biochemical analysis were selected based on the shorter time between animal death and sampling. Ambient temperature during tissue collection ranged from -10°C to 4°C. Samples were frozen for later biochemical analysis or formalin-fixed for histology.

The non-integumentary glandular tissue collected included the parotid gland and the anterior portion of the vomeronasal organ. The integumentary glands collected included the facial forehead, preorbital, lateral vestibular nasal glands, and the leg tarsal, metatarsal, and hind interdigital glands (**Figure 2.1**).

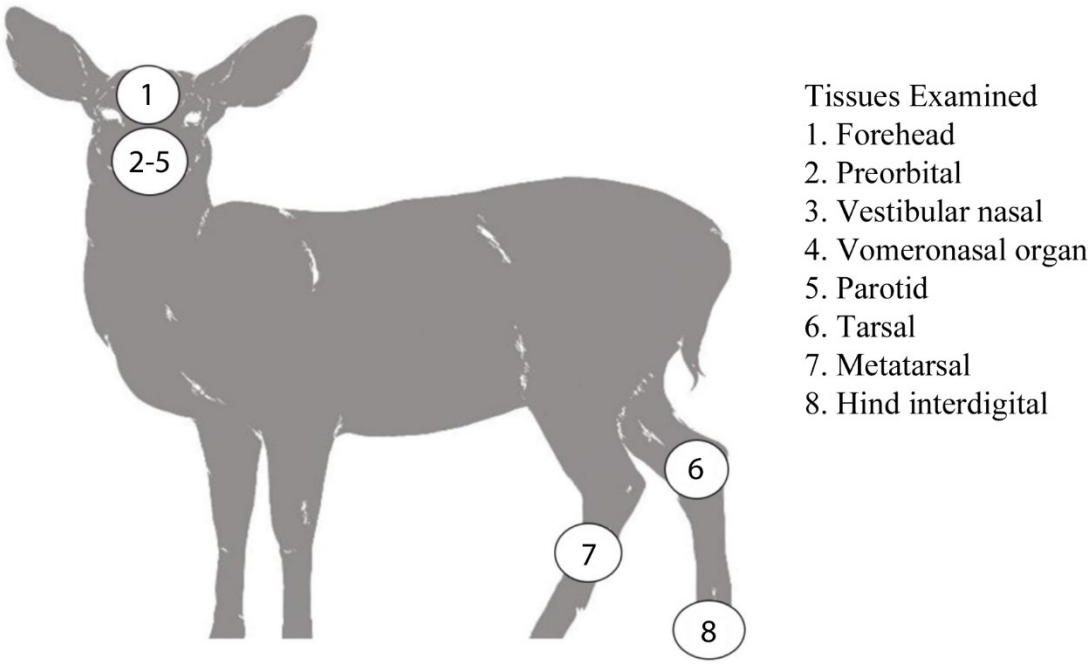

Figure 2.1. Scent glands and non-integumentary tissues sampled from mule deer and white-tailed deer from CFB Wainwright, Alberta.

2.3.2 Tissue homogenization and protein content determination

Glandular tissues were trimmed of non-glandular tissue, fat, hair, and secretory exudate, weighed, minced, then homogenized in RIPA lysis buffer (50mM Tris, 150mM NaCl, 1% IGEPAL CA-630, 0.25% deoxycholate, 1mM EDTA, pH 7.4) supplemented with cOmplete™ EDTA-Free Protease Inhibitor Cocktail (Roche Diagnostics GmbH, Switzerland). Samples were mechanically homogenized in a Bead Ruptor 24 (Omni International, USA) bead mill homogenizer in the presence of a cold air flow supplied by an OMNI BR-Cryo cooling unit to minimize heat-denaturation. Tissues were subjected to 25 minutes of high-energy ceramic bead milling-assisted agitation cycles of 10 second intervals of milling followed by 15 seconds of cooling. Homogenate supernatants were collected following a brief microcentrifugation to yield clarified 10% (w/v) homogenates for biochemical analysis. Total protein content of clarified 10% (w/v) gland homogenates was determined using a Pierce™ BCA Protein Assay Kit

(Thermo Fisher Scientific, USA). Homogenate protein concentrations were compared by non-repeated-measures two-way ANOVA with GraphPad Prism software (GraphPad Software, USA).

2.3.3 Western blot analysis

Visualization of cellular prion protein by western blot under denaturing conditions required atypical conditions to prevent aberrant protein separation. Samples were denatured for 15 minutes at 100°C having first been mixed one part 10% clarified gland homogenate, one part water, and two parts 5x Laemmli buffer. Samples (7.5µL per well) were loaded into 15-well Invitrogen NuPAGE™ 12% Bis-Tris gels (Thermo Fisher Scientific, USA). Gels were run slowly at 70V for 5 hours in MOPS (3-(N-Morpholino)propane sulfonic acid) buffer. Proteins were transferred onto Immobilon®-FL (MilliporeSigma, USA) PVDF (polyvinylidene fluoride) membranes at 35V for 1.5 hours followed by blocking with 2% (w/v) bovine serum albumin in phosphate buffered saline (130mM NaCl, 7mM $Na_2HPO_4 \cdot 7H_2O$, 3mM $NaH_2PO_4 \cdot 1H_2O$, pH 7.4). PrP^C was probed with the mouse IgG_1 anti-prion protein SHA31 monoclonal primary antibody (1:10,000) (Cayman Chemical, USA) which binds to an epitope of 148-155 (*Odocoileus* amino acid sequence). Secondary goat anti-mouse IgG (H+L) AP Conjugate (Promega Corporation, USA) detection antibody (1:10,000) was enzymatically developed with AttoPhos® AP Fluorescent Substrate System (Promega Corporation, USA). Membrane fluorescent imaging was performed using an ImageQuant LAS 4000 (GE Life Sciences, USA) system.

Relative protein abundance was compared using pixel intensity analysis with ImageJ software. A box enclosing individual western blot lane regions of interest (ROI) ranging from the unglycosylated PrP fragments to the diglycosylated forms of PrP^C recognized by the anti-PrP SHA31 antibody (14-37KDa) were used to determine average pixel intensity. Average western

blot background-adjusted pixel intensity was compared using Mann-Whitney tests (* $p < 0.05$, ** $p < 0.01$, *** $p < 0.001$).

2.3.4 Capillary electrophoresis immunoassay

Unless otherwise stated, all reagents for capillary electrophoresis immunoassays were purchased from Protein Simple (Bio-Techne Corporation, USA). Capillary Western assay analysis was used to compare PrP^C in protein concentration-adjusted samples. Clarified 10% (w/v) gland homogenates and 1% white-tailed deer whole brain homogenate controls were adjusted with capillary assay diluent and master mix to a final protein concentration of 1.5µg/µL for capillary electrophoresis. PrP^C was detected with SHA31 primary antibody (1:10,000) and Protein Simple anti-mouse secondary antibody were consistent with that described in Castle, *et al*., 2018 [596]. Samples were loaded into 12-230 kDa 25-capillary cartridges for automated separation and chemiluminescent imaging in a Protein Simple Wes™ machine (Bio-Techne Corporation, USA). Analysis was performed with the associated Compass for Simple Western software. Baseline-fit corrected peak areas (as determined by the perpendicular drop method) corresponding with expected PrP^C molecular weights were compared between deer species and sex by two-way ANOVA with additional comparison of sex and species by Bonferroni post-hoc tests for tissues with significant interaction effects.

2.3.5 Enzyme-linked immunosorbent assay

The concentration of PrP^C in 10% (w/v) clarified gland homogenates was quantified by sandwich enzyme-linked immunosorbent assay (ELISA). Anti-PrP SHA31 (*Odocoileus* sequence epitope of amino acids 148-155, YEDRYYRE) capture antibody (1:5,000) and horseradish peroxidase-conjugated N5 (*Odocoileus* sequence epitope of amino acids 101-104, QWNK) detection antibodies (1:5,000) were used in custom sandwich ELISA. Recombinant wild-type sequence

full-length deer prion protein was used for quantitative standardization (courtesy of Dr. Leonardo Cortez (University of Alberta)). Capture antibody was coated onto high-binding polystyrene strip plates (Greiner Bio-One International, Austria) with 50mM carbonate-bicarbonate (pH 9.6) buffer. Clarified gland homogenate (25µL) was diluted into 75µL of phosphate buffered saline in the ELISA plates, in triplicate. White-tailed deer whole-brain homogenate (1% w/v) was used for comparison. Recombinant deer PrP and brain homogenate controls were diluted to final concentrations of 25% RIPA lysis buffer to match gland samples. Plates were developed with TMB (3,3',5,5'-tetramethylbenzidine) One Component HRP (horseradish peroxidase) Microwell Substrate (Surmodics, Inc., USA) chromogen and scanned at 650nm and, following addition of 2N sulfuric acid stop solution to be scanned at 450nm. Quantified gland homogenate concentrations of PrP^C variants detectable by the SHA31-N5 sandwich combination were compared between deer species and sex by two-way ANOVA with additional comparison of sex and species by Bonferroni post-hoc tests for tissues with significant interaction effects.

2.3.6 Histology and immunohistochemical detection of the cellular prion protein in gland tissues

Formalin-fixed glands were trimmed and embedded in paraffin. 4µm thick sections were cut, using a microtome, and mounted on glass slides. Sections were stained using hematoxylin and eosin (H&E) to identify the histological structures of the glands. Immunohistochemical labeling for the detection of cellular prion protein (PrP^C) was performed similarly to that previously described [597]. Briefly, tissue sections were deparaffinized and dehydrated by immersion in xylene and decreasing concentrations of ethanol (100%, 95% and 70%). Epitope retrieval was performed by hydrated autoclaving at 121°C in citrate buffer (pH 6) for 5 minutes. Endogenous peroxidase was blocked using a 3% hydrogen peroxide solution for 12 minutes. Sections were exposed to 5% goat serum for 1 hour to block non-specific sites followed by 15 minutes of

blocking with avidin and biotin (Vector Laboratories, USA), respectively. Immunodetection was completed by incubating the samples with the monoclonal antibody BAR224 (1:50; Cayman Chemical, USA) overnight at 4°C followed by 1 hour of incubation with Immun-Star anti-mouse HRP secondary antibody (1:250) (Bio-Rad, USA). SHA31 is not suitable for immunohistochemistry. DAB (3,3′-Diaminobenzidine) (MilliporeSigma, USA) was used as the HRP chromogen substrate. After counterstaining with hematoxylin, sections were mounted with DPX (distyrene, plasticizer, xylene) mounting medium (MilliporeSigma, USA). Control slides in which incubation with the primary antibody was omitted were used for specificity controls. Slides were scanned with a NanoZoomer 2.ORS (Hamamatsu Photonics K.K., Japan) and the images analyzed with the manufacturer's NDP.view2 software. For each tissue examined by immunohistochemistry, 6 deer of each species were used (3 of each sex).

2.4 Results

2.4.1 Integumentary gland sample gross examination

Species- and sex-dependent gross morphological differences of the glands were consistent with historical descriptions. Male forehead gland dermal and epidermal layers were thicker than those of female white-tailed deer [272]. Sampled male mule deer also had thicker forehead glandular tissue than females. Mule deer metatarsal glands are considerably larger than those of white-tailed deer [271, 405, 598]. The interdigital glands of white-tailed deer possessed more externalized ceraceous secreta than mule deer - consistent with historical observations [271]. The preorbital gland sacs of mule deer were larger than white-tailed deer [430, 598]. We observed more ceraceous accumulations in mule deer preorbital sacs relative to white-tailed deer. The anal and preputial glands were not collected as they were damaged or destroyed during hunter field dressing.

2.4.2 Clarified gland homogenate total protein concentration:

Total protein concentration of clarified 10% (w/v) mule deer and white-tailed deer gland homogenates was generally consistent between species and sex for individual glands (**Figure 2.2**, **Table 2.1**). Gland homogenate total protein concentration was not significantly influenced by species or sex in 4 of 7 glands - the preorbital, vestibular nasal, tarsal, and metatarsal glands - and the vomeronasal organ. Total protein content was significantly higher in the female forehead and parotid glands relative to males. Protein concentration was higher in white-tailed deer parotid gland homogenates while mule deer interdigital glands yielded higher protein concentrations. The average total protein concentrations of clarified 10% (w/v) homogenates from the integumentary glands and the vomeronasal organ of both deer species ranged from 3.09µg/µL to 5.86µg/µL. The parotid gland homogenate protein content was notably higher than other glands examined with an average protein concentration of 9.76µg/µL in mule deer and 10.85µg/µL in white-tailed deer. Reference control 10% (w/v) white-tailed deer whole brain homogenate (not clarified) total protein concentration averaged 9.64µg/µL.

Table 2.1. Mean total protein concentration and 95% confidence intervals of deer clarified 10% (w/v) gland homogenates as determined by standard bicinchoninic acid assay.

Exocrine Tissue	Total Protein Concentration (µg/µL)						2-Way ANOVA P Values		
	Mule Deer			White-tailed Deer					
		Male	Female		Male	Female	Interaction	Species	Sex
Vomeronasal	3.89 ± 0.40 n=13	4.26 ± 0.66 n=7	3.47 ± 0.80 n=6	4.01 ± 0.52 n=12	3.96 ± 1.20 n=6	4.07 ± 0.41 n=6	0.2306 n.s.	0.0779 n.s.	0.0842 n.s.
Parotid	9.76 ± 0.93 n=12	8.94 ± 1.72 n=6	10.59 ± 0.68 n=6	10.85 ± 0.90 n=12	10.12 ± 1.56 n=6	11.59 ± 0.99 n=6	0.8586 n.s.	0.0443 *	0.0062 **
Forehead	3.90 ± 0.38 n=11	3.86 ± 0.68 n=5	3.93 ± 0.48 n=6	3.96 ± 0.44 n=11	3.66 ± 0.50 n=6	4.33 ± 0.88 n=5	0.7899 n.s.	0.5734 n.s.	0.0200 *
Preorbital	3.54 ± 0.47 n=12	3.93 ± 0.35 n=6	3.15 ± 0.89 n=6	3.23 ± 0.43 n=12	3.3 ± 0.71 n=6	3.16 ± 0.76 n=6	0.2519 n.s.	0.2735 n.s.	0.1124 n.s.
Nasal	4.22 ± 0.37 n=12	4.30 ± 0.55 n=6	4.15 ± 0.72 n=6	4.51 ± 0.21 n=12	4.35 ± 0.29 n=6	4.67 ± 0.34 n=6	0.2417 n.s.	0.1599 n.s.	0.6666 n.s.
Tarsal	3.09 ± 0.41 n=12	3.01 ± 0.68 n=6	3.17 ± 0.74 n=6	3.26 ± 0.58 n=13	3.17 ± 0.90 n=7	3.38 ± 1.06 n=6	0.9484 n.s.	0.5943 n.s.	0.5948 n.s.
Metatarsal	4.17 ± 0.58 n=11	4.36 ± 1.45 n=5	4.01 ± 0.60 n=6	4.56 ± 0.60 n=12	4.34 ± 0.90 n=6	4.77 ± 1.13 n=6	0.3241 n.s.	0.3535 n.s.	0.9300 n.s.
Interdigital	5.86 ± 1.14 n=12	5.25 ± 1.38 n=6	6.47 ± 2.19 n=6	3.35 ± 0.52 n=13	3.62 ± 0.53 n=7	3.02 ± 1.14 n=6	0.1078 n.s.	0.0001 ***	0.5724 n.s.

2-way ANOVA significance indicators: n.s. $p \geq 0.05$, * $p < 0.05$, ** $p < 0.01$, *** $p < 0.001$

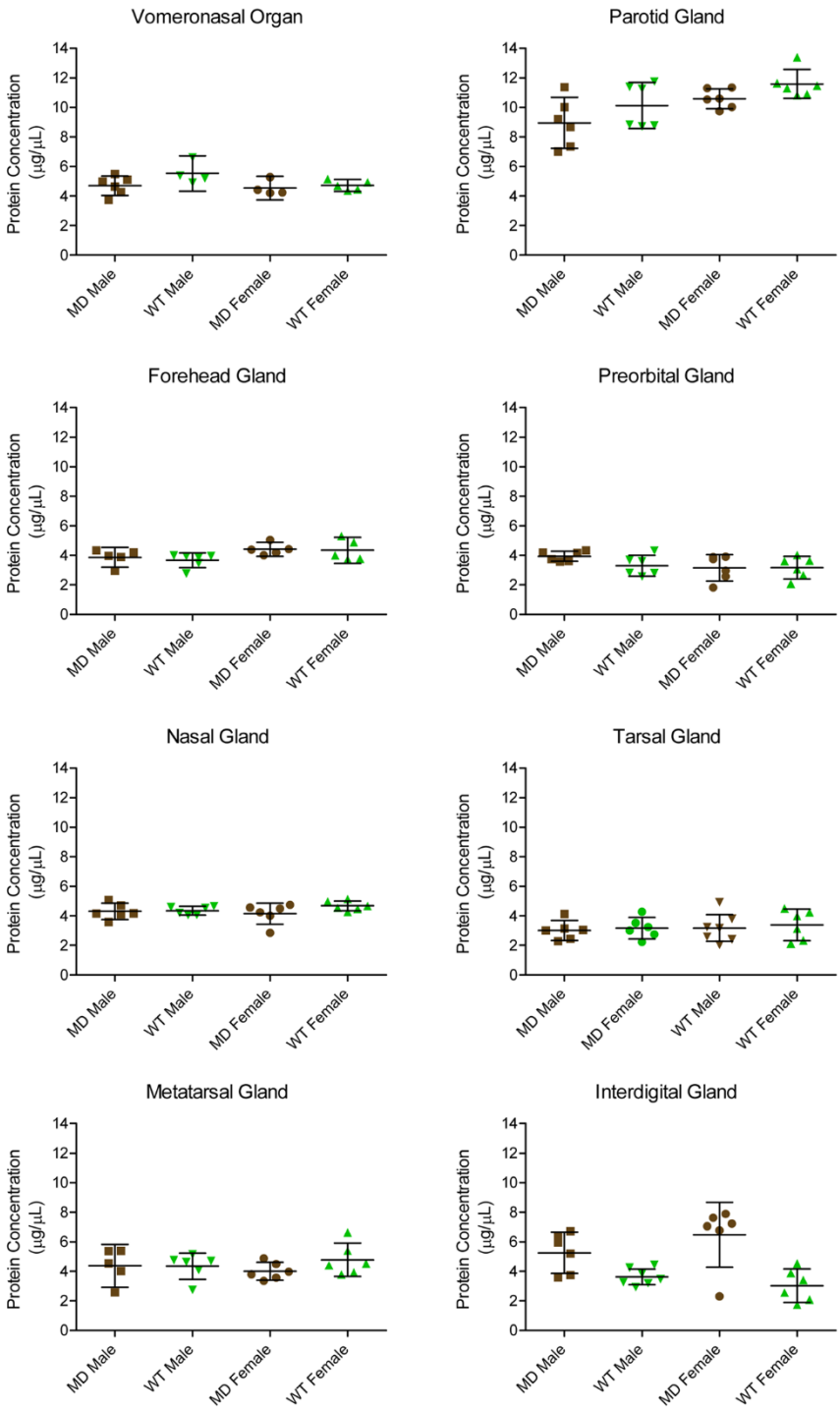

Figure 2.2. Clarified gland homogenate protein concentrations. Total protein concentrations (µg/µL), mean, and 95% confidence intervals of clarified 10% (w/v) deer gland homogenates prepared in RIPA buffer as determined by standard bicinchoninic acid assay. Individual mule deer (MD) and white-tailed deer (WT) homogenate samples were assayed in triplicate.

2.4.3 Western blot analysis of PrP^C expression in exocrine glands

Relative PrP^C protein expression in uninfected deer was detected, by western blot, in all exocrine glands examined (**Figure 2.3** – **Figure 2.5**). Male and female PrP^C expression was compared for each species. 10% (w/v) gland homogenate (not adjusted for total protein content) PrP^C detected with anti-PrP SHA31 antibody was comparable to 0.5-1% white-tailed deer whole-brain homogenates (**Figure 2.6** – **Figure 2.8**). Broadly, facial and leg gland homogenates express at least 10-fold less PrP^C than 10% brain homogenates. Glycosylation patterns of PrP^C varied between glands and were distinguishably different from brain homogenate-derived PrP^C (**Figure 2.3** – **Figure 2.5**). Among a representative panel of deer (4-6 deer of each sex), female deer of both species expressed significantly more PrP^C than their male counterparts in the forehead and preorbital integumentary glands as determined by pixel intensity analysis (**Figure 2.7**).

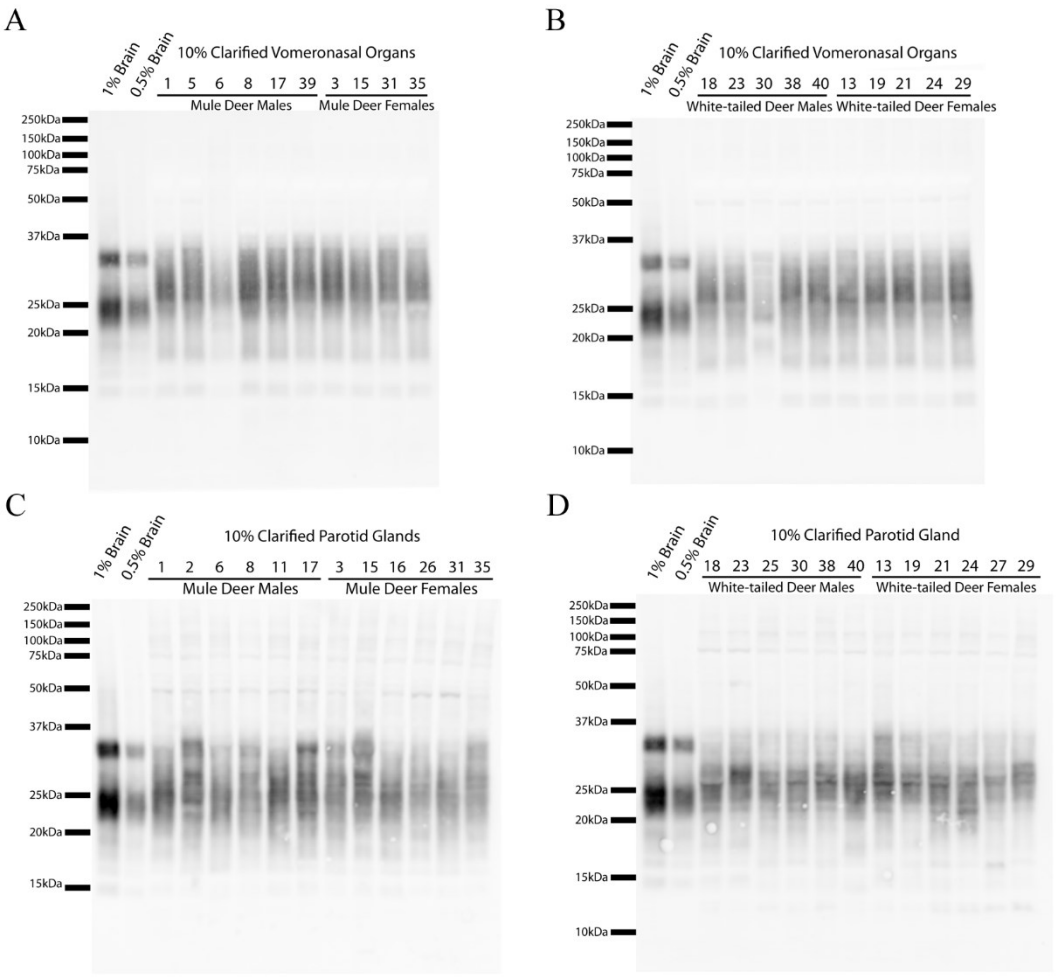

Figure 2.3. Immunodetection of PrP^C expression in non-integumentary cranial exocrine clarified 10% (w/v) gland homogenates of mule deer (A, C) and white-tailed deer (B, D). Vomeronasal organs (A-B) and parotid glands (C-D) were compared with unclarified white-tailed deer whole brain homogenate. Membranes were probed with 1:10,000 anti-PrP SHA31.

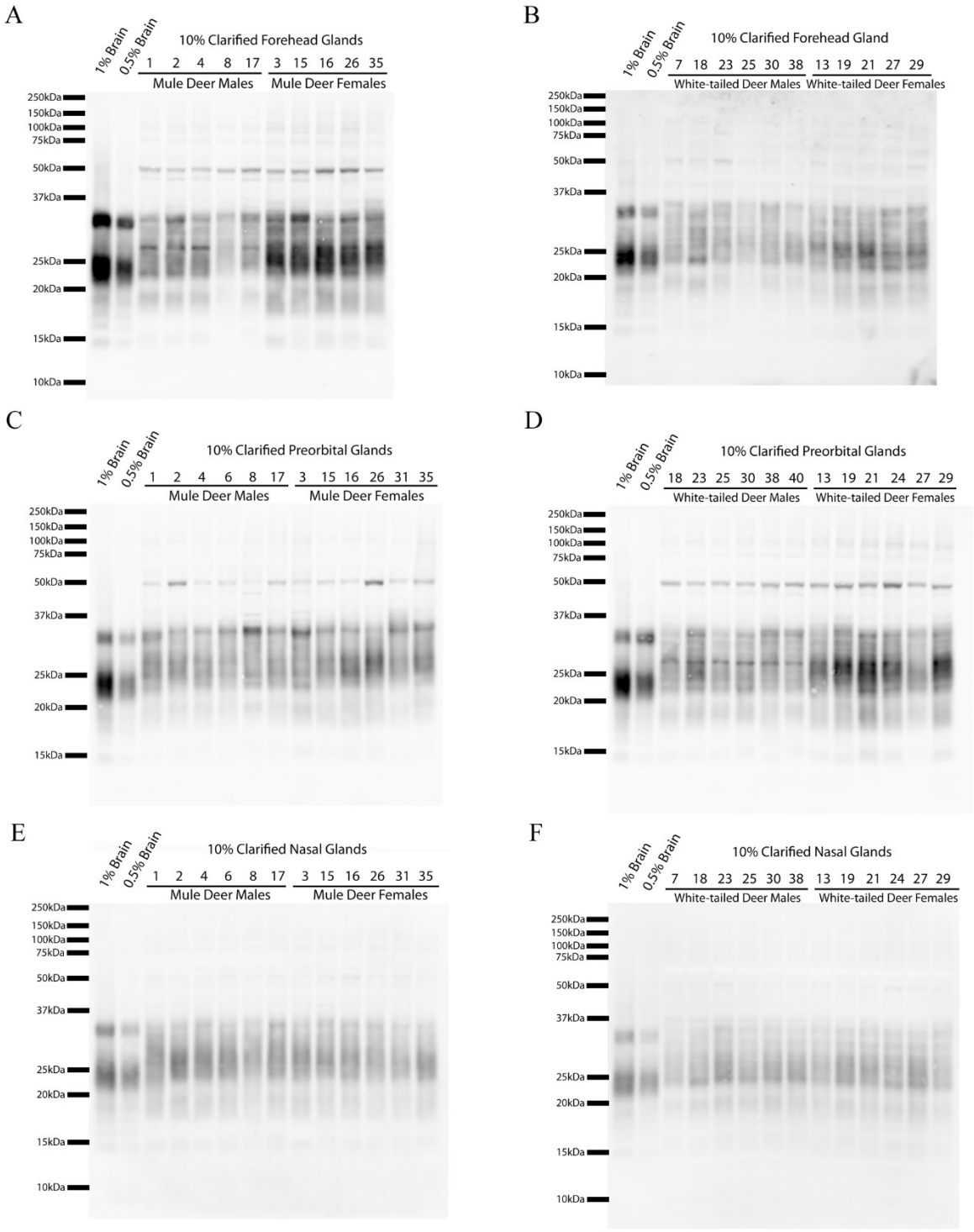

Figure 2.4. Immunodetection of PrP^C expression in facial integumentary clarified 10% (w/v) gland homogenates of mule deer (A, C, E) and white-tailed deer (B, D, F). Forehead (A-B) and preorbital (C-D), and nasal (E-F) glands were compared with unclarified white-tailed deer whole brain homogenate. Membranes were probed with 1:10,000 anti-PrP SHA31.

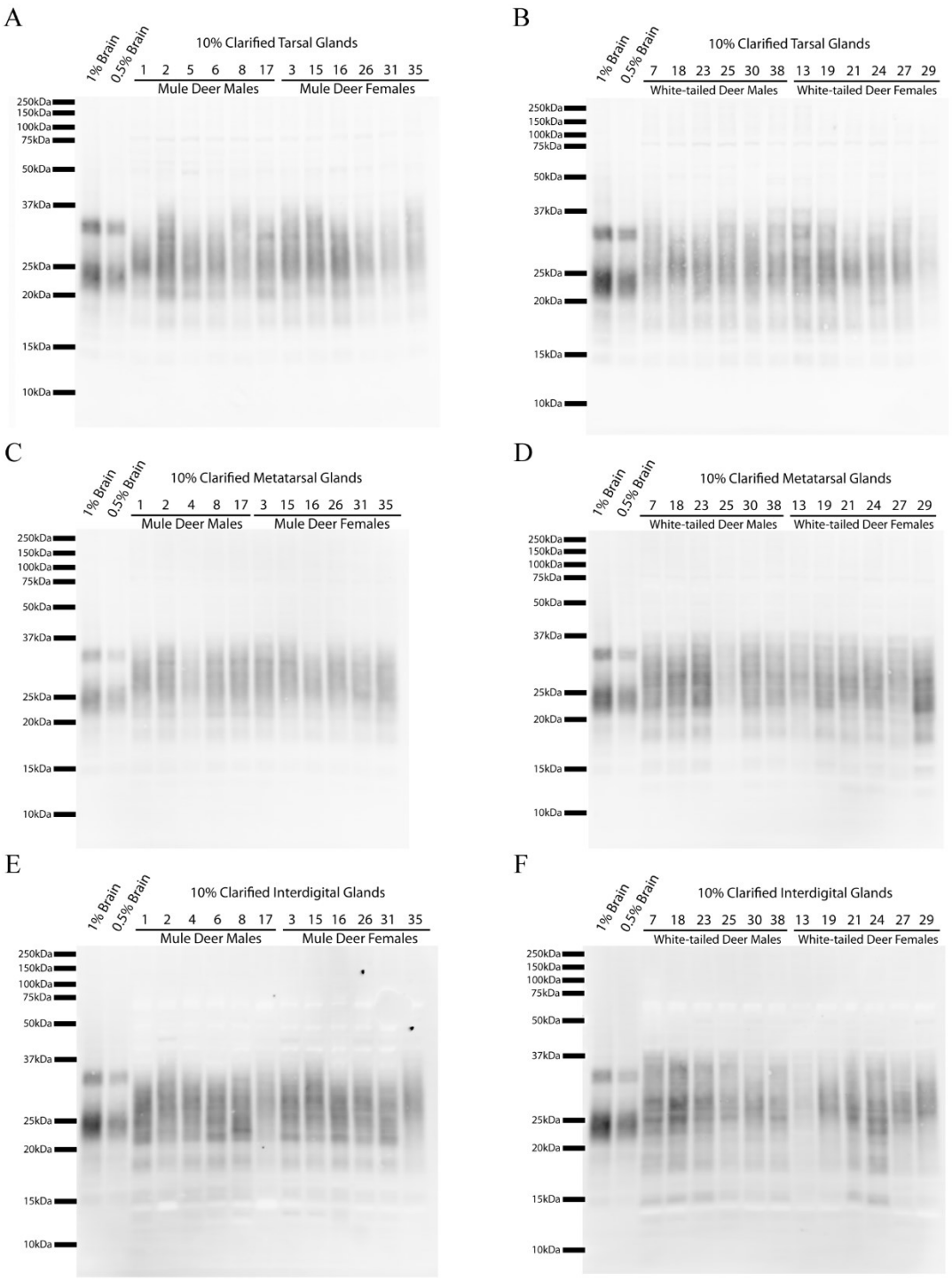

Figure 2.5. Immunodetection of PrP^C expression in leg integumentary clarified 10% (w/v) gland homogenates of mule deer (A, C, D) and white-tailed deer (B, D, F). Tarsal (A-B), metatarsal (C-D), and interdigital (E-F) glands were compared with unclarified white-tailed deer whole brain homogenate. Membranes were probed with 1:10,000 anti-PrP SHA31.

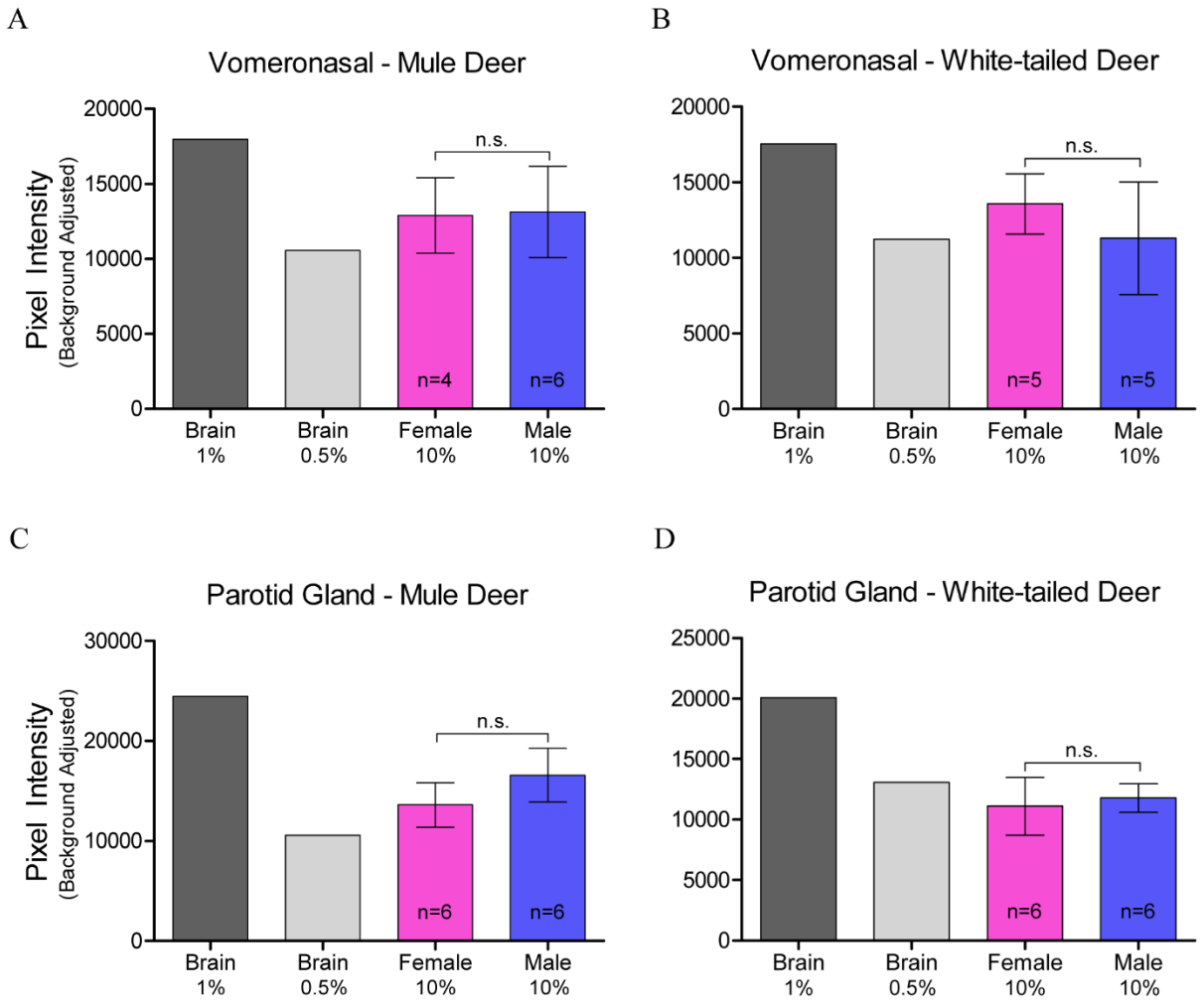

Figure 2.6. Relative pixel intensity analysis of PrP^C expression in non-integumentary cranial exocrine clarified 10% (w/v) gland homogenates of mule deer (A, C) and white-tailed deer (B, D). Background-adjusted average pixel intensities of PrP^C bands of the vomeronasal organs (A-B) and parotid glands (C-D) as detected by anti-PrP SHA31 were compared. Unclarified white-tailed deer whole brain homogenate was used for reference. Sample size, mean, 95% confidence intervals, and significance by Mann-Whitney tests are shown.

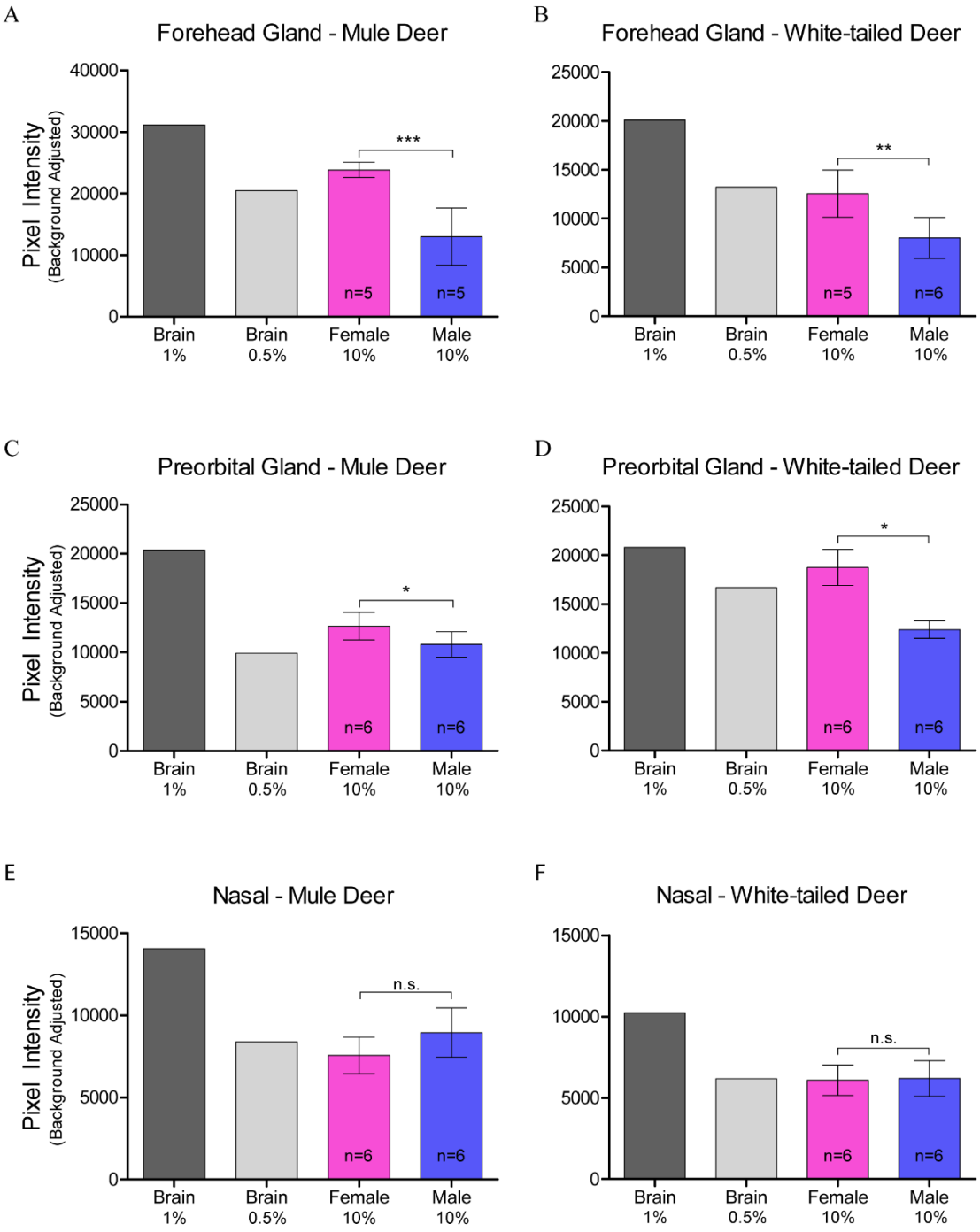

Figure 2.7. Relative pixel intensity analysis of PrP^C expression in facial integumentary clarified 10% (w/v) gland homogenates of mule deer (A, C, E) and white-tailed deer (B, D, F). Background-adjusted average pixel intensities of PrP^C bands of forehead (A-B), preorbital (C-D), and vestibular nasal glands as detected by anti-PrP SHA31 were compared. Unclarified white-tailed deer whole brain homogenate was used for reference. Sample size, mean, 95% confidence intervals, and significance by Mann-Whitney tests are shown.

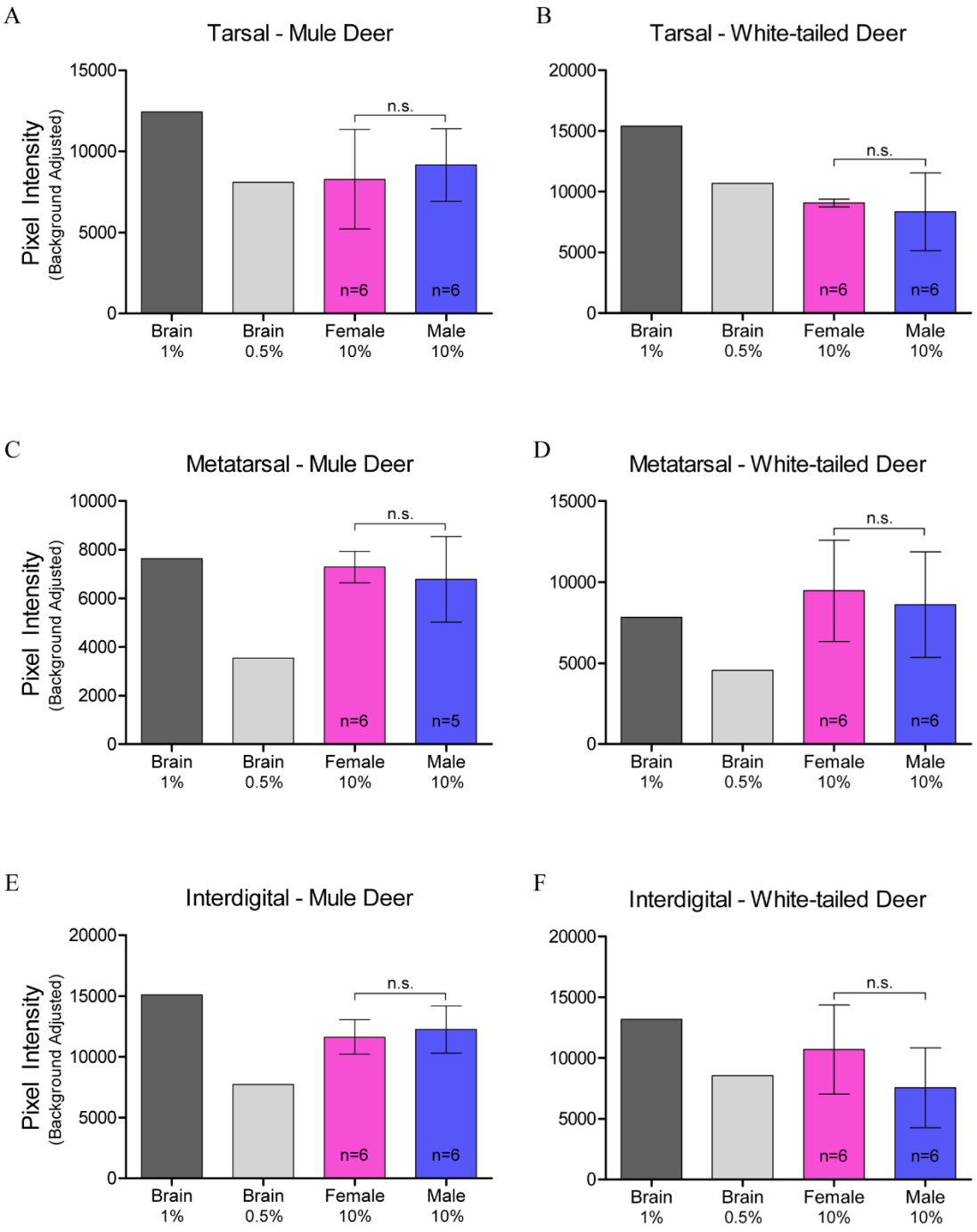

Figure 2.8. Relative pixel intensity analysis of PrP^C expression in leg integumentary clarified 10% (w/v) gland homogenates of mule deer (A, C, D) and white-tailed deer (B, D, F). Background-adjusted average pixel intensities of PrP^C bands of tarsal (A-B), metatarsal (C-D), and interdigital (E-F) glands as detected by anti-PrP SHA31 were compared. Unclarified white-tailed deer whole brain homogenate was used for reference. Sample size, mean, 95% confidence intervals, and significance by Mann-Whitney tests are shown.

2.4.4 Protein-adjusted PrP^C expression examined by capillary electrophoresis immunoassay

Sample homogenates were not adjusted for protein concentration for the western blot analysis. Capillary electrophoresis immunoassay, using the anti-PrP SHA31 antibody, allowed for comparison of PrP^C protein expression between deer species and sex using total protein concentration-adjusted samples from clarified 10% (w/v) gland homogenates (**Figure 2.9** – **Figure 2.11**, **Table 2.2**). Sex significantly influenced PrP^C expression in the forehead gland with expression higher in females than males. When the species was influential, white-tailed deer had higher levels of PrP^C expression. White-tailed deer expressed more PrP^C in the parotid, metatarsal, and interdigital glands than mule deer. Following significant interactions between species and sex, post-hoc tests indicated that white-tailed females had higher PrP^C expression in the parotid, nasal, and metatarsal glands than mule deer males, and white-tailed males expressed more PrP^C than mule deer males. Within species, white-tailed deer females expressed more PrP^C in the metatarsal glands than males, and mule deer males expressed PrP^C more than in females (**Figure 2.12**).

Table 2.2. Species and sex influence on PrP^C detection by anti-PrP SHA31 using capillary gel electrophoresis.

Exocrine Tissue	Sample Size						2-Way ANOVA P Values					
	Mule Deer			White-tailed Deer								
		Male	Female		Male	Female	Interaction		Species		Sex	
Vomeronasal	n=10	n=6	n=4	n=9	n=4	n=5	0.0241	*	0.1322	n.s.	0.5962	n.s.
Parotid	n=11	n=6	n=5	n=10	n=6	n=4	0.0250	*	0.0011	* *	0.9608	n.s.
Forehead	n=10	n=5	n=5	n=11	n=6	n=5	0.6200	n.s.	0.3282	n.s.	0.0054	**
Preorbital	n=11	n=6	n=5	n=12	n=6	n=6	0.1997	n.s.	0.0564	n.s.	0.0517	n.s.
Nasal	n=11	n=6	n=5	n=12	n=6	n=6	0.0049	**	0.3594	n.s.	0.6823	n.s.
Tarsal	n=11	n=6	n=5	n=12	n=6	n=6	0.2779	n.s.	0.1540	n.s.	0.4555	n.s.
Metatarsal	n=11	n=5	n=6	n=12	n=6	n=6	0.0050	**	0.0106	*	0.3302	n.s.
Interdigital	n=12	n=6	n=6	n=11	n=6	n=5	0.2029	n.s.	0.0002	***	0.4598	n.s.

PrP^C-associated chemiluminescent baseline-fit corrected peak areas were compared between species and sex.
2-Way ANOVA significance indicators: n.s. $p \geq 0.05$, * $p < 0.05$, ** $p < 0.01$, *** $p < 0.001$

A Vomeronasal Organ

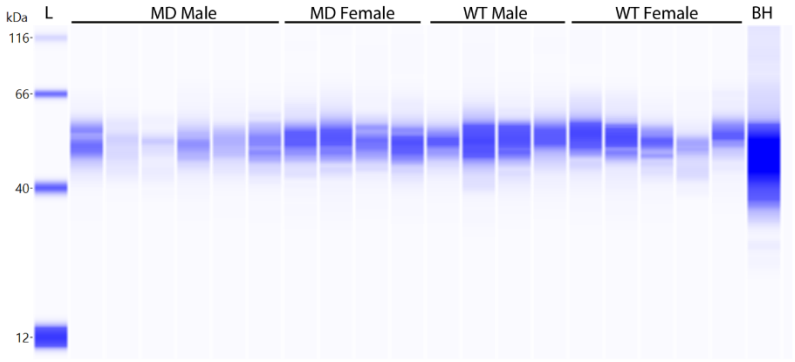

B Parotid Gland

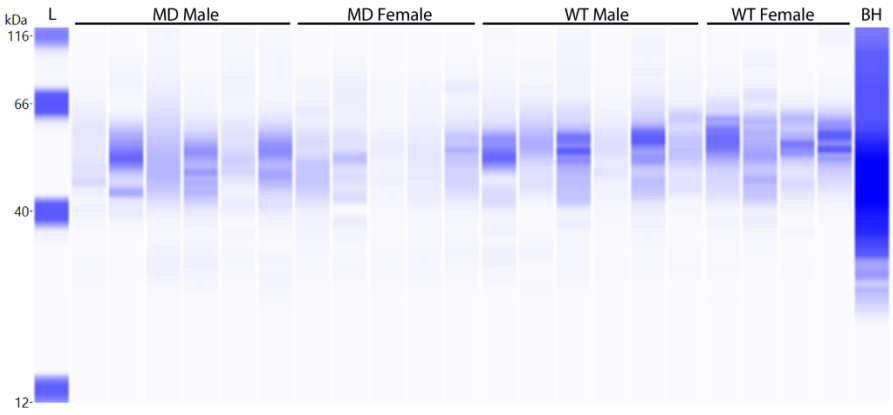

Figure 2.9. Capillary electrophoresis immunoassay of deer facial non-integumentary exocrine glands. Chemiluminescence virtual blot-like image data of PrP^C expression in clarified 10% (w/v) homogenates of mule deer (MD) and white-tailed deer (WT) detected anti-PrP SHA31. Biotinylated protein ladder (L) and unclarified white-tailed deer whole brain homogenate (BH) were used for reference. Homogenates were adjusted to final protein concentrations of 1.5µg/µL for the immunoassay.

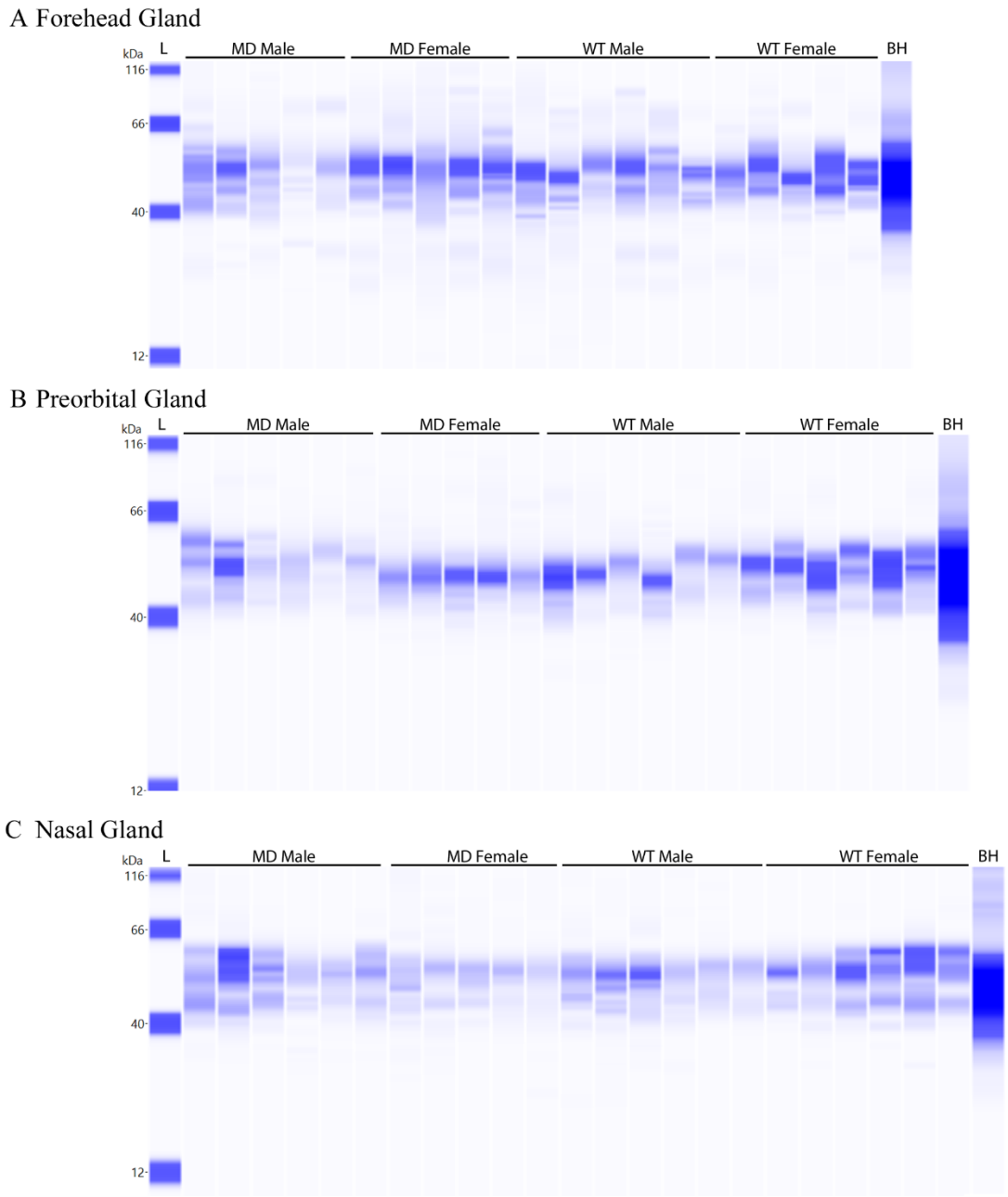

Figure 2.10. Capillary electrophoresis immunoassay of deer facial integumentary exocrine glands. Chemiluminescence virtual blot-like image data of PrP^C expression in clarified 10% (w/v) gland homogenates of mule deer (MD) and white-tailed deer (WT) detected anti-PrP SHA31. Biotinylated protein ladder (L) and unclarified white-tailed deer whole brain homogenate (BH) was used for reference. Homogenates were adjusted to final protein concentrations of 1.5µg/µL for the immunoassay.

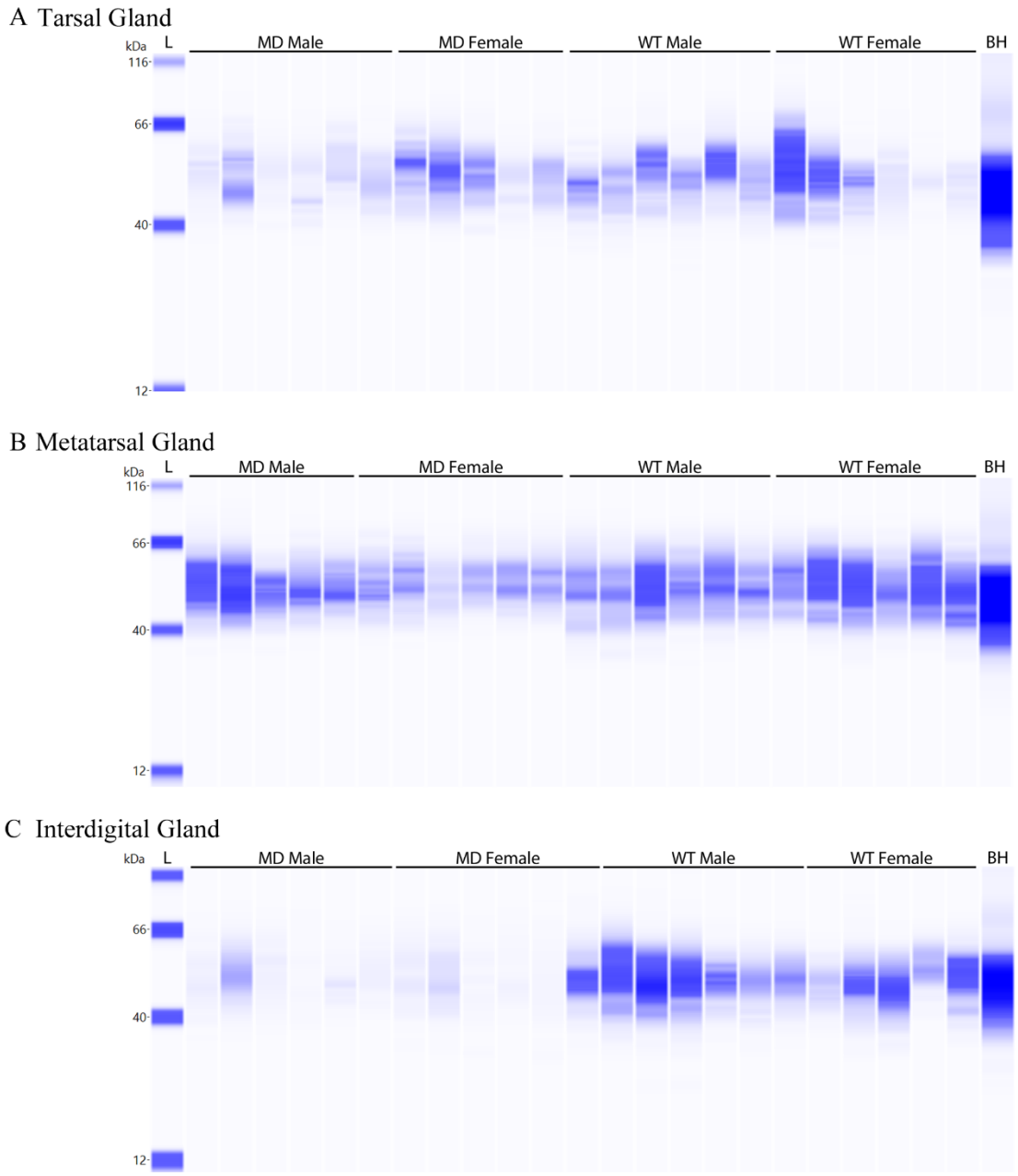

Figure 2.11. Capillary electrophoresis immunoassay of deer leg integumentary exocrine glands. Chemiluminescence virtual blot-like image data of PrP^C expression in leg integumentary clarified 10% (w/v) gland homogenates of mule deer (MD) and white-tailed deer (WT) detected anti-PrP SHA31. Biotinylated protein ladder and unclarified white-tailed deer whole brain homogenate (BH) was used for reference. Homogenates were adjusted to final protein concentrations of 1.5µg/µL for the immunoassay.

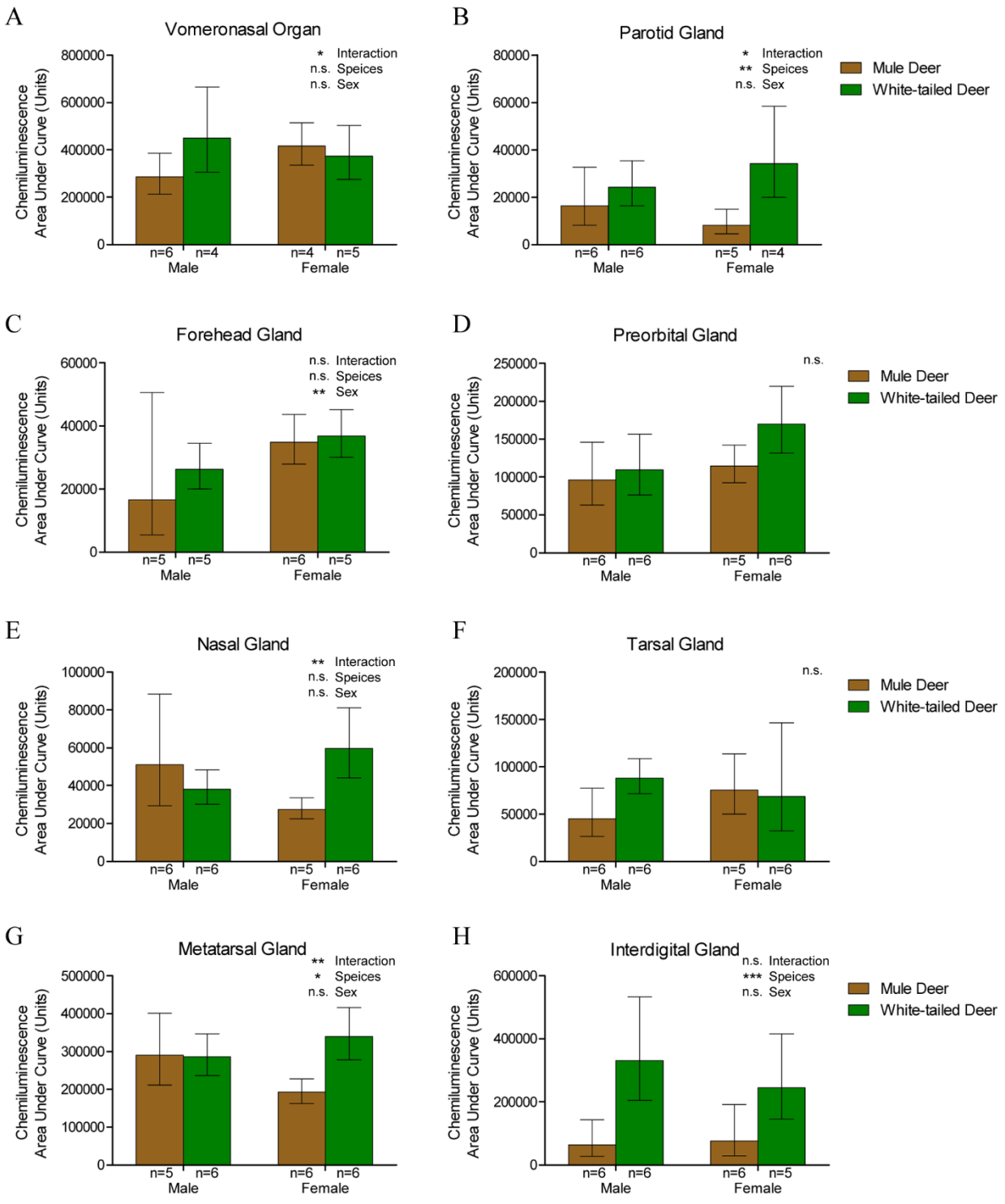

Figure 2.12. Protein concentration-adjusted PrP^C protein expression in deer exocrine glands. Capillary electrophoresis immunoassay chemiluminescence sample size, mean, and 95% confidence intervals of clarified 10% (w/v) gland homogenates. Deer facial (A-E) and leg (F-H) tissue and gland homogenate samples were adjusted to final protein concentrations of 1.5µg/µL and detected by anti-PrP SHA31.

2.4.5 Protein PrP^C concentration quantitation by ELISA

The SHA31-N5 sandwich ELISA combination used for this study is limited to the detection of full-length and C2 PrP^C fragments. Average PrP^C protein concentrations of homogenates (not adjusted for total protein concentration) ranged from 2.03ng/μL in mule deer nasal glands to 13.02ng/μL in white-tailed deer metatarsal glands (**Figure 2.13**, **Table 2.3**). White-tailed deer 1% whole-brain homogenate control PrP^C concentration averaged 4.78ng/μL between the 8 SHA31-N5 ELISAs. When the homogenates are adjusted for protein concentration, 10% (w/v) brain homogenate contains 3.7-23.5 fold more PrP^C than the clarified 10% (w/v) deer glands. Species but not sex influenced PrP^C concentration in tissues. White-tailed deer expressed more PrP^C than mule deer in the parotid, metatarsal, and interdigital glands than mule deer. Following significant interactions between species and sex, post-hoc tests indicated that white-tailed females expressed more PrP^C in the nasal gland than mule deer females, and that mule deer females expressed more PrP^C in the forehead gland than male mule deer (**Figure 2.13C, E**).

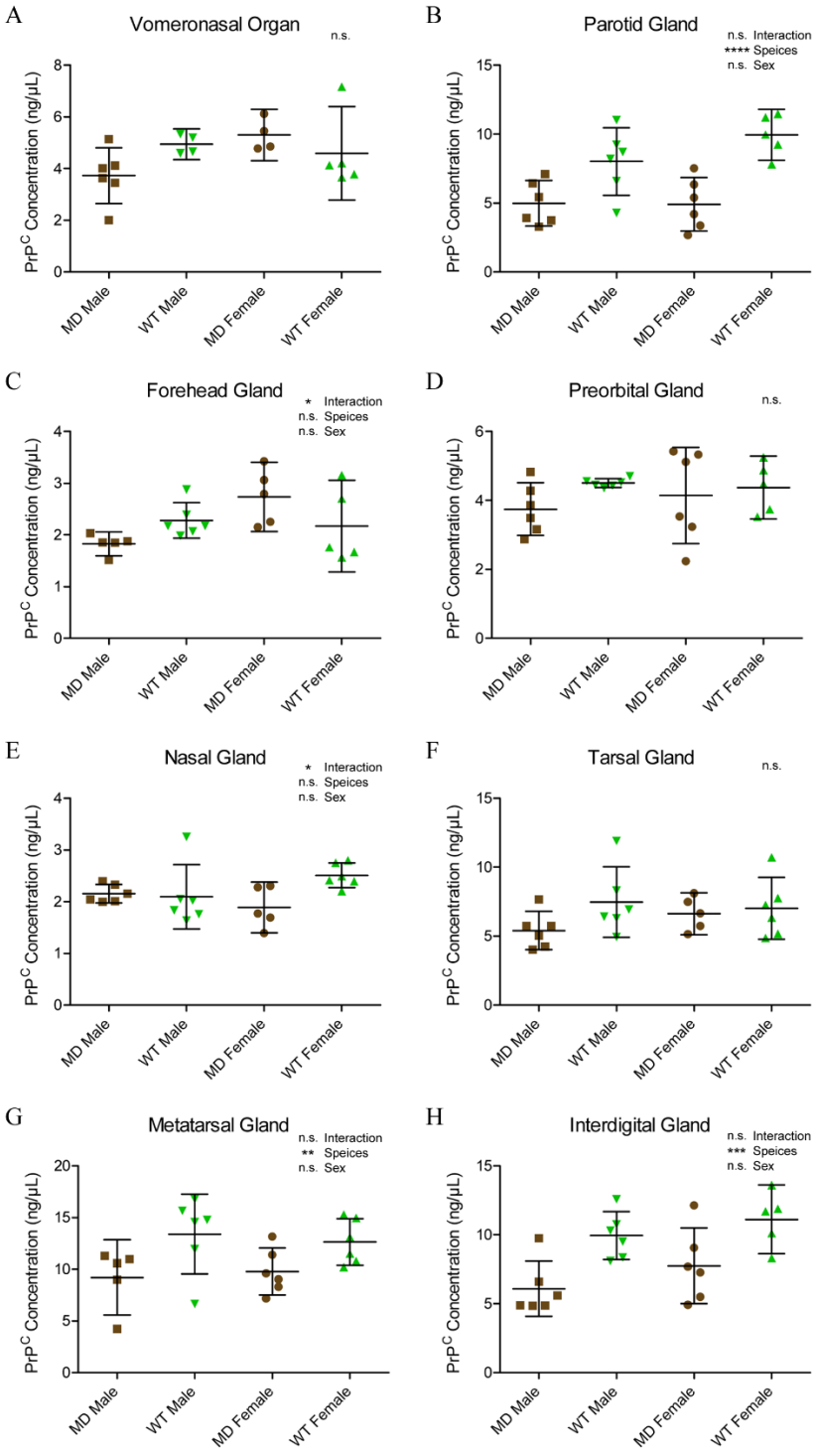

Figure 2.13. PrP^C protein concentration in deer gland homogenates. Total PrP^C concentrations of individuals, means, and 95% confidence intervals of clarified 10% (w/v) mule deer (MD) and white-tailed deer (WT) facial (A-E) and leg (F-H) gland homogenates prepared in RIPA buffer as determined by SHA31-N5 sandwich ELISA. Protein concentration was calculated using a full-length recombinant deer prion protein standard curve.

Table 2.3. Mean PrP^C concentrations and 95% confidence intervals of clarified 10% (w/v) gland homogenates as determined by SHA31-N5 sandwich ELISA.

Exocrine Tissue	PrP^C Concentration (ng/µL)						2-Way ANOVA P Values		
	Mule Deer			White-tailed Deer					
		Male	Female		Male	Female	Interaction	Species	Sex
Vomeronasal	4.36 ± 0.84 n=10	3.73 ± 1.08 n=6	5.30 ± 1.00 n=4	4.75 ± 0.82 n=9	4.95 ± 0.59 n=4	4.49 ± 1.81 n=5	0.0579 n.s.	0.5961 n.s.	0.2159 n.s.
Parotid	4.96 ± 1.04 n=12	4.99 ± 1.65 n=6	4.92 ± 1.94 n=6	8.89 ± 1.45 n=11	8.01 ± 2.44 n=6	9.95 ± 1.86 n=5	0.2116 n.s.	<0.0001 ****	0.2441 n.s.
Forehead	2.28 ± 0.44 n=10	1.83 ± 0.23 n=5	2.74 ± 0.67 n=5	2.23 ± 0.34 n=11	2.28 ± 0.34 n=6	2.17 ± 0.89 n=5	0.0261 *	0.7878 n.s.	0.0731 n.s.
Preorbital	3.95 ± 0.66 n=12	3.75 ± 0.76 n=6	4.15 ± 1.40 n=6	4.45 ± 0.32 n=11	4.51 ± 0.13 n=6	4.37 ± 0.91 n=5	0.4621 n.s.	0.1812 n.s.	0.7143 n.s.
Nasal	2.03 ± 0.21 n=11	2.16 ± 0.18 n=6	1.89 ± 0.49 n=5	2.30 ± 0.30 n=12	2.10 ± 0.62 n=6	2.51 ± 0.24 n=6	0.0469 *	0.0962 n.s.	0.6493 n.s.
Tarsal	5.96 ± 0.92 n=11	5.41 ± 1.39 n=6	6.63 ± 1.52 n=5	7.25 ± 1.39 n=12	7.47 ± 2.55 n=6	7.02 ± 2.24 n=6	0.3013 n.s.	0.1342 n.s.	0.6316 n.s.
Metatarsal	9.52 ± 1.63 n=11	9.21 ± 3.64 n=5	9.78 ± 2.28 n=6	13.02 ± 1.84 n=12	13.40 ± 3.86 n=6	12.64 ± 2.26 n=6	0.5771 n.s.	0.0071 **	0.9359 n.s.
Interdigital	6.93 ± 1.50 n=12	6.09 ± 2.01 n=6	7.76 ± 2.75 n=6	10.48 ± 1.23 n=11	9.94 ± 1.75 n=6	11.12 ± 2.49 n=5	0.7841 n.s.	0.0006 ***	0.1187 n.s.

Tissue homogenates were not adjusted for total protein concentration.
2-Way ANOVA significance indicated: n.s. $p \geq 0.05$, * $p < 0.05$, ** $p < 0.01$, *** $p < 0.001$

2.4.6 Distribution of PrP^C in exocrine glands

Glandular PrP^C distribution was visualized by immunohistochemistry using the anti-PrP BAR224 monoclonal antibody. PrP^C-associated immunohistochemistry intensity and glandular structures were confirmed by no-primary antibody negative controls and H&E staining (**Figure 2.14**). No differences were observed in the distribution of PrP^C within specific glandular structures between deer species or sex, although it must be noted that a smaller number of deer were selected for histological examination relative to the number used for the biochemical characterization methods.

The non-integumentary vomeronasal organ presented with PrP^C in the tubular serous glands and the vomeronasal respiratory epithelium, immune cell infiltrates in the submucosa (**Figure**

2.15A). This study was limited to anterior sections of the vomeronasal organ. The sections we examined did not contain any vomeronasal sensory epithelium - consistent with anterior sections of Scandinavian moose vomeronasal organs [446]. Parotid gland PrP^C immunolabeling was disseminated throughout the glandular serous acini (**Figure 2.15B**).

All six integumentary exocrine glands examined contained PrP^C in the holocrine sebaceous glandular cells, nearby epidermis, and hair root sheaths, and the nucleated regions of the hair follicles except for the dermal papilla (**Figure 2.16** – **Figure 2.17**) Sudoriferous glands were observed in all integumentary glands with the exception of the vestibular nasal glands. Contrary to Atkeson, *et al*., who reported the nasal glands of white-tailed deer and mule deer to be hairless epithelium [273], we observed hair follicles directly adjacent to the lateral vestibular nasal glands (**Figure 2.14**). Of a cautionary note for future surveys, DAB labeling can be mistaken for melanocytes among hair follicle matrix cells surrounding the hair bulb papilla and in the respiratory epithelium of vomeronasal organs.

Immunolabeling was observed in sudoriferous gland tubules of all integumentary glands except in the lateral vestibular nasal gland where these structures were absent. Non-integumentary nasal mucosa serous glands and skeletal muscle immunolabeled for PrP^C in sections of the vestibular nasal glands. Similarly, PrP^C immunolabeling was observed in the skeletal muscle of forehead gland sections. Sebaceous gland arrector pili smooth muscles were devoid of PrP^C immunolabeling. Collections of infiltrating leukocytes colocalized with PrP^C immunolabeling were observed in the preorbital and interdigital gland submucosa. The interdigital glands of mule deer contained notably abundant PrP^C-expressing leukocytes between sudoriferous ducts, sebaceous glands, and in large leukocytic infiltrates (**Figure 2.17C**). Leukocytic infiltrates were present in the interdigital glands of white-tailed deer, but less conspicuous. The remarkably

concentrated presence of immune cells in mule deer interdigital glands is consistent with prior cervid integumentary gland observations [252]. The interdigital gland sebaceous zone was thicker in white-tailed deer compared to mule deer - consistent with past observations [252]. Structurally, the interdigital glands of white-tailed deer have more developed sebaceous glands, but less developed sudoriferous glands than mule deer - consistent with observations by Quay [252, 474].

Protozoal *Sarcocystis sp.* parasitic cysts were observed in the non-glandular skeletal muscle portions of the vestibular nasal, preorbital, and forehead glands of white-tailed deer and mule deer. *Sarcocystis sp*. sarcocysts had been previously described in mule deer and white-tailed deer of CFB Wainwright [599]. The parasite's presence in specific organs is considered extraneous with respect to CWD or any gland-associated behaviours given that muscular invasion within cervids follows oral sporocyst ingestion. Sarcocysts observed were not associated with inflammation that could be expected to recruit PrP^{CWD}-containing infiltrates.

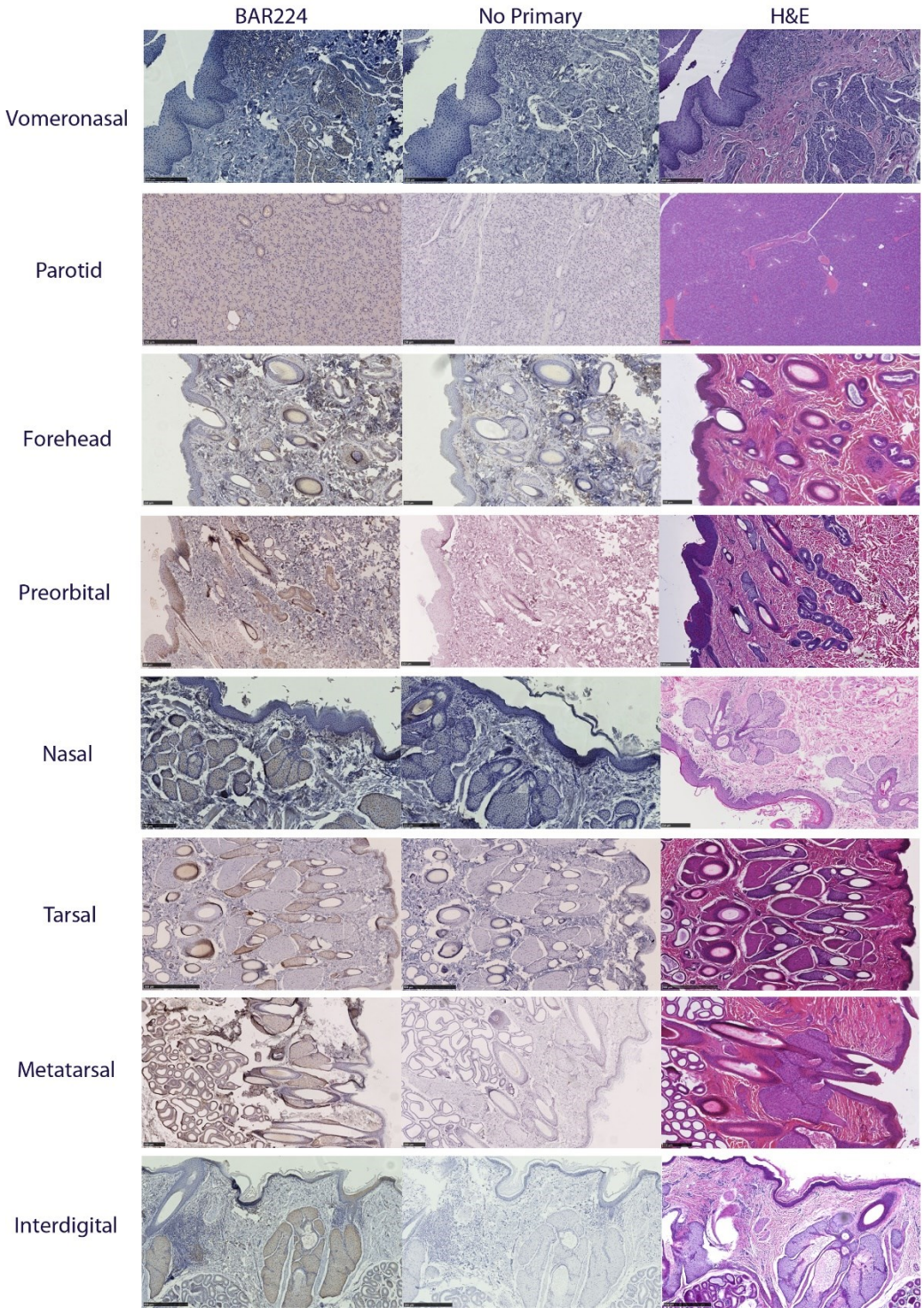

Figure 2.14. Tissue structure PrP^{C} distribution in mule deer and white-tailed deer exocrine glands. Anti-PrP BAR224 immunohistochemistry is contrasted with hematoxylin counterstain. BAR224 and no-primary antibody control immunohistochemistry slides of each gland were developed in the same batches. Scale bars for tarsal and metatarsal glands: 500µm. All other scale bars: 250µm.

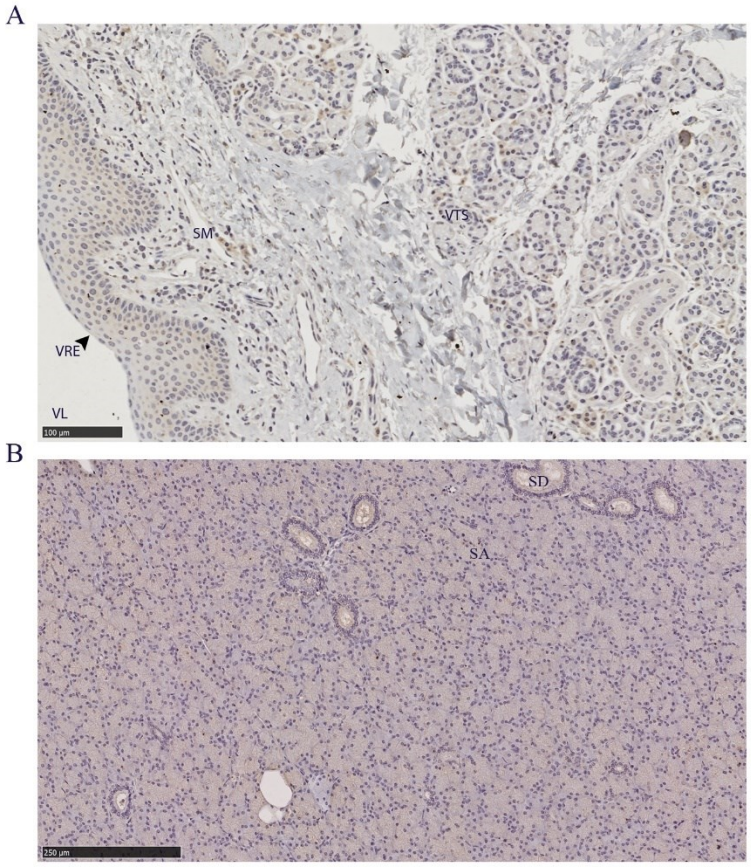

Figure 2.15. PrP^C distribution within non-integumentary facial glands. Immunohistochemical BAR224 detection of PrP^C (brown) with hematoxylin counterstaining. Female mule deer A) vomeronasal organ, and B) parotid gland. Structure abbreviations: SA, serous acini; SD, striated duct; SM, submucosa; VL, vomeronasal lumen; VRE, vomeronasal respiratory epithelium; VTS, vomeronasal tubular serous glands.

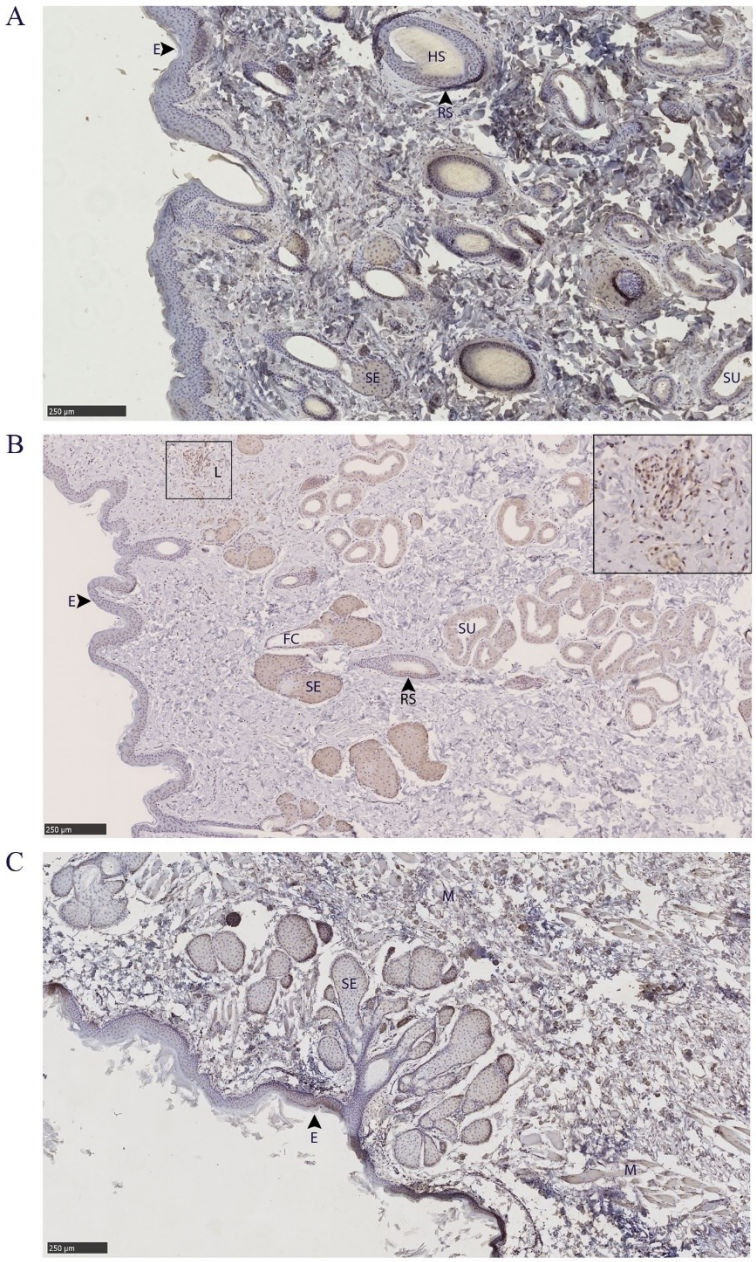

Figure 2.16. PrP^C distribution within facial integumentary glands. Immunohistochemical BAR224 detection of PrP^C (brown) with hematoxylin counterstaining. White-tailed male deer A) forehead gland, B) preorbital gland with magnified inset of infiltrating leukocytes, and mule deer female C) lateral vestibular nasal gland. Structure abbreviations: E, epidermis; FC, follicular canal; HS, hair shaft; L, leukocytic infiltrates; M, skeletal muscle; RS, follicular root sheath; SE, sebaceous glands; and SU, sudoriferous glands.

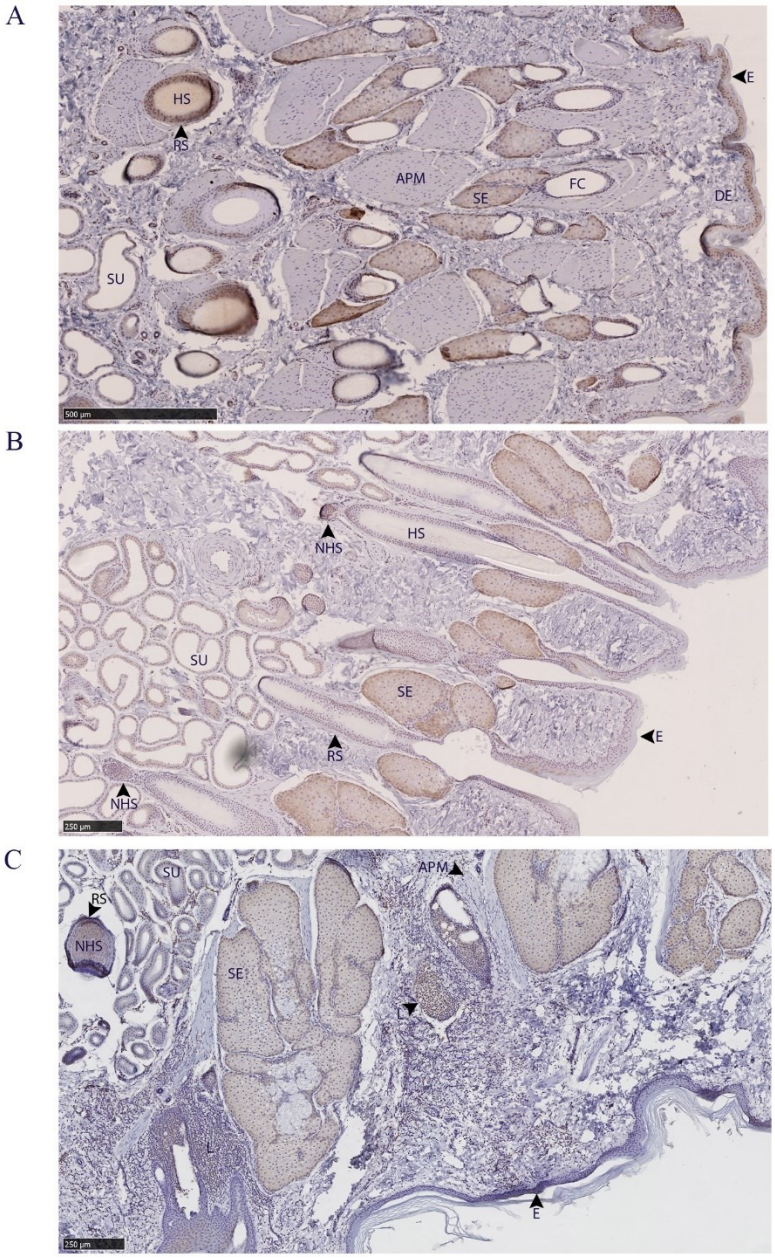

Figure 2.17. PrP^C distribution within leg integumentary glands. Immunohistochemical BAR224 detection of PrP^C (brown) with hematoxylin counterstaining. White-tailed male deer A) tarsal gland, B) metatarsal gland, and mule deer female C) interdigital gland. Structure abbreviations: APM, arrector pili muscle; DE, dermis elastic layer; E, epidermis; FC, follicular canal; HS, hair shaft; L, leukocytic infiltrates; NHS, nucleated region of the hair shaft; RS, follicular root sheath; SE, sebaceous glands; and SU, sudoriferous glands.

2.5 Discussion

The presence and distribution of white-tailed deer and mule deer PrP^{C} within 6 integumentary facial and leg glands, and the non-integumentary vomeronasal organ and parotid gland were investigated to assess their potential for the disease-associated PrP^{CWD} isoform uptake or shedding. Secondarily, we were interested if PrP^{C} abundance corresponds to the sex and species differences in CWD prevalence. Mule deer, and male cervids, have been consistently observed to be more prone to CWD infection [190-191, 193-194, 197, 595].

PrP^{C} was detected by multiple methods in all 8 tissues examined in this survey. Based on western blot, the clarified 10% (w/v) gland homogenates are estimated to possess approximately 10-25 fold less PrP^{C} than 10% (w/v) brain homogenates. Similarly, sandwich ELISA determined the gland homogenates to contain between 3.7 and 23.5 fold less PrP^{C} than brain homogenate - the difference in estimates being attributed to restricted PrP^{C} fragment detection by sandwich ELISA relative to western blot. Time between the animals death and sample collection may have contributed to individual variation of PrP^{C} detection via protein degradation. The impact of protein degradation as a factor in PrP^{C} detection was mitigated by cold ambient temperature during the hunt and by the preferential selection of shorter times between death and sampling. The deer examined in this study were sampled exclusively near the end of the breeding season. The possibility that PrP^{C} protein expression and gland activity varies cyclically throughout the year cannot be excluded.

Contrary to CWD wild population prevalence patterns, we observed that glandular PrP^{C} expression was significantly higher in females and in white-tailed deer - regardless of whether homogenates were adjusted for total protein content. Western blot analysis showed that female deer of both species expressed more PrP^{C} in the forehead and preorbital glands than male deer

(**Figure 2.7A-D**). Capillary electrophoresis immunoassay of protein concentration-adjusted samples confirmed the western blot analysis of the females having more PrP^C expression in the forehead glands, and also indicated that white-tailed deer express more PrP^C than mule deer in the interdigital glands (**Table 2.2**). ELISA quantification of unadjusted gland homogenates similarly indicated that white-tailed deer express more PrP^C than mule deer in the parotid, metatarsal, and interdigital glands (**Table 2.3**). Discrepancies in tissues identified to have significant PrP^C abundance differences between the capillary electrophoresis and ELISA methods can be explained by a lack of total protein adjustment in ELISA and fewer PrP^C molecular species being detected by the sandwich ELISA relative to the single antibody-based detection of western blot or capillary electrophoresis immunoassays.

The lack of correlation between deer gland PrP^C expression and known CWD sex and species prevalence patterns are not the only variables to be considered. Our determination of PrP^C concentrations do not take into consideration glandular size and secretion differences between season, species, and sex. For example, western blot and capillary electrophoresis immunoassay determined that females express more PrP^C than males; however, male deer have thicker forehead glands [272]. Likewise, white-tailed deer were identified as having significantly more PrP^C expression in the metatarsal glands by ELISA and capillary electrophoresis immunoassay, but this may be counterbalanced by mule deer having larger metatarsal glands [271, 598]. Capillary electrophoresis and ELISA determined that white-tailed deer express more PrP^C than mule deer.

Data on cervid PrP^C abundance and distribution in non-neuronal tissues is limited, but has been examined in the alimentary tract and associated lymph nodes in white-tailed deer [594]. Such tissues variably expressed PrP^C and accumulated PrP^{CWD} prion seeding activity in symptomatic

animals [594]. The authors also determined that higher relative PrP^{C} expression between tissues did not correlate well with early preclinical PrP^{CWD} prion seeding activity [594]. Relative sex and species expression differences between the 6 integumentary glands and 2 non-integumentary tissues were generally low in magnitude; PrP^{C} was readily detectable in all deer tested and ELISA quantification of PrP^{C} concentrations determined that all differences were less than two-fold (**Table 2.3**). Although yet to be investigated, all tissues contained expressed PrP^{C} at levels that could feasibly replicate PrP^{CWD}. The PrP^{C} abundance differences of the tissues investigated may not be sufficient in magnitude to influence horizontal CWD transmission and broad disease prevalence patterns.

Immunohistochemistry of the integumentary gland sections identified PrP^{C} localized in the integumentary glandular cells, hair follicles, epidermis near glandular ducts, and local immune cells. Resident immune cells - especially the large clusters observed in the interdigital glands - and *in situ* nerve endings are envisioned to be accommodating to prion conversion and trafficking. Many of the structures identified in the exocrine gland sections that labeled for PrP^{C} are composed of actively replicating cells that would be anticipated to have a low propensity for PrP^{CWD} replication based on cell division rate [601]. Although the glandular cells and hair follicles are suspected to be poorly tropismatic for PrP^{CWD}, these integumentary structures are innervated in cervids [252, 404, 475] which could permit direct nervous system access for PrP^{CWD} uptake or shedding. Parotid glands of orally infected deer at clinical stage of disease were observed to have PrP^{CWD} in parasympathetic nerves and the interstitial space of the gland rather than the acini or glandular ducts [123]. Supportive of infectious prion replication in glandular cells is the observation of PrP^{Sc} of scrapie-infected sheep in the parotid gland acinar cells, ductal cells, and interstitia - depending on the antibody used [155]. PrP^{CWD} labeling by 6H4

in the deer study is analogous to PrP^{SC} labeling by L42 in scrapie-infected sheep work. The anti-prion protein 6H4 monoclonal antibody has an epitope that encapsulates the epitope of L42. Both antibodies identified infectious prions in the interstitium of the parotid gland. Alternative anti-prion antibody use in deer may identify PrP^{CWD} in the acinar cells and glandular ducts of the parotid gland (and other glands) as observed in scrapie.

The integumentary glands examined expressed similar levels of PrP^{C} to the parotid gland, which is known to accumulate PrP^{CWD} [41, 123, 180, 232]. PrP^{Sc} is present in the vomeronasal organ sensory epithelium, but not the respiratory epithelium of Hyper prion strain-infected hamsters [530]. To be considered for future studies is the lack of sensory epithelium in the anterior portions of the vomeronasal organ we examined. Although PrP^{C} abuncance was lower than in brain homogenate, the 8 tissues examined expressed PrP^{C} at levels that could feasibly replicate PrP^{CWD}. The PrP^{C} expression in the glands examined (of both species and sex), therefore, has CWD transmission potential.

Species and sex differences in cervid behaviours, including grouping and movement patterns, sparring, courtship behaviour, scent-marking, and other advertisement activities, have been proposed to explain the disease prevalence differences of wild animal populations [193, 220, 229, 276]; however, uniting cervid behaviours, physiology, and CWD transmission is currently lacking. Our identification of PrP^{C} presence in the vomeronasal organ and integumentary scent glands associated with mule deer and white-tailed deer behaviors provides a biochemical foundation for understanding these tissues if they are demonstrated to be involved in CWD transmission. Investigations into PrP^{CWD} presence in the described tissues will provide further insights into possible mechanisms of CWD transmission that drive asymmetrical disease prevalence.

Chapter 3 Chronic wasting disease prions in mule deer interdigital glands

Data in this chapter has been included in one manuscript, published in PLOS ONE, as:

Ness, Anthony; Zeng, Doris; Kuznetsova, Alsu; Otero, Alicia; Kim, Chiye; Saboraki, Kelsey; Lingle, Susan; Pybus, Margo; Aiken, Judd; Gilch, Sabine; McKenzie, Debbie (2022). Presence and evidence of chronic wasting disease prion secretion from the hoof interdigital glands of mule deer

3.1 Abstract

Chronic wasting disease (CWD) is a geographically expanding, fatal neurodegenerative disease in cervids. The disease can be transmitted directly (animal-animal) or indirectly, via infectious prions shed into the environment. The precise mechanisms of indirect CWD transmission are unclear but known sources of the infectious prions that contaminate the environment include saliva, urine and feces. We previously identified PrP^{C} expression in deer interdigital glands, sac-like exocrine structures located between the digits of the hooves. In this study, we assayed for CWD prions within the interdigital glands of CWD infected deer to determine if they could serve as a source of prion shedding and potentially contribute to CWD transmission. Immunohistochemical analysis of interdigital glands from a CWD-infected female mule deer identified disease-associated PrP^{CWD} within clusters of infiltrating leukocytes adjacent to sudoriferous and sebaceous glands, and within the acrosyringeal epidermis of a sudoriferous gland tubule. Proteinase K-resistant PrP^{CWD} material was amplified by serial protein misfolding cyclic amplification (sPMCA) from soil retrieved from between the hoof digits of a clinically affected mule deer. Blinded testing of interdigital glands from 11 mule deer by real-time quake-induced conversion (RT-QuIC) accurately identified CWD-infected animals. Our data suggests that interdigital glands may play a role in the dissemination of CWD prions into the environment.

3.2 Introduction

Chronic wasting disease (CWD) is a contagious, fatal transmissible spongiform encephalopathy of cervids. The pathological agent of CWD (PrP^{CWD}) is a misfolded isoform of the cellular prion protein (PrP^{C}) that propagates by a template misfolding-like mechanism [1-2, 4]. The environments of CWD-endemic areas are contaminated by PrP^{CWD} by carcasses, feces, urine, and saliva from clinically and subclinically affected animals [38-39, 41, 44-46, 243, 602-603].

Prions shed into the environment remain infectious for years to decades - contributing to horizontal disease transmission [35, 154, 181-183]. Shed prions bind to soil, vegetation, and other fomites that provide reservoirs for naïve deer exposure [37, 46-51, 185].

Deer possess a number of integumentary glands that are hypothesized to be involved in CWD transmission (Chapter 2) [276, 359, 604]. Many cervids, including mule deer (*Odocoileus hemionus*) and white-tailed deer (*Odocoileus virginianus*), but not elk (*Cervus canadensis*), possess interdigital glands - anteriorly-facing pocket structures between the two first phalangeal bones - in the fore and hind feet [252, 405, 474]. Interdigital glands secrete volatile compounds that are believed to create scent trails [252, 458, 474, 605-606]. We previously reported the distribution of PrP^{C} in mule deer and white-tailed deer integumentary glands (Chapter 2) [604]. PrP^{C} in the interdigital glands was observed within the sebaceous glands, sudoriferous glands, portions of epidermis, hair root sheaths, and infiltrating immune cells. A parallel survey for the presence of disease-associated PrP^{CWD} in the tissues was performed. We identified PrP^{CWD} in the hind interdigital gland of a CWD-infected female mule deer, leading to a further investigation of this cutaneous gland. Our subsequent analysis of blinded interdigital gland samples from 11 mule deer resulted in the correct identification of infected animals. We describe the findings of PrP^{CWD} being found within the interdigital glands of mule deer and discuss the associated implications.

3.3 Methods

3.3.1 Tissue collection

All deer samples were obtained from animals harvested by hunters or found dead. Institutional animal care and use approval was not required for the tissues used this study. Tissue samples used in this study were collected at three different times (**Figure 3.1**). Hunter harvested deer samples from 2017 and 2019 used in this study were collected from Albertan Canadian Forces

Base (CFB) Wainwright, Alberta. Tissues collected for the 2017 PrP^{CWD} survey included the apical portion of the vomeronasal organ, the parotid gland, and 6 integumentary glands - forehead, preorbital, vestibular nasal, tarsal, metatarsal, and hind interdigital glands. This study focuses on the interdigital glands. Samples were frozen for later biochemical analysis or formalin-fixed for histology. Investigation into the distribution of PrP^{CWD} in the tissues described was limited by random selection of deer to be sampled. CWD status of individual deer was unknown during tissue collection. The CWD status (positive or negative) of sampled deer was later determined by the Alberta Ministry of Agriculture and Forestry using the BioRad TeSeE ELISA on retropharyngeal lymph nodes and/or obex samples [191]. Consequently, for the broad gland collection of 41 deer in 2017 (including mule deer and white-tailed deer), only 2 were positive for CWD - both mule deer. The two hunter-harvested adult mule deer (1 of each sex) were CWD-positive in the retropharyngeal lymph nodes and obex (specific obex scoring unavailable). Hunter-reported fat levels (indicative of possible clinical-stage wasting) of the two infected deer was listed as normal.

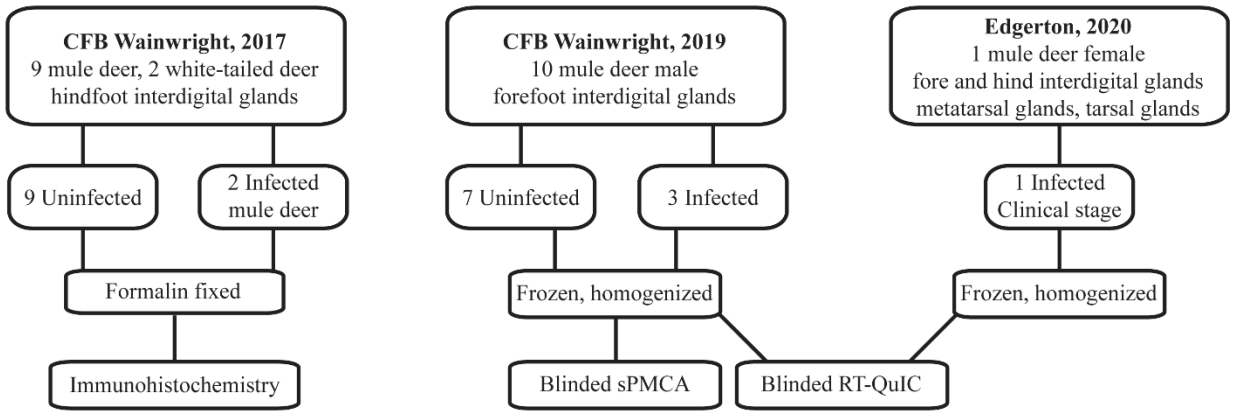

Figure 3.1. Conceptual diagram of sample origin and use.

Additional frozen forelegs were obtained from 10 male mule deer harvested by hunters within CFB Wainwright in the autumn of 2019. Male mule deer have the highest prevalence of CWD in Alberta relative to females and white-tailed deer [191]. During the 2019 harvest, male mule deer at CFB Wainwright (wildlife management units 728 and 730) had an estimated prevalence of 11-30% [77]. Interdigital glands were extracted from the hooves as follows: forelegs were thawed by warm water, local pelage was trimmed with stainless steel operating scissors. Scissors were decontaminated with 2M NaOH submersion for 24 hours between leg sets. Each interdigital gland was excised with a single-use disposable scalpel to prevent cross contamination. Once the interdigital gland was exposed (**Figure 3.2A**), the fundus of each gland sac was excised with a disposable razor (**Figure 3.2B**) and frozen for later homogenization.

Additional samples were collected from a collared yearling female mule deer with signs of wasting that was found dead in eastern Alberta in October, 2020. The animal is presumed to have died of CWD. The animal was tested by the Alberta Ministry of Agriculture and Forestry as described above and was CWD-positive. All four legs (including the hind tarsal and metatarsal glands) were removed and frozen. The interdigital gland from each leg and both tarsal and metatarsal glands from the hind legs were extracted and individually homogenized.

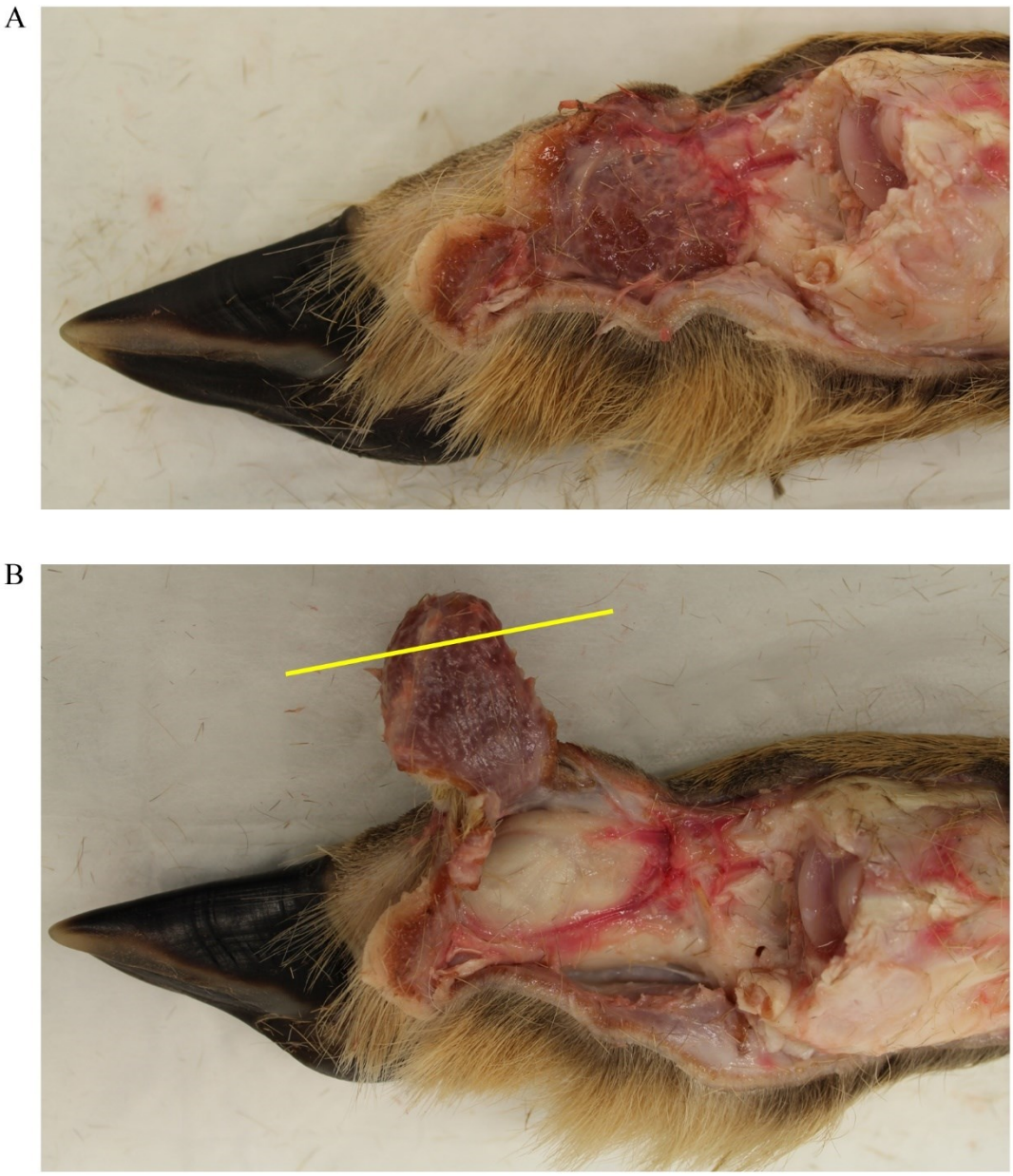

Figure 3.2. Extraction of the interdigital gland fundus for homogenization. A) Half of the hoof was disarticulated leaving the entire interdigital gland intact. B) The glandular sac is exposed and the fundus excised by cutting at the yellow line.

3.3.2 *PRNP* gene amplification and sequencing

DNA from all CWD-infected animals was extracted and sequenced to identify *PRNP* genotypes.

Genomic DNA was isolated from deer tissues by methanol precipitation. The cervid *PRNP* gene

was amplified by a primer set targeting the coding region of the mature mule deer prion protein using GoTaq® Long PCR Master Mix (Promega Corporation, USA). To avoid amplification of the mule deer prion protein pseudogene (GenBank accession no. AY371694) or white-tailed deer prion protein pseudogene (GenBank accession no. AY425673), primers (DeerPCR1F and DeerPCR7F) were specifically designed for the sequence region with high variation between the white-tailed deer and mule deer prion protein pseudogenes and the functional mule deer *PRNP* gene (GenBank accession no. AY228473). The forward primer, DeerPCR1F (5'-ACCTACAATTACTTTCGTGAGATGT-3'), overlaps intron 2 and the reverse primer, DeerPCR1R (5'-CAAGAAATGAGACACCACCACTA-3'), was located 1059 bp downstream of the forward primer (GenBank accession no. AY228473). PCR thermocycling conditions were 95°C for 3 min for initial denaturation followed by 35 cycles of 95°C for 30 s, 62°C for 30 s, and 65°C for 2 min, and the final extension at 72°C for 10 min. PCR fragments were sequenced by Sanger DNA sequencing at the University of Alberta Molecular Biology Facility using the forward primer DeerPCR7F (5'-CTGATGCCACTGCTATGCAGTCAT-3') and the reverse primer DeerPCR1R with BigDye® sequencing reagents (ThermoFisher Scientific, United States).

3.3.3 Histological and immunohistochemical detection of PrP^{CWD} in gland tissues

Formalin fixed glands were trimmed and embedded in paraffin. 4µm thick sections were cut using a microtome and mounted on glass slides. Sections were then stained using the hematoxylin and eosin (H&E) protocol to identify the histological structures of the glands. Immunohistochemical labeling for the detection of PrP^{CWD} in glandular tissues required modifications to prevent the loss of fine structures and leukocytic infiltrates [597]. Tissue sections were incubated at 65°C overnight, deparaffinized and dehydrated by immersion in

xylene and decreasing concentrations of ethanol (100%, 95% and 70%). Epitope retrieval was performed by hydrated autoclaving at 121°C in deionized water for 10 minutes, incubated with 98% formic acid for 10 minutes, digested with proteinase K (4µg/mL) (Invitrogen, USA) at 37°C for 15 minutes, and incubation with 4M guanidine thiocyanate for 2 hours. Endogenous peroxidase was blocked using a 3% hydrogen peroxide solution for 12 minutes. Sections were exposed to 5% goat serum for 1 hour to block non-specific sites followed by 15 minutes of blocking with avidin and biotin (Vector Laboratories, USA) respectively. Immunodetection was completed by incubating the samples with the monoclonal antibody BAR224 (1:2,000; Cayman Chemical, USA) overnight at 4°C followed by 1 hour of incubation with an anti-mouse horseradish peroxidase (HRP) secondary antibody (1:250; Immun-Star). AEC (3-Amino-9-ethylcarbazole) (Vector Laboratories, USA) was used as the HRP chromogen substrate. After counterstaining with hematoxylin, sections were mounted with DPX mounting medium (MilliporeSigma, USA). Control slides in which incubation with the primary antibody was omitted were used as specificity controls. Slides were scanned with a NanoZoomer 2.ORS (Hamamatsu Photonics K.K., Japan) and images analyzed with the manufacturer's NDP.view2 software.

3.3.4 Tissue homogenization

Glandular tissue was processed as detailed previously (Chapter 2) [604]. The tissues were weighed and minced to create 10% (w/v) homogenates in RIPA lysis buffer (50mM Tris, 150mM NaCl, 1% IGEPAL CA-630, 0.25% deoxycholate, 1mM EDTA, pH 7.4) supplemented with cOmplete™ EDTA-Free Protease Inhibitor Cocktail (Roche Diagnostics GmbH, Switzerland). Samples were mechanically homogenized in a Bead Ruptor 24 (Omni International, USA) ceramic bead mill homogenizer in the presence of a cold air flow supplied

by an OMNI BR-Cryo cooling unit (Omni International, USA) to minimize heat-denaturation. Tissues were subjected to 25 minutes of high-energy milling using cycles of 10 second milling intervals followed by 15 seconds of cooling. Homogenate supernatants were collected following a brief centrifugation to yield clarified 10% gland homogenates for biochemical analysis.

3.3.5 Serial protein misfolding cyclic amplification and western blot analysis

Interdigital clarified gland homogenates blinded for CWD status were analyzed by sPMCA. PMCA substrate preparation was prepared from transgenic mice expressing elk 132MM prion protein (tgElk) [607]. Mice were perfused, after euthanasia by isoflurane inhalation, using phosphate buffered saline (PBS) (130mM NaCl, 7mM $Na_2HPO_4 \cdot 7H_2O$, 3mM $NaH_2PO_4 \cdot 1H_2O$, pH 7.4) with 5mM EDTA (in compliance with the University of Alberta Animal Care and Use Committee approved animal use protocol AUP914). Brains were extracted and immediately frozen at -80ºC. The brain substrate (10% w/v brain homogenate) was prepared using a Dounce tissue grinder, homogenizing the brain tissue in chilled PMCA conversion buffer (PBS, 150mM NaCl, 1% Triton X-100, 4mM EDTA) with cOmplete™ EDTA-Free Protease Inhibitor Cocktail (Roche Diagnostics GmbH, Switzerland) and clarified by centrifugation at 800g for 5 min. Supernatant aliquots (90µL each) were stored in 0.2mL PCR tubes (Corning, USA) at -80ºC. *In vitro* amplification of PrP^{CWD} present in gland homogenates was performed using serial protein misfolding cyclic amplification (sPMCA) similarly to that described previously [608-611]. Each PMCA reaction included three 3/32″ PTFE beads (McMaster-Carr, USA) to increase the efficiency of prion amplification. Substrates seeded with 10µL of samples were placed on the plate holder of a S-4000 Misonix sonicator (QSonica, USA) and were subjected to 24 hour rounds of serial PMCA consisting of incubation cycles of 15 min at 37 ºC followed by sonication pulses of 30s at 60% power.

Reaction products sPMCA rounds were examined for evidence of PrP^{CWD} seeding by western blot. Samples of sPMCA round products were proteolytically digested using 50µg/ml of proteinase K (PK) for 1 h at 37ºC with agitation. Digestion was terminated by the addition of 2x Laemmli sample buffer (150mM Tris-HCl (pH 6.8), 0.5% bromophenol blue, 25% (v/v) glycerol, 5% (w/v) SDS, 12.5% (v/v) β-mercaptoethanol) and boiling at 100ºC for 10min. Samples were analyzed by western blot using Invitrogen NuPAGE™ 12% Bis-Tris protein gels (Thermo Fisher Scientific Inc., USA) separated in MOPS buffer. Proteins were transferred onto PVDF membranes, followed by immunodetection of PrP^{CWD} with mouse anti-PrP monoclonal antibody SHA31 (1:10,000; Cayman Chemical, USA). Blots were developed using the AttoPhos AP Fluorescent Substrate System (1:10,000; Promega Corporation, USA). Secondary goat anti-mouse IgG (H+L) AP Conjugate (Promega Corporation, USA) detection antibody was enzymatically developed with AttoPhos® AP Fluorescent Substrate System (Promega Corporation, USA). Fluorescent imaging of the membranes was performed using an ImageQuant LAS 4000 (GE Life Sciences, USA) system.

3.3.6 Real-time Quake-Induced Conversion (RT-QuIC)

RT-QuIC using recombinant mouse PrP substrate was performed as previously described [612-613]. Uninfected mule deer and CWD-infected reindeer brain homogenates were used for negative and positive controls. Briefly, RT-QuIC reactions were prepared in assay buffer containing 20 mM sodium phosphate (pH 6.9), 300 mM NaCl, 1 mM EDTA, 10 µM thioflavin T (ThT), and 0.1 mg/ml full-length mouse recombinant PrP (amino acids 23-230) substrate. Aliquots (98µL) were added to the wells of a 96 well optical bottom plate (Nalge Nunc International, USA). Quadruplicate reactions were seeded with 2µl of sample. Clarified 10% (w/v) interdigital, metatarsal, and tarsal gland homogenates were blinded for CWD status and

assayed for the presence of prion infectivity by RT-QuIC. Mouse recombinant PrP, in our hands, efficiently amplifies CWD prions with minimal spontaneous conversion (we find higher levels of spontaneous conversion with both bank vole and truncated hamster PrP). Gland and control brain homogenates were assayed at dilutions of 1:20 (0.5% final concentration), and 1:200 (0.05% final concentration).

The plate was sealed with Nunc Amplification Tape (Nalge Nunc International, USA) and placed in a FLUOstar Omega fluorescence plate reader (BMG LABTECH GmbH, Germany) pre-heated to 42˚C. The RT-QuIC assay was run for a total of 50 hours with cycles of 1 minute of double orbital shaking (700 rpm) incubation and 1 minute of resting throughout the incubation. ThT fluorescence signals (450nm excitation, 480nm emission) were recorded every 15 minutes. The positive sample threshold was calculated using the average ThT fluorescence signals of the negative control +5 standard deviations. Values were plotted as the average of quadruplicate reactions by using GraphPad Prism software (GraphPad Software, USA).

3.3.7 Soil collection and prion detection

A soil sample was found lodged between the two hoof digits in the vicinity of the interdigital gland of the clinically affected female mule deer. The hoof soil was not characterized due to limited sample size, but the deer legs were collected near Edgerton, Alberta where dark brown and black chernozemic soils are predominant [614]. A comparable negative control (orthic black chernozem, humic horizon Ah) soil sample was sourced from the Leduc region of Alberta in 2010 when the area was CWD-free. The control soil sample has been previous described [592]. Bound PrP^{CWD} was extracted from soil samples as follows: soil samples were mixed with 5x Laemmli buffer (300mM tris base, 50% (v/v) glycerol, 10% (w/v) sodium dodecyl sulfate, 25% (v/v) 2-mercaptoethanol) in ratio 1:1 and heated for 10 minutes at 100°C. Samples were briefly

centrifuged and 10µL of sample supernatants were used to seed tgElk PMCA substrate following brief centrifugation. Subsequent sPMCA was performed as described above.

3.4 Results

3.4.1 Detection of interdigital PrP^{CWD} by immunohistochemistry

Dense leukocytic infiltrates unrelated to CWD were observed within all 2017 mule deer interdigital gland samples examined by histology - consistent with past observations (Chapter 2) [252, 604]. No PrP^{CWD} was observed in the interdigital glands of CWD-negative deer (7 mule deer and 2 white-tailed deer). Histology was available for two CWD-infected mule deer collected in 2017. PrP^{CWD} was observed in the interdigital gland of the CWD-infected female mule deer, but not in the CWD-infected male mule deer. Of note, the male had visibly less severe leukocytic infiltration than the female. In the CWD-infected female mule deer, PrP^{CWD} was present among leukocytic infiltrates between and adjacent to sudoriferous (**Figure 3.3** – **Figure 3.4**) and sebaceous glands (**Figure 3.4B**). Further PrP^{CWD} immunolabeling was identified within the acrosyringeal epidermis of a dilated, blocked sudoriferous duct (miliaria rubra) (**Figure 3.5**) [615-616]. Deposition of PrP^{CWD} was confirmed by analysis of sequential tissues sections (**Figure 3.6**, **Figure 3.7**). Acrosyringium structure was confirmed by serial haematoxylin and eosin sections (**Figure 3.8**). PrP^{CWD} was located close to the epidermis with 6 foci of PrP^{CWD} immunolabeling averaging 623µm from the external surface of the epidermal stratum granulosum. Aberrant infiltration of sudoriferous tubule lumen by leukocytes was observed in uninfected and CWD-infected mule deer without PrP^{CWD} (**Figure 3.8**, **Figure 3.9**). PrP^{CWD} was not observed in nerves associated with interdigital glands.

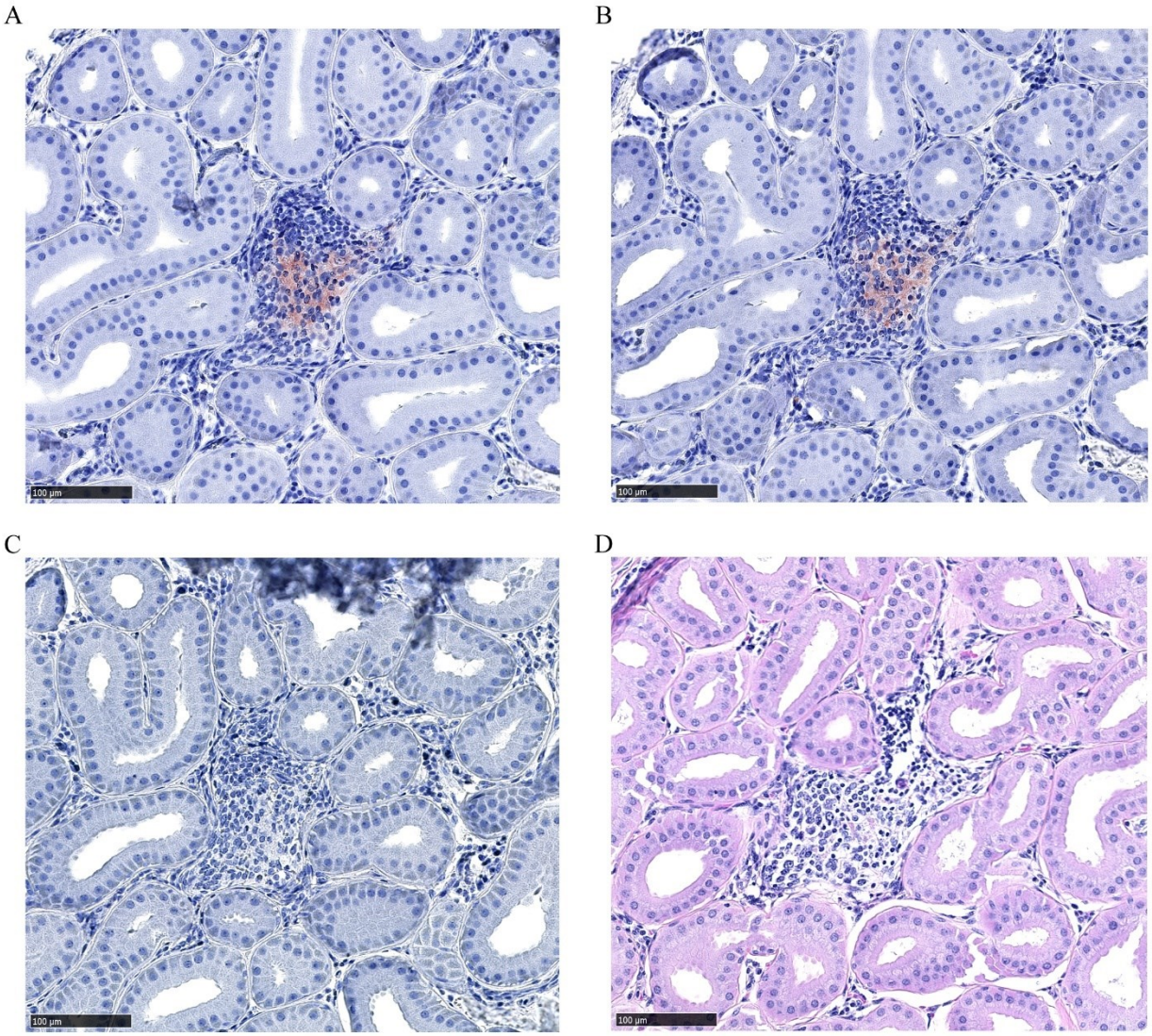

Figure 3.3. PrP^{CWD} immunolabeling between sudoriferous glands of a female mule deer hind interdigital gland. A-B) Adjacent sections of immune cell infiltrates between sudoriferous glands with PrP^{CWD} immunolabeling (red) with anti-PrP BAR224 (1:2,000). C) Negative control section without primary antibody. D) Haematoxylin and eosin staining.

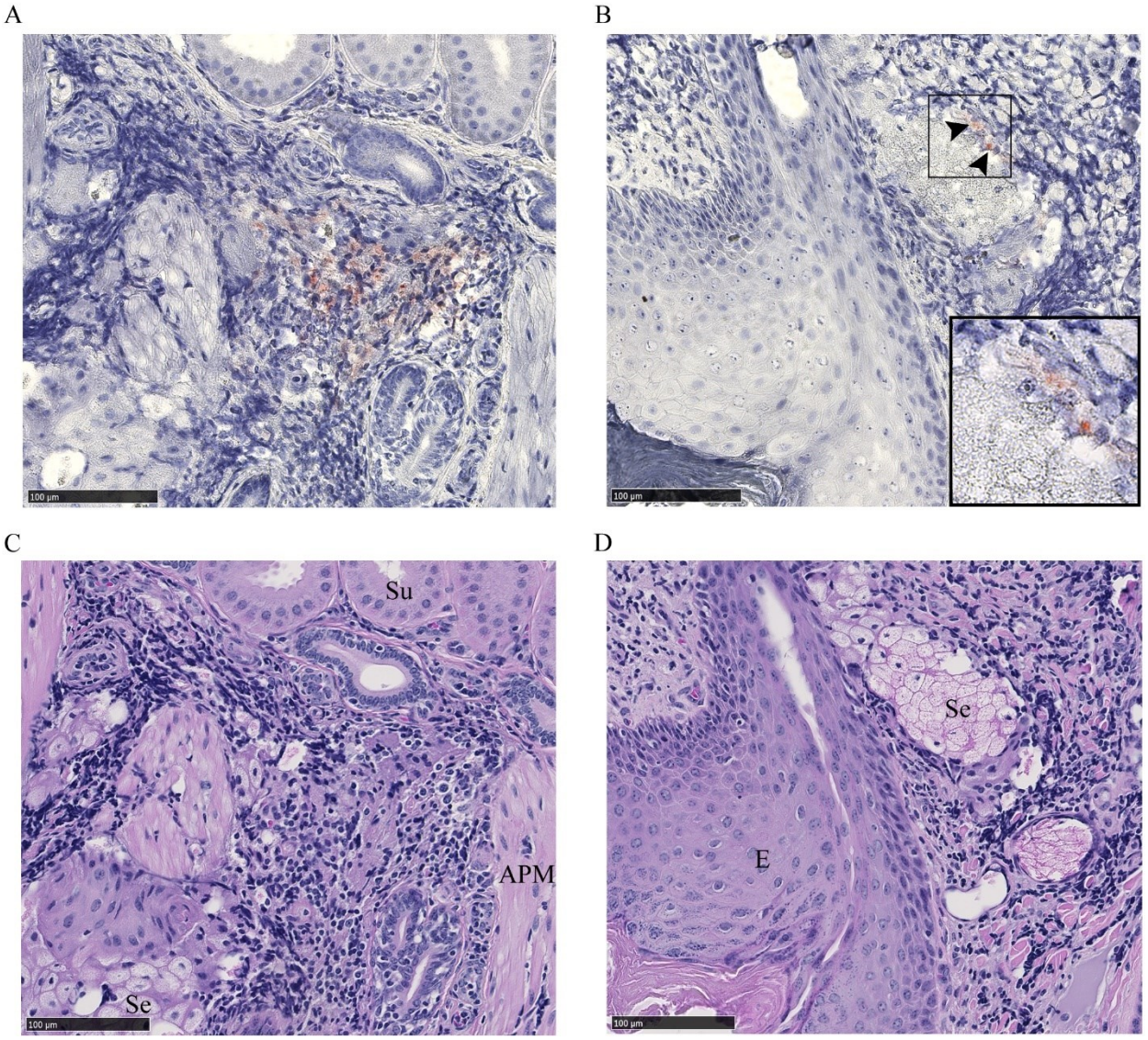

Figure 3.4. PrP^{CWD} immunolabeling adjacent to sudoriferous and sebaceous glands of a female mule deer hind interdigital gland. A) Immune cell infiltrates between sebaceous and sudoriferous glands with PrP^{CWD} immunolabeling (red) with anti-PrP BAR224 (1:2,000). B) Immune cell infiltratres near the epidermis with PrP^{CWD} immunolabeling (arrows) adjacent to a sebaceous glandular element. Inset shows PrP^{CWD} with increased magnification. C-D) Adjacent section haematoxylin and eosin staining. Abbreviations: APM, arrector pili muscle; E, epidermis; Se, sebaceous gland; Su, sudoriferous gland.

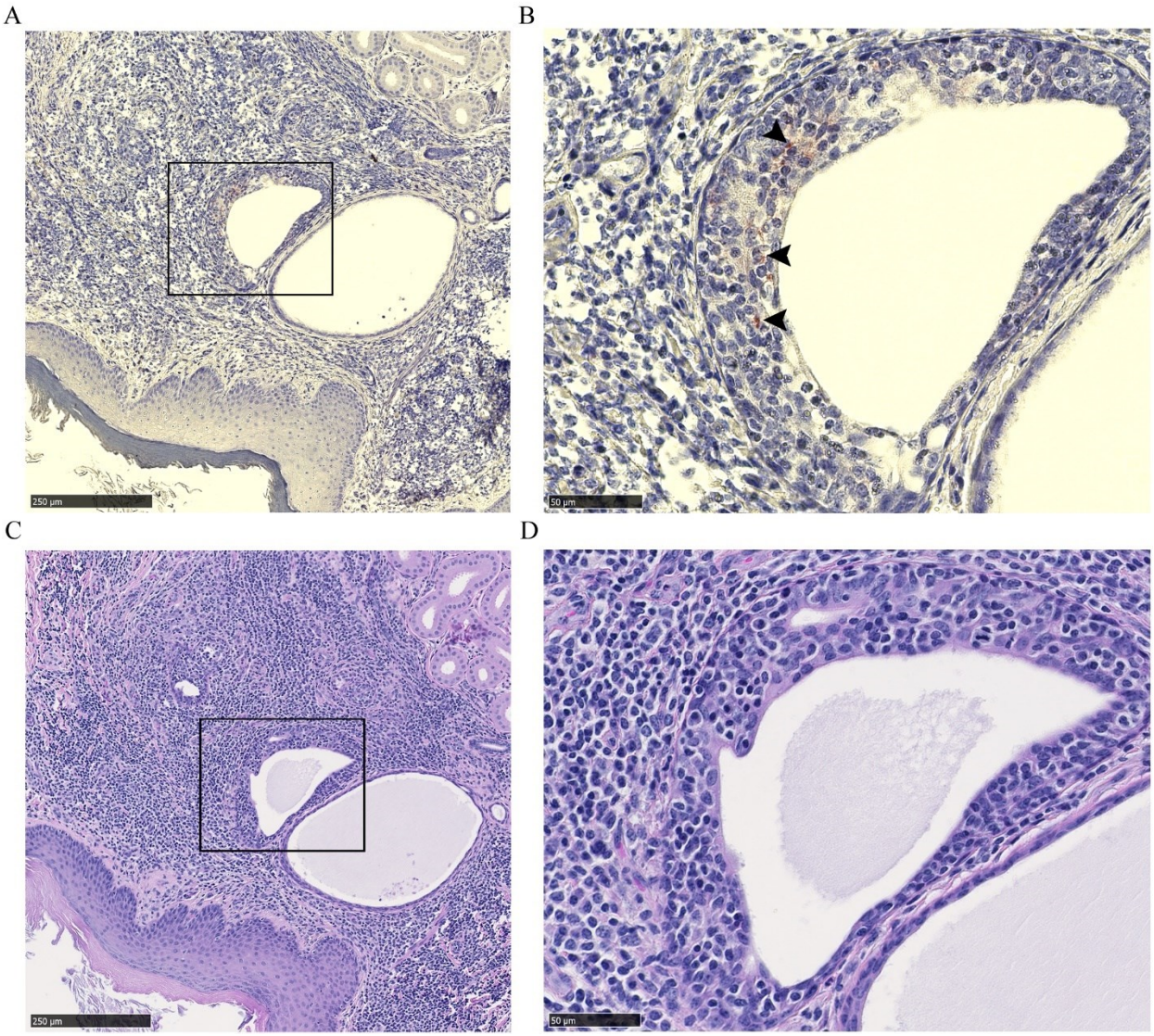

Figure 3.5. PrP^{CWD} immunolabeling within the acrosyringeal epidermis of a female mule deer hind interdigital gland. A) Immune cell infiltrates between epidermis and sudoriferous glands. B) Increased magnification of the inset showing PrP^{CWD} (red, arrows) within the acrosyringeal epidermis of a dilated sudoriferous tubule immunolabeled with anti-PrP BAR224 (1:2,000). C-D) Adjacent section haematoxylin and eosin staining.

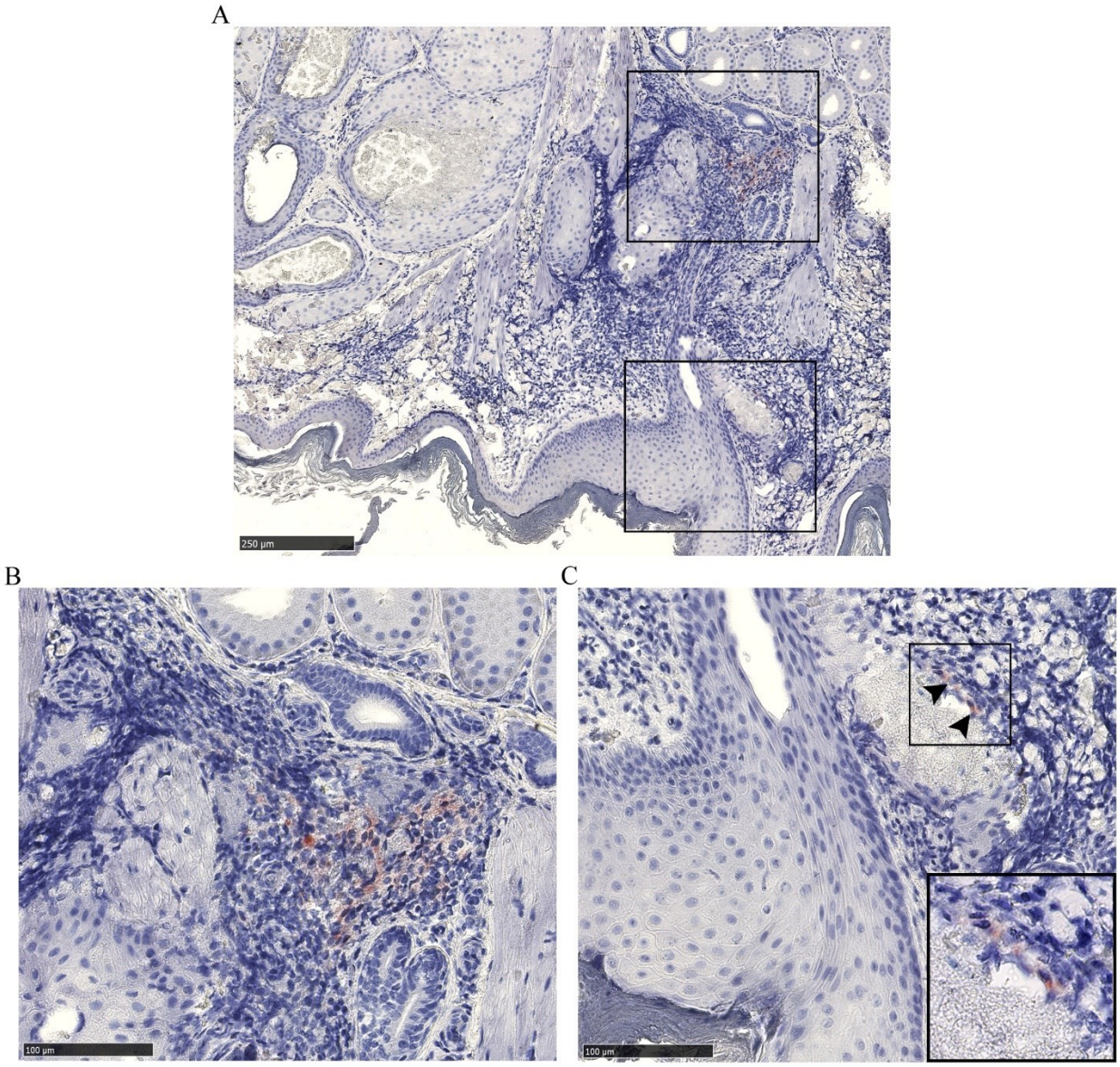

Figure 3.6. Adjacent section to **Figure 3.4** showing hind interdigital gland PrP^{CWD} immunolabeling in a CWD-infected mule deer. Immune cell infiltrates near the epidermis, between sebaceous and sudoriferous glands. B) Increased magnification of the upper inset showing PrP^{CWD} immunolabeling adjacent to sudoriferous gland tubules. C) Increased magnification of the lower inset showing PrP^{CWD} immunolabeling (red, arrows) adjacent to a sebaceous glandular element. Inset shows PrP^{CWD} with increased magnification. PrP^{CWD} was immunolabeled with anti-PrP BAR224 (1:2,000).

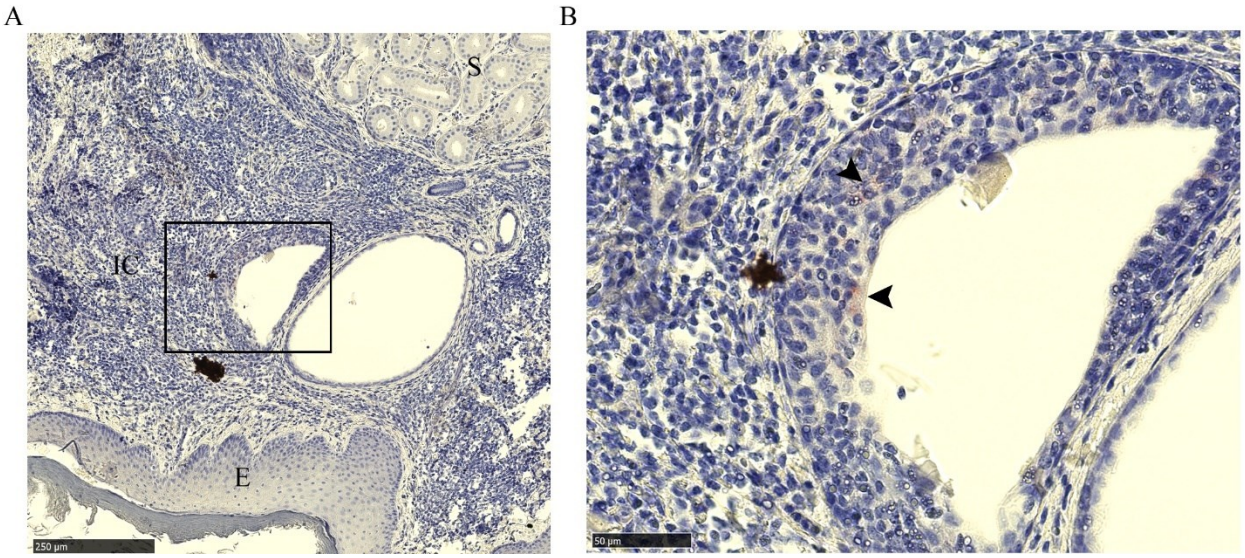

Figure 3.7. Sequential section to **Figure 3.5** showing hind interdigital gland PrP^{CWD} immunolabeling in the acrosyringeal epidermis of a dilated sudoriferous gland from a CWD-infected mule deer. A) Immune cell infiltrates and vessels between the epidermis and sudoriferous glands. B) Increased magnification of the inset showing acrosyringeal epidermis with PrP^{CWD} (arrows). PrP^{CWD} was immunolabeled with anti-PrP BAR224 (1:2,000). Abbreviations: E, epidermis; IC, immune cell infiltrates; S, sudoriferous glands.

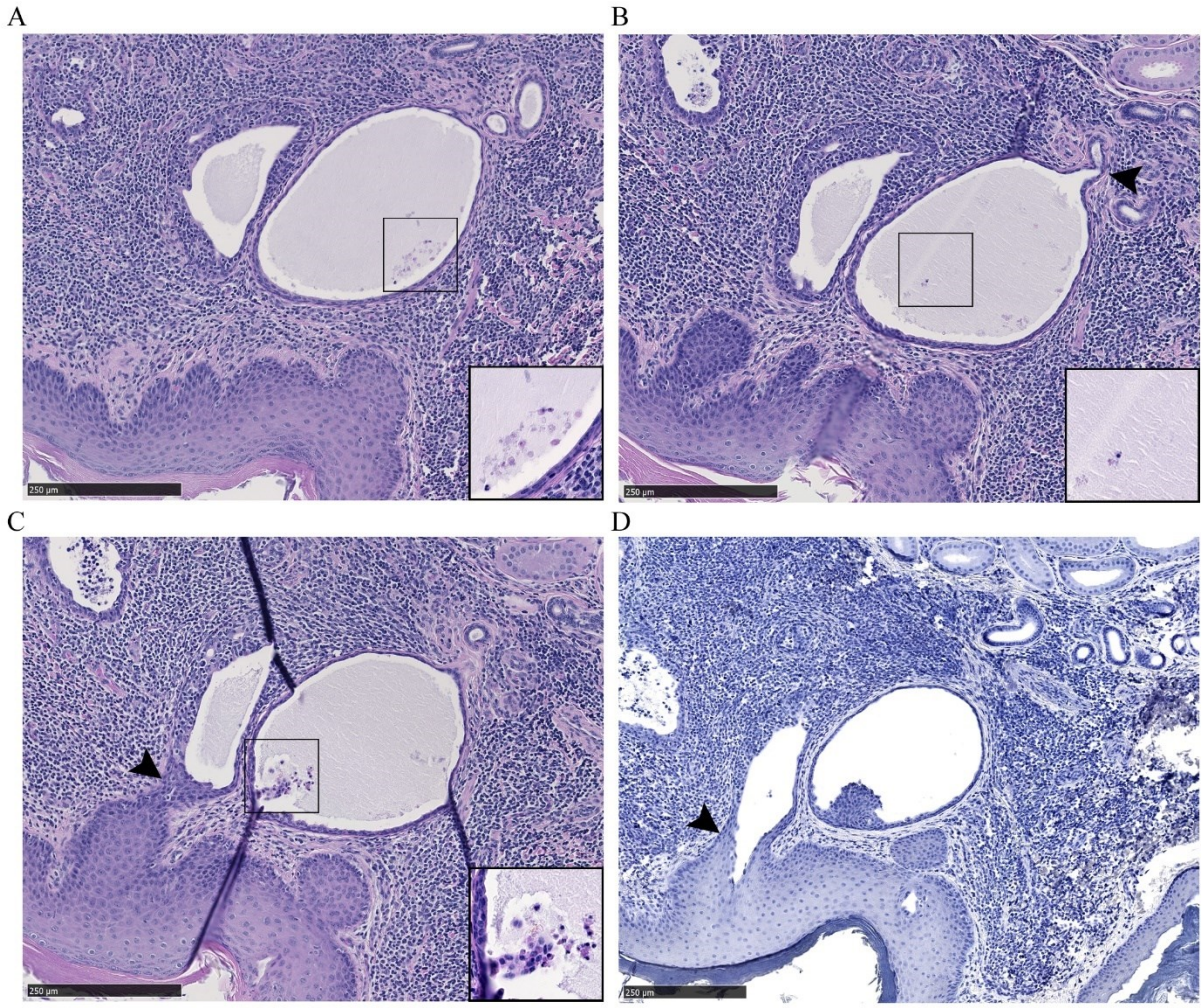

Figure 3.8. Identification of the acrosyringium and miliaria. A) Section adjacent to **Figure 3.5A** which presented with PrP^{CWD} immunolabeling in the acrosyringeal epidermis. B) Deeper sections showing the joining of the larger dilated sudoriferous duct to narrower coils (black arrow) indicating miliaria profundum. C-D) Visualization of the dilated acrosyringeal epidermis (miliaria rubra) joining to the external epidermis (black arrows). Ectopic lymphocytes in the lumen of the larger dilated tubule are observed in most sections (insets). Sections (A-C) were stained by haematoxylin and eosin. Section (D) was probed with BAR224 (1:2,000) with haematoxylin counterstaining.

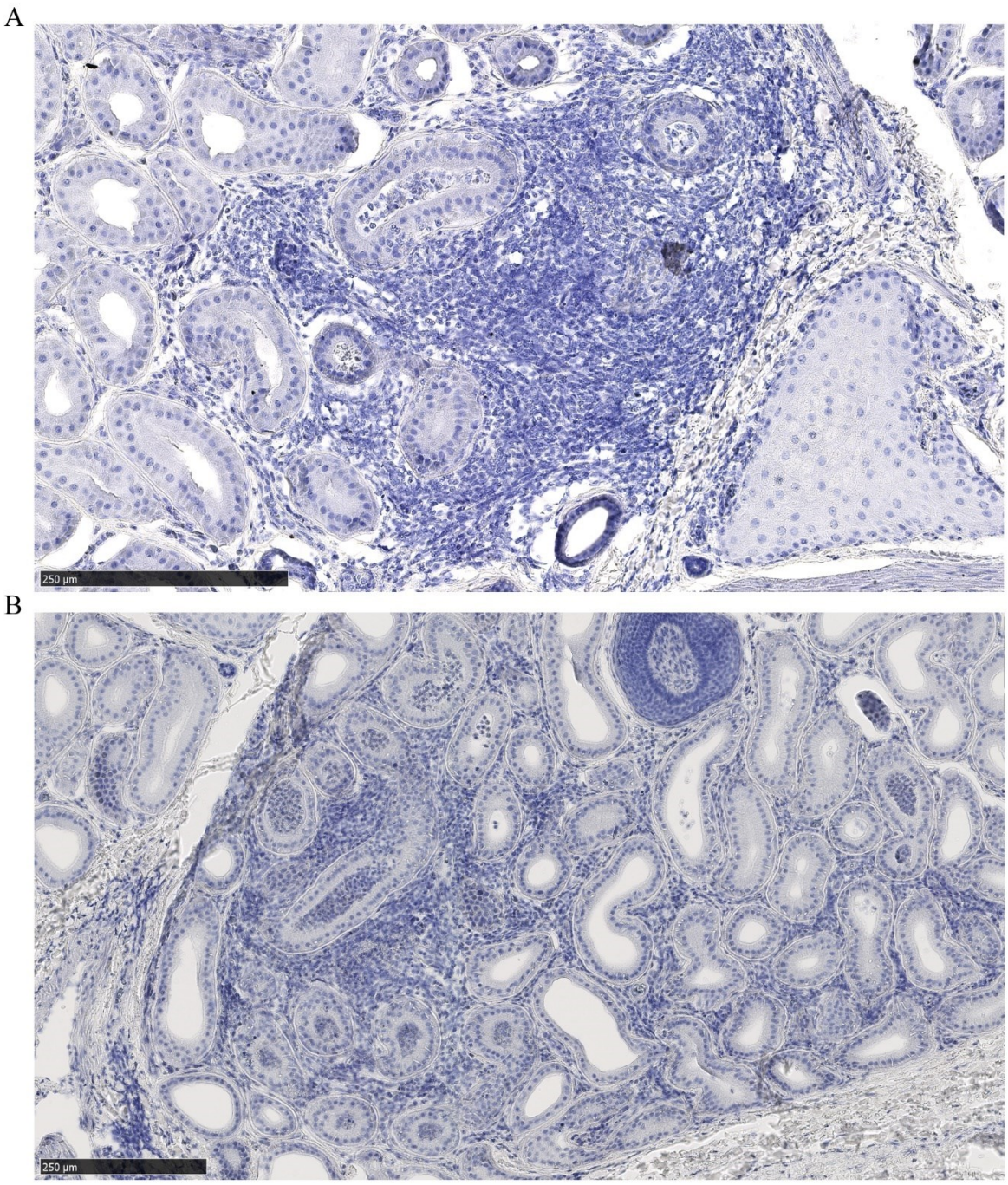

Figure 3.9. Leukocytic infiltration of sudoriferous gland lumen in the hind leg interdigital glands of A) female mule deer with PrP^{CWD} deposits in other regions of the section, and B) an uninfected male mule deer. PrP^{CWD} probed with BAR224 (1:2,000) and counterstained with haematoxylin.

3.4.2 Detection of interdigital PrP^{CWD} by RT-QuIC and sPMCA

Interdigital glands of male mule deer forefeet harvested in 2018 on CFB Wainwright, Alberta were tested for the presence of PrP^{CWD} by sPMCA in a blinded study. 19 interdigital glands from the forefeet of 10 male mule deer were tested (only one interdigital gland was collected from one of the animals). Seven rounds of sPMCA were required to amplify detectable levels of PrP^{CWD}. All samples were retested by sPMCA in a second trial to examine result consistency (**Figure 3.10**). sPMCA yielded several inconsistencies between trials and a high rate of false positives when provided the provincial CWD surveillance results (**Table 3.1**). sPMCA successfully identified 2 of 3 CWD-infected animals, but with 3 false positives from a sample size of 10 animals.

The RT-QuIC analysis included 4 interdigital, 2 tarsal, and 2 metatarsal glands of a clinically-positive female mule deer and 19 interdigital glands from 10 male mule deer also used for sPMCA testing. Blinded RT-QuIC testing returned faster, single-round results with accurate diagnostic results (**Figure 3.11**, **Table 3.1**). The best results were obtained using 0.5% (w/v) interdigital gland homogenates. RT-QuIC of interdigital glands correctly identified all CWD-positive animals with no false positives or negatives (**Table 3.1**). Infectivity was not identified by RT-QuIC in the metatarsal and tarsal glands of the clinically-affected deer. Interdigital gland samples (0.5%) that tested positive crossed the negative control threshold between 30 and 46 hours - later than all CWD-infected reindeer brain positive controls. All CWD-infected mule deer were determined to have wildtype *PRNP* protein sequences with the exception of individual 136227 which was heterozygous for a previously known D20G polymorphism [617].

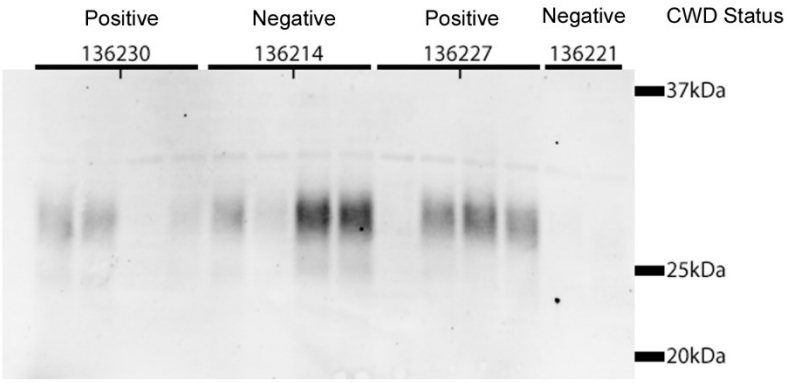

Figure 3.10. Detection of PrP^{CWD} in blinded mule deer leg interdigital gland samples by sPMCA. Representative western blot of 7th round sPMCA testing of each interdigital gland in duplicate.

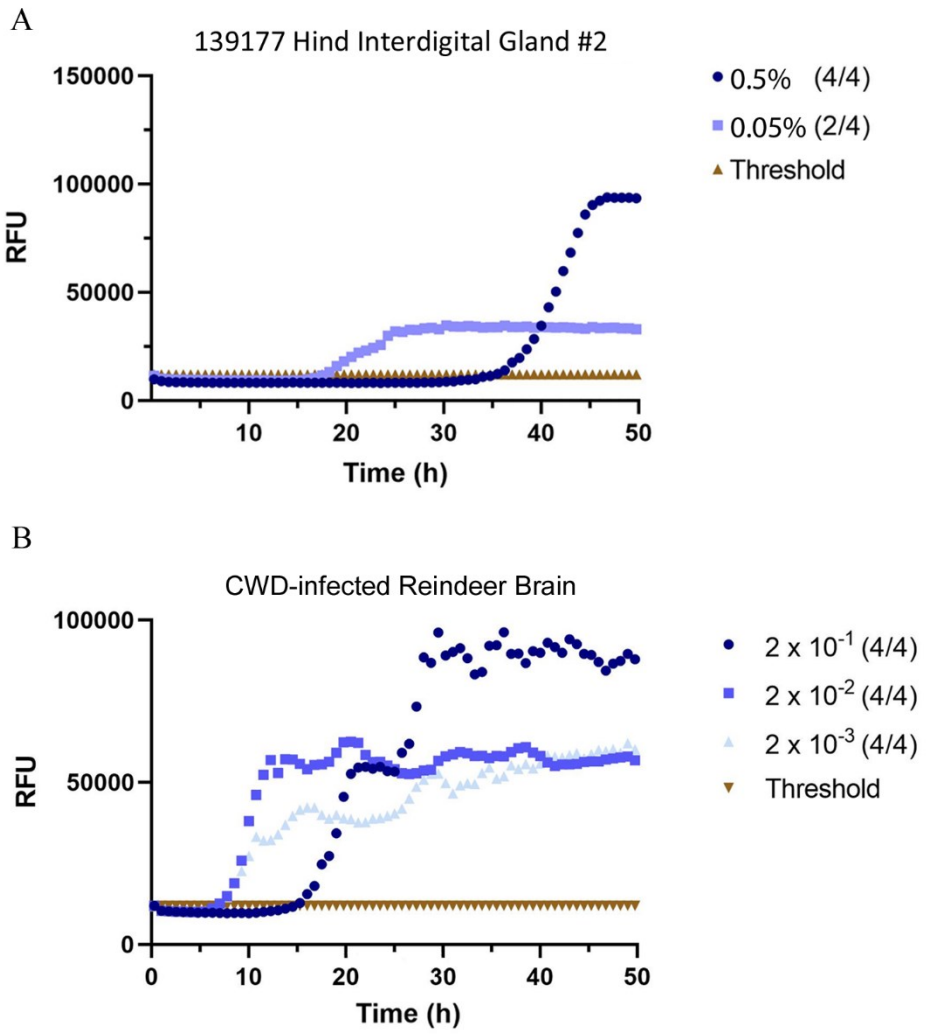

Figure 3.11. RT-QuIC detection of PrP^{CWD} in blinded mule deer leg interdigital glands. A) Representative example of single-round RT-QuIC detection of PrP^{CWD} in one interdigital gland of a CWD-infected mule deer. B) CWD-infected reindeer brain homogenate positive control. Samples were tested in quadruplicate with average relative fluorescence units (RFU) displayed. Gland homogenates were diluted to 0.5% and 0.05% (w/v) final concentrations.

Table 3.1. Blinded detection of PrP^{CWD} in interdigital (ID), metatarsal (MET), and tarsal (TAR) glands by sPMCA and RT-QuIC.

Deer Tissue & Identification	Provincial CWD Status	sPMCA		RT-QuIC				
		Trial 1	Trial 2	0.5% GH			0.05% GH	
136179 ID	Negative	n=2 (0/4)	(0/4)	n=2	(0/4)	(0/4)	(0/4)	(0/4)
136180 ID	Negative	n=2 **(2/4)**	**(2/4)**	n=2	(0/4)	(0/4)	(0/4)	(0/4)
136207 ID	Negative	n=2 (0/4)	(1/4)	n=2	(0/4)	(0/4)	(0/4)	(0/4)
136214 ID	Negative	n=2 (1/4)	**(3/4)**	n=2	(0/4)	(0/4)	(0/4)	(0/4)
136216 ID	Negative	n=2 (0/4)	(0/4)	n=2	(0/4)	(0/4)	(0/4)	(0/4)
136221 ID	Negative	n=2 **(2/4)**	(1/4)	n=2	(0/4)	(0/4)	(0/4)	(0/4)
136227 ID	**Positive**	n=2 **(4/4)**	**(3/4)**	n=2	(1/4)	**(2/4)**	(0/4)	(1/4)
136229 ID	Negative	n=2 (0/4)	(0/4)	n=2	(0/4)	(0/4)	(0/4)	(0/4)
136230 ID	**Positive**	n=2 **(3/4)**	**(3/4)**	n=2	(1/4)	**(4/4)**	(0/4)	**(2/4)**
136237 ID	**Positive**	n=1 (0/2)	(0/2)	n=1	**(2/4)**		(1/4)	
139177[a] ID	**Positive**			n=4	**(3/4)**	**(4/4)**	(1/4)	**(2/4)**
MET					**(4/4)**	**(4/4)**	(0/4)	(0/4)
TAR				n=2	(1/4)	(0/4)	(0/4)	(0/4)
				n=2	(0/4)	(0/4)	(0/4)	(0/4)

Number of glands (n) tested by 7 rounds of sPMCA in duplicate or by one round of RT-QuIC in quadruplicate. Samples with 2 or more positive replicates are bolded.
Gland homogenates (GH) (0.5% or 0.05% (w/v)) were tested by RT-QuIC in quadruplicate.
[a]Individual 139177 was a mule deer clinically affected with CWD

3.4.3 Detection of PrP^{CWD} in soil extracted from a hoof by sPMCA

A soil sample was obtained from between the hoof digits of clinically positive mule deer 139177. All four interdigital glands of this deer tested positive by RT-QuIC, but fixed samples were not available for immunohistochemistry. CWD-infected brain, the hoof soil sample, and negative control soil from Alberta were analyzed by 5 rounds of sPMCA. The hoof soil amplified proteinase K-resistant material - indicating the possible presence of PrP^{CWD} (**Figure 3.12**).

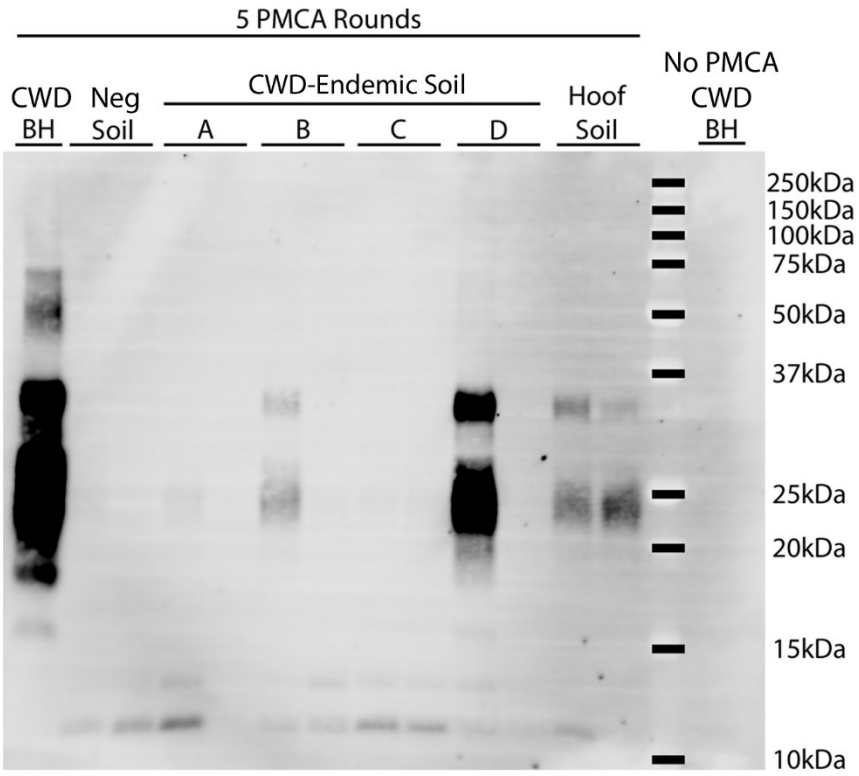

Figure 3.12. Detection of PrP^{CWD} from soil samples of CWD-endemic regions. Soil samples from a CWD-free region (Neg soil) and from CWD-endemic areas that had undergone a PrP^{CWD}-extraction procedure were subjected to 5 rounds of PMCA in duplicate. Samples were compared to 0.1% CWD-infected brain homogenate (BH) controls with and without PMCA. Hoof digits of CWD positive 139177 female mule deer.

3.5 Discussion

PrP^{CWD} was detected in the interdigital glands of CWD-positive mule deer. CWD-infected white-tailed deer hooves were not available for this study. PrP^{CWD} accumulation of the female mule deer occurred primarily in the immune cells of the glandular leukocytic infiltrates (**Figure 3.3**, **Figure 3.4**). The structures associated with the PrP^{CWD} we describe - namely the infiltrating immune cells, but also the sudoriferous and sebaceous glands – were previously found to express PrP^{C} (Chapter 2) [604]. Initiation and establishment of CWD infection in the interdigital gland is possible; however, centrifugal spread of PrP^{CWD} to the interdigital glands is a strong and more

plausible possibility. Circulating immune cells carrying PrP^{CWD} or PrP^{Sc} in prion infected animals are known to be concentrated in sites of inflammation - making them easier to identify by immunohistochemistry [152, 173, 175, 249, 618-620]. The interdigital glands of mule deer possess numerous dense leukocytic infiltrates, indicating that they are subject to more inflammation relative to other integumentary glands or deer (Chapter 2) [252, 404, 604] which likely explains why infectivity was readily observed in the interdigital gland and not in the metatarsal or tarsal glands (**Table 3.1**). Leukocytic infiltrates in the interdigital glands of white-tailed deer are either less dense or absent relative to mule deer (Chapter 2) [252, 474, 604]. The reduced propensity for white-tailed deer to have dense leukocytic infiltrates in the interdigital glands may translate into less sensitive detection of PrP^{CWD} using interdigital gland tissues for that species. The presence of leukocytic infiltrates in the interdigital skin of healthy sheep [621-622] suggests that interdigital tissue testing could also be valuable for diagnosis of scrapie.

We report the presence of PrP^{CWD} by immunohistochemistry within the interdigital gland of a CWD-infected female mule deer. The other CWD-infected mule deer examined by immunohistochemistry had no observable PrP^{CWD} which could be attributed to lesser grade of immune cell infiltration in that individual. Cautioned interpretation of the results is warranted when considering that PrP^{CWD} was observed by immunohistochemistry in only one of two CWD-infected animals where fixed samples were available. Immunolabeling of PrP^{CWD} was observed immediately adjacent to sudoriferous and sebaceous glands (**Figure 3.3A-B**). The source of the PrP^{CWD} observed within the acrosyringeal epidermis (**Figure 3.5B**) could either represent a novel prion tropism or, based on the dense lymphocytic infiltration, PrP^{CWD}-containing lymphocytes infiltrating the epidermis. The PrP^{CWD} immunolabeling was located closer to the lumen of the acrosyringium and was not observed among the adjacent infiltrating interstitial lymphocytes

(**Figure 3.5B**, **Figure 3.7**). The novel tropism of the acrosyringium is supported by observation of PrP^{C} in the interdigital gland epidermis including the glandular ducts (Chapter 2) [604], but is countered by higher cell division rates which are generally inversely correlated with cell propensity for prion replication [601]. Prions have been detected in the skin of a variety of prion diseases [154, 623-626]. Using proteinase K-digested tissue blot immunoassay, Thomzig *et al*. identified structures with PrP^{Sc} deposition in clinically affected hamsters infected with the 263K prion strain [154]. Differing from our findings, the authors found PrP^{Sc} in a variety of cutaneous nerve fibers, plexuses, and follicular hair innervations.

Dissemination of CWD prions into the environment from the interdigital glands is a possible consequence of infectivity in a secreting gland. Cervid salivary glands are a source of PrP^{CWD} [38-39, 41, 44-45, 123, 243, 261-262, 603], so detecting PrP^{CWD} in other secretory glands could be expected. Direct secretion of PrP^{CWD} could occur as infiltrating immune cells disrupt the architecture of the sebaceous glands (**Figure 3.4B**) or invade the sudoriferous tubules (**Figure 3.8**, **Figure 3.9**). The presence of PrP^{CWD} immunolabeling within the acrosyringeal epithelium is supportive of possible interdigital gland secretion. An analogous mechanism of integumentary gland secretion of prions exists in scrapie. Comparable to our results, immunohistochemistry of sheep with mastitis identified scrapie-associated PrP^{Sc} in lymphoid follicles adjacent to mammary gland ducts and within mammary gland ducts and acini [152, 173-175]. Mastitis is not required for secretion of PrP^{Sc} into milk of scrapie-infected ewes [152, 156, 175]. More disseminated leukocytic infiltration in the interdigital and mammary glands is expected to assist with visualizing PrP^{CWD} and PrP^{Sc} by immunohistochemistry. Visibly less immune cell infiltration of the interdigital glands of the single infected male mule deer analyzed may explain why PrP^{CWD} was not visualized by immunohistochemistry in those samples.

Detection of PrP^{CWD} from soil adventitiously lodged between the hoof digits of a clinically-affected deer (**Figure 3.12**) that had all four interdigital glands test positive by RT-QuIC lends credence to the theory of soil contamination by interdigital gland secretions. Due to the avidity of binding of prions to soil and soil components, detection using sPMCA is challenging. Analysis of additional soil collected from deer hooves will validate these current results and provide further information regarding the amount of infectivity present. The feasibility of uninfected deer being exposed to and infected by PrP^{CWD} through the interdigital glands could not be determined by our study.

Our study demonstrated that RT-QuIC was more specific and sensitive interdigital gland than sPMCA under the conditions tested. Slow interdigital gland sample RT-QuIC reactions (0.5% homogenates crossing the negative control thresholds between 30 and 46 hours) indicate that the seeding activity in the tissue homogenate is very low, or that reaction conditions for gland tissue could be optimized. Inaccurate detection of PrP^{CWD} in the interdigital glands of deer by 7 rounds of sPMCA is further suggestive of low infectivity. False positive results can be attributed to the high number of PMCA rounds [611]. It is possible that unidentified components of the interdigital gland homogenates, possibly ceraceous gland secreta, inhibit the PMCA reactions. Disintegration of sebum and other homogenate components by sonication may sequester prion seeding activity. For the RT-QuIC reactions, uninfected gland homogenates may have been more appropriate negative controls but, as our samples were blinded, we did not have material for this use. An opportunity exists to explore post- and antemortem CWD diagnosis using interdigital gland biopsies or possibly the hair and secretions. Larger sample sizes of both white-tailed deer and mule deer will be required to determine what stage of disease PrP^{CWD} first accumulates in the interdigital glands and for determining the diagnostic value of testing interdigital gland

tissues. Our small sample size prevents us from determining the frequency and abundance of PrP^{CWD} accumulation in interdigital glands. Perhaps more importantly, any possible contribution of interdigital gland PrP^{CWD} secretion into the environment and any associated disease transmission effects has yet to be investigated.

Detection of PrP^{CWD} in the interdigital glands is a novel finding that has implications for ante- and post-mortem prion diagnosis. RT-QuIC was determined to be the preferred method of prion detection over sPMCA using interdigital gland homogenates. The presence of PrP^{CWD} in the interdigital glands is likely reflective of the dense leukocytic infiltrates that are commonly observed in the interdigital glands of mule deer. Future bioassays will provide an assessment of the infectivity present in the interdigital glands relative to other tissues. Secretion of PrP^{CWD} into the environment is suspected due to the presence of PrP^{CWD} near secreting sebaceous and sudoriferous glands. Identification of PrP^{CWD} in additional interdigital glands would suggest a role for these glandular secretions in horizontal CWD transmission. Exposure of uninfected animals through the interdigital glands is possible but is currently lacking evidence when considering that PrP^{CWD} was only detected in the interdigital glands of animals identified as CWD-positive by existing CWD-surveillance methods.

Chapter 4 Quantification of prion inactivation and denaturation using enzyme-linked immunosorbent assay

Data in this chapter has been included in a manuscript to be submitted to Chemosphere, a peer-reviewed journal, as: Ness, Anthony; Dzhabrailov, Isa; Kuznetsova, Alsu; Martinez Moreno, Diana; Tang, Xinli; Aiken, Judd; McKenzie, Debbie (2022). Quantification of prion inactivation by humic acid using enzyme-linked immunosorbent assay

4.1 Abstract

Chronic wasting disease (CWD) is a contagious neurodegenerative prion disease of cervids. Infectious CWD prions are shed from infected hosts - contaminating the environment for years. Soil-derived humic substances possess anti-prion properties. We have developed an indirect enzyme-linked immunosorbent assay (ELISA) to quantify decontamination of prion-contaminated surfaces by humic acid. The method better represents environmental prion contamination by using adsorbed prions in contrast to older aqueous inactivation experiments. Enriched preparations of infectious prions (cervid PrP^{CWD} and hamster PrP^{Sc}) were adsorbed to a solid support prior to humic acid exposure and subsequent immunodetection. PrP^{CWD} and PrP^{Sc} levels decreased following humic acid exposure in a dose-dependent manner. The N-terminal regions of PrP^{CWD} and PrP^{Sc} were more sensitive to humic acid than the central region either when adsorbed or in solution. Adsorbed prions are less susceptible to humic acid inactivation than prions in solution. This high throughput ELISA will permit quantitative analysis of different putative anti-prion compounds for their impact on adsorbed prions to simulate environmental prion decontamination.

4.2 Introduction

Chronic wasting disease (CWD) is a contagious, fatal prion disease affecting farmed and free ranging cervids. Both the geographic range and disease prevalence of CWD have expanded over the past two decades, with 30 American states, 4 Canadian provinces, Northern Europe and South Korea all reporting cases in captive and/or free-ranging animals. In captive cervid farms, the majority of animals can become infected [231-232]. In CWD infections, as with all prion diseases, the cellular form of the prion protein (PrP^{C}) is converted to the infectious isoform (PrP^{CWD}) [1-2, 4, 627]. PrP^{CWD} prions are shed into the environment by body fluids, feces, and

carcasses during the preclinical and clinical phases of disease [38-39, 41, 44-46, 177]. CWD-contaminated environments, including soils, vegetation, salt licks, and feeding sites, contribute to indirect transmission of CWD [37, 46-51, 185]. Prions are notoriously difficult to destroy, remaining infectious in the environment for years to decades [35, 181-183]. Repeated applications of sodium hypochlorite to a contaminated farm site failed to prevent naïve animal infection - infectious dust being implicated as a possible source of reinfection [570-572]. South Korea attempted to eradicate CWD by an aggressive protocol involving stripping the top 30cm of soil, multiple 2N sodium hydroxide sprays, and the use of a flamethrower [573] - an expensive and destructive procedure that requires further land reclamation. With few exceptions, CWD-endemic environments are not currently remediated.

Humic substances, including humic acids and fulvic acids, have anti-prion properties [592-593]. CWD-infected brain homogenates exposed to humic acid in solution resulted in decreasing PrP^{CWD} detection by western blot. Infectious prion titre is also reduced by humic acid as demonstrated by animal bioassays [592-593]. Past studies of humic acid inactivation of prions have focussed on prions in solution. To be effective in the environment, humic acids and other putative decontaminants must inactivate prions adsorbed to solids. We have developed a high throughput enzyme-linked immunosorbent assay (ELISA) for measuring the impact of humic acid solutions on adsorbed prions. This assay allows for the quantification and comparison of anti-prion compound effects on adsorbed prions to simulate environmental prion decontamination.

4.3 Methods

4.3.1 Enrichment of PrP^{CWD} and PrP^{Sc} from brain homogenates

Brain samples from CWD-positive deer (hunter harvested) were provided by Alberta Environment and Parks. Brain samples, from the brainstem at the level of the obex, were homogenized in phosphate buffered saline (PBS) (130mM NaCl, 7mM $Na_2HPO_4 \cdot 7H_2O$, 3mM $NaH_2PO_4 \cdot 1H_2O$, pH 7.4) to 10% (w/v). Homogenates were screened for disease-associated proteinase-K (PK) resistant prion protein (PrP^{res}) by dot blot, and western blot using the anti-PrP SHA31 antibody (Cayman Chemical, USA); those with high levels of PrP^{res} were selected for PrP^{CWD} enrichment. CWD-negative whole-brain homogenates were sourced from adult white-tailed deer in Saskatchewan, Canada and Wisconsin, USA. Brains from clinically affected Syrian golden hamsters were homogenized and enriched for PrP^{Sc} (Hyper, Drowsy, 263K hamster prion strains).

A combination of protease digestion, phosphotungstic acid hydrate (PTA) precipitation, and size-exclusion filtration were utilized to enrich PrP^{CWD} and PrP^{Sc}. Enrichment protocols followed that of Wenborn *et al*., [627] with the following modifications. Brain homogenates (10% (w/v) were clarified by centrifugation for 1 minute at 100 rcf. Clarified supernatant (500µL) was digested with either pronase E (PE) (MilliporeSigma, USA) (100µg/mL) for 2 hours at 37°C with agitation or with PK (MilliporeSigma, USA) (50µg/mL) with 10mM $CaCl_2$ for 30 minutes at 37°C with agitation. Proteins were precipitated by the addition of 500µL of 4% (w/v) sodium lauroylsarcosine in PBS and 81.3µL of 4% (w/v) phosphotungstic acid hydrate, 170mM magnesium chloride (pH 7.40), incubated for 30 minutes at 37°C with agitation and centrifuged at 16,100 rcf for 30 minutes. The supernatant was removed and discarded. PTA-precipitated pellets were resuspended in 80µL PBS, multiple pellets generated from the same brain

homogenate were combined and filtered with a 0.45µm Millex-HA syringe filter (MilliporeSigma, USA). For PK-digested samples, AEBSF (4-(2-aminoethyl)benzenesulfonyl fluoride hydrochloride) protease inhibitor (Thermo Fisher Scientific Inc., USA) was added to the filtrate to a final concentration of 0.25mM. Protein concentrations were determined using the Pierce™ BCA Protein Assay Kit (Thermo Fisher Scientific Inc., USA).

4.3.2 Assaying of protein desorption from microplates by humic acid

High-binding 96 well flat-bottomed strip microplates (Greiner Bio-One International, GmbH, Austria) were coated with 3% (w/v) bovine serum albumin (BSA) (VWR International, LLC., USA) in 50mM sodium carbonate-bicarbonate (pH 9.6). The BSA was adsorbed to the plate by incubating at room temperature (RT) for 2 hours, then overnight at 4°C. Two microplate rows were left uncoated for no-protein controls and for a BSA concentration standard curve. Following washes with tris-buffered saline (TBS-T) (0.1% tween-20, pH 7.4), the samples were treated with either humic acid (MilliporeSigma, USA) (in PBS) or PK (MilliporeSigma, USA) (in PBS with 1mM calcium chloride) in sextuplicate. Wells were exposed to dilution series of PK or humic acid, incubated for 2 hours at RT, then washed with TBS-T. An epitope exposure step to mimic the prion detection ELISA was performed by the addition of 4M guanidine hydrochloride (GdnHCl) in PBS (200µL) for 10 minutes at RT with shaking. After washing with TBS-T, desorption of protein from the microplate was measured at 562nm using a Pierce™ BCA Protein Assay Kit (Thermo Fisher Scientific Inc.). Reference humic acid and BSA (both at 0.1g/L) ultraviolet-visible light (190-840nm) absorbance spectra were measured with a NanoDrop 2000 Spectrophotometer (Thermo Fisher Scientific Inc., USA).

4.3.3 Prion detection by indirect ELISA

In-well detection of adsorbed infectious prions to anti-prion compounds was restricted to direct or indirect ELISAs (**Figure 4.1**). High-binding 96 well flat-bottomed strip microplates (Greiner Bio-One International, GmbH, Austria) were coated with 300ng (hamster) or 500ng (deer) prion preparation per well in 50mM sodium carbonate-bicarbonate buffer (pH 9.6). A reference standard curve was created with a dilution series of recombinant full-length deer PrP or recombinant full-length hamster PrP (Impact Biologicals, USA). Coated plates were incubated at RT for 2 hours, then overnight at 4°C. Humic acid (MilliporeSigma, USA) was prepared in HyClone™ Molecular Biology Grade water (Cytiva, USA). Wells coated with cervid (300ng of total protein per well) or hamster prion (200ng of total protein per well) enriched preparations were exposed to humic acid dilution series (125uL per well) for 2 hours at RT (**Figure 4.2**) or overnight at 4°C, then washed three times with TBS-T. Epitopes were exposed by the addition of 4M GdnHCL (200µL) for 10 minutes at RT with gentle shaking. Wells were blocked with 200µL of 3% (w/v) bovine serum albumin (VWR International, LLC., USA) for 2 hours at RT. Samples were probed with 1:5,000 anti-PrP SHA31 or 1:5,000 SAF32 primary antibody overnight at 4°C, followed by 1:5,000 goat anti-mouse IgG HRP conjugate (Bio-Rad Laboratories, Inc., USA) secondary antibody for 2 hours at RT. Following washes with TBS-T, samples were developed with BioFX® TMB One Component HRP Microwell Substrate (Surmodics, Inc., USA) chromagen. Reactions were terminated by the addition of 50µL of 2N sulfuric acid and absorbance at 450nm measured (**Figure 4.1C**). Matched humic acid dilution treatments of coated preparations were compared with two-way ANOVA multiple comparisons tests with the Bonferroni correction (* $p < 0.05$, ** $p < 0.01$, *** $p < 0.001$).

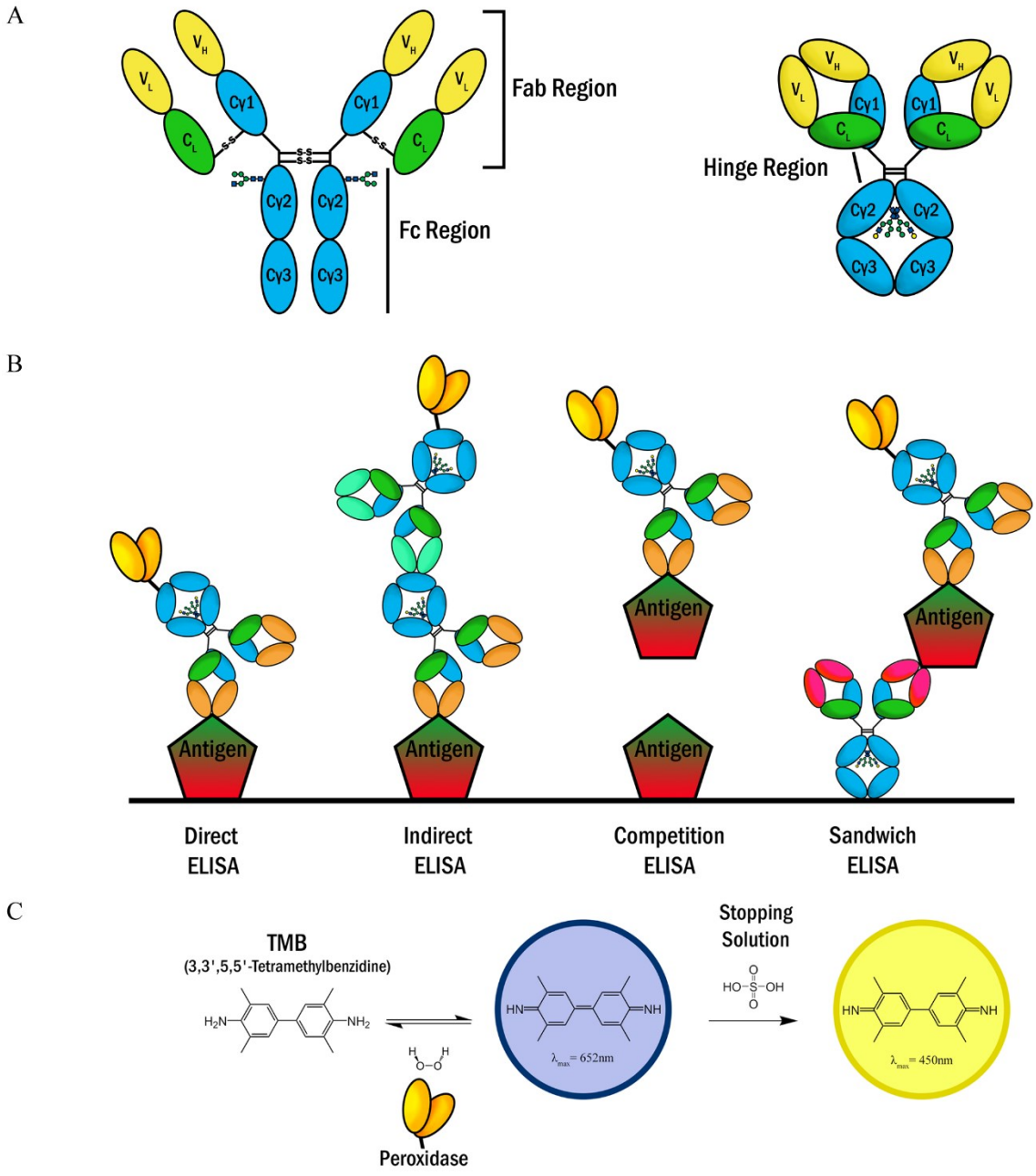

Figure 4.1. Enzyme-linked immunosorbent assay types and TMB detection. A) Antibody structure and B) the four major configurations of ELISA to detect antigen using perodidase-conjugated detection antibodies. C) Reaction mechanism for peroxidase-induced TMB chromogen visualization and reaction product peak absorbance wavelengths. Abbreviations: VL, light chain variable domain; VH, heavy chain variable domain; CL, light chain conserved domain; Cγ, gamma heavy chain conserved domain.

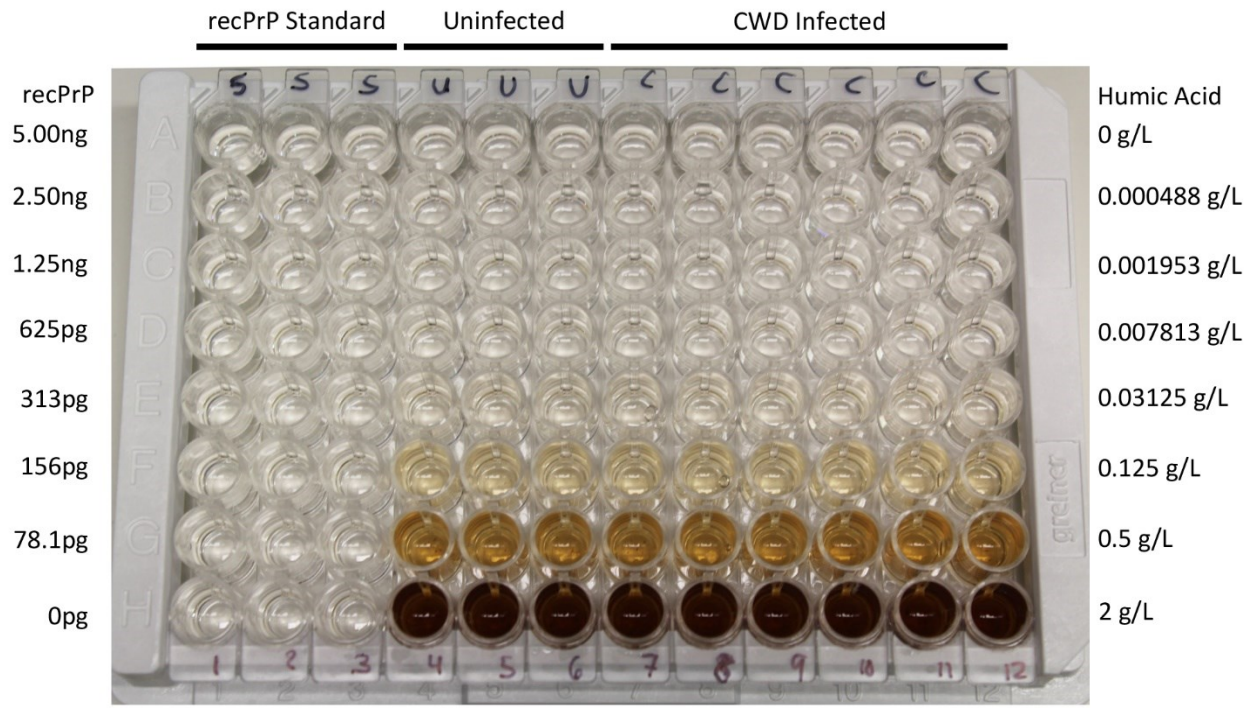

Figure 4.2. Representative ELISA plate with humic acid dilutions. Three sets of samples were coated on the plate: recombinant PrP standard (recPrP), and enriched preparations from uninfected and CWD-infected brains. Concentrations of coated recPrP are presented on the left; humic acid concentrations to the right.

4.3.4 Western blot and silver staining

Prion-enriched samples, adjusted for total protein concentration, were diluted 1:1 with sample buffer [517], denatured for 10 minutes at 100°C. Samples were loaded into 15-well Invitrogen NuPAGE™ 12% Bis-Tris protein gels (Thermo Fisher Scientific Inc., USA), separated in MOPS buffer and transferred to PVDF membranes. Membranes were blocked with 2% (w/v) bovine serum albumin and then probed with anti-prion protein SHA31 monoclonal primary antibody (Cayman Chemical, USA; epitope of 148-155 (*Odocoileus* amino acid sequence)), N5 monoclonal antibody (epitope of 101-104 (*Odocoileus* amino acid sequence)), or SAF32 (epitope is the N-terminal octapeptide repeat region) (**Figure 1.1**). Secondary goat anti-mouse IgG (H+L) AP Conjugate (Promega Corporation, USA) detection antibody was detected using AttoPhos®

AP Fluorescent Substrate System (Promega Corporation, USA) and an ImageQuant LAS 4000 (GE Life Sciences, USA) system. Silver staining of 15-well polyacrylamide Invitrogen NuPAGE™ 12% Bis-Tris protein gels (Thermo Fisher Scientific Inc., USA) was performed with a Pierce™ Silver Stain Kit (Thermo Fisher Scientific Inc., USA) as per the manufacturer's instructions.

For humic acid treatment of PrP^{CWD}- and PrP^{Sc}-enriched preparations in solution, 4µg of protein was mixed with humic acid (0-10g/L) solutions to a final volume of 45µL. Silanized microcentrifuge tubes minimized protein loss to adsorption to the tubes. The mixtures were incubated overnight at 4°C, diluted by the addition of 15µL of 5x Laemmli sample buffer, denatured for 10 minutes at 100°C and analyzed by western blot as described above. Relative total PrP protein expression was compared using pixel intensity analysis with ImageJ software. A box enclosing individual lanes from 15-75kDa were used to determine average pixel intensity.

4.3.5 Synthesis of polystyrene sulfonate microplates

Falcon® 96-well clear flat bottom polystyrene plates (Corning Inc., USA) were modified by the addition of concentrated sulfuric acid to generate polystyrene sulfonate surfaces [628-632]. Polystyrene microplate wells were modified by the addition of 200µL concentrated sulfuric acid (approximately 36 normality) (Thermo Fisher Scientific, USA) to each well. Plates were incubated overnight at room temperature, then washed with deionized water, dried, and sealed for later use.

4.4 Results

4.4.1 Prion enrichments for humic acid inactivation

Infectious prion enrichment methods were compared using silver staining and western blot detection with the anti-PrP SHA31 antibody. Cervid PrP^{CWD} enrichment by pronase E digestion,

PTA precipitation, and 0.45µm filtration (PE-PTA-Filter) eliminated PrP^{C} while contemporaneously concentrating disease-associated PrP^{CWD} (**Figure 4.3**). Enrichment of three hamster prion strains using PE-PTA-Filter or proteinase K digestion, PTA precipitation, and 0.45µm filtration (PK-PTA-Filter) yielded comparable results (**Figure 4.4A, C**). PTA precipitation alone was insufficient for effectively removing PrP^{C} of uninfected controls (data not shown). Silver staining confirmed efficient removal of most contaminants by the enrichment described method (**Figure 4.3B**, **Figure 4.4B, D**). Enriching deer CWD preparations yielded final protein concentrations ranging from 0.07-1.31µg/µL versus 0.03-0.25µg/µL for uninfected, enriched preparations as determined by BCA assay. Hamster purifications yielded concentrations ranging from 0.12-21µg/µL. Beginning with 10mL of 10% brain homogenate would typically yield 1mL of prion-enriched final product.

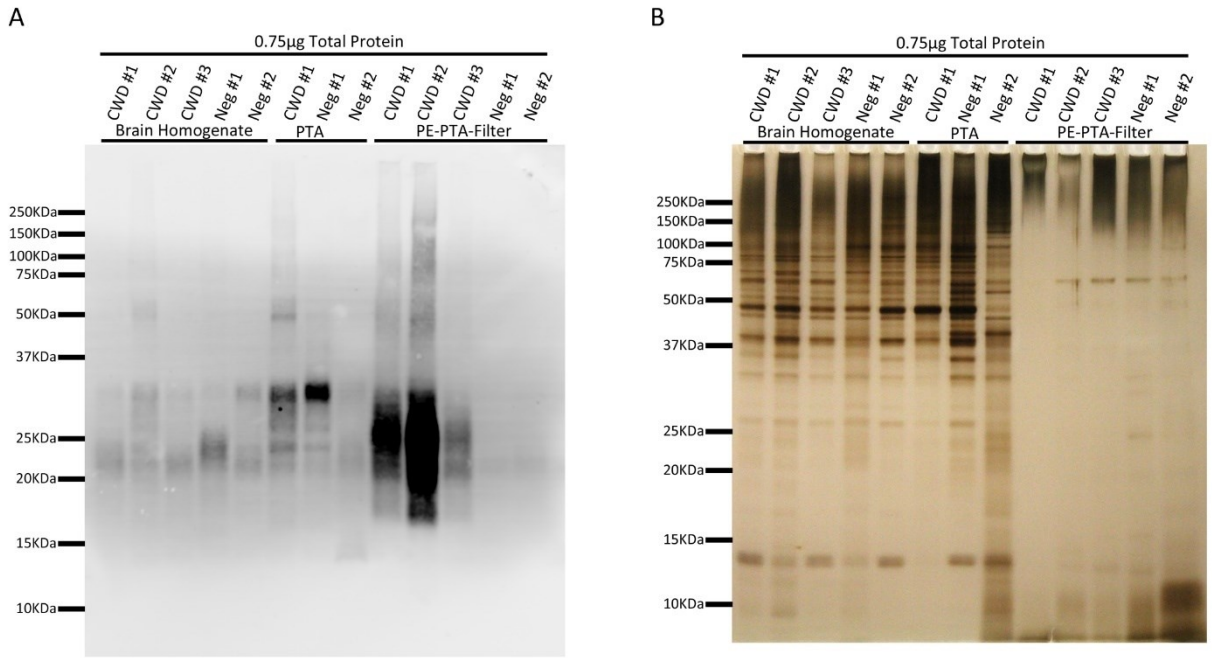

Figure 4.3. Enrichment of deer PrP^{CWD}. Total protein-adjusted preparations of deer prion-infected and uninfected (Neg) brain homogenates with and without PrP^{CWD} enrichment. A) Immunodetection of total PrP by SHA31 and (B) silver stain of the brain preparations. Samples were precipitated with phosphotungstic acid (PTA) or a combination of pronase E (PE), PTA precipitation, and filtered with a 0.45µm pore size membrane.

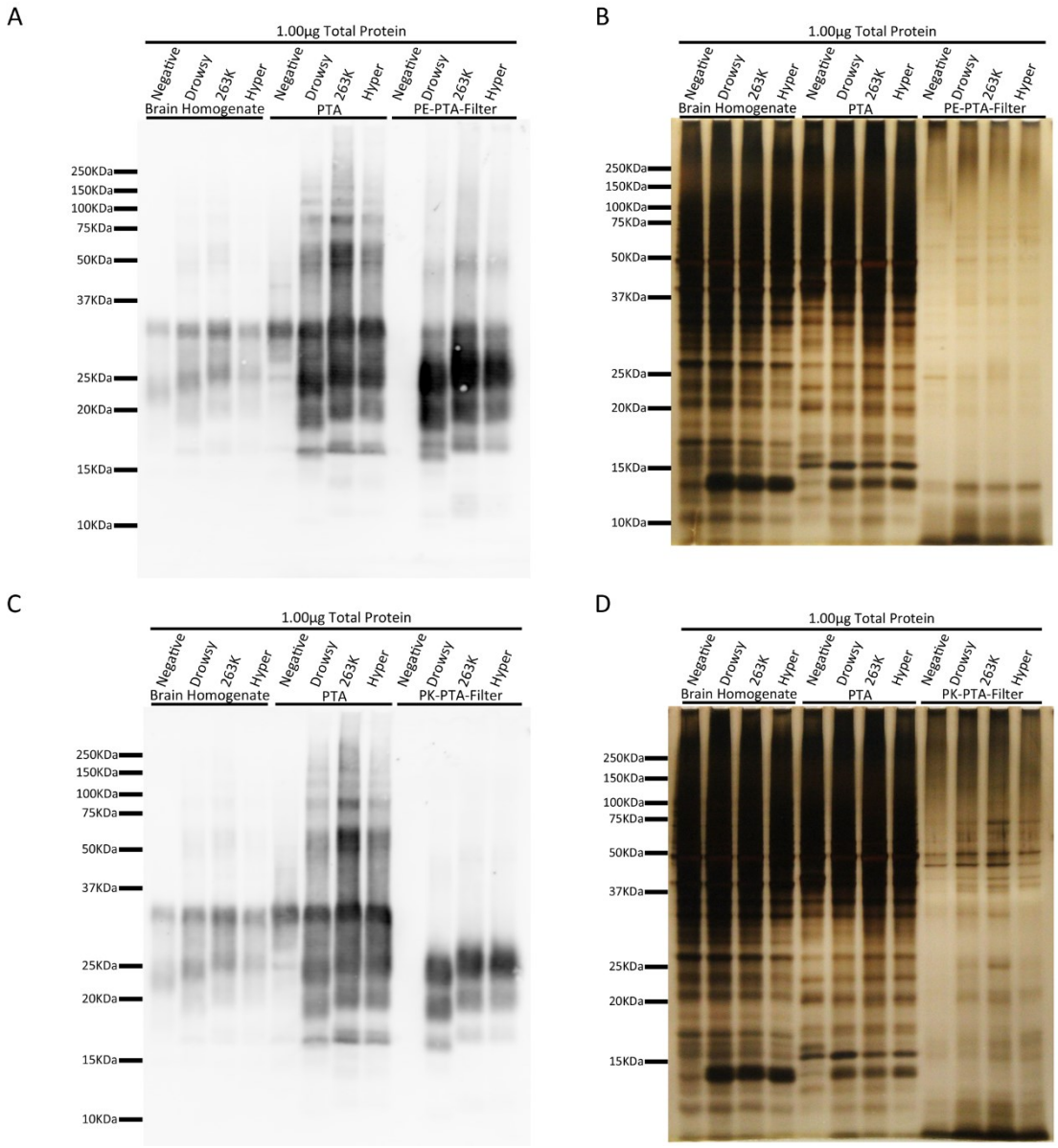

Figure 4.4. Enrichment of hamster PrP^{Sc}. Total protein-adjusted preparations of hamster prion-infected and uninfected (Negative) brain homogenates with and without PrP^{Sc} enrichment. A, C) Immunodetection of total PrP by SHA31 and (C, D) silver stain of the brain preparations. Samples were either precipitated with phosphotungstic acid (PTA) or a combination of pronase E (PE) (A-B), proteinase K (PK) (C-D), PTA precipitation, and filtered with a 0.45µm pore size membrane.

4.4.2 Effect of humic acid and proteinase K on adsorbed protein

To determine whether humic acid treatment desorbs proteins from a microplate surface, a test using bovine serum albumin (BSA) was designed. BSA adsorbed to the surface of microplate wells was exposed to dilution series of humic acid or PK for 2 hours at room temperature. Wells were washed, exposed to 4M GdnHCl for 10 minutes to simulate the epitope exposure step of the prion-coated ELISAs, and washed again. Adsorbed protein was detected using a Pierce™ BCA Protein Assay Kit (Thermo Fisher Scientific Inc.) (**Figure 4.5A**). Elevated 562nm absorbance in samples exposed to humic acid concentrations above 5g/L suggested an increase in adsorbed protein. The increased BCA 562nm absorbance can be explained by co-adsorbed humic acid contributing to the BCA biuret reaction or by humic acid 562nm absorbance (**Figure 4.5B**). In contrast, PK-treated wells demonstrated concentration-dependent reductions of 562nm absorbance indicating loss of enzymatically digested peptide fragments from the wells during washing steps.

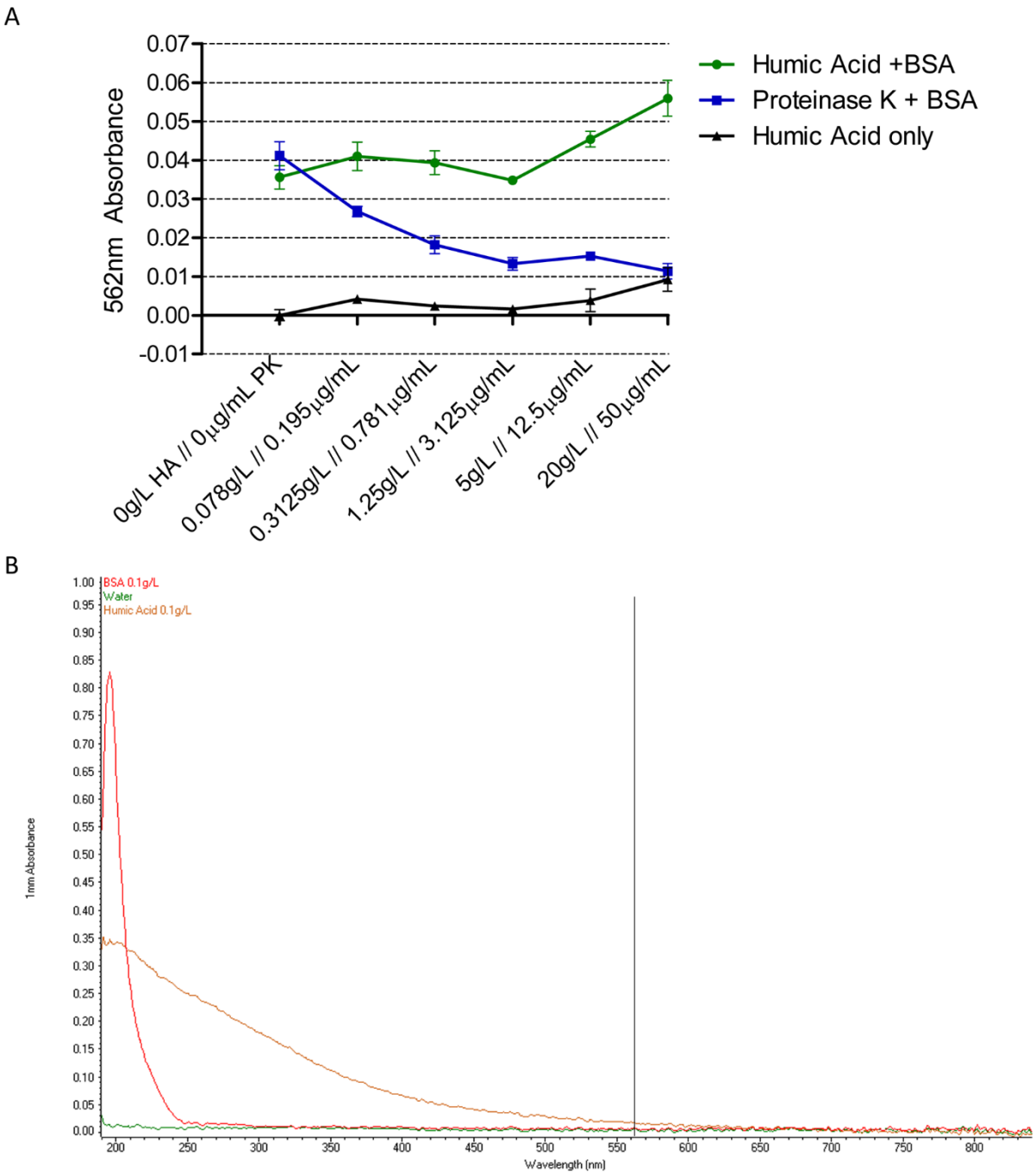

Figure 4.5. Humic acid and proteinase K effects on adsorbed bovine serum albumin. A) Intra-well BCA assay of wells with adsorbed bovine serum albumin (BSA) exposed to dilutions of humic acid or proteinase K for 2 hours at room temperature. Wells were exposed to 4M guanidine hydrochloride for 10 minutes, then washed. B) Ultraviolet-visible light absorbance spectra of humic acid and BSA in water with the 562nm BCA assay absorbance marked. Error bars represent standard error of the mean.

4.4.3 ELISA quantification of prion inactivation by humic acid

PTA precipitations without enzymatic digestion were insufficient for removing PrP^{C} for ELISA detection (**Figure 4.6**). The enhanced purifications (**Figure 4.3** and **Figure 4.4**) were required for the prion inactivation assay. PrP^{CWD} enrichment by PE digestion, PTA precipitation, and 0.45µm filtration is demonstrated by comparing CWD-infected preparations with negative control uninfected preparations (**Figure 4.7**). Total detectable PrP was calculated using a protein standard curve using full-length deer recombinant PrP (**Figure 4.7A-B**). Humic acid treatment of PrP^{CWD} decreased immunodetection in a concentration-dependent manner (**Figure 4.7**). Average PrP^{CWD} detected decreased from 2.253ng for untreated wells to 1.732ng for 2g/L HA-exposed wells while PrP in the uninfected controls (residual PrP^{C}) decreased from 0.097 to 0.045ng for the respective treatments (**Figure 4.7C**). Adsorbed PrP detection was reduced by 23.1% of control signal when treated with 2g/L humic acid for 2 hours at room temperature (**Figure 4.7D**). Assuming an equivalent mass and reduced detection of residual PrP^{C} was present in the infected preparation, total loss of the residual PrP^{C} (0.052ng difference) could account for at most 2.3% of reduced signal detection.

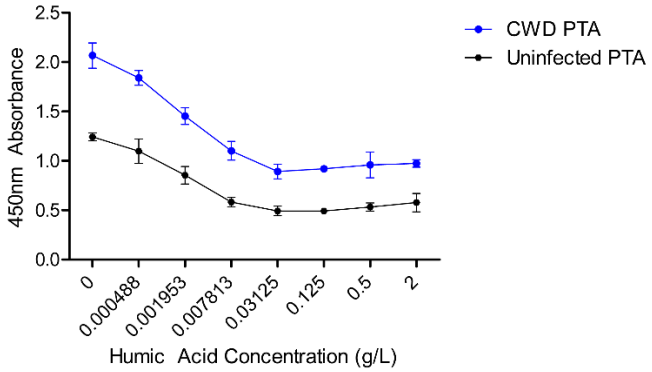

Figure 4.6. Incomplete removal of PrP^{C} by PTA precipitation without enzymatic digestion. Adsorbed precipitate products were exposed for to humic acid with a proprietary additive for either 2 hours at room temperature. Total PrP was detected with anti-PrP SHA31. Error bars represent 95% confidence intervals.

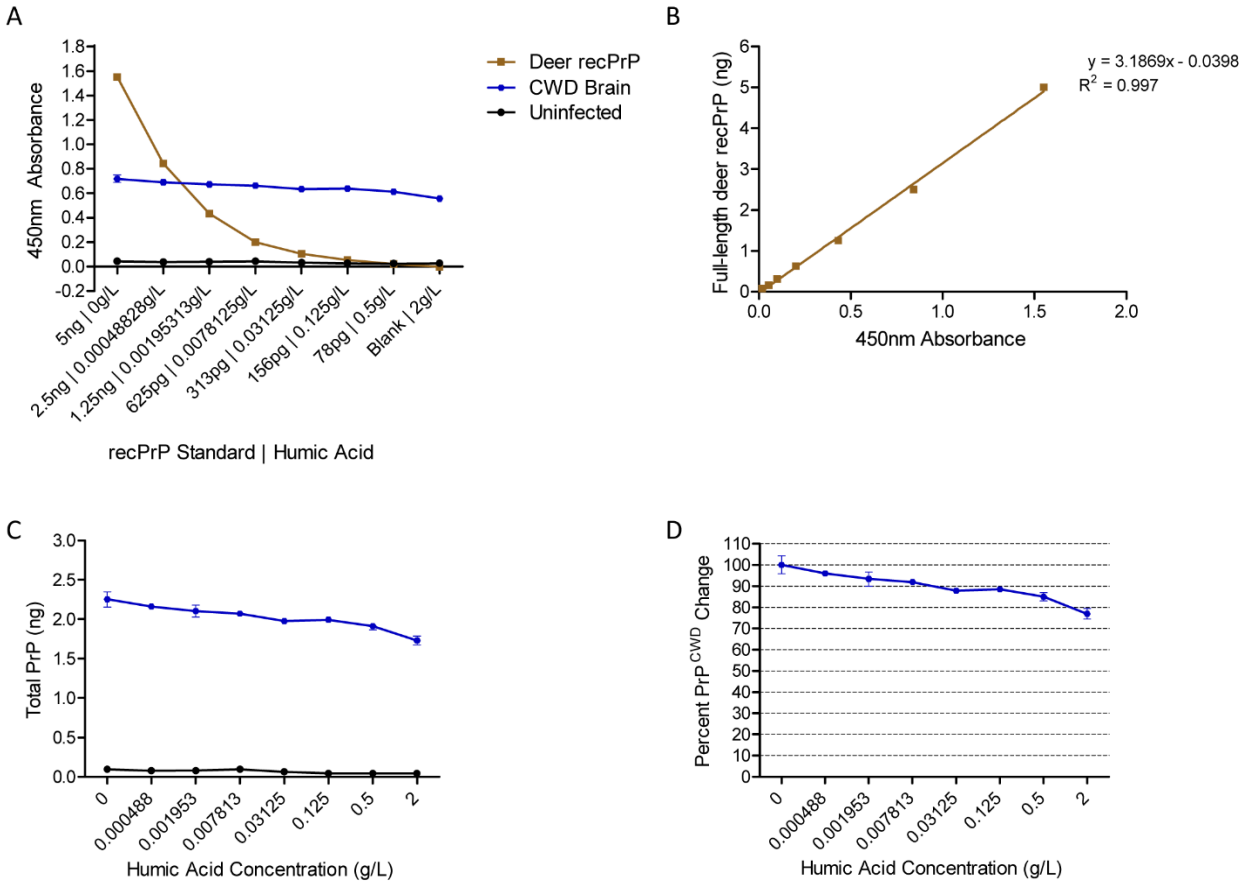

Figure 4.7. Reduction of PrP^{CWD} detection following a 2 hour exposure to humic acid. A) Average blank-adjusted 450nm absorbance of full-length deer recPrP protein standard and humic-acid treated uninfected white-tailed and CWD-infected mule deer pronase E-digested, phosphotugstic acid precipitated, and 0.45µm pore size filtered preparations. Coated brain homogenate was exposed to humic acid dilutions for 2 hours at room temperature. Total PrP was detected with anti-PrP SHA31 primary antibody. B) Deer recPrP standard linear regression, R-squared value, and linear equation used for calculating (C) total PrP mass detectable by the anti-PrP SHA31 antibody. D) Percent change of detected PrP^{CWD} exposed to humic acid dilutions relative to 0g/L humic acid controls. Error bars represent standard error of the mean.

4.4.4 Effect of humic acid on adsorbed proteinase K and pronase E PrP^{CWD} and PrP^{Sc} preparations

Differences in humic acid inactivation of PrP^{CWD} from proteolytically trimmed PK and full-length PE preparations was investigated by ELISA. Cervid PE-PTA-Filter and PK-PTA-Filter

enrichments from the same source brains were compared. PrP^{C} from uninfected controls were more readily eliminated by PK digestion (**Figure 4.8A**). Uninfected, untreated control wells coated with PK-digested preparations averaged 0.06ng/well of PrP^{C} versus 0.10ng/well for PE-digested preparations of equivalently coated total protein. Using the same source CWD-infected brain homogenate, PK-digested preparations yielded a calculated total PrP of 1.35ng/well versus 1.99ng/well for PE preparations when equivalent total protein mass was coated. When comparing an overnight humic acid exposure of PrP^{CWD} enriched preparations, PK-treated preparations were more susceptible to humic acid exposure than PE preparations when using a central region PrP-detecting antibody (**Figure 4.8B**). The highest humic acid concentration, 25g/L, reduced detection of the central PrP region by 58.8% and 38.1% for PK and PE-digested preparations, respectively. PrP^{CWD}-coated wells, exposed to high concentrations of humic acid overnight, demonstrated dose-dependent increases in absorbance at 450nm in uninfected control preparations - translating into increased apparent total PrP detection (**Figure 4.8A-B**). The increased signal is indicative of humic acid co-adsorption to the wells. Shorter incubation of CWD-infected PE and PK preparations for 2 hours at room temperature with humic acid concentrations of 2g/L or less did not result in significant differences between the two preparations (**Figure 4.9**).

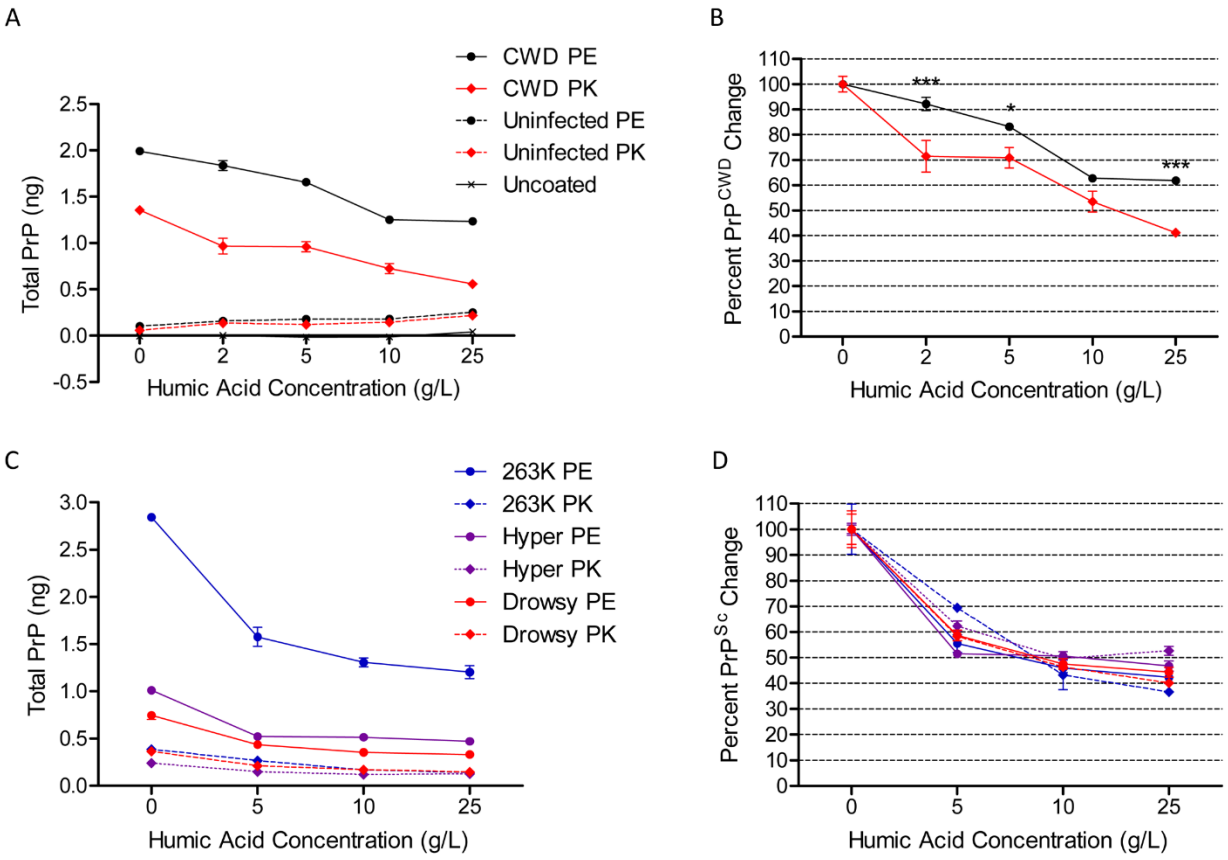

Figure 4.8. Humic acid treatment of pronase E (PE) and proteinase K (PK) deer PrP^{CWD} and hamster PrP^{Sc}. Total PrP mass calculated by recPrP standard curve for A) deer preparations and C) hamster preparations. The corresponding humic acid-induced percent changes of detected B) PrP^{CWD} and D) PrP^{Sc}. Infectious prions were enriched by sequential PE or PK digestion, PTA precipitation, and 0.45µm filtration. The same brain material was used for the PE and PK preparations. Adsorbed preparations were exposed to humic acid overnight at 4°C. Total PrP was detected by anti-PrP SHA31 (1:5,000). Error bars represent standard error of the mean.

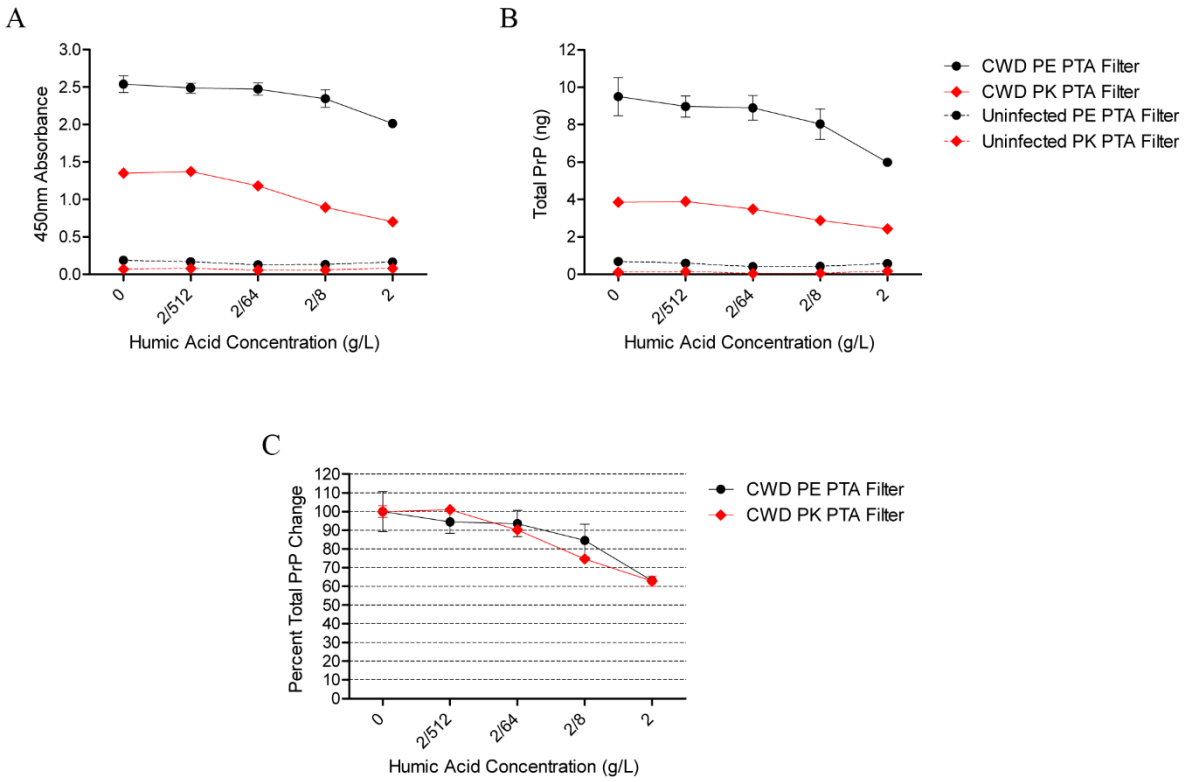

Figure 4.9. Inactivation of pronase E and proteinase K-enriched prions by 2 hour humic acid exposure. A) 450nm absorbance, B) quantified total PrP as determined by a recombinant PrP standard curve, and C) the calculated percent of remaining total PrP detected by anti-PrP SHA31 (1:5,000). Error bars represent standard error of the mean.

Similar to cervid preparations, more total PrP was detected by SHA31 in hamster PE-PTA-Filter preparations than PK-PTA-Filter preparations from the same source brains for three prion strains - 263K, Hyper, and Drowsy (**Figure 4.8C**). Average total PrP detected from the PE-PTA-Filter preparations without humic acid treatment were 2.84ng, 1.01ng, and 0.75ng per well for 263K, Hyper, and Drowsy, respectively. The PK-PTA-Filter preparations (from the same source brains used for the PE preparations) yielded 0.39ng, 0.24ng, and 0.36ng per well for the 263K, Hyper and Drowsy strains. Residual PrP^{C} from uninfected hamster PE-PTA-Filter preparations yielded slightly higher detection than uninfected PK-PTA-Filter preparations with detected masses for both lower than 0.0625ng/well - the lowest recPrP standard used (data not shown). Average

percent reduction of detection of PrP^{Sc} exposed to 25g/L humic acid varied from 63.4% for 263K PK preparations to 47.3% for Hyper PK preparations (**Figure 4.8D**). Statistical 2-way ANOVA analysis found no significant differences between PE and PK-digested preparations treated with 25g/L humic acid of the same hamster prion strains.

4.4.5 Overnight humic acid exposure of adsorbed pronase E PrP^{CWD} and PrP^{Sc} preparations

PE-digested cervid and hamster preparations treated with humic acid concentrations overnight were probed for total PrP with antibodies targeting varying regions of the PrP molecule (**Figure 4.10**, **Figure 4.11**). Average total PrP central region detection of the two CWD PE preparations was reduced by 41.3% following 25g/L humic acid treatment as detected by SHA31 (central prion protein region). The result is contrasted by a 78.2% reduction when SAF32 antibody (N-terminal octapeptide domain) is used. Cervid brains preparations of different hunter-harvested individuals expectedly resulted in varying enriched PrP^{CWD} concentrations (**Figure 4.10A, C**); however, following humic acid exposure the percent change of total PrP detection was not significant (**Figure 4.10B, D**).

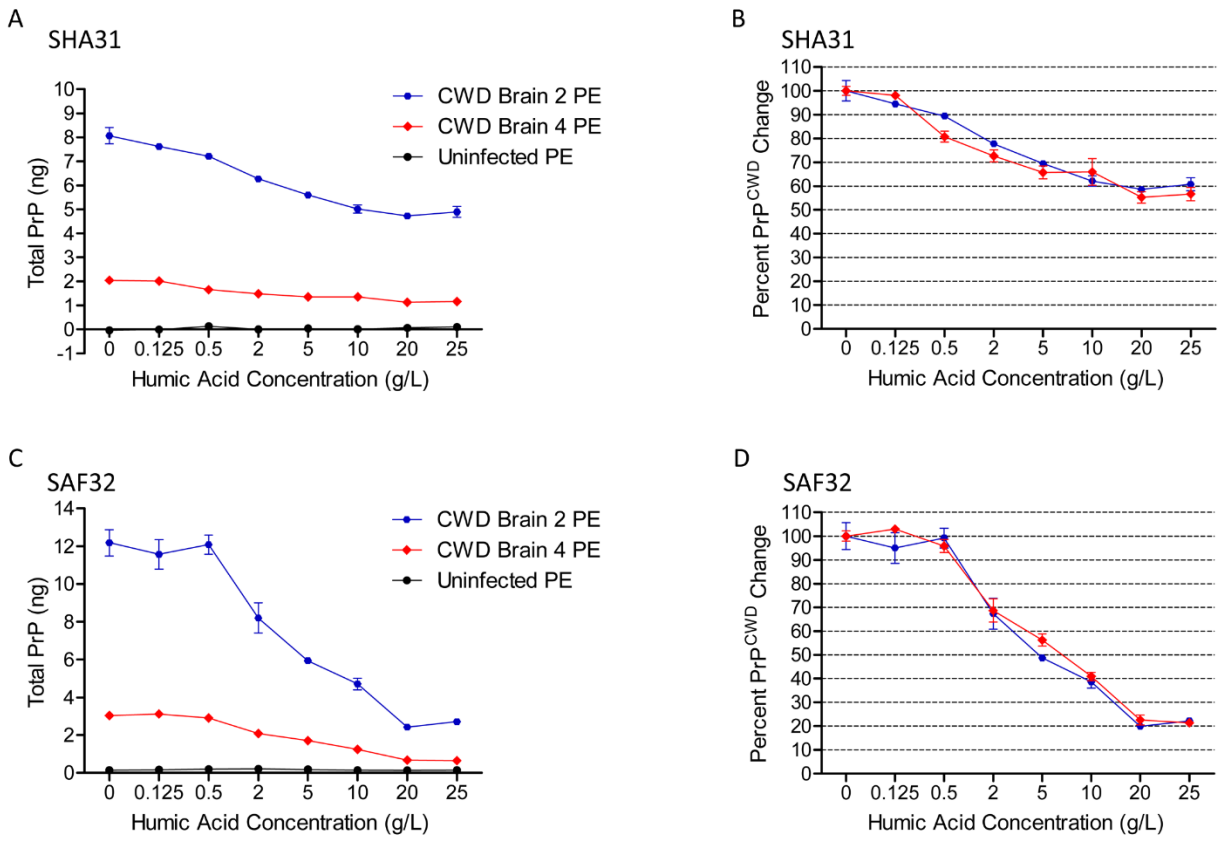

Figure 4.10. Detection of PrP^{CWD} following overnight exposure to humic acid. Total PrP was quantified by recPrP standard curves as detected by A) central region-detecting SHA31 and C) N-terminal octapeptide repeat-detecting SAF32. Corresponding percent reductions of PrP^{CWD} for B) SHA31 and D) SAF32 detection are shown. Microplates were coated with enrichments of CWD-infected mule deer and uninfected white-tailed deer brain homogenates enriched for PrP^{CWD} using sequential pronase E (PE) digestion, PTA precipitation, and 0.45µm filtration. Error bars represent standard error of the mean.

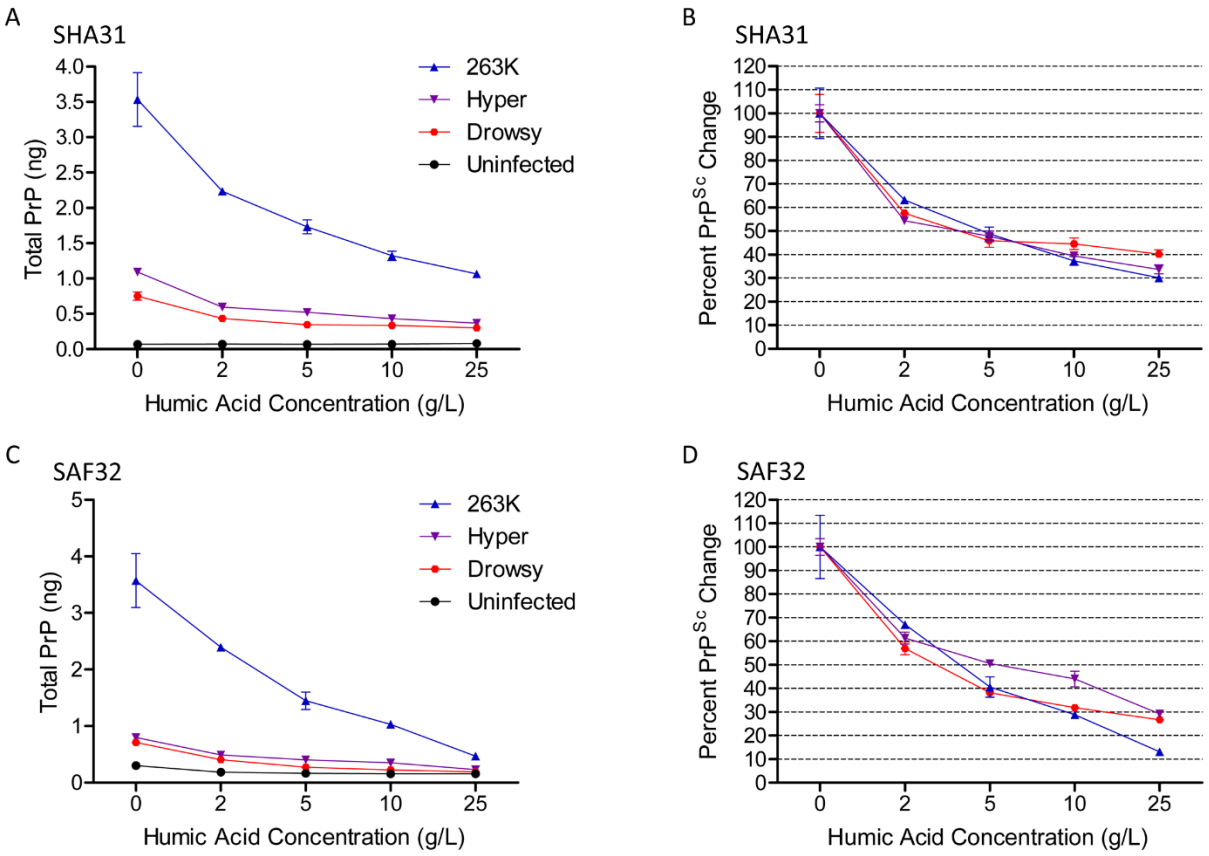

Figure 4.11. Detection of PrP^{Sc} following overnight exposure to humic acid. Quantified total PrP calculated by recPrP standard curves as detected by anti-PrP A) central region-detecting SHA31 and C) N-terminal octapeptide repeat region-detecting SAF32. Corresponding percent reductions of total PrP mass for B) SHA31 and D) SAF32 detection are shown. Microplates were coated with enrichments of uninfected and end-stage prion disease-infected hamster brain homogenates enriched for PrP^{Sc} using sequential pronase E digestion, PTA precipitation, and 0.45µm filtration. Error bars represent standard error of the mean.

Epitope-dependent differences in humic acid detection of hamster PE-digested preparations under the same conditions resembled those of deer prions. Total PrP detection of 263K, Hyper, and Drowsy brain preparations by SHA31 and SAF32 demonstrated humic acid dose-dependent decreases of detection (**Figure 4.11A, C**). Detection of the central PrP region was reduced by 69.9%, 66.2%, and 59.7% for 263K, Hyper, and Drowsy, respectively (**Figure 4.11B**). The N-terminal octapeptide repeat region of the three hamster strains was more susceptible to humic

acid with a detection reduction of 86.9%, 70.7%, and 73.3% for 263K, Hyper, and Drowsy respectively (**Figure 4.11D**), although no significant differences between the three hamster prion strains were found by 2-way ANOVA analysis found for any of the humic acid concentrations.

4.4.6 Humic acid-prion interaction in free solution

Prion inactivation without adsorption to a solid support was examined by western blot using the PrP^{CWD}- and PrP^{Sc}-enriched PE treated preparations. The protein concentrations of the preparations limited the final humic acid concentration to 10g/L for western blot detection. Relative CWD detection was reduced by 75.6% and 67.3% for 10g/L exposure of two CWD brain PrP^{CWD} enrichments as detected by SHA31 (**Figure 4.12A-B**). Detection with SAF32 (N-terminal epitope) resulted in reductions of 98.5% and 97.5% of PrP^{CWD} (**Figure 4.12C-D**). Hamster PE enrichment exposure to 10g/L humic acid overnight resulted in reductions of 79.5%, 64.5%, and 80.5% (SHA31 antibody) (**Figure 4.13A-B**) and 85.4%, 95.3%, and 95.1% (N5 antibody) for the Drowsy, 263K, and Hyper strains (**Figure 4.13C-D**). Humic acid contributions to background pixel intensity were taken into account for signal intensity calculations (**Figure 4.14**).

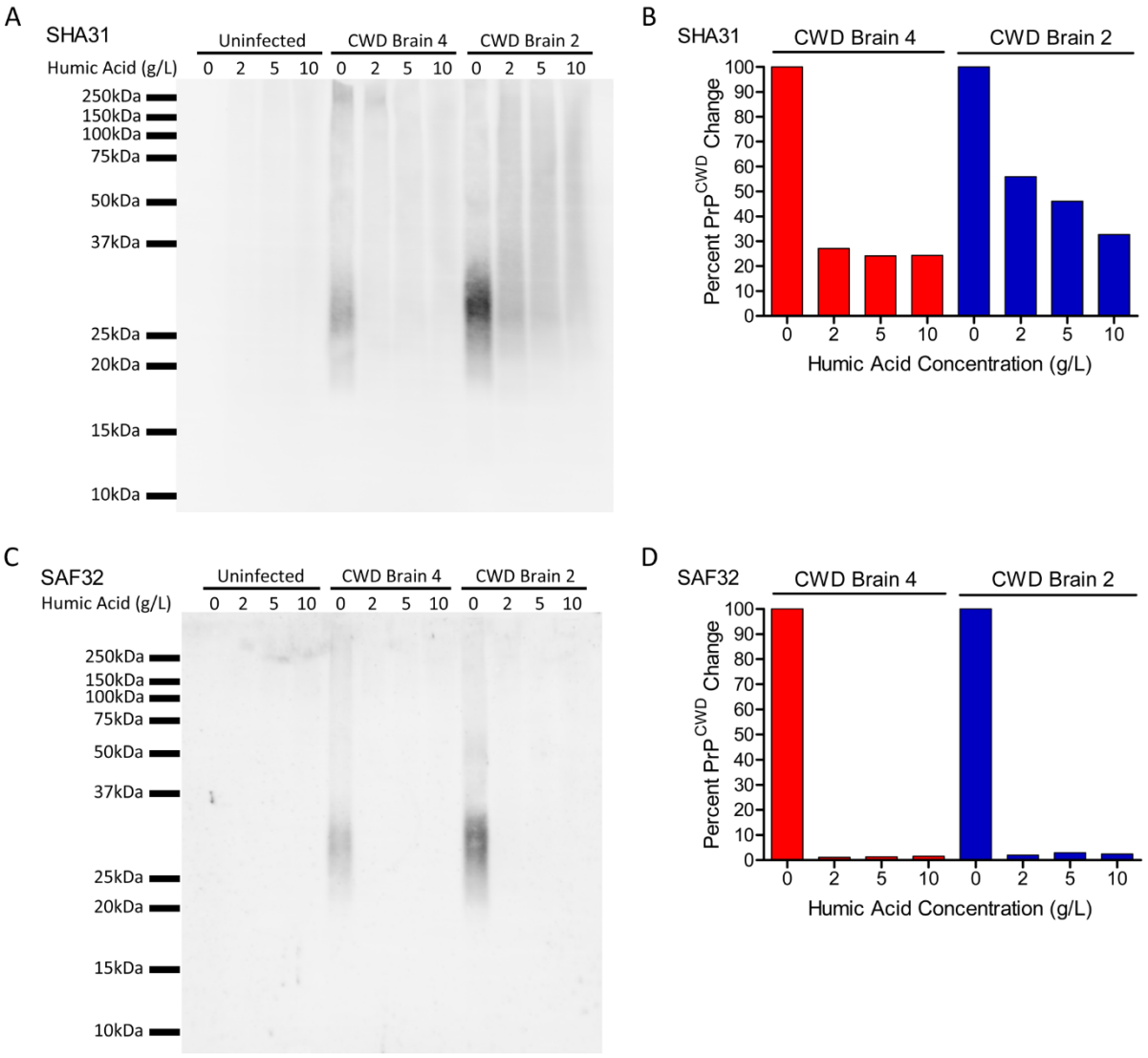

Figure 4.12. Humic acid-PrP^{CWD} interactions in solution. PrP^{CWD} was detected with anti-PrP A) central region-detecting SHA31 and C) N-terminal region-detecting SAF32 antibodies. B, D) Adjusted mean pixel intensity demonstrate dose-dependent loss of PrP^{CWD} detection. Lanes were loaded with 0.75µg of total protein per well. Samples enriched by sequential pronase E digestion, PTA precipitation, and 0.45µm filtration.

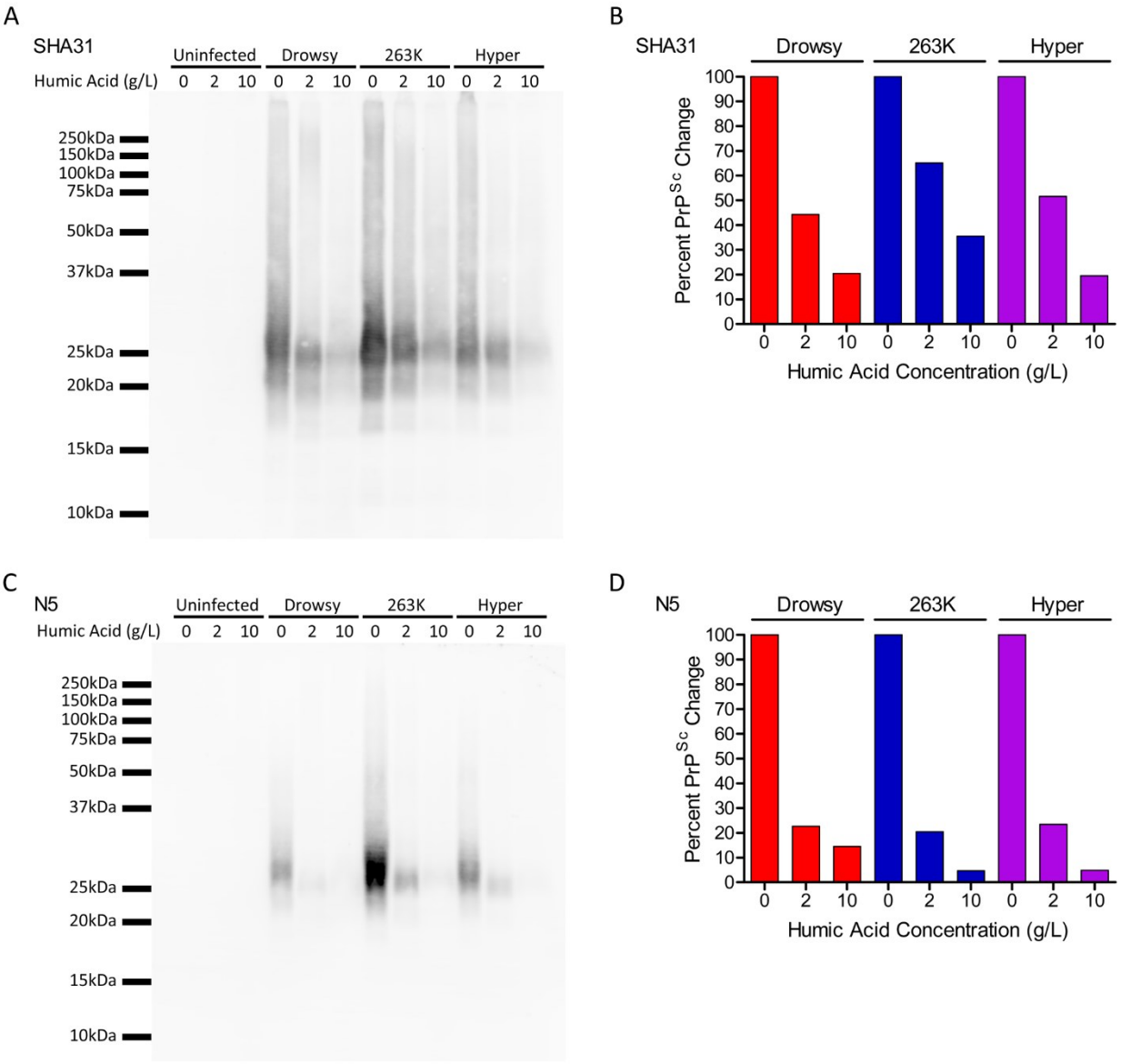

Figure 4.13. Humic acid-PrP^{Sc} interactions in solution with hamster prion disease strains. PrP^{Sc} was detected with anti-PrP A) central region-detecting SHA31 and C) N-terminal region-detecting N5 antibodies. B, D) Adjusted mean pixel intensity demonstrate dose-dependent loss of PrP^{Sc} detection. Lanes were loaded with 0.75µg of total protein per well. Samples were enriched by sequential pronase E digestion, PTA precipitation, and 0.45µm filtration.

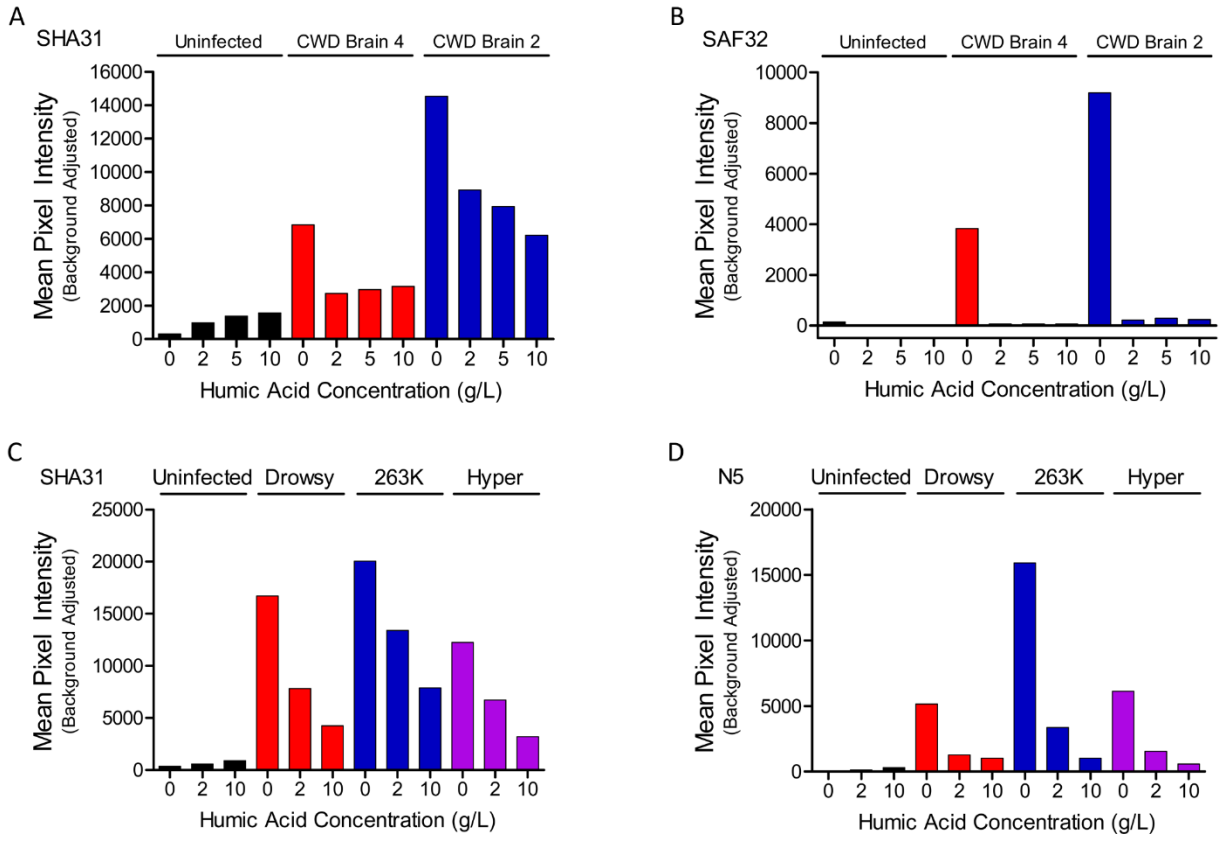

Figure 4.14. Background-adjusted mean pixel intensities for Figure 4.12, Figure 4.13. Aqueous overnight 4˚C humic acid exposure of pronase E, PTA, and filtered A-B) deer PrP^{CWD} and C-D) hamster PrP^{Sc}-enriched prions. Total PrP pixel analysis of western blots with 15-75kDa regions of interest for western blots detected with A, C) central region-detecting SHA31, B) N-terminal-detecting SAF32, and D) N-terminal-detecting N5 antibodies.

4.4.7 Improvement of humic acid ability to inactivate adsorbed prions

The utility of the ELISA prion inactivation assay lies, in part, in the ability to quantify the effects of anti-prion agents. Improvements to the anti-prion effects of humic acid were investigated. A proprietary diluent formulation was tested for its ability to enhance the anti-prion effects of humic acid. Humic acid powder (MilliporeSigma, USA) and diluted in HyClone™ Molecular Biology Grade water (Cytiva, USA) was compared to the same humic acid diluted in the proprietary mixture using the prion inactivation assay. Adsorbed PE-PTA-Filter PrP^{CWD}-

enriched prions from mule deer brain were exposed to a range of humic acid concentrations diluted in water or the proprietary mixture overnight at 4˚C (**Figure 4.15**). Humic acid diluted in the proprietary mixture was significantly more effective at reducing PrP^{CWD} detection at all humic acid concentrations (**Figure 4.15B**). The highest concentration of humic acid, 25g/L, diluted in water reduced PrP^{CWD} detection by 21.4% versus a reduction of 52.0% for humic acid diluted in the proprietary mixture as detected by SHA31 (**Figure 4.15C**).

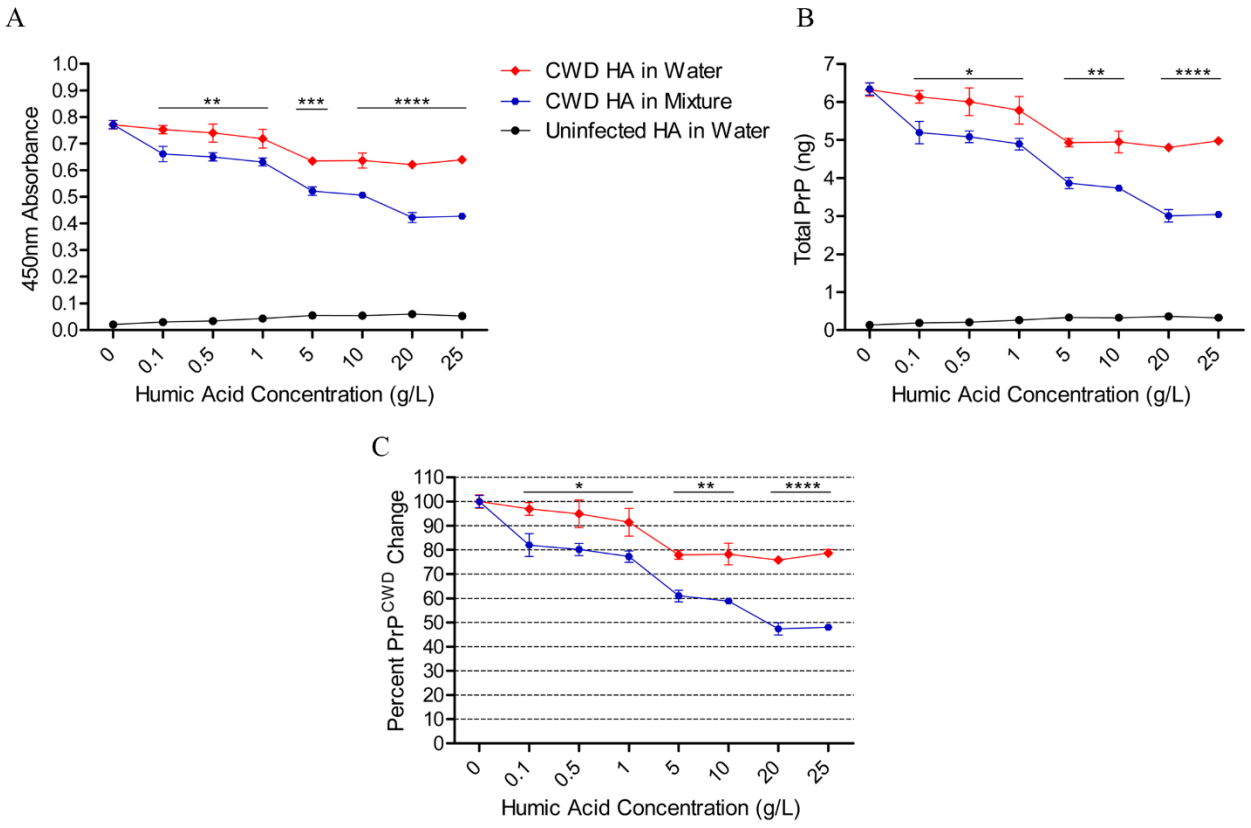

Figure 4.15. Enhanced inactivation of adsorbed prions by an improved humic acid formulation. CWD-infected mule deer male and uninfected white-tailed deer brains enriched by pronase E (PE) digestion, PTA precipitation, and 0.45µm filtration. Adsorbed purifications were exposed to humic acid solutions of water or a proprietary mixture overnight at 4°C. A) 450nm absorbance, B) quantified total PrP as determined by a recombinant PrP standard curve, and C) the calculated percent of remaining total PrP detected by anti-PrP SHA31. Error bars represent standard error of the mean.

The effect of humic acid diluted in water versus the proprietary mixture was tested on prions in solution. CWD-infected mule deer brain homogenate (10%) was mixed with humic acid diluted either in water or proprietary mixture. Tubes were incubated overnight at 4˚C prior to PrP detection by western blot using the SHA31 or N5 antibodies. Consistent with section 5.4.6, detection of the N-terminal region was more impacted by humic acid exposure than the central region (**Figure 4.16**). Differences between humic acid in water or proprietary mixture were difficult to distinguish visually. Pixel intensity analysis determined that the proprietary mixture enhancement of the anti-prion effects of humic acid when free in solution was modest (**Figure 4.16B, D**).

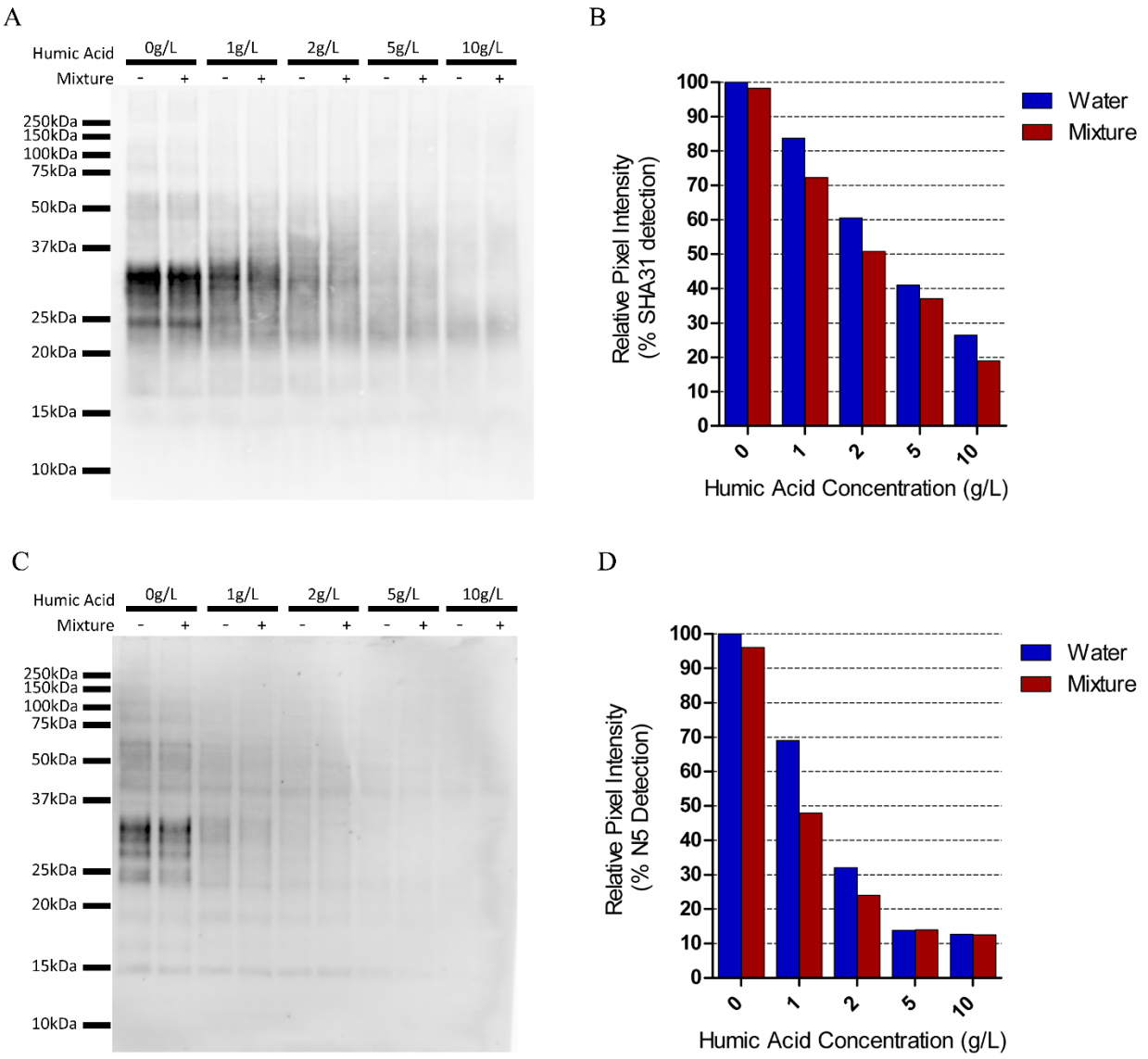

Figure 4.16. Effect of humic acid diluted in water or proprietary mixture on CWD-infected mule deer brain homogenate (10%) in solution. Total PrP was detected with anti-PrP A) SHA31 and C) N5 antibodies following 24 hour incubation with humic acid at 4˚C. Background-adjusted pixel intensity reduction B, D) relative to water-only control was calculated for the PrP protein size range.

We then determined whether the anti-prion effects of resuspended humic acid changes with long-term storage. Humic acid diluted either in water or in water with an ingredient of the proprietary mixture was stored at room temperature for up to 13 months. Aliquots of the humic acid samples were frozen at designated time points for later simultaneous testing. Mule deer 10% brain homogenate, and PE-PTA-Filter PrP^{CWD}-enriched prions were exposed to 10g/L of the humic acid solutions overnight at 4˚C (**Figure 4.17**). Similar to the comparison between humic acid in water and the proprietary mixture, differences between time and diluent were difficult to distinguish visually. Pixel intensity analysis (**Figure 4.17C**) revealed no clear indications of altered anti-prion effects with time that could translate to biological relevance.

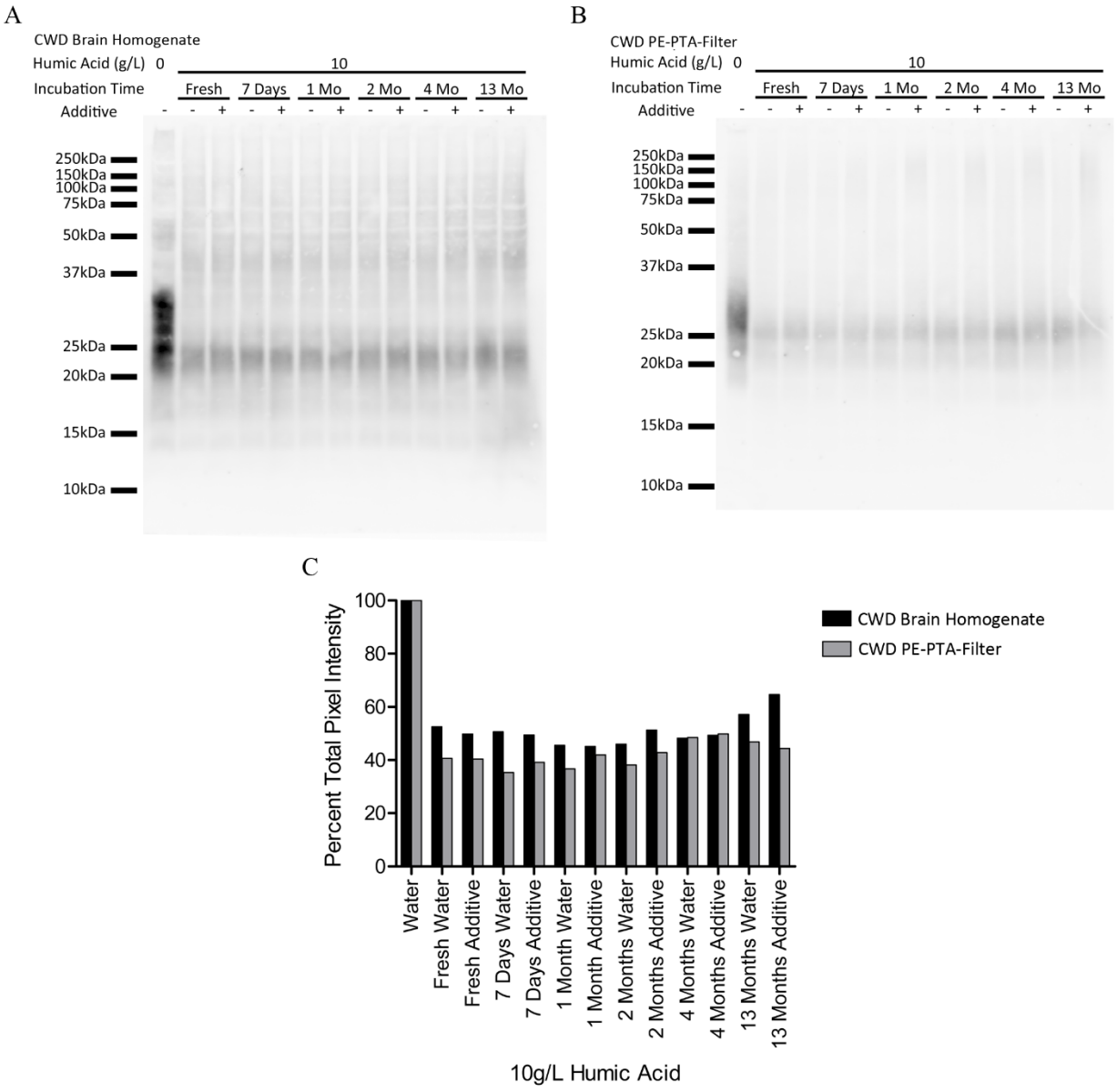

Figure 4.17. Effects of long-term storage on the anti-prion effects of humic acid solutions. Aged humic acid used to treat A) CWD-infected mule deer brain homogenate (10%) and B) PE-PTA-Filter enriched prion preparations from the same deer brain were incubated with humic acid overnight at 4˚C. C) Percent average pixel intensity of individual lanes relative to untreated controls as measured from the loading well to 10kDa. PrP was detected by anti-PrP SHA31.

4.4.8 Testing of alternative binding surfaces for quantifying prion inactivation

Alternative adsorption surfaces were investigated for assaying prion inactivation by humic acid to optimize prion binding. Stronger relative prion binding characteristics of the assay microplate surface would be expected to translate into less antigen desorption and more accurate prion inactivation results. The proprietary hydrophilic microplate surface modification of the Microlon High Binding (Greiner Bio-One GmbH) used for prion inactivation studies in sections was compared to hydrophobic polystyrene and to hydrophilic, anionic polystyrene sulfonate microplates.

Polystyrene microplates were chemically modified by a sulfonation substitution reaction [631] to have surface-exposed polystyrene sulfonate groups (**Figure 4.18A**). Urea was chosen over guanidine hydrocholoride as an epitope-exposing chaotropic agent when using the polyanionic polystyrene sulfonate microplates to avoid displacement of the adsorbed antigen by the guanidine cations (**Figure 4.18B**). PBS (pH 7.4) was determined to be a better coating buffer for IgG1 adsorption to polystyrene sulfonate plates than carbonate bicarbonate buffer (pH 9.6), formate buffer (pH 4.0), or acetate buffer (pH 4.0) (data not shown). Although the polystyrene sulfonate microplates bound mouse IgG1 well (**Figure 4.19**), the sulfonated plates failed to adsorb deer recPrP (**Figure 4.20A**) or PE-digested mule deer CWD preparations (**Figure 4.20B**). Polystyrene plates returned more variable absorbance readings for adsorbed CWD prion preparations relative to Greiner Bio-One High Binding microplates (**Figure 4.20B**).

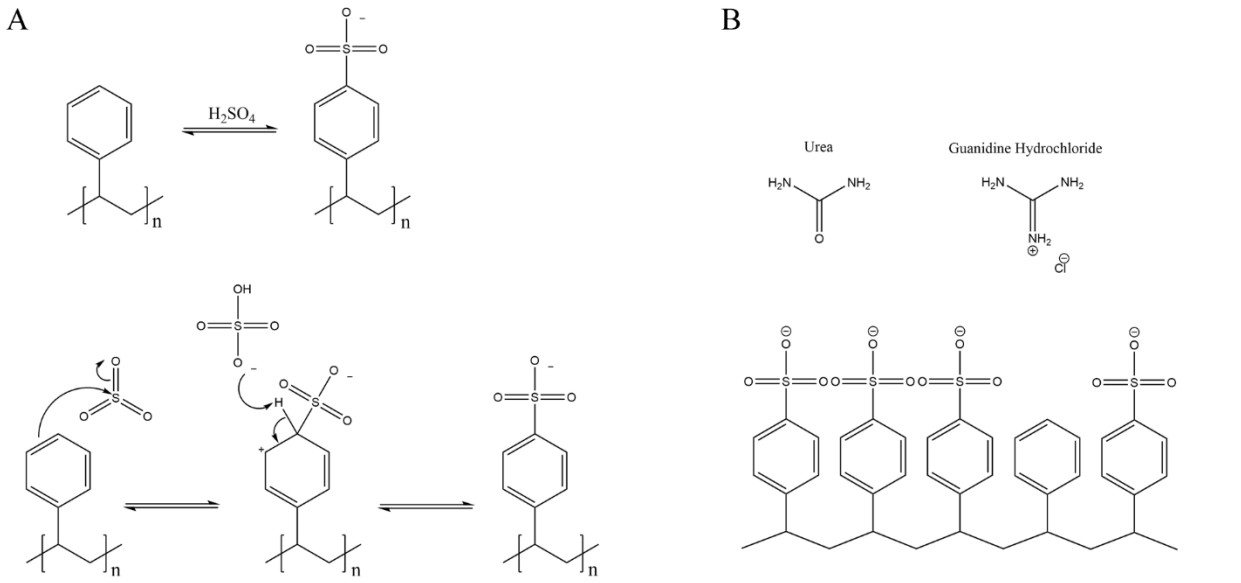

Figure 4.18. Synthesis of polysulfonated microplate surfaces from polystyrene for protein binding. A) Reversible modification of polystyrene into polystyrene sulfonate by concentrated sulfuric acid. B) Importance of chaotropic agent charge selection for epitope exposure use of bound antigens.

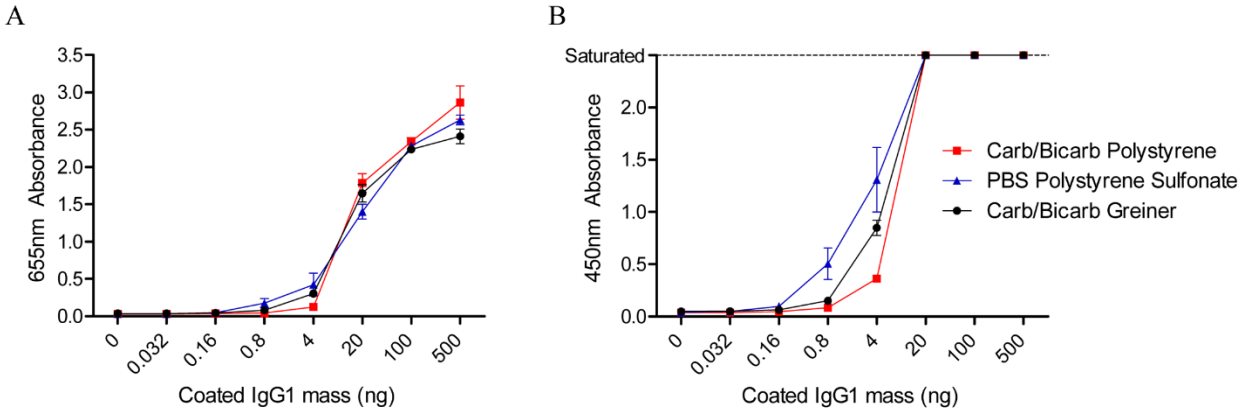

Figure 4.19. Effect of solid support surface chemical composition on adsorption of mouse IgG1. A) 650nm and B) 450nm absorbance readings of IgG1 to polystyrene, polystyrene sulfonate, and Greiner Bio-One plates were coated with IgG1 in carbonate bicarbonate (pH 9.6). Polystyrene sulfonate wells were coated with IgG1 in phosphate-buffered saline. Error bars represent standard error of the mean.

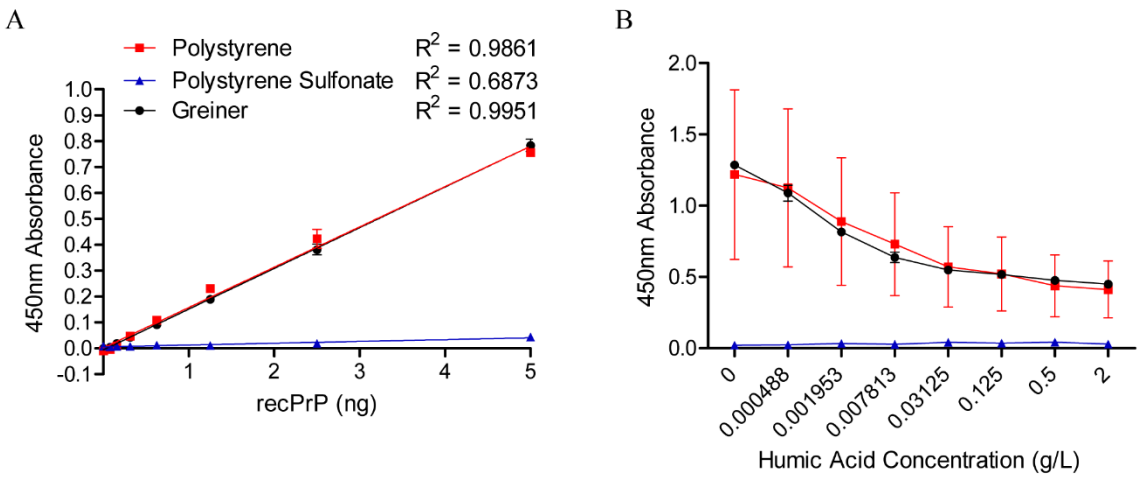

Figure 4.20. Effect of solid support surface chemical composition on recPrP and enriched PrP^{CWD} adsorption. A) Standard recPrP protein curve generation using polystyrene, polystyrene sulfonate, and Greiner Bio-One Microlon High Binding microplates. B) Humic acid inactivation of PrP^{CWD} from a male mule deer enriched by pronase E digestion, PTA precipitation, and 0.45µm filtration using the three differing binding surfaces. Coated wells were exposed to humic acid in a proprietary mixture for 2 hours at room temperature in triplicate. PrP^{CWD} was detected by SHA31 (1:5,000) Error bars represent standard error of the mean.

4.5 Discussion

The anti-prion effects of humic substances are poorly understood - largely due to the heterogeneous, indeterminate structures of humic substances that vary depending on the initial soil source [587, 589, 633]. Possible mechanisms of prion inactivation by humic substances include sequestration by encapsulation, covalent crosslinking, and chemical degradation - possibly by hydrolysis [592-593, 634-636]. Exposure of PrP^{CWD} to the numerous chemical groups of complex humic substances could contribute to prion inactivation by any of the listed mechanisms. Aromatic moieties of humic substances have been proposed to contribute to the loss of infectious prion detection [593].

Validation of humic acid inactivation of prions using ELISA is contingent on adsorbed PrP^{CWD} being retained throughout the assay. Indirect testing of humic acid-induced protein desorption

from the microplate surface was assayed by BCA. Bovine serum albumin was selected as a proteinaceous substitute to elucidate the effect of humic acids on adsorbed protein (**Figure 4.5**). Comprehensive desorption or proteolysis of adsorbed protein would be expected to manifest in a reduced 562nm absorbance. PK treatment of BSA-coated wells resulted in an expected concentration-dependent reduction of 562nm absorbance - reflecting loss of proteolysed peptide fragments during washing steps. BSA-adsorbed and uncoated wells treated with humic acid solutions had increased calculated protein content at high humic acid concentrations (by 5g/L). Increased 562nm absorbance (**Figure 4.5A**) is likely due to humic acid coating the well surface and adsorbed proteins. Peptide components of coating humic acid molecules [587] may contribute to the Biuret reaction of the BCA assay together with broad spectrum humic acid absorbance - including weak 562nm absorbance (**Figure 4.5B**). Likewise, humic acid concentration-dependent increases of uninfected control ELISA absorbance readings with overnight exposures (**Figure 4.5A**) indicates co-adsorption of HA to the plate surface. Co-adsorption instead of desorption supports the encapsulation theory of prion inactivation by humic acids, although contribution of chemical crosslinking cannot be excluded. Humic acid binding to adsorbed PrP^{CWD} in our ELISA format may allude to the inactivation mechanism of soil, plant, or mineral-bound prions in the environment by humic acids. The results of the presented ELISAs are consistent with encapsulation or crosslinking mechanisms of prion inactivation.

Enrichment of infectious prions allows for study of humic acid interactions with PrP^{CWD} and PrP^{Sc}. PrP^{CWD} enrichment by detergent-assisted phosphotungstic acid precipitations [637] without enzymatic digestion was insufficient for reducing uninfected control PrP^{C} as detected by western blot (**Figure 4.3A**, **Figure 4.4A, C**) and ELISA (**Figure 4.6**). A prion enrichment scheme similar to Wenborn *et al*., (2015) generated PrP^{CWD}- and PrP^{Sc}-enriched preparations

with minimal contaminating PrP^{C} [627]. Our enrichment protocol resulted in PrP^{CWD} less pure than Wenborn *et al*., but sufficient for ELISA use. Balancing sample purity and quantity was a decisive consideration for the assay. The reduction of contaminants by the PE-PTA-Filter and PK-PTA-Filter methods allowed us to better study prion interactions with humic acids. Unlike PK, limited enzymatic digestion by PE destroys most PrP^{C} while maintaining full-length PrP^{CWD} and PrP^{Sc} [638-639] (**Figure 4.3A**, **Figure 4.4A, C**). The difference between quantified total PrP of infected and uninfected control preparations in our experiments is interpreted to represent disease-associated PrP^{CWD} or PrP^{Sc} of infected samples. Digestion with PK was more aggressive than PE [638] - degrading more PrP^{C}, PrP^{CWD}, and PrP^{Sc} (**Figure 4.8A, C**). PE-digested preparations allowed for the study of humic acid solution interactions with full-length, infectious PrP^{CWD} and PrP^{Sc}. Size exclusion 0.45µm filtration is removes impurities, including DNA and collagen fibrils [627], that would compete with PrP for microplate adsorption surface area. Sarkosyl-enhanced PTA precipitation induces fibrillization of infectious prions [638]. Loss of large PrP^{CWD} fibrils and aggregates during the filtration step favors detection of smaller infectious units. The described humic acid-PrP^{CWD} ELISA experiments are therefore biased towards humic acid interactions with the smaller, fibrillar species. The PrP^{CWD} enrichment methods described are hampered by large volumes of brain homogenates required for preparations.

Adsorbed PrP^{CWD}- and PrP^{Sc}-enriched preparations were detected and quantified by ELISA using chaotrope-induced antigen exposure in conjunction with a recombinant PrP standard (**Figure 4.7**). Infectious prions have been previously quantified by ELISA from a variety of agents including bovine spongiform encephalopathy, sheep scrapie, and mouse prions using recombinant PrP and synthetic peptide epitopes [640-643]. Epitope exposure of adsorbed PrP^{CWD}

in direct, antigen capture, and sandwich ELISAs by guanidine hydrochloride and guanidine thiocyanate is effective for enhancing PrP^{CWD} detection [641-645]. Use of guanidine epitope exposure with the described PrP^{CWD}-enriched preparations alludes to potential use in conformational stability assays to differentiate prion strains (Appendix 3) [646-647].

Humic acid concentration-dependent loss of PrP^{CWD} and PrP^{Sc} detection by ELISA and western blot differed by prion epitope. The N-terminal region of hamster and deer prions was more susceptible to humic acid than the central region (**Figure 4.10**, **Figure 4.11**), a finding consistent with Smith *et al*., [593]. The N-terminal region of the prion protein is similarly susceptible to environmental degradation and PK digestion [648-650]. CWD prions were more resistant to humic acid inactivation than the hamster strains when SHA31 (detecting the central region) was used (**Figure 4.10B**, **Figure 4.11B**). This difference in humic acid response could reflect species-specific prion conformation. Interestingly, no significant differences were observed between the three hamster prion strains exposed to humic acid.

Comparing adsorbed and aqueous PrP^{CWD} and PrP^{Sc} interactions with humic acid produced insights into potential environmental decontamination strategies. When controlling for time and temperature, deer PrP^{CWD} and hamster PrP^{Sc} were more resistant to inactivation by humic acid when adsorbed to a solid support (**Figure 4.10**, **Figure 4.11**) than in solution (**Figure 4.12**, **Figure 4.13**). Greater sensitivity of ELISA relative to western blot is a possible explanation of the differing responses, although our results agree with the observations that adsorption of Hyper hamster prions to montmorillonite partially protects the pathogen from inactivation by sodium hydroxide, sodium hypochlorite, and Environ LpH [577]. Further, prions bound to some soils and clays (particularly those containing montmorillonite) enhance CWD infectivity [47-48, 651]. Adsorption of infectious prions to a surface may reduce humic acid-prion chemical reaction rates

and surface area available for encapsulation or cross-linking. PrP^{CWD} binding to soil, minerals, vegetation, and other fomites presents a challenge for CWD decontamination. Resistance of adsorbed prions to refined humic acid may explain how prions readily exist in a variety of soils with high soil organic matter content [652].

The ELISA assay was used to test and optimize anti-prion solutions designed to decontaminate CWD-endemic areas. A proprietary HA diluent was tested for anti-prion activity by both ELISA (**Figure 4.15**) and western blot (**Figure 4.16**). The enhanced HA formulated demonstrated improved anti-prion activity, especially when the prions were adsorbed. Future testing of enhance HA formulations using bioassay or other means are required to assess the utility solutions for prion decontamination.

Microplates with surface-exposed polystyrene sulfonate was selected as a test solid support based on the propensity of prions to bind polyanionic compounds (including polysulfated compounds). PrP^{C} has long been recognized to bind to polyanionic compounds [653-658], but the disease-associated PrP^{Sc} isoform can also bind to such molecules [659-661]. Infectious prion binding to polyanionic compounds is a key principle for the HerdChek (IDEXX Laboratories, Inc.) prion diagnostic antigen capture ELISA [662-663]. Discriminating agents are used in the HerdChek ELISA to reduce PrP^{C} binding to the polyanionic surfaces of the HerdChek ELISA antigen binding surface [663]. Using PrP^{C}-depleted prion preparations, we hoped that microplates modified to have a polystyrene sulfonate binding surface would readily bind PrP^{CWD}.

Intriguingly, polyanionic polystyrene polysulfate microplates failed to adsorb recombinant deer PrP and PE-digested CWD-infected deer preparations using a PBS coating buffer at physiological pH (**Figure 4.20**). Immobilized polyanionic polysulfated molecules have

previously been found to bind to recombinant PrP at physiological pH with enhanced binding being provided by the presence of divalent copper and zinc cations [656-657]. Future work could determine whether the addition of copper and zinc divalent ions enhance the binding of recombinant PrP and enriched prions to the polystyrene polysulfate microplates. Differences in binding capacity could be partly attributed to the helical structure of prion fibrils [18-19, 664-665]. Planar polystyrene polysulfate microplate surfaces would differ from more flexible immobilized polysulfated molecules such as heparin sulfate and pentosan polysulfate that could better accommodate the helical prion fibril structures.

In vitro investigations into infectious prion-humic acid interactions have primarily used liquid mixtures with detection by western blot [592-593]. In contrast, indirect transmission of CWD via environmental contamination is certain to involve PrP^{CWD} adsorbed to surfaces including soil and vegetation. Using an ELISA format, we sought to study humic acid-prion interactions in a context more representative of environmental prion adsorption. By comparing inactivation of prions in solution and adsorbed to a solid support by humic acid solutions, we determined that the central prion region is more resistant to humic acid than the N-terminal region. Experimental results indicating humic acid co-adsorption suggest that humic acid likely inactivates prions by encapsulation or chemical cross-linking. The results also question the utility of humic acid as a means of environmental decontamination of prions without optimizing or enhancing formulations. Testing of anti-prion compounds by ELISA is rapid and cost effective relative to long animal prion bioassays.

Chapter 5 Contributions to prion research

5.1 Remarks on prion and cervid historiography

The rapid advance of machine translation, digitalization, and accessibility of global library and archival material has greatly accelerated the efficiency of historical research. The early investigators of scrapie history had been largely hobbled by inaccessible documents, language barriers, and slow, uncertain response times from agriculturalist historians. Prior to this thesis, the first known report of scrapie came from the Electorate of Saxony (part of the Holy Roman Empire) in 1750 [144]. The first known description of scrapie in Britain was from 1772 with a second-hand anecdote claiming that the disease had been present since 1732 [83]. With thanks to readily accessible digitalized archival documents, the first recorded description of scrapie can now be attributed to between 1693-1706 by Edward Lisle (Appendix 1) [666]. Although James Parry's historic study into scrapie had previously recognized two centers of scrapie outbreaks in England (Wessex and East Anglia) [667], a more accurate geographical description of the two major outbreaks of scrapie in England prior to 1800 has now been detailed (Appendix 1).

As more historic documents become digitalized earlier reports of scrapie are almost certain to be gleaned from archival material. Albrecht Daniel Thaer wrote in 1826 that he had been unable to find any Spanish, English, Danish, or Swedish writers that described scrapie prior to Leopoldt in 1759 [668]. Likewise, aside from Edward Lisle, I was unsuccessful uncovering any other documentation related to scrapie predating 1750 from German, Polish, French, Latin, Italian, or Spanish sources. Johann George Leopoldt, who published the 1750 description of scrapie, had a very detailed knowledge of the disease and its transmission – suggesting that the scrapie had been well established in Saxony [144]. German sources predating 1750 will likely be found as more documents become digitalized. Spain had long been hypothesized to have been an original source of scrapie in Merino sheep [149, 667, 669], but verifiable documentation has yet to be put forward to support this.

The next leap in TSE historiography, I believe, will come from the newly described camel prion disease. The symptoms of camel prion disease are conspicuous and local knowledge of the disease remains to be detailed beyond anecdotes that the disease had been present in Algeria as far back as the 1980s [13]. Arab scholars of old have documented an incredible wealth of knowledge regarding natural sciences, including on camel diseases. The accessible volume of historical Arabic sources that have been digitally archived by optical character recognition is, unfortunately, limited. Further, difficulties in machine translation between Arabic and the Germanic or Latin languages have prevented me from fully investigating the history of camel prion disease. I will recommend a place to start an investigation: "رجز" (*rajuz*) was translated by European sources as early as 1781 as a disease in camels marked by trembling and weakness of the buttocks and hind limbs with difficulty rising from a recumbent state [670-671]. Hind limb ataxia and recumbency are symptoms of camel prion disease, but more symptoms (notably tooth grating) are required for camel prion disease identification beyond a reasonable doubt. The presence of the term in multiple language lexicons suggests the disease to have been established local knowledge in some regions.

Other historical revelations now recognized from the historical record include the identification of deer rabies outbreaks in England as early as 1772 and 1789 (previously thought to have been first reported in 1856) (Appendix 1). Anatoly Ivanovich Akaevsky is now recognized to have identified the vestibular nasal glands in 1939 before the 1976 description by Jacob and von Lehmann (Chapter 1). The first accurate description of white-tailed deer scraping behaviour can now be attributed to Tony Alexander in 1887 (previously attributed to Pruitt in 1954) (Chapter 1).

5.2 Implications for the study of chronic wasting disease transmission

Cervid scent glands (and their associated behaviours) are hypothesized to be involved in the transmission of CWD. Results from this thesis provide insights into possible mechanisms of CWD environmental contamination, transmission, and the cervid behaviours likely involved. To investigate the feasibility of skin gland involvement, mule deer and white-tailed deer integumentary glands were surveyed for the presence of PrP^{C} (Chapter 2). We had initially hypothesized that PrP^{C} was expressed in white-tailed deer and mule deer integumentary glands. PrP^{C} was detected, quantified, and structurally located in all glands analyzed. The presence and distribution of PrP^{C} was similar between species and sex, but some nominally small, but statistically significant differences were found. White-tailed deer and female deer expressed more PrP^{C} in some skin glands relative to mule deer and males – findings that surprised us as wild mule deer and males have higher CWD prevalence. Relative PrP^{C} expression, however, between tissues does not correlate well with early preclinical PrP^{CWD} prion seeding activity [594]. Behavioural aspects of cervids were concluded to impact CWD transmission more than relative glandular PrP^{C} presence. Nonetheless, the largely ubiquitous distribution of PrP^{C} within the tissues examined in Chapter 2 suggests that all tissues examined had potential for PrP^{CWD} accumulation and replication. The work used samples collected during the deer rut – potential for seasonal changes in PrP^{C} distribution were not examined.

PrP^{CWD} had been hypothesized to be present within some of the integumentary glands examined. The identification of PrP^{CWD} in the interdigital glands of mule deer (Chapter 3) was a novel finding of this work that opens the door to many research approaches. Consistent, dense immune cell infiltration of all mule deer interdigital glands examined appears to be the primary source of PrP^{CWD} localization in the glands. Further investigation into the possible secretion of PrP^{CWD} from the interdigital glands into the environment will be interesting to pursue. CWD-infected

white-tailed deer have yet to be examined for PrP^{CWD} in the interdigital glands. Future investigation into the facial glands will also be of interest. The small sample size of infected animals studies prevented an accurate assessment of PrP^{CWD} presence in the facial glands. RT-QuIC and PMCA were not used to assay for PrP^{CWD} in the facial glands. If PrP^{CWD} is found in other skin glands in future studies, the PrP^{C} presence and quantification has already been detailed for most of the cervid skin glands. As the facial gland lymphatics all drain to the lateral retropharyngeal lymph nodes, CWD infections established in these glands, through animal scent-marking and social behaviours, would be identified by current CWD surveillance programs that test RPLNs. The theory of facial gland involvement and contribution to CWD transmission cannot be excluded with the current evidence. If the interdigital glands are involved in CWD transmission, they may also be involved in scrapie transmission. Sheep have interdigital glands, but the structure is lacking in goats. It would be interesting to examine whether the absence of interdigital glands in goats alters susceptibility of goats to environmental PrP^{Sc} relative to sheep.

Detection of prions in soil samples is a methodology that will likely see a rapid growth in interest for both CWD and scrapie surveillance. PMCA detection of abnormal PrP in the hoof soil sample reported in Chapter 3 was preliminary and requires more samples to verify possible secretion of PrP^{CWD} from the interdigital glands into the soil. Testing of soil samples by both PMCA and RT-QuIC may provide more convincing results.

5.3 Future direction for the quantification of prion inactivation

We have developed a method for quantifying adsorbed prion inactivation using ELISA after initially hypothesizing that ELISA could be used to as a platform for quantifying PrP^{CWD} inactivation. The use of ELISA for testing adsorbed prion inactivation is of valuable use for comparing anti-prion compounds (Chapter 4). The methodology allows for a quantitative

measure of inactivation that was previously lacking outside of expensive and lengthy bioassay experiments. Using this methodology, I quantified prion inactivation following humic acid exposure. Importantly, the assay allowed for studying the impacts of anti-prion compounds when the target prions are adsorbed. Past studies on prion inactivation by humic substances primarily used aqueous mixtures. The ELISA-based assay simulates adsorbed prions that are encountered by animals being naturally infected. Experiments determined that humic acid did not desorb proteins from the ELISA plate, but instead likely co-adsorbed to the surface. The implication surrounding the lack of desorption is that humic acid inactivates prions by either encapsulation and sequestration of the prions with or without chemical crosslinking.

The prion inactivation ELISA is a tool that can be used for early testing of environmental prion decontamination methods. Enhanced anti-prion formulations of humic acid have been tested using the methods described (Chapter 4) but not with prion-contaminated soil. Anti-prion compounds other than humic acids can and will be tested with this ELISA. This ELISA-based inactivation assay may also be useful for other protein misfolding diseases involving amyloid beta, tau, and alpha-synuclein. Use of such an assay with adsorbed amyloids could show promising results with testing of anti-amyloid abzymes or other amyloid-degrading compounds.

I am curious as to why the adsorbed prion strains failed to demonstrate strain-specific differences by CSA (Appendix 3). Three hamster prion strains were tested simultaneously on a single plate, yet chaotropic agents failed to demonstrate significant differences in epitope exposure. Different PrP-detecting antibodies may shine light on this question. More sensitive detection methods are recommended for further investigation into the matter given the large volumes of hamster brain homogenates required to coat plates for the CSAs I performed.

The first of the appendices begin on page 231.

Literature cited

1. Prusiner SB. The prion diseases. Brain Pathol. 1998 Jul;8(3):499-513.

2. Jarrett JT, Lansbury PT. Seeding "one-dimensional crystallization" of amyloid: a pathogenic mechanism in Alzheimer's disease and scrapie? Cell. 1993 Jun 18;73(6):1055-8.

3. Aguzzi A, Calella AM. Prions: protein aggregation and infectious diseases. Physiol Rev. 2009 Oct;89(4):1105-52.

4. Colby DW, Prusiner SB. Prions. Cold Spring Harb Perspect Biol. 2011 Jan 01;3(1):a006833.

5. Glatzel M, Stoeck K, Seeger H, et al. Human prion diseases: molecular and clinical aspects. Arch Neurol. 2005 Apr;62(4):545-52.

6. Ritchie DL, Ironside JW. Neuropathology of Human Prion Diseases. Prog Mol Biol Transl Sci. 2017;150:319-339.

7. Kimberlin RH. Bovine spongiform encephalopathy. Rev Sci Tech. 1992 Jun;11(2):347-489.

8. Wells GA, Wilesmith JW. The neuropathology and epidemiology of bovine spongiform encephalopathy. Brain Pathol. 1995 Jan;5(1):91-103.

9. Houston F, Andréoletti O. Animal prion diseases: the risks to human health. Brain Pathol. 2019 03;29(2):248-262.

10. Williams ES. Chronic wasting disease. Vet Pathol. 2005 Sep;42(5):530-49.

11. Mathiason CK. Scrapie, CWD, and Transmissible Mink Encephalopathy. Prog Mol Biol Transl Sci. 2017;150:267-292.

12. Greenlee JJ. Review: Update on Classical and Atypical Scrapie in Sheep and Goats. Vet Pathol. 2019 Jan;56(1):6-16.

13. Babelhadj B, Di Bari MA, Pirisinu L, et al. Prion disease in dromedary camels, Algeria. Emerg Infect Dis. 2018 Jun;24(6):1029-1036.

14. World Organization for Animal Health. Camel prion disease: a possible emerging disease in dromedary camel populations? World Organization for Animal Health; 2019 Dec. (Bulletin).

15. Wulf MA, Senatore A, Aguzzi A. The biological function of the cellular prion protein: an update. BMC Biol. 2017 05 02;15(1):34.

16. Vázquez-Fernández E, Young HS, Requena JR, et al. The Structure of Mammalian Prions and Their Aggregates. Int Rev Cell Mol Biol. 2017;329:277-301.

17. Marín-Moreno A, Fernández-Borges N, Espinosa JC, et al. Transmission and Replication of Prions. Prog Mol Biol Transl Sci. 2017;150:181-201.

18. Glynn C, Sawaya MR, Ge P, et al. Cryo-EM structure of a human prion fibril with a hydrophobic, protease-resistant core. Nat Struct Mol Biol. 2020 05;27(5):417-423.

19. Wang LQ, Zhao K, Yuan HY, et al. Genetic prion disease-related mutation E196K displays a novel amyloid fibril structure revealed by cryo-EM. Sci Adv. 2021 Sep 10;7(37):eabg9676.

20. Hoyt F, Standke HG, Artikis E, et al. Cryo-EM structure of anchorless RML prion reveals variations in shared motifs between distinct strains. Nat Commun. 2022 07 13;13(1):4005.

21. Hallinan GI, Ozcan KA, Hoq MR, et al. Cryo-EM structures of prion protein filaments from Gerstmann-Sträussler-Scheinker disease. Acta Neuropathol. 2022 Sep;144(3):509-520.

22. Manka SW, Zhang W, Wenborn A, et al. 2.7 Å cryo-EM structure of ex vivo RML prion fibrils. Nat Commun. 2022 07 13;13(1):4004.

23. Ironside JW, Ritchie DL, Head MW. Prion diseases. Handb Clin Neurol. 2017;145:393-403.

24. Ersdal C, Simmons MM, González L, et al. Relationships between ultrastructural scrapie pathology and patterns of abnormal prion protein accumulation. Acta Neuropathol. 2004 May;107(5):428-38.

25. Orge L, Lima C, Machado C, et al. Neuropathology of Animal Prion Diseases. Biomolecules. 2021 03 21;11(3).

26. Frontzek K, Aguzzi A. Recent developments in antibody therapeutics against prion disease. Emerg Top Life Sci. 2020 09 08;4(2):169-173.

27. Giles K, Olson SH, Prusiner SB. Developing Therapeutics for PrP Prion Diseases. Cold Spring Harb Perspect Med. 2017 Apr 03;7(4).

28. Sigurdson CJ, Bartz JC, Glatzel M. Cellular and Molecular Mechanisms of Prion Disease. Annu Rev Pathol. 2019 01 24;14:497-516.

29. Zafar S, Noor A, Zerr I. Therapies for prion diseases. Handb Clin Neurol. 2019;165:47-58.

30. Taylor DM. Inactivation of prions by physical and chemical means. J Hosp Infect. 1999 Dec;43 Suppl:S69-76.

31. Giles K, Woerman AL, Berry DB, et al. Bioassays and Inactivation of Prions. Cold Spring Harb Perspect Biol. 2017 Aug 01;9(8).

32. Sakudo A, Ano Y, Onodera T, et al. Fundamentals of prions and their inactivation (review). Int J Mol Med. 2011 Apr;27(4):483-9.

33. Bonda DJ, Manjila S, Mehndiratta P, et al. Human prion diseases: surgical lessons learned from iatrogenic prion transmission. Neurosurg Focus. 2016 Jul;41(1):E10.

34. Smith PG, Cousens SN, d' Huillard Aignaux JN, et al. The epidemiology of variant Creutzfeldt-Jakob disease. Curr Top Microbiol Immunol. 2004;284:161-91.

35. Georgsson G, Sigurdarson S, Brown P. Infectious agent of sheep scrapie may persist in the environment for at least 16 years. J Gen Virol. 2006 Dec;87(Pt 12):3737-3740.

36. Williams ES, Young S. Chronic wasting disease of captive mule deer: a spongiform encephalopathy. J Wildl Dis. 1980 Jan;16(1):89-98.

37. Williams ES, Miller MW, Kreeger TJ, et al. Chronic wasting disease of deer and elk: A review with recommendations for management [Article]. Journal of Wildlife Management. 2002 July, 2002;66(3):551-563.

38. Mathiason CK, Powers JG, Dahmes SJ, et al. Infectious prions in the saliva and blood of deer with chronic wasting disease. Science. 2006 Oct 06;314(5796):133-6.

39. Davenport KA, Hoover CE, Denkers ND, et al. Modified Protein Misfolding Cyclic Amplification Overcomes Real-Time Quaking-Induced Conversion Assay Inhibitors in Deer Saliva To Detect Chronic Wasting Disease Prions. J Clin Microbiol. 2018 09;56(9).

40. Rubenstein R, Chang B, Gray P, et al. Prion disease detection, PMCA kinetics, and IgG in urine from sheep naturally/experimentally infected with scrapie and deer with preclinical/clinical chronic wasting disease. J Virol. 2011 Sep;85(17):9031-8.

41. Haley NJ, Mathiason CK, Carver S, et al. Detection of chronic wasting disease prions in salivary, urinary, and intestinal tissues of deer: potential mechanisms of prion shedding and transmission. J Virol. 2011 Jul;85(13):6309-18.

42. Tamgüney G, Miller MW, Wolfe LL, et al. Asymptomatic deer excrete infectious prions in faeces. Nature. 2009 Sep 24;461(7263):529-32.

43. Pulford B, Spraker TR, Wyckoff AC, et al. Detection of PrPCWD in feces from naturally exposed Rocky Mountain elk (Cervus elaphus nelsoni) using protein misfolding cyclic amplification. J Wildl Dis. 2012 Apr;48(2):425-34.

44. Tamgüney G, Richt JA, Hamir AN, et al. Salivary prions in sheep and deer. Prion. 2012 2012 Jan-Mar;6(1):52-61.

45. Mathiason CK, Hays SA, Powers J, et al. Infectious prions in pre-clinical deer and transmission of chronic wasting disease solely by environmental exposure. PLoS One. 2009 Jun 16;4(6):e5916.

46. Miller MW, Williams ES, Hobbs NT, et al. Environmental sources of prion transmission in mule deer. Emerg Infect Dis. 2004 Jun;10(6):1003-6.

47. Johnson CJ, Phillips KE, Schramm PT, et al. Prions adhere to soil minerals and remain infectious. PLoS Pathog. 2006 Apr;2(4):e32.

48. Johnson CJ, Pedersen JA, Chappell RJ, et al. Oral transmissibility of prion disease is enhanced by binding to soil particles. PLoS Pathog. 2007 Jul;3(7):e93.

49. Nichols TA, Spraker TR, Rigg TD, et al. Intranasal inoculation of white-tailed deer (Odocoileus virginianus) with lyophilized chronic wasting disease prion particulate complexed to montmorillonite clay. PLoS One. 2013;8(5):e62455.

50. Pritzkow S, Morales R, Moda F, et al. Grass plants bind, retain, uptake, and transport infectious prions. Cell Rep. 2015 May 26;11(8):1168-75.

51. Plummer IH, Johnson CJ, Chesney AR, et al. Mineral licks as environmental reservoirs of chronic wasting disease prions. PLoS One. 2018;13(5):e0196745.

52. Miller MW, Fischer JR. The first five (or more) decades of chronic wasting disease: Lessons for the five decades to come. In: Transactions of the 81st North American Wildlife and Natural Resources Conference; 2016 Mar 13-16; Pittsburgh (PA). Washington (DC): Wildlife Management Institute; 2016. p. 110-120.

53. Williams ES, Young S. Spongiform encephalopathy of Rocky Mountain elk. J Wildl Dis. 1982 Oct;18(4):465-71.

54. Spraker TR, Miller MW, Williams ES, et al. Spongiform encephalopathy in free-ranging mule deer (Odocoileus hemionus), white-tailed deer (Odocoileus virginianus) and Rocky Mountain elk (Cervus elaphus nelsoni) in northcentral Colorado. J Wildl Dis. 1997 Jan;33(1):1-6.

55. Dubé C, Mehren KG, Barker IK, et al. Retrospective investigation of chronic wasting disease of cervids at the Toronto Zoo, 1973-2003. Can Vet J. 2006 Dec;47(12):1185-93.

56. Williams ES, Young S. Spongiform encephalopathies in Cervidae. Rev Sci Tech Off Int Epiz. 1992;11(2):551-567.

57. Inch C, Doré A. The impact of Canada's animal health status on trade. Can Vet J. 1999 Jun;40(6):435-9.

58. Sohn H, Kim J, Choi K, et al. A case of chronic wasting disease in an elk imported to Korea from Canada. J Vet Med Sci. 2002;64(9):855-858.

59. Lee YH, Sohn HJ, Kim MJ, et al. Experimental chronic wasting disease in wild type VM mice. J Vet Med Sci. 2013;75(8):1107-10.

60. Roh I-S, Kim H-J, Suh T-Y, et al.Outbreak of Chronic Wasting Disease in captive deer, 2016. Korean Veterinary Society Conference Presentation. 2016;56(3):281-282.

61. Doster GL, editor. Special CWD Issue. SCWS Briefs. 2002 Apr;18(1):1-16.

62. Chronic Wasting Disease – History in Alberta [Internet]. Alberta (CA). Government of Alberta; 2022 [cited 2022 Sep 2]. Available from: https://www.alberta.ca/chronic-wasting-disease-history-in-alberta.aspx

63. Bryon JR. Expanding Distribution of Chronic Wasting Disease [Internet]. Updated 2022 Apr 1 [Cited 2022 Sep 2]. United States Geological Survey, Available from: https://www.usgs.gov/centers/nwhc/science/expanding-distribution-chronic-wasting-disease

64. Government of Alberta. Chronic wasting disease in Alberta: year of first detection in a Wildlife Management Unit (WMU) [map]. Alberta (CA): Government of Alberta. 2021 Apr. Available from: https://open.alberta.ca/publications/chronic-wasting-disease-in-alberta-year-of-first-detection-in-a-wildlife-management-unit-wmu

65. Government of Alberta. Alberta Caribou Ranges [map]. Alberta (CA): Government of Alberta. 2017 Dec 18. Available from: https://open.alberta.ca/publications/9781460137055

66. CWD Surveillance Program Results [Internet]. Saskatchewan (CA): Government of Saskatchewan. Updated 2022 May 17 [Cited 2022 Sep 2]. Available from: https://www.saskatchewan.ca/residents/environment-public-health-and-safety/wildlife-issues/fish-and-wildlife-diseases/chronic-wasting-disease/cwd-map

67. Government of Saskatchewan. Woodland Caribou 2019 Woodland Caribou Conservation Program Update. Saskatchewan (CA): Government of Saskatchewan; 2020.

68. Benestad SL, Mitchell G, Simmons M, et al. First case of chronic wasting disease in Europe in a Norwegian free-ranging reindeer. Vet Res. 2016 09 15;47(1):88.

69. Pirisinu L, Tran L, Chiappini B, et al. Novel Type of Chronic Wasting Disease Detected in Moose (Alces alces), Norway. Emerg Infect Dis. 2018 Dec;24(12):2210-2218.

70. Mysterud A, Rolandsen CM. A reindeer cull to prevent chronic wasting disease in Europe. Nat Ecol Evol. 2018 09;2(9):1343-1345.

71. Vikøren T, Våge J, Madslien KI, et al. First Detection of Chronic Wasting Disease in a Wild Red Deer (J Wildl Dis. 2019 10;55(4):970-972.

72. Ågren EO, Sörén K, Gavier-Widén D, et al. First Detection of Chronic Wasting Disease in Moose (Alces alces) in Sweden. J Wildl Dis. 2021 04 01;57(2):461-463.

73. Tranulis MA, Gavier-Widén D, Våge J, et al. Chronic wasting disease in Europe: new strains on the horizon. Acta Vet Scand. 2021 Nov 25;63(1):48.

74. Kekkonen J, Wikström M, Brommer JE. Heterozygosity in an isolated population of a large mammal founded by four individuals is predicted by an individual-based genetic model. PLoS One. 2012;7(9):e43482.

75. Laaksonen S, Oksanen A, Hoberg E. A lymphatic dwelling filarioid nematode, Rumenfilaria andersoni (Filarioidea; Splendidofilariinae), is an emerging parasite in Finnish cervids. Parasit Vectors. 2015 Apr 16;8:228.

76. Sauvala M, Laaksonen S, Laukkanen-Ninios R, et al. Microbial contamination of moose (Alces alces) and white-tailed deer (Odocoileus virginianus) carcasses harvested by hunters. Food Microbiol. 2019 Apr;78:82-88.

77. Chronic Wasting Disease – Updates [Internet]. Government of Alberta. Chronic Wasting Disease (CWD) surveillance update: May 31, 2022. Available from: https://web.archive.org/web/20220610094431/https://www.alberta.ca/chronic-wasting-disease-updates.aspx

78. Benestad SL, Sarradin P, Thu B, et al. Cases of scrapie with unusual features in Norway and designation of a new type, Nor98. Vet Rec. 2003 Aug 16;153(7):202-8.

79. Chong A, Kennedy I, Goldmann W, et al. Archival search for historical atypical scrapie in sheep reveals evidence for mixed infections. J Gen Virol. 2015 Oct;96(10):3165-3178.

80. Gill ON, Spencer Y, Richard-Loendt A, et al. Prevalence in Britain of abnormal prion protein in human appendices before and after exposure to the cattle BSE epizootic. Acta Neuropathol. 2020 06;139(6):965-976.

81. Detwiler LA, Rubenstein R. Bovine spongiform encephalopathy: an overview. ASAIO J. 2000 2000 Nov-Dec;46(6):S73-9.

82. Smith PG, Bradley R. Bovine spongiform encephalopathy (BSE) and its epidemiology. Br Med Bull. 2003;66:185-98.

83. Comber T. A letter to Dr. Hunter, physician in York. Concerning the rickets in sheep. In: Real Improvements in Agriculture. London (England): W. Nicoll; 1772. p. 73-83.

84. Chatelain J, Cathala F, Brown P, et al. Epidemiologic comparisons between Creutzfeldt-Jakob disease and scrapie in France during the 12-year period 1968-1979. J Neurol Sci. 1981 Sep;51(3):329-37.

85. Brown P, Cathala F, Raubertas RF, et al. The epidemiology of Creutzfeldt-Jakob disease: conclusion of a 15-year investigation in France and review of the world literature. Neurology. 1987 Jun;37(6):895-904.

86. van Duijn CM, Delasnerie-Lauprêtre N, Masullo C, et al. Case-control study of risk factors of Creutzfeldt-Jakob disease in Europe during 1993-95. European Union (EU) Collaborative Study Group of Creutzfeldt-Jakob disease (CJD). Lancet. 1998 Apr 11;351(9109):1081-5.

87. Ironside JW. Variant Creutzfeldt-Jakob disease. Haemophilia. 2010 Jul;16 Suppl 5:175-80.

88. Sikorska B, Knight R, Ironside JW, et al. Creutzfeldt-Jakob disease. Adv Exp Med Biol. 2012;724:76-90.

89. Collee JG, Bradley R, Liberski PP. Variant CJD (vCJD) and bovine spongiform encephalopathy (BSE): 10 and 20 years on: part 2. Folia Neuropathol. 2006;44(2):102-10.

90. Will RG, Ironside JW, Zeidler M, et al. A new variant of Creutzfeldt-Jakob disease in the UK. Lancet. 1996 Apr 06;347(9006):921-5.

91. Hilton DA, Ghani AC, Conyers L, et al. Prevalence of lymphoreticular prion protein accumulation in UK tissue samples. J Pathol. 2004 Jul;203(3):733-9.

92. Gill ON, Spencer Y, Richard-Loendt A, et al. Prevalent abnormal prion protein in human appendixes after bovine spongiform encephalopathy epizootic: large scale survey. BMJ. 2013 Oct 15;347:f5675.

93. Whitfield JT, Pako WH, Collinge J, et al. Cultural factors that affected the spatial and temporal epidemiology of kuru. R Soc Open Sci. 2017 Jan;4(1):160789.

94. Hill AF, Desbruslais M, Joiner S, et al. The same prion strain causes vCJD and BSE. Nature. 1997 Oct 02;389(6650):448-50, 526.

95. Asante EA, Linehan JM, Desbruslais M, et al. BSE prions propagate as either variant CJD-like or sporadic CJD-like prion strains in transgenic mice expressing human prion protein. EMBO J. 2002 Dec 02;21(23):6358-66.

96. Béringue V, Herzog L, Reine F, et al. Transmission of atypical bovine prions to mice transgenic for human prion protein. Emerg Infect Dis. 2008 Dec;14(12):1898-901.

97. Wadsworth JD, Asante EA, Collinge J. Review: contribution of transgenic models to understanding human prion disease. Neuropathol Appl Neurobiol. 2010 Dec;36(7):576-97.

98. Wadsworth JD, Joiner S, Linehan JM, et al. Atypical scrapie prions from sheep and lack of disease in transgenic mice overexpressing human prion protein. Emerg Infect Dis. 2013 Nov;19(11):1731-9.

99. Cassard H, Torres JM, Lacroux C, et al. Evidence for zoonotic potential of ovine scrapie prions. Nat Commun. 2014 Dec 16;5:5821.

100. Kong Q, Huang S, Zou W, et al. Chronic wasting disease of elk: transmissibility to humans examined by transgenic mouse models. J Neurosci. 2005 Aug 31;25(35):7944-9.

101. Tamgüney G, Giles K, Bouzamondo-Bernstein E, et al. Transmission of elk and deer prions to transgenic mice. J Virol. 2006 Sep;80(18):9104-14.

102. Sandberg MK, Al-Doujaily H, Sigurdson CJ, et al. Chronic wasting disease prions are not transmissible to transgenic mice overexpressing human prion protein. J Gen Virol. 2010 Oct;91(Pt 10):2651-7.

103. Wilson R, Plinston C, Hunter N, et al. Chronic wasting disease and atypical forms of bovine spongiform encephalopathy and scrapie are not transmissible to mice expressing wild-type levels of human prion protein. J Gen Virol. 2012 Jul;93(Pt 7):1624-1629.

104. Kurt TD, Jiang L, Fernández-Borges N, et al. Human prion protein sequence elements impede cross-species chronic wasting disease transmission. J Clin Invest. 2015 Jun;125(6):2548.

105. Wadsworth JDF, Joiner S, Linehan JM, et al. Humanised transgenic mice are resistant to chronic wasting disease prions from Norwegian reindeer and moose. J Infect Dis. 2021 Jan 27.

106. Race B, Williams K, Chesebro B. Transmission studies of chronic wasting disease to transgenic mice overexpressing human prion protein using the RT-QuIC assay. Vet Res. 2019 Jan 22;50(1):6.

107. Hannaoui S, Zemlyankina I, Chang SC, et al. Transmission of cervid prions to humanized mice demonstrates the zoonotic potential of CWD. Acta Neuropathol. 2022 Aug 22.

108. Diack AB, Ritchie DL, Peden AH, et al. Variably protease-sensitive prionopathy, a unique prion variant with inefficient transmission properties. Emerg Infect Dis. 2014 Dec;20(12):1969-79.

109. Piccardo P, Cervenak J, Goldmann W, et al. Experimental Bovine Spongiform Encephalopathy in Squirrel Monkeys: The Same Complex Proteinopathy Appearing after Very Different Incubation Times. Pathogens. 2022 May 20;11(5).

110. Marsh RF, Kincaid AE, Bessen RA, et al. Interspecies transmission of chronic wasting disease prions to squirrel monkeys (Saimiri sciureus). J Virol. 2005 Nov;79(21):13794-6.

111. Race B, Meade-White KD, Miller MW, et al. Susceptibilities of nonhuman primates to chronic wasting disease. Emerg Infect Dis. 2009 Sep;15(9):1366-76.

112. Race B, Meade-White KD, Phillips K, et al. Chronic wasting disease agents in nonhuman primates. Emerg Infect Dis. 2014 May;20(5):833-7.

113. Gibbs CJ, Gajdusek DC, Latarjet R. Unusual resistance to ionizing radiation of the viruses of kuru, Creutzfeldt-Jakob disease, and scrapie. Proc Natl Acad Sci U S A. 1978 Dec;75(12):6268-70.

114. Lasmézas CI, Deslys JP, Demaimay R, et al. BSE transmission to macaques. Nature. 1996 Jun 27;381(6585):743-4.

115. Herzog C, Salès N, Etchegaray N, et al. Tissue distribution of bovine spongiform encephalopathy agent in primates after intravenous or oral infection. Lancet. 2004 Feb 07;363(9407):422-8.

116. Comoy EE, Mikol J, Luccantoni-Freire S, et al. Transmission of scrapie prions to primate after an extended silent incubation period. Sci Rep. 2015 Jun 30;5:11573.

117. Gibbs CJ, Gajdusek DC. Transmission of scrapie to the cynomolgus monkey (Macaca fascicularis). Nature. 1972 Mar 10;236(5341):73-4.

118. Race B, Williams K, Orrú CD, et al. Lack of Transmission of Chronic Wasting Disease to Cynomolgus Macaques. J Virol. 2018 07 15;92(14).

119. Czub S, Schulz-Schaeffer W, Stahl-Hennig, et al. First Evidence of intracranial and peroral transmission of chronic wasting disease (CWD) into Cynomolgus macaques: a work in progress. Paper presented at: PRION 2017; 2017 May 23-26; Edinburgh, Scotland.

120. Angers RC, Browning SR, Seward TS, et al. Prions in skeletal muscles of deer with chronic wasting disease. Science. 2006 Feb 24;311(5764):1117.

121. Daus ML, Breyer J, Wagenfuehr K, et al. Presence and seeding activity of pathological prion protein (PrP(TSE)) in skeletal muscles of white-tailed deer infected with chronic wasting disease. PLoS One. 2011 Apr 01;6(4):e18345.

122. Hoover CE, Davenport KA, Henderson DM, et al. Pathways of prion spread during early chronic wasting disease in deer. J Virol. 2017 Apr 28;91(10):e00077-17.

123. Otero A, Duque Velásquez C, Johnson C, et al. Prion protein polymorphisms associated with reduced CWD susceptibility limit peripheral PrP. BMC Vet Res. 2019 Feb 04;15(1):50.

124. Kramm C, Gomez-Gutierrez R, Soto C, et al. In Vitro detection of Chronic Wasting Disease (CWD) prions in semen and reproductive tissues of white tailed deer bucks (Odocoileus virginianus). PLoS One. 2019;14(12):e0226560.

125. Li M, Schwabenlander MD, Rowden GR, et al. RT-QuIC detection of CWD prion seeding activity in white-tailed deer muscle tissues. Sci Rep. 2021 08 18;11(1):16759.

126. Buschmann A, Groschup MH. Highly bovine spongiform encephalopathy-sensitive transgenic mice confirm the essential restriction of infectivity to the nervous system in clinically diseased cattle. J Infect Dis. 2005 Sep 01;192(5):934-42.

127. Iwata N, Sato Y, Higuchi Y, et al. Distribution of PrP(Sc) in cattle with bovine spongiform encephalopathy slaughtered at abattoirs in Japan. Jpn J Infect Dis. 2006 Apr;59(2):100-7.

128. Balkema-Buschmann A, Eiden M, Hoffmann C, et al. BSE infectivity in the absence of detectable PrP(Sc) accumulation in the tongue and nasal mucosa of terminally diseased cattle. J Gen Virol. 2011 Feb;92(Pt 2):467-76.

129. Franz M, Eiden M, Balkema-Buschmann A, et al. Detection of PrP(Sc) in peripheral tissues of clinically affected cattle after oral challenge with bovine spongiform encephalopathy. J Gen Virol. 2012 Dec;93(Pt 12):2740-2748.

130. Geist V, Clausen D, Crichton V, et al. The Challenge of CWD: Insidious and Dire. Alliance for Public Wildlife; 2017. (Living Legacy White Paper Series).

131. Gavin C, Henderson D, Benestad SL, et al. Estimating the amount of Chronic Wasting Disease infectivity passing through abattoirs and field slaughter. Prev Vet Med. 2019 May 01;166:28-38.

132. Belay ED, Gambetti P, Schonberger LB, et al. Creutzfeldt-Jakob disease in unusually young patients who consumed venison. Arch Neurol. 2001 Oct;58(10):1673-8.

133. Mawhinney S, Pape WJ, Forster JE, et al. Human prion disease and relative risk associated with chronic wasting disease. Emerg Infect Dis. 2006 Oct;12(10):1527-35.

134. Anderson CA, Bosque P, Filley CM, et al. Colorado surveillance program for chronic wasting disease transmission to humans: lessons from 2 highly suspicious but negative cases. Arch Neurol. 2007 Mar;64(3):439-41.

135. Olszowy KM, Lavelle J, Rachfal K, et al. Six-year follow-up of a point-source exposure to CWD contaminated venison in an Upstate New York community: risk behaviours and health outcomes 2005-2011. Public Health. 2014 Sep;128(9):860-8.

136. Liu Y, Camacho M, Zou W, et al. Screening and characterization of unusual sCJD cases in a CWD endemic state in the USA. In: Westaway D, Schätzl H, Keough K, editors. PRION 2019 emerging concepts; 2019 May 21-24; Edmonton (AB): Prion. 2019 May 18;13(sup1):1-141.

137. Diack AB, Head MW, McCutcheon S, et al. Variant CJD. 18 years of research and surveillance. Prion. 2014;8(4):286-95.

138. Brandel JP, Knight R. Variant Creutzfeldt-Jakob disease. Handb Clin Neurol. 2018;153:191-205.

139. Mok T, Jaunmuktane Z, Joiner S, et al. Variant Creutzfeldt-Jakob Disease in a Patient with Heterozygosity at PRNP Codon 129. N Engl J Med. 2017 01 19;376(3):292-294.

140. Kaski D, Mead S, Hyare H, et al. Variant CJD in an individual heterozygous for PRNP codon 129. Lancet. 2009 Dec 19;374(9707):2128.

141. Nurmi MH, Bishop M, Strain L, et al. The normal population distribution of PRNP codon 129 polymorphism. Acta Neurol Scand. 2003 Nov;108(5):374-8.

142. Ironside JW, Bishop MT, Connolly K, et al. Variant Creutzfeldt-Jakob disease: prion protein genotype analysis of positive appendix tissue samples from a retrospective prevalence study. BMJ. 2006 May 20;332(7551):1186-8.

143. Schneider K, Fangerau H, Michaelsen B, et al. The early history of the transmissible spongiform encephalopathies exemplified by scrapie. Brain Res Bull. 2008 Dec 16;77(6):343-55.

144. Leopoldt JG. Nützliche und auf die Erfahrung gegründete Einleitung zu der Land-Wirthschafft [Useful and experience-based introduction to agriculture]. Sorau: Johann Gottlieb Rothen; 1750. German.

145. Soltmann H. Gothaisches genealogisches taschenbuch der freiherrlichen häuser auf das jahr 1859. Gotha: Justus Pertha; 1859. German.

146. von Richthofen AKS. Die traberkrankheit der schaafe, verglichen mit der sogenannten schaffräudekrankheit. Breslau: Wilhelm Gottlich Korn; 1827. German.

147. Obituary: J. P. McGowan, M.D., M.R.C.P.Ed., D.T.M.&H. Brit Med J. 1961 Oct 28;2(5260):1155-1156.

148. Boulton F. Thomas Addis (1881-1949); Scottish pioneer in haemophilia research. J R Coll Physicians Edinb. 2003;33(2):135–142.

149. M'Gowan JP. Investigation into the disease of sheep called "scrapie" (traberkrankheit; la tremblante): with especial reference to its association with sarcosporidiosis. Edinburgh (UK): William Blackwood and Sons; 1914.

150. Cuillé J, Chelle PL. La maladie dite "tremblante" du mouton; est-elle inoculable? Compte Rend Acad Sci. 1936;203:1552–1554. French.

151. Greig JR. Scrapie: Observations on the transmission of the disease by mediate contact. Vet J (1900). 1940 May;96(5):203-206.

152. Lacroux C, Simon S, Benestad SL, et al. Prions in milk from ewes incubating natural scrapie. PLoS Pathog. 2008 Dec;4(12):e1000238.

153. Konold T, Hawkins SA, Thurston LC, et al. Objects in Contact with Classical Scrapie Sheep Act as a Reservoir for Scrapie Transmission. Front Vet Sci. 2015;2:32.

154. Thomzig A, Schulz-Schaeffer W, Wrede A, et al. Accumulation of pathological prion protein PrPSc in the skin of animals with experimental and natural scrapie. PLoS Pathog. 2007 May 25;3(5):e66.

155. Vascellari M, Nonno R, Mutinelli F, et al. PrPSc in salivary glands of scrapie-affected sheep. J Virol. 2007 May;81(9):4872-6.

156. Maddison BC, Baker CA, Rees HC, et al. Prions are secreted in milk from clinically normal scrapie-exposed sheep. J Virol. 2009 Aug;83(16):8293-6.

157. Gough KC, Maddison BC. Prion transmission: prion excretion and occurrence in the environment. Prion. 2010 Oct-Dec;4(4):275-82.

158. Maddison BC, Rees HC, Baker CA, et al. Prions are secreted into the oral cavity in sheep with preclinical scrapie. J Infect Dis. 2010 Jun 01;201(11):1672-6.

159. Terry LA, Howells L, Bishop K, et al. Detection of prions in the faeces of sheep naturally infected with classical scrapie. Vet Res. 2011 May 18;42:65.

160. Touzeau S, Chase-Topping ME, Matthews L, et al. Modelling the spread of scrapie in a sheep flock: evidence for increased transmission during lambing seasons. Arch Virol. 2006 Apr;151(4):735-51.

161. Dexter G, Tongue SC, Heasman L, et al. The evaluation of exposure risks for natural transmission of scrapie within an infected flock. BMC Vet Res. 2009 Oct 09;5:38.

162. Garza MC, Fernández-Borges N, Bolea R, et al. Detection of PrPres in genetically susceptible fetuses from sheep with natural scrapie. PLoS One. 2011;6(12):e27525.

163. Foster JD, Goldmann W, Hunter N. Evidence in sheep for pre-natal transmission of scrapie to lambs from infected mothers. PLoS One. 2013;8(11):e79433.

164. Spiropoulos J, Hawkins SA, Simmons MM, et al. Evidence of in utero transmission of classical scrapie in sheep. J Virol. 2014 Apr;88(8):4591-4.

165. Brotherston JG, Renwick CC, Stamp JT, et al. Spread and scrapie by contact to goats and sheep. J Comp Pathol. 1968 Jan;78(1):9-17.

166. Hourrigan JL, Klingsporn AL. Scrapie: studies on vertical and horizontal transmission. In: Gibbs CJ, editor. Bovine spongiform encephalopathy: The BSE dilemma. New York (NY): Springer; 1996. p. 59-83.

167. Hadlow WJ, Kennedy RC, Race RE. Natural infection of Suffolk sheep with scrapie virus. J Infect Dis. 1982 Nov;146(5):657-64.

168. Heggebø R, Press CM, Gunnes G, et al. Distribution of prion protein in the ileal Peyer's patch of scrapie-free lambs and lambs naturally and experimentally exposed to the scrapie agent. J Gen Virol. 2000 Sep;81(Pt 9):2327-2337.

169. Onodera T, Ikeda T, Muramatsu Y, et al. Isolation of scrapie agent from the placenta of sheep with natural scrapie in Japan. Microbiol Immunol. 1993;37(4):311-6.

170. Race R, Jenny A, Sutton D. Scrapie infectivity and proteinase K-resistant prion protein in sheep placenta, brain, spleen, and lymph node: implications for transmission and antemortem diagnosis. J Infect Dis. 1998 Oct;178(4):949-53.

171. Schneider DA, Madsen-Bouterse SA, Zhuang D, et al. The placenta shed from goats with classical scrapie is infectious to goat kids and lambs. J Gen Virol. 2015 Aug;96(8):2464-2469.

172. Konold T, Moore SJ, Bellworthy SJ, et al. Evidence of effective scrapie transmission via colostrum and milk in sheep. BMC Vet Res. 2013 May 07;9:99.

173. Ligios C, Sigurdson CJ, Santucciu C, et al. PrPSc in mammary glands of sheep affected by scrapie and mastitis. Nat Med. 2005 Nov;11(11):1137-8.

174. Salazar E, Monleón E, Bolea R, et al. Detection of PrPSc in lung and mammary gland is favored by the presence of Visna/maedi virus lesions in naturally coinfected sheep. Vet Res. 2010 2010 Sep-Oct;41(5):58.

175. Ligios C, Cancedda MG, Carta A, et al. Sheep with scrapie and mastitis transmit infectious prions through the milk. J Virol. 2011 Jan;85(2):1136-9.

176. Haley NJ, Seelig DM, Zabel MD, et al. Detection of CWD prions in urine and saliva of deer by transgenic mouse bioassay. PLoS One. 2009;4(3):e4848.

177. Tennant JM, Li M, Henderson DM, et al. Shedding and stability of CWD prion seeding activity in cervid feces. PLoS One. 2020;15(3):e0227094.

178. Miller MW, Williams ES. Detection of PrP(CWD) in mule deer by immunohistochemistry of lymphoid tissues. Vet Rec. 2002 Nov 16;151(20):610-2.

179. Fox KA, Jewell JE, Williams ES, et al. Patterns of PrPCWD accumulation during the course of chronic wasting disease infection in orally inoculated mule deer (Odocoileus hemionus). J Gen Virol. 2006 Nov;87(Pt 11):3451-3461.

180. Spraker TR, Zink RR, Cummings BA, et al. Distribution of protease-resistant prion protein and spongiform encephalopathy in free-ranging mule deer (Odocoileus hemionus) with chronic wasting disease. Vet Pathol. 2002 Sep;39(5):546-56.

181. Somerville RA, Fernie K, Smith A, et al. BSE infectivity survives burial for five years with only limited spread. Arch Virol. 2019 Apr;164(4):1135-1145.

182. Seidel B, Thomzig A, Buschmann A, et al. Scrapie Agent (Strain 263K) can transmit disease via the oral route after persistence in soil over years. PLoS One. 2007 May 09;2(5):e435.

183. Brown P, Gajdusek DC. Survival of scrapie virus after 3 years' interment. Lancet. 1991 Feb 02;337(8736):269-70.

184. Miller MW, Wild MA, Williams ES. Epidemiology of chronic wasting disease in captive Rocky Mountain elk. J Wildl Dis. 1998 Jul;34(3):532-8.

185. Thompson AK, Samuel MD, Van Deelen TR. Alternative feeding strategies and potential disease transmission in Wisconsin white-tailed deer. J Wildl Manage. 2008 Feb;72(2):416-421.

186. Herbst A, Wohlgemuth S, Yang J, et al. Susceptibility of Beavers to Chronic Wasting Disease. Biology (Basel). 2022 Apr 26;11(5).

187. Heisey DM, Mickelsen NA, Schneider JR, et al. Chronic wasting disease (CWD) susceptibility of several North American rodents that are sympatric with cervid CWD epidemics. J Virol. 2010 Jan;84(1):210-5.

188. Moore SJ, Smith JD, Richt JA, et al. Raccoons accumulate PrP. J Vet Diagn Invest. 2019 Mar;31(2):200-209.

189. Moore SJ, Carlson CM, Schneider JR, et al. Increased Attack Rates and Decreased Incubation Periods in Raccoons with Chronic Wasting Disease Passaged through Meadow Voles. Emerg Infect Dis. 2022 04;28(4):793-801.

190. DeVivo MT, Edmunds DR, Kauffman MJ, et al. Endemic chronic wasting disease causes mule deer population decline in Wyoming. PLoS One. 2017;12(10):e0186512.

191. Smolko P, Seidel D, Pybus M, et al. Spatio-temporal changes in chronic wasting disease risk in wild deer during 14 years of surveillance in Alberta, Canada. Prev Vet Med. 2021 Dec;197:105512.

192. Almberg E, Becker M, Thornburg J et al. Montana fish, wildlife & parks' 2020 chronic wasting disease surveillance and monitoring report. Bozeman (MT): Montana Fish, Wildlife & Parks; 2021 May 14.

193. Grear DA, Samuel MD, Langenberg JA, et al. Demographic patterns and harvest vulnerability of chronic wasting disease infected white-tailed deer in Wisconsin [Article]. Journal of Wildlife Management. 2006 2006;70(2):546-553.

194. Osnas EE, Heisey DM, Rolley RE, et al. Spatial and temporal patterns of chronic wasting disease: fine-scale mapping of a wildlife epidemic in Wisconsin. Ecol Appl. 2009 Jul;19(5):1311-22.

195. CWD prevalence in Wisconsin [Internet]. Madison (WI): Wisconsin Department of Natural Resources. [Cited 2022 Jun 26] Available from: https://dnr.wi.gov/topic/wildlifehabitat/prevalence.html#prevalence.

196. Wolfe LL, Watry MK, Sirochman MA, et al. Evaluation of a test and cull strategy for reducing prevalence of chronic wasting disease in mule deer (Odocoileus hemionus). J Wildl Dis. 2018 07;54(3):511-519.

197. Mysterud A, Madslien K, Viljugrein H, et al. The demographic pattern of infection with chronic wasting disease in reindeer at an early epidemic stage [Article]. Ecosphere. 2019 Nov;10(11):Article No.: e02931.

198. Edmunds DR, Kauffman MJ, Schumaker BA, et al. Chronic wasting disease drives population decline of white-tailed deer. PLoS One. 2016 Aug 30;11(8): e0161127.

199. Edmunds DR, Albeke SE, Grogan RG, et al. Chronic wasting disease influences activity and behavior in white-tailed deer. J Wildl Manage. 2018;82(1):138-154.

200. Almberg ES, Cross PC, Johnson CJ, et al. Modeling routes of chronic wasting disease transmission: environmental prion persistence promotes deer population decline and extinction. PLoS One. 2011;6(5):e19896.

201. Montana Fish, Wildlife & Parks Reports. First-ever CWD deer case in Montana? Outdoor News [Internet]. 2017 Nov 8 [cited 2022 Jul 3]. Available from: https://www.outdoornews.com/2017/11/08/first-ever-cwd-deer-case-montana/

202. O'Brien DJ, Schmitt SM, Fierke JS, et al. Epidemiology of Mycobacterium bovis in free-ranging white-tailed deer, Michigan, USA, 1995-2000. Prev Vet Med. 2002 May 30;54(1):47-63.

203. Sundberg JP, Nielsen SW. Deer fibroma: a review. Can Vet J. 1981 Dec;22(12):385-8.

204. Sundberg JP, Nielsen SW. Prevalence of cutaneous fibromas in white-tailed deer (Odocoileus virginianus) in New York and Vermont. J Wildl Dis. 1982 Jul;18(3):359-60.

205. Jokelainen P, Näreaho A, Knaapi S, et al. Toxoplasma gondii in wild cervids and sheep in Finland: north-south gradient in seroprevalence. Vet Parasitol. 2010 Aug 04;171(3-4):331-6.

206. Rosenfeld I, Beath OA. Contagious panophthalmitis in deer. J Wildl Manage. 1944 Jul;8(3):247-250.

207. Muñoz Gutiérrez JF, Sondgeroth KS, Williams ES, et al. Infectious keratoconjunctivitis in free-ranging mule deer in Wyoming: a retrospective study and identification of a novel alphaherpesvirus. J Vet Diagn Invest. 2018 Sep;30(5):663-670.

208. Allen SE, Vogt NA, Stevens B, et al. A retrospective summary of cervid morbidity and mortality in Ontario and Nunavut regions of Canada (1991-2017). J Wildl Dis. 2020 10 01;56(4):884-895.

209. Cohen BS, Belser EH, Keeler SP, et al. A headache from our past? Intracranial abscess disease, virulence factors of Trueperella pyogenes, and a legacy of translocating white-tailed deer (Odocoileus virgianus). J Wildl Dis. 2018 10;54(4):671-679.

210. Belser EH, Cohen BS, Keeler SP, et al. Epethelial presence of Trueperella pyogenes predicts site-level presence of cranial abscess disease in white-tailed deer (Odocoileus virginianus). PLoS One. 2015;10(3):e0120028.

211. Karns GR, Lancia RA, Deperno CS, et al. Intracranial abscessation as a natural mortality factor for adult male white-tailed deer (Odocoileus virginianus) in Kent County, Maryland, USA. J Wildl Dis. 2009 Jan;45(1):196-200.

212. Hale VL, Dennis PM, McBride DS, et al. SARS-CoV-2 infection in free-ranging white-tailed deer. Nature. 2022 02;602(7897):481-486.

213. Palermo PM, Orbegozo J, Watts DM, et al. SARS-CoV-2 Neutralizing Antibodies in White-Tailed Deer from Texas. Vector Borne Zoonotic Dis. 2022 01;22(1):62-64.

214. Holman RC, Belay ED, Christensen KY, et al. Human prion diseases in the United States. PLoS One. 2010 Jan 01;5(1):e8521.

215. Klug GM, Boyd A, Lewis V, et al. Creutzfeldt-Jakob disease: Australian surveillance update to 31 December 2004. Commun Dis Intell Q Rep. 2005;29(3):269-71.

216. Nakamura Y, Yanagawa H, Hoshi K, et al. Incidence rate of Creutzfeldt-Jakob disease in Japan. Int J Epidemiol. 1999 Feb;28(1):130-4.

217. Lai CH, Tseng HF. Population-based epidemiological study of neurological diseases in Taiwan: I. Creutzfeldt-Jakob disease and multiple sclerosis. Neuroepidemiology. 2009;33(3):247-53.

218. Elsen JM, Amigues Y, Schelcher F, et al. Genetic susceptibility and transmission factors in scrapie: detailed analysis of an epidemic in a closed flock of Romanov. Arch Virol. 1999;144(3):431-45.

219. Del Rio Vilas VJ, Gutian J, Pfeiffer DU et al. Analysis of data from the passive surveillance of scrapie in Great Britain between 1993 and 2002. Vet Record. 2006 Dec 9;159:799-804.

220. Miller MW, Conner MM. Epidemiology of chronic wasting disease in free-ranging mule deer: spatial, temporal, and demographic influences on observed prevalence patterns. J Wildl Dis. 2005 Apr;41(2):275-290.

221. Heisey DM, Osnas EE, Cross PC, et al. Linking process to pattern: estimating spatiotemporal dynamics of a wildlife epidemic from cross-sectional data. Ecol Monogr. 2010;80(2):221-240.

222. Samuel MD, Storm DJ. Chronic wasting disease in white-tailed deer: infection, mortality, and implications for heterogeneous transmission. Ecology. 2016;97(11):3195-3205.

223. Wilesmith JW. An epidemiologist's view of bovine spongiform encephalopathy. Philos Trans R Soc Lond B Biol Sci. 1994 Mar 29;343(1306):357-61.

224. Anderson RM, Donnelly CA, Ferguson NM, et al. Transmission dynamics and epidemiology of BSE in British cattle. Nature. 1996 Aug 29;382(6594):779-88.

225. Redman CA, Coen PG, Matthews L, et al. Comparative epidemiology of scrapie outbreaks in individual sheep flocks. Epidemiol Infect. 2002 Jun;128(3):513-21.

226. Bacchetti P. Age and variant Creutzfeldt-Jakob disease. Emerg Infect Dis. 2003 Dec;9(12):1611-2.

227. The National CJD Research & Surveillance Unit (UK). 25th Annual report 2016: Creutzfeldt-Jakob Disease surveillance in the UK. Edinburgh (UK): The National CJD Research & Surveillance Unit (UK); 2016.

228. Schramm PT, Johnson CJ, Mathews NE, et al. Potential role of soil in the transmission of prion disease. Rev Mineral Geochem. 2006;64:135-152.

229. Potapov A, Merrill E, Pybus M, et al. Chronic wasting disease: Possible transmission mechanisms in deer. Ecol Modell. 2013 Feb 10;250:244-257.

230. Miller MW, Wild MA. Epidemiology of chronic wasting disease in captive white-tailed and mule deer. J Wildl Dis. 2004;40(2):320-327.

231. Argue CK, Ribble C, Lees VW, et al. Epidemiology of an outbreak of chronic wasting disease on elk farms in Saskatchewan. Can Vet J. 2007 Dec;48(12):1241-1248.

232. Keane DP, Barr DJ, Bochsler PN, et al. Chronic wasting disease in a Wisconsin white-tailed deer farm. J Vet Diagn Invest. 2008 Sep;20(5):698-703.

233. Peters J, Miller JM, Jenny AL, et al. Immunohistochemical diagnosis of chronic wasting disease in preclinically affected elk from a captive herd. J Vet Diagn Invest. 2000 Nov;12(6):579-82.

234. Miller MW, Williams ES, McCarty CW, et al. Epizootiology of chronic wasting disease in free-ranging cervids in Colorado and Wyoming. J Wildl Dis. 2000 Oct;36(4):676-90.

235. Jacques CN, Jenks JA, Jenny AL, et al. Prevalence of chronic wasting disease and bovine tuberculosis in free-ranging deer and elk in South Dakota. J Wildl Dis. 2003 Jan;39(1):29-34.

236. Saunders SE, Bartelt-Hunt SL, Bartz JC. Occurrence, transmission, and zoonotic potential of chronic wasting disease. Emerg Infect Dis. 2012 Mar;18(3):369-76.

237. Rivera NA, Brandt AL, Novakofski JE, et al. Chronic Wasting Disease In Cervids: Prevalence, Impact And Management Strategies. Vet Med (Auckl). 2019;10:123-139.

238. Monello RJ, Powers JG, Hobbs NT, et al. Survival and Population Growth of a Free-Ranging Elk Population With a Long History of Exposure to Chronic Wasting Disease. Journal of Wildlife Management. 2014 Feb 2014;78(2):214-223.

239. Sargeant GA, Wild AW, Schroeder GM, et al. Spatial network clustering reveals elk population structure and local variation in prevalence of chronic wasting disease. Ecosphere. 2021 Dec;12(12):e03781.

240. Haley NJ, Hoover EA. Chronic wasting disease of cervids: current knowledge and future perspectives. Annu Rev Anim Biosci. 2015;3:305-25.

241. Mysterud A, Edmunds DR. A review of chronic wasting disease in North America with implications for Europe. Eur J Wildl Res. 2019 Feb 21;65,26.

242. Baeten LA, Powers BE, Jewell JE, et al. A natural case of chronic wasting disease in a free-ranging moose (Alces alces shirasi). J Wildl Dis. 2007 Apr;43(2):309-14.

243. Henderson DM, Denkers ND, Hoover CE, et al. Longitudinal Detection of Prion Shedding in Saliva and Urine by Chronic Wasting Disease-Infected Deer by Real-Time Quaking-Induced Conversion. J Virol. 2015 Sep;89(18):9338-47.

244. Davenport KA, Mosher BA, Brost BM, et al. Assessment of Chronic Wasting Disease Prion Shedding in Deer Saliva with Occupancy Modeling. J Clin Microbiol. 2018 01;56(1).

245. Plummer IH, Wright SD, Johnson CJ, et al. Temporal patterns of chronic wasting disease prion excretion in three cervid species. J Gen Virol. 2017 Jul;98(7):1932-1942.

246. Hwang S, Greenlee JJ, Nicholson EM. Real-Time Quaking-Induced Conversion Detection of PrP. Front Vet Sci. 2021;8:643754.

247. Cheng YC, Hannaoui S, John TR, et al. Early and Non-Invasive Detection of Chronic Wasting Disease Prions in Elk Feces by Real-Time Quaking Induced Conversion. PLoS One. 2016;11(11):e0166187.

248. Aguzzi A, Heikenwalder M, Miele G. Progress and problems in the biology, diagnostics, and therapeutics of prion diseases. J Clin Invest. 2004 Jul;114(2):153-60.

249. Aguzzi A, Nuvolone M, Zhu C. The immunobiology of prion diseases. Nat Rev Immunol. 2013 Dec;13(12):888-902.

250. Davenport KA, Christiansen JR, Bian J, et al. Comparative analysis of prions in nervous and lymphoid tissues of chronic wasting disease-infected cervids. J Gen Virol. 2018 05;99(5):753-758.

251. Race BL, Meade-White KD, Ward A, et al. Levels of abnormal prion protein in deer and elk with chronic wasting disease. Emerg Infect Dis. 2007 Jun;13(6):824-30.

252. Quay WB, Müller-Schwarze D. Functional histology of integumentary glandular regions in black-tailed deer (Odocoileus hemionus columbianus). J Mammal. 1970 Nov;51(4):675-694.

253. Suzuki Y, Komatsu T, Yamamoto Y, et al. Pathology of interdigital glands in a wild Japanese serow (Capricornis crispus) infected with parapoxvirus. J Vet Med Sci. 1997 Nov;59(11):1063-5.

254. Dego OK, Van Dijk JE, Nederbragt H. Factors involved in the early pathogenesis of bovine Staphylococcus aureus mastitis with emphasis on bacterial adhesion and invasion. A review. [Article]. Veterinary Quarterly. 2002 December 2002;24(4):181-198.

255. Jain NC. Common mammary pathogens and factors in infection and mastitis. J Dairy Sci. 1979 Jan;62(1):128-34.

256. Fragkou IA, Gougoulis DA, Billinis C, et al. Transmission of Mannheimia haemolytica from the tonsils of lambs to the teat of ewes during sucking. Vet Microbiol. 2011 Feb 24;148(1):66-74.

257. Azizi S, Tehrani AA, Dalir-Naghadeh B, et al. The effects of farming system and season on the prevalence of lameness in sheep in northwest Iran. N Z Vet J. 2011 Nov;59(6):311-6.

258. Arteche-Villasol N, Fernández M, Gutiérrez-Expósito D, et al. Pathology of the Mammary Gland in Sheep and Goats. J Comp Pathol. 2022 May;193:37-49.

259. Didier A, Gebert R, Dietrich R, et al. Cellular prion protein in mammary gland and milk fractions of domestic ruminants. Biochem Biophys Res Commun. 2008 May 09;369(3):841-4.

260. Sigurdson CJ, Williams ES, Miller MW, et al. Oral transmission and early lymphoid tropism of chronic wasting disease PrPres in mule deer fawns (Odocoileus hemionus). J Gen Virol. 1999 Oct;80 (Pt 10):2757-2764.

261. Balachandran A, Harrington NP, Algire J, et al. Experimental oral transmission of chronic wasting disease to red deer (Cervus elaphus elaphus): early detection and late stage distribution of protease-resistant prion protein. Can Vet J. 2010 Feb;51(2):169-78.

262. Mitchell GB, Sigurdson CJ, O'Rourke KI, et al. Experimental oral transmission of chronic wasting disease to reindeer (Rangifer tarandus tarandus). PLoS One. 2012;7(6):e39055.

263. Alexander KA, Sanderson CE, Larsen MH, et al. Emerging Tuberculosis Pathogen Hijacks Social Communication Behavior in the Group-Living Banded Mongoose (Mungos mungo). mBio. 2016 05 10;7(3).

264. Alexander KA, Laver PN, Williams MC, et al. Pathology of the Emerging Mycobacterium tuberculosis Complex Pathogen, Mycobacterium mungi, in the Banded Mongoose (Mungos mungo). Vet Pathol. 2018 03;55(2):303-309.

265. Deane MP, Lenzi HL, Jansen A. Trypanosoma cruzi: vertebrate and invertebrate cycles in the same mammal host, the opossum Didelphis marsupialis. Mem Inst Oswaldo Cruz. 1984 Oct-Dec;79(4):513-5.

266. Jansen AM, Xavier SCC, Roque ALR. Trypanosoma cruzi transmission in the wild and its most important reservoir hosts in Brazil. Parasit Vectors. 2018 Sep 06;11(1):502.

267. Barros FNL, Sampaio Júnior FD, Costa SM, et al. First report of natural infection by Trypanosoma cruzi in secretions of the scent glands and myocardium of Philander opossum (Marsupialia: Didelphidae): Parasitological and clinicopathological findings. Vet Parasitol Reg Stud Reports. 2020 12;22:100463.

268. Springer A, Mellmann A, Fichtel C, et al. Social structure and Escherichia coli sharing in a group-living wild primate, Verreaux's sifaka. BMC Ecol. 2016 Feb 12;16:6.

269. Perofsky AC, Lewis RJ, Abondano LA, et al. Hierarchical social networks shape gut microbial composition in wild Verreaux's sifaka. Proc Biol Sci. 2017 Dec 06;284(1868).

270. Miller KV, Marchinton RL, Bush PB. Signpost communication by white-tailed deer: research since Calgary 1991. Appl Anim Behav Sci. 1991 Feb;29:195-204.

271. Caton JD. The antelope and deer of America. New York (NY): Hurd and Houghton; 1877.

272. Atkeson TD, Marchinton RL. Forehead glands in white-tailed deer. J Mammal. 1982 Nov;63(4):613-617.

273. Atkeson TD, Nettles VF, Marchinton RL, et al. Nasal glands in Cervidae. J Mammal. 1988 Feb;69(1):153-156.

274. Nalls AV, McNulty EE, Mayfield A, et al. Detection of Chronic Wasting Disease Prions in Fetal Tissues of Free-Ranging White-Tailed Deer. Viruses. 2021 12 03;13(12).

275. Selariu A, Powers JG, Nalls A, et al. In utero transmission and tissue distribution of chronic wasting disease-associated prions in free-ranging Rocky Mountain elk. J Gen Virol. 2015 Nov;96(11):3444-3455.

276. Saboraki KL. Chronic wasting disease in mule deer and white-tailed deer: the potential for behavioural transmission of prions [master's thesis]. Winnipeg (CA): University of Winnipeg; 2019.

277. Conner MM, Miller MW. Movement patterns and spatial epidemiology of a prion disease in mule deer population units. Ecol Appl. 2004 Dec;14(6):1870-1881.

278. Miller MW, Williams ES. Prion disease: horizontal prion transmission in mule deer. Nature. 2003 Sep 04;425(6953):35-6.

279. Schauber EM, Woolf A. Chronic wasting disease in deer and elk: a critique of current models and their application. Wildl Soc Bull. 2003 Autumn;31(3):610-616.

280. Oyer AM, Matthews NE, Skuldt LH. Long-distance movement of a white-tailed deer away from a chronic wasting disease area. J Wildl Manage. 2007 Jul;71(5):1635-1638.

281. Belsare AV, Gompper ME, Keller B, et al. An agent-based framework for improving wildlife disease surveillance: A case study of chronic wasting disease in Missouri white-tailed deer. Ecol Modell. 2020 Feb 01;417.

282. Grear DA, Samuel MD, Scribner KT, et al. Influence of genetic relatedness and spatial proximity on chronic wasting disease infection among female white-tailed deer. J Appl Ecol. 2010 Jun;47(3):532-540.

283. McFarlane LR. Breeding behavior and space use of male and female mule deer: An examination of potential risk differences for chronic wasting disease infection [master's thesis]. Logan (UT): Utah State University; 2007.

284. Mejía-Salazar MF, Goldizen AW, Menz CS, et al. Mule deer spatial association patterns and potential implications for transmission of an epizootic disease. PLoS One. 2017;12(4):e0175385.

285. Wood AK, Mackie RJ, Hamlin KL. Ecology of sympatric populations of mule deer and white-tailed deer in a prairie environment. Bozeman (MT): Color World Printers; 1989.

286. Purdue JR, Smith MH, Patton JC. Female philopatry and extreme spatial genetic heterogeneity in white-tailed der. J Mammal. 2000 Feb 1;81(1):179-185.

287. Brunjes KJ, Ballard WB, Humphrey MH, et al. Home ranges of sympatric mule deer and white-tailed deer in Texas. Southw Natural. 2009 Sep;54(3):253-260.

288. Bose S, Forrester TD, Brazeal JR, et al. Implications of fidelity and philopatry for the population structure of female black-tailed deer. Behav Ecol. 2017 Jul-Aug;28(4):983-990.

289. Cullingham CI, Nakada SM, Merrill EH, et al. Multiscale population genetic analysis of mule deer (Odocoileus hemionus hemionus) in western Canada sheds new light on the spread of chronic wasting disease. Can J Zool. 2011;89:134-147.

290. Brown BA. Social organization in male groups of white-tailed deer. In: Geist V, Walther F, editors. The behaviour of ungulates and its relation to management: The papers of an International Symposium held at the University of Calgary, Alberta, Canada 2-5 November 1971. Vol 1; Morgues (Switzerland): International Union for Conservation of Nature and Natural Resources; 1974. p. 436-446.

291. Hirth DH. Social behavior of white-tailed deer in relation to habitat. Wildl Monogr. 1977 Apr;53:3-55.

292. Bowyer RT. Sexual segregation in southern mule deer. J Mammal. 1984 Aug;65(3):410-417.

293. Bowyer RT. Antler characteristics as related to social status of male southern mule deer. Southw Natural. 1986 Sep 11;31(3):289-298.

294. Bowyer RT, McCullough DR, Belovsky GE. Causes and consequences of sociality in mule deer. Alces. 2001 Jan 1;37(2):371-402.

295. Mejía Salazar MF, Waldner C, Stookey J, et al. Infectious disease and grouping patterns in mule deer. PLoS One. 2016 Mar 23;11(3):e0150830.

296. Lingle S. Group composition and cohesion in sympatric white-tailed deer and mule deer. Can J Zool. 2003 Jul;81:1119-1130.

297. Hardin JW, Silvy NJ, Klimstra WD. Group size and composition of the Florida key deer. J Wild Manage. 1976 Jul;40(3):454-463.

298. Koutnik DL. Sex-related differences in the seasonality of agonistic behavior in mule deer. J Mammal. 1981 Mar 31;62(1):1-11.

299. Bender CL. Relationships between social group size of Columbian black-tailed deer and habitat cover in Washington. Northwest Nat. 2000 Autumn;81(2):49-53.

300. Richardson KE, Weckerly FW. Intersexual social behavior of urban white-tailed deer and its evolutionary implications. Can J Zool. 2007;85:759-766.

301. Bowyer RT, Kie JG. Effects of foraging activity on sexual segregation in mule deer. J Mammal. 2004;85(3):498-504.

302. Linsdale JM, Tomich PQ. A herd of mule deer. Berkeley (CA): University of California Press; 1953.

303. Kucera TE. Social behavior and breeding system of the desert mule deer. J Mammal. 1978 Aug 21;59(3):463-476.

304. Airst JI, Lingle S. Male size and alternative mating tactics in white-tailed deer and mule deer. J Mammal. 2020 Oct 3;101(5):1231-1243.

305. Newbolt CH, Acker PK, Neuman TJ, et al. Factors influencing reproductive success in male white-tailed deer. J Wildl Manage. 2017 Feb;81(2):206-217.

306. Rue LL. The world of the white-tailed deer. Philadelphia (PA): J. B. Lippincott Company; 1962. Chapter I, The deer itself; p. 1-18.

307. Nelson ME, Mech LD. Deer social organization and wolf predation in northeastern Minnesota. Wildl Monogr. 1981 Jul;77:3-53.

308. Ozoga JJ, Gysel LW. Response of white-tailed deer to winter weather. J Wildl Manage. 1972 Jul;36(3):892-896.

309. Brown CG. Movement and migration patterns of mule deer in southeastern Idaho. J Wildl Manage. 1992 Apr;56(2):246-253.

310. Lingle S. Anti-Predator Strategies and Grouping Patterns in White-Tailed Deer and Mule Deer. Ethology. 2001 Dec 21;107(4):295-314.

311. Lingle S, Pellis SM. Fight or flight? Antipredator behavior and the escalation of coyote encounters with deer. Oecologia. 2002;131:154-164.

312. Lingle S, Pellis SM, Wilson WF. Interspecific variation in antipredator behaviour leads to differential vulnerability of mule deer and white-tailed deer fawns early in life. J Anim Ecol. 2005 Nov 2;74:1140-1149.

313. Airst J, Lingle S. Courtship strategies of white-tailed deer and mule deer males when living in sympatry. Behaviour. 2019 Mar 19;156:307-330.

314. Hundertmark KJ. Home range, dispersal and migration. In: Franzmann AW, Schwartz CC, editors. Ecology and management of the North American moose. Boulder (CO): University Press of Colorado; 2007. p. 303-336.

315. Smith BL. Winter feeding of elk in western North America. J Wildl Manage. 2001 Apr;65(2):173-190.

316. Lyon LJ, Ward AL. Elk and land management. In: Thomas JW, Toweill DE, editors. Elk of North America : ecology and management. Harrisburg (PA): Stackpole Books; 1982. p. 443-478.

317. Thorn ET, Morton JK, Blunt FM, et al. Brucellosis in elk. II. Clinical effects and means of transmission as determined through artificial infections. J Wildl Dis. 1978 Jul;14(3):280-291.

318. Scurlock BM, Edwards WH. Status of brucellosis in free-ranging elk and bison in Wyoming. J Wildl Dis. 2010 Apr;46(2):442-449.

319. Lankester MW, Peterson WJ. The possible importance of wintering yards in the transmission of Parelaphostrongylus tenuis to white-tailed deer and moose. J Wildl Dis. 1996 Jan;32(1):31-38.

320. McIntosh T, Rosatte R, Campbell D, et al. Evidence of Parelaphostrongylus tenuis infections in free-ranging elk (Cervus elaphus) in southern Ontario. Can Vet J. 2007 Nov;48(11):1146-1154.

321. Mejía-Salazar MF, Waldner CL, Hwang YT, et al. Use of environmental sites by mule deer: a proxy for relative risk of chronic wasting disease exposure and transmission. Ecosphere. 2018 Jan;9(1):e02055.

322. Calef GW, Lortie GM. A mineral lick of barren-ground caribou. J Mammal. 1975 Feb;56(1):240-242.

323. Couturier S, Barrette C. The behavior of moose at natural mineral springs in Quebec. Can J Zool. 1987 Feb;66(2):522-528.

324. Schultz SR, Johnson MK. Use of artificial mineral licks by white-tailed deer in Louisiana. J Range Manage. 1992 Nov;45(6):546-548.

325. Atwood TC, Weeks HP. Sex- and age-specific patterns of mineral lick use by white-tailed deer (Odocoileus virginianus). Am Midl Nat. 2002 Oct 1;148(2):289-296.

326. Lavelle MJ, Phillips GE, Fischer JW, et al. Mineral licks: motivational factors for visitation and accompanying disease risk at communal use sites of elk and deer. Environ Geochem Health. 2014 Dec;36(6):1049-61.

327. Drewe JA. Who infects whom? Social networks and tuberculosis transmission in wild meerkats. Proc Biol Sci. 2010 Feb 22;277(1681):633-42.

328. Rimbach R, Bisanzio D, Galvis N, et al. Brown spider monkeys (Ateles hybridus): a model for differentiating the role of social networks and physical contact on parasite transmission dynamics. Philos Trans R Soc Lond B Biol Sci. 2015 May 26;370(1669).

329. MacIntosh AJ, Jacobs A, Garcia C, et al. Monkeys in the middle: parasite transmission through the social network of a wild primate. PLoS One. 2012;7(12):e51144.

330. Bailey ED. Behavior of the Rattlesnake mule deer on their winter range [master's thesis]. Bozeman (MT): Montana State University; 1960.

331. Fairman LL. Movements populations and behavior of deer on a western Montana winter range [master's thesis]. Missoula (MT): University of Montana; 1966.

332. Mooring MS. Ontogeny of allogrooming in mule deer (Odocoileus hemionus). J Mammal. 1989 May;70(2):434-437.

333. Forand KJ, Marchinton RL. Patterns of social grooming in adult white-tailed deer. Am Midl Nat. 1989 Oct;122(2):357-364.

334. Miller FL. Mutual grooming by black-tailed deer in Northwestern Oregon. Can Field-Nat. 1971 Oct-Dec;85(4):295-301.

335. Müller-Schwarze D. Social functions of various scent glands in certain ungulates and the problems encountered in experimental studies of scent communication. In: Geist V, Walther F, editors. The behaviour of ungulates and its relation to management: The papers of an International Symposium held at the University of Calgary, Alberta, Canada 2-5 November 1971. Vol 1; Morgues (Switzerland): International Union for Conservation of Nature and Natural Resources; 1974. p. 107-113.

336. Browman LG, Hudson P. Observations on the Behavior of Penned Mule Deer. J Mammal. 1957 May;38(2):247-253.

337. Müller-Schwarze D. Social significance of forehead rubbing in blacktailed deer (Odocoileus heiminus columbianus). Anim Behav. 1972;20:788-797.

338. Struhsaker TT. Behavior of elk (Cervus canadensis) during the rut. Z Tierpsychol. 1967 Jan-Dec;24(1):80-114.

339. Livezey KB. Social behavior of Rocky Mountain elk at the National Bison Range [master's thesis]. Missoula (MT): University of Montana; 1979.

340. Rhyal J, Nol P, Wehtje M, et al. Partial protection in balb/c house mice (Mus musculus) and Rocky Mountain elk (Cervus canadensis) after vaccination with a killed, mucosally delivered Brucella abortus vaccine. J Wildl Dis. 2019;55(4):794-803.

341. Thomson BR. The behaviour of wild reindeer in Norway [dissertation]. Edinburgh (UK): University of Edinburgh; 1977.

342. Müller-Schwarze D, Källquist L, Mossing T. Social behavior and chemical communication in reindeer (Rangifer t. tarandus L.). J Chem Ecol. 1979;5(4):483-517.

343. Bergerud AT. Rutting behaviour of Newfoundland caribou. In: Geist V, Walther F, editors. The behaviour of ungulates and its relation to management: The papers of an International Symposium held at the University of Calgary, Alberta, Canada 2-5 November 1971. Vol 1; Morgues (Switzerland): International Union for Conservation of Nature and Natural Resources; 1974. p. 395-435.

344. Murie A. The moose of Isle Royale. Ann Arbor (MI): University of Michigan Press; 1934. (University of Michigan Museum of Zoology Miscellaneous Publications No. 25).

345. Murie OJ. Alaska-Yukon caribou. Washington (DC): United States Department of Agriculture Bureau of Biological Survey; 1935. (North American Fauna; No. 54).

346. Altman M. The role of juvenile elk and moose in the social dynamics of their space. Zoologica (N. Y.). 1960;45(4):35-39.

347. Pruitt WO. Behavior of the barren-ground caribou. Lancaster (PA): The Intelligencer Printing Company. 1960. (Biological Papers of the University of Alaska; No. 3).

348. Geist V. On the behaviour of the North American moose (Alces alces andersoni Peterson 1950) in British Columbia. Behaviour. 1963;20(3/4):377-416.

349. Franklin WL, Mossman AS, Dole M. Social organization and home range of Roosevelt elk. J Mammal. 1975 Feb 20;56(1):102-118.

350. Peek JM, van Ballenberghe V, Miquelle DG. Intensity of interactions between rutting bull moose in central Alaska. J Mammal. 1986 May;67(2):423-426.

351. Bowyer RT, Kitchen DW. Significance of scent-marking by Roosevelt elk. J Mammal. 1987 May;68(2):418-423.

352. Weckerly FW. Are large male Roosevelt elk less social because of aggression? [Article]. Journal of Mammalogy. 2001 May, 2001;82(2):414-421.

353. Barrette C, Vandal D. Sparring, relative antler size, and assessment in male caribou. Behav Ecol Sociobiol. 1990;26(6):383-387.

354. Geist V. Behavior: Adaptive strategies in mule deer. In: Wallmo OC, editor. Mule and black-tailed deer of North America. Lincoln (NE): University of Nebraska Press; 1981. p. 157-223.

355. Van Ballenberghe V, Miquelle DG. Rutting behavior of moose in central Alaska. Alces. 1996;32:109-130.

356. Denkers ND, Hayes-Klug J, Anderson KR, et al. Aerosol transmission of chronic wasting disease in white-tailed deer. J Virol. 2013 Feb;87(3):1890-1892.

357. Denkers ND, Hoover CE, Davenport KA, et al. Very low oral exposure to prions of brain or saliva origin can transmit chronic wasting disease. PLoS One. 2020 Aug 20;15(8):e0237410.

358. Moore WG, Marchinton L. Marking behaviour and its social function in white-tailed deer. In: Geist V, Walther F, editors. The behaviour of ungulates and its relation to management: The papers of an International Symposium held at the University of Calgary, Alberta, Canada 2-5 November 1971. Vol 1; Morgues (Switzerland): International Union for Conservation of Nature and Natural Resources; 1974. p. 447-456.

359. Kinsell TC. Scraping behavior in male white-tailed deer as a potential means of transmitting chronic wasting disease [master's thesis]. Lincoln (NE): University of Nebraska at Lincoln; 2010.

360. de Vos A, Brokx P, Geist V. A review of social behavior of the North American cervids during the reproductive. Am Midl Nat. 1967 Apr;77(2):390-417.

361. Müller-Schwarze D. Pheromones in black-tailed deer (Odocoileus hemionus columbianus). Anim Behav. 1971;19:141-152.

362. Sawyer TG, Marchinton RL, Miller KV. Response of female white-tailed deer to scrapes and antler rubs. J Mammal. 1989 May;70(2):431-433.

363. Relyea RA, Demarais S. Activity of desert mule deer during the breeding season. J Mammal. 1994 Nov;75(4):940-949.

364. Ozoga JJ, Verme LJ. Comparative breeding behavior and performance of yearling vs. prime-age white-tailed bucks. J Wildl Manage. 1985 Apr;49(2):364-372.

365. Marchinton RL, Johansen KL, Miller KV. Behavioural components of white-tailed deer scent marking: social and seasonal effects. In: Macdonald DW, Müller-Schwarze D, Natynczuk SE, editors. Chemical signals in vertebrates 5. Oxford (UK): Oxford University Press; 1990. p. 295-301.

366. Geist V. Deer of the world : their evolution, behaviour, and ecology. Mechanicsburg (PA): Stackpole Books; 1998.

367. Volkman NJ, Zemanek KF, Müller-Schwarze D. Antorbital and forehead secretions of black-tailed deer (Odocoileus hemionus columbianus): their role in age-class recognition. Anim Behav. 1978;26:1098-1106.

368. Graf W. Territorialism in deer. J Mammal. 1956 May;37(2):165-170.

369. Bowyer RT, Van Ballenberghe V, Rock KR. Scent marking by Alaskan moose: characteristics and spatial distribution of rubbed trees. Can J Zool. 1994;72:2186-2192.

370. Adams CA, Bowyer RT, Rowell JE, et al. Scent marking by male caribou: an experimental test of rubbing behavior. Rangifer. 2001;21(1):21-27.

371. Geist V. Adaptive behavioral strategies. In: Thomas JW, Toweill DE, editors. Elk of North America : ecology and management. Harrisburg (PA): Stackpole Books; 1982. p. 219-278.

372. Pruitt WO. The function of the brow-tine in caribou antlers. Arctic. 1966 Jun;19(2):111-113.

373. Lent PC. Rutting behaviour in a barren-ground caribou population. Anim Behav. 1965 Apr-Jul;13(2-3):259-264.

374. Kojola I. Rutting behaviour in an enclosured group of wild forest reindeer (Rangifer tarandus fennicus Lönnb.). Rangifer. 1986;6(special issue no.1):173-179.

375. Van Ballenberghe V, Miquelle DG. Mating in moose: timing, behavior, and male access patterns. Can J Zool. 1993;71:1687-1690.

376. Kile TL, Marchinton RL. White-tailed deer rubs and scrapes: spatial, temporal and physical characteristics and social role. Am Midl Nat. 1977 Apr;97(2):257-266.

377. Baumann CD, Davidson WR, Roscoe DE, et al. Intracranial abscessation in white-tailed deer of North America. J Wildl Dis. 2001 Oct;37(4):661-670.

378. Crichton V, Wowchuk R. A possible source of brain abscesses in bull moose. Alces. 2019;55:61-65.

379. Pruitt WO. Behavior of the whitetail deer (Odocoileus virginianus). J Mammal. 1954 Feb;35(1):129-130.

380. Alexy KJ, Gassett JW, Osborn DA, et al. Remote monitoring of scraping behaviors of a wild population of white-tailed deer. Wildl Soc Bull. 2001 Autumn;29(3):873-878.

381. Ozoga JJ. Induced scraping activity in white-tailed deer. J Wildl Manage. 1989 Oct;53(4):877-880.

382. Sawyer TG, Marchinton RL, Berisford CW. Scraping behavior in female white-tailed deer. J Mammal. 1982;63(4):696-697.

383. Alexander T. Tony Alexander's practical hunter's & trapper's guide. New York (NY): J. J. Little & Co.; 1887.

384. Sawyer TG, Miller KV, Marchinton RL. Patterns of urination and rub-urination in female white-tailed deer. J Mammal. 1993 May;74(2):477-479.

385. VerCauteren KC, Burke PW, Phillips GE, et al. Elk use of wallows and potential chronic wasting disease transmission. J Wildl Dis. 2007 Oct;43(4):784-788.

386. Altman M. Group dynamics in Wyoming moose during the rutting season. J Mammal. 1959 Aug;40(3):420-424.

387. Miquelle DG. Are moose mice? The function of scent urination in moose. Am Net. 1991 Aug;138(2):460-477.

388. Bubenik AB. Behavior. In: Franzmann AW, Schwartz CC, editors. Ecology and management of the North American moose. Boulder (CO): University Press of Colorado; 2007. p. 173-222.

389. Bubenik AB. Behavioural significance of the moose bell. Alces. 1983;19:238-245.

390. Miquelle DG, Van Ballenberghe V. The moose bell: A visual or olfactory communicator? Alces. 1985;21:191-213.

391. von Schumancher S. Das Stirnorgan des Rehbockes (Capreolus capreolus capreolus L.), ein bisher unbekanntes Duftorgan. Z Mikr-Anat Forsch. 1936;39:215-230.

392. Rehorek SJ, Hillenius WJ, Kennaugh J, et al. The gland and the sac – the preorbital apparatus of muntjacs. In: Mason RT, LeMaster MP, Müller-Schwarze, D, editors. Chemical Signals in Vertebrates 10. New York (NY): Springer; 2005. p. 152-158.

393. Schaffer J. Die hautdrüsenorgane der Säugetiere. Berlin: Urban & Schwarzenberg; 1940. German.

394. Clifford AB, Witmer LM. Case studies in novel narial anatomy: 2. The enigmatic nose of moose (Artiodactyla: Cervidae: Alces alces). J Zool Lond. 2004;262:339-360.

395. Bubenik AB. Evolution, taxonomy and morphophysiology. In: Franzmann AW, Schwartz CC, editors. Ecology and management of the North American moose. Boulder (CO): University Press of Colorado; 2007. p. 77-124.

396. Sokolov VE, Chernova OF. Morphology of the skin of moose (Alces alces L.). Swed Wildl Res. 1987 Jan;Suppl. 1:367-375.

397. Bowyer RT, Van Ballenberghe V, Kie JG. Moose. In: Feldhamer GA, Thompson BC, Chapman JA, editors. Wild mammals of North America: biology, management, and conservation. 2nd ed. Baltimore (MD): The Johns Hopkins University Press; 2003. p. 931-964.

398. Mearn EA. Mammals of the Mexican boundary of the United States Part 1. Washington (DC): Smithsonian Institution. 1907. (United States National Museum; Bulletin 56).

399. Anderson AE, Wallmo OC. Odocoileus hemionus. Mamm Species. 1984 Apr 27;219:1-9.

400. Oates DW. Differentiation of mule deer and white-tailed deer. Lincoln (NE): 1989. (Nebraska Wildlife Bulletin; No. 89-1).

401. Mossing T, Damber J. Rutting behavior and androgen variation in reindeer (Rangifer tarandus L.). J Chem Ecol. 1981;7(2):377-389.

402. McTaggart Cowan I, Geist V. Aggressive behavior in deer of the genus Odocoileus. J Mammal. 1961 Nov;42(4):522-526.

403. Hillenius WJ, Phillips DA, Rehorek SJ. "A new lachrymal gland with an excretory duct in red and fallow deer" by Johann Jacob Harder (1694): English translation and historical perspective. Ann Anat. 2007 Sep 10;189(5):423-433.

404. Quay WB, Müller-Schwarze D. Relations of age and sex to integumentary glandular regions in Rocky Mountain mule deer (Odocoileus hemionus hemionus). J Mammal. 1971 Nov;52(4):670-685.

405. McTaggart Cowan I. Distribution and variation in deer (genus Odocoileus) of the Pacific coastal region of North America. Cal Fish Game. 1936 Jul;22(3):155-246.

406. Modell W, Noback CV. Histogenesis of bone in the growing antler of the Cervidae. Am J Anat. 1931;49(1):65-95.

407. Wislocki GB. Studies on the growth of deer antlers. Am J Anat. 1942;71(3):371-415.

408. Wislocki GB, Singer M. The occurrence and function of nerves in the growing antlers of deer. J Comp Neurol. 1946 Aug;85(1):1-19.

409. Vacek, Z. Innervace lýčí rostoucích parohů u Cervidů. Československá Morfologie, 1955;3(3):249-264. Czech.

410. Lojda, Z. Histogenese parohů našich Cervidů a její histochemický obraz. Československá Morfologie. 1956;4:43–62. Czech.

411. Murie OJ. The elk of North America. Harrisburg (PA): Stackpole Co. and The Wildlife Management Institute; 1951.

412. Palmer LJ. Raising reindeer in Alaska. Washington (DC): United States Department of Agriculture; 1934. (Miscellaneous publication; Number 207).

413. Altmann M. Social behavior of elk, Cervus canadensis nelsoni, in the Jackson Hole area of Wyoming. Behaviour. 1952;4(2):116-143.

414. Hirth DH. Observations of loss of antler velvet in white-tailed deer. Southwest Nat. 1977 Jun 3;22(2):278-280.

415. Van Ballenberghe V. In the company of moose. 2nd ed. Mechanicsburg (PA): Stackpole Books; 2013. Giants of the northern forests; p. 1-20.

416. Abascal K, Yarnell E. Botanical alternatives to velvet antler. Altern Complement Ther. 2002 Feb;8(1):30-33.

417. Angers RC, Seward TS, Napier D, et al. Chronic wasting disease prions in elk antler velvet. Emerg Infect Dis. 2009 May;15(5):696-703.

418. Halford DK, Arthur WJ, Alldredge AW. Observations of captive Rocky Mountain mule deer behavior. Great Basin Nat. 1987 Jan 31;47(1):105-109.

419. Mysterud A, Ytrehus B, Tranulis MA, et al. Antler cannibalism in reindeer. Sci Rep. 2020 Dec 17;10(1):22168.

420. Huor A, Douet JY, Lacroux C, et al. Infectivity in bone marrow from sporadic CJD patients. J Pathol. 2017;243(3):273-278.

421. Barrette C. Antler eating and antler growth in wild Axis deer. Mammalia. 1985;45(4):491-499.

422. McCabe RA. Observations on the disappearance of shed caribou antlers. J Mammal. 1957 May;38(2):275-277.

423. Kelsall JP. Continued barren-ground caribou studies. Ottawa (CA): Department of Northern Affairs and Natural Resources National Parks Branch Canadian Wildlife Service; 1957. (Wildlife Management Bulletin; Series 1, Number 12).

424. Sutcliffe AJ. Similarities of bones and antlers gnawed by deer to human artefacts. Nature. 1973 Dec 14;246:428-430.

425. Wika M. Antlers – a mineral source in Rangifer. Acta Zool. 1982;63(1):7-10.

426. Millais JG. Newfoundland and its untrodden ways. London: Longmans, Green, and co.; 1907.

427. Bowyer RT. Osteophagia and antler breakage among Roosevelt elk. Cal Fish Game. 1983;69(2):84-88.

428. Walter WD, Bryant RL, Leslie DM. Unusual documentation of elk behaviors using automated cameras. Proc Okla Acad Sci. 2005;85:81-83.

429. McTaggart Cowan I. The ecological relationships of the food of the Columbian black-tailed deer, Odocoileus hemionus columbianus (Richardson), in the coast forest region of southern Vancouver Island, British Columbia. Ecol Monogr. 1945 Apr;15(2):109-139.

430. Michael ED. Characteristics of shed antlers from white-tailed deer in south Texas. J Wildl Manage. 1965 Apr;29(2):376-380.

431. Krausman PR, Bissonette JA. Bone-chewing behavior of desert mule deer. Southw Natural. 1977 Mar 1;22(1):149-150.

432. Meckel LA, McDaneld CP, Wescott DJ, et al. White-tailed deer as a taphonomic agent: photographic evidence of white-tailed deer gnawing on human bone. J Forensic Sci. 2018 Jan;63(1):292-294.

433. Clough M, Zentilli M, Broders HG, et al. Elemental composition of incisors in Nova Scotia Moose: Evaluation of a population with abnormal incisor breakage. Alces. 2006;42:55-64.

434. Akaeiewsky AJ. Anatomy of the reindeer. Leningrad (USSR): The institute of polar agriculture, animal husbandry and fishing and hunting industry; 1939. Russian.

435. Jacob J, von Lehmann E. Bemerkungen zu einer Nasendrüse des Sumpfhirsches, Odocoileus (Dorcocephalus) dichotomus (Illiger, 1811). Säugetierkundliche Mitteilungen. 1976;24:151–156. German.

436. Langguth A, Jackson J. Cutaneous scent glands in pampas deer Blastoceros bezoarticus (L., 1758). Z Säugetierkund. 1980;45:82-90.

437. McCrady WA. Assessment of animal-borne video systems for studying behavior and energetics of male white-tailed deer (Odocoileus virginianus) [master's thesis]. Nacogdoches (TX): Stephen F. Austin State University; 2013.

438. VerCauteren KC, Lavelle MJ, Seward NW. Fence-line contact between wild and farmed cervids in Colorado: potential for disease transmission. J Wildl Manage. 2007 Jul 1;71(5):1594-1602.

439. Thomas JW, Robinson RM, Marburger RG. Social behavior in a white-tailed deer herd containing hypogonadal males. J Mammal. 1965 May;46(2):314-327.

440. Døving KB, Trotier D. Structure and function of the vomeronasal organ. J Exp Biol. 1998 Nov;201(21):2913-2925.

441. Estes RD. The role of the vomeronasal organ in mammalian reproduction. Mammalia. 1972;36:315-341.

442. Ladewig J, Hart BL. Flehmen and vomeronasal organ function in male goats. Physiol Behav. 1980 Jun;24(6):1067-1071.

443. Blissitt MJ, Bland KP, Cottrell DF. Olfactory and vomeronasal chemoreception and the discrimination of oestrous and non-oestrous ewe urine odours by the ram. Appl Anim Behav Sci. 1990 Oct;27(4):325-335.

444. Halpern M, Martínez-Marcos A. Structure and function of the vomeronasal system: an update. Prog Neurobiol. 2003 Jun;70(3):245-318.

445. Bertmar G. Variations in size and structure of vomeronasal organs in reindeer Rangifer tarandus tarandus L. Arch Biol. (Bruxelles) 1981;92:343-366.

446. Vedin V, Eriksson B, Berghard A. Organization of the chemosensory neuroepithelium of the vomeronasal organ of the Scandinavian moose Alces alces. Brain Res. 2010 Jan 8;1306:53-61.

447. Park C, Ahn M, Lee J-Y, et al. A morphological study of the vomeronasal organ and the accessory olfactory bulb in the Korean roe deer, Capreolus pygargus. Acta Histochem. 2014 Jan;116(1):258-264.

448. Gassett JW, Osborn DA, Rickard JK, et al. Stimuli-related variation in urination frequency of female white-tailed deer during the estrous cycle. Appl Anim Behav Sci. 1998 Feb;56(1):71-75.

449. Henderson J, Altieri R, Müller-Schwarze D. The annual cycle of Flehmen in black-tailed deer (Odocoileus hemionus columbianus). J Chem Ecol. 1980 May;6(3):537-547.

450. Altieri R, Müller-Schwarze D. Seasonal changes in flehmen to constant urine stimuli. J Chem Ecol. 1980 Sep;6(5):905-909.

451. Crump D, Swigar AA, West JR, et al. Urine fractions that release flehmen in black-tailed deer, Odocoileus hemionus columbianus. J Chem Ecol. 1984 Feb;10(2):203-215.

452. Broadfoot JD, Addison EM, McLaughlin RF, et al. Flehmen in captive moose calves (Alces alces americana). Alces. 1997;33:43-47.

453. Müller-Schwarze D. Flehmen in the context of mammalian urine communication. In: Ritter F, editor. Chemical Ecology: Odour Communication in Animals. New York (NY): Elsevier North-Holland Publishing Co.; 1979. p. 85-96.

454. Warren RJ, Vogelsang RW, Kirkpatrick RL, et al. Reproductive behaviour of captive white-tailed deer. Anim Behav. 1978 Feb;26(1):179-183.

455. DeYoung RW, Miller KV. White-tailed deer behavior. In: Hewitt DG, editor. Biology and management of white-tailed deer. Boca Raton (FL): CRC Press; 2011. p. 311-351.

456. Haugen AO. Breeding records of captive white-tailed deer in Alabama. J Mammal. 1959 Feb;40(1):108-113.

457. Fudge JR, Miller KV, Marchinton RL, et al. Effects of exogenous testosterone on the scent-marking and agonistic behaviors of white-tailed deer. In: Doty RL, Müller-Schwarze D, editors. Chemical signals in vertebrates VI. New York (NY): Plenum Press; 1992. p. 477-484.

458. Nichol AA. Experimental feeding of deer. Tuscon (AZ): University of Arizona; 1938. (Technical bulletin No. 75).

459. Espmark Y. Rutting behaviour in reindeer (Rangifer tarandus L.). Anim Behav. 1964 Jan;12(1):159-163.

460. Müller-Schwarze D, Müller-Schwarze C. Subspecies specificity of response to a mammalian social odor. J Chem Ecol. 1975 Mar;1(1):125-131.

461. Gassett JW, Dasher KA, Miller KV, et al. White-tailed deer tarsal glands : sex and age-related variation in microbial flora. Mammalia. 2000;64(3):371-377.

462. Müller-Schwarze D, Volkman NJ, Zemanek KF. Osmetrichia: specialized scent hair in black-tailed deer. J Ultrastruct Res. 1977 Jun;59(3):223-230.

463. Hoffman DM, Miller KV, Marchinton RL, et al. Ultrastructure of hairs associated with the skin glands of white-tailed deer (Odocoileus virginianus). GA J Sci. 1997;55(4):209-214.

464. Alexy KJ, Gassett JW, Osborn DA, et al. Bacterial Fauna of the Tarsal Tufts of White-tailed Deer (Odocoileus virginianus). Am Midl Nat. 2003 Jan 1;149(1):237-240.

465. Li K, Siefkes MJ, Li W. Cervidins A-D: Novel glycine conjugated fatty acids from the tarsal gland of male whitetail deer, Odocoileus virginianus. J Chem Ecol. 2021 Mar;47(3):243-247.

466. Andersson G, Andersson K, Brundin A, et al. Volatile compounds from the tarsal scent gland of reindeer (Rangifer tarandus). J Chem Ecol. 1975 Jun;1(2):275-281.

467. Bubenik AB, Dombalagian M, Wheeler JW. The role of the tarsal glands in the olfactory communication of the Ontario moose – a preliminary report. Alces. 1979;15:119-147.

468. Müller-Schwarze D, Altieri R, Porter N. Alert odor from skin gland in deer. J Chem Ecol. 1984 Dec;10(12):1707-1729.

469. Anderson AE, Medin DE, Bowden DC. Growth and morphometry of the carcass, selected bones, organs, and glands of mule deer. Wildl Monogr. 1974 Oct;39:3-122.

470. Quay WB. Geographic variation in the metatarsal “gland” of the white-tailed deer (Odocoileus virginianus). J Mammal. 1971 Feb 26;52(1):1-11.

471. Pocock RI. On the specialized cutaneous glands of ruminants. Proc Zool Soc Lond. 1910 Apr-Jun:840-986.

472. Hundertmark KJ, Bowyer RT, Shields GF, et al. Mitochondrial phylogeography of moose (Alces alces) in North America. J Mammal. 2003 May 30;84(2):718-728.

473. Hundertmark KJ, Bowyer RT. Genetics, evolution, and phylogeography of moose. Alces. 2004;40:103-122.

474. Quay WB. Microscopic structure and variation in the cutaneous glands of the deer, Odocoileus virginianus. J Mammal. 1959 Feb 20;40(1):114-128.

475. Quay WB. Histology and cytochemistry of skin gland areas in the caribou, Rangifer. J Mammal. 1955 May;36(2):187-201.

476. Mossing T, Källquist L. Variation in cutaneous glandular structures in reindeer (Rangifer tarandus). J Mammal. 1981 Aug;62(3):606-612.

477. Sokolov VE. Mammal skin. Berkeley (CA): University of California Press; 1982. Subordo Ruminantia; p. 478-572.

478. Chapman DM. Histology of moose (Alces alces andersoni) interdigital glands and associated green hairs. Can J Zool. 1985 Apr;63(4):899-911.

479. Tempel M. Die Drüsen der Zwischenklauenhaut der Paarzeher. Arch Wiss Prakt Tierheilkd. 1897:1-48. German.

480. Källquist L, Mossing T. The distribution of sudoriferous glands in the hairy skin of reindeer (Rangifer tarandus L.). Acta Zool (Stockh). 1977 Jun;58(2):65-68.

481. Mossing T. Seasonal variations in general activity, behaviour and cutaneous glandular structures in reindeer (Rangifer tarandus L.) [dissertation]. Umeå (Sweden): Umeå Universitet; 1980.

482. Handeland K, Boye M, Bergsjø B, et al. Digital Necrobacillosis in Norwegian wild tundra reindeer (Rangifer tarandus tarandus). J Comp Pathol. 2010 Jul;143(1):29-38.

483. Riseth JA, Tømmervik H, Tryland M. Spreading or gathering? Can traditional knowledge be a resource to tackle reindeer diseases associated with climate change? Int J Environ Res Public Health. 2020;17(16):6002.

484. Hardin JW. Behavior, socio-biology, and reproductive life history of the Florida Key deer, Odocoileus virginianus clavium [dissertation]. Carbondale (IL): Southern Illinois University Graduate School; 1974.

485. Anderson JR. The behavior of nose bot flies (Cephenemyia apicata and C. jellisoni) when attacking black-tailed deer (Odocoileus hemionus columbianus) and the resulting reactions of the deer. Can J Zool. 1975 Jul;53(7):977-992.

486. Genovesi S, Leita L, Sequi P, et al. Direct detection of soil-bound prions. PLoS One. 2007 Oct;10:e1069.

487. Arthur WJ, Alldredge AW. Soil ingestion by Mmule deer in northcentral Colorado. J Range Manage. 1979 Jan;32(1):67-71.

488. Beyer WN, Connor EE, Gerould S. Estimates of soil ingestion by wildlife. J Wildl Manage. 1994 Apr;58(2):375-382.

489. Müller-Schwarze D, Källquist L, Mossing T, et al. Responses of reindeer to interdigital secretions of conspecifics. J Chem Ecol. 1978;4(3):325-335.

490. Skerman TM. Isolation of Bacteroides nodosus from hoof lesions in farmed red deer (Cervus elaphus). NZ Vet J. 1983;31:102-103.

491. Han S, Mansfield KG, Bradway DS. Treponeme-associated hoof disease of free-ranging elk (Cervus elaphus) in southwestern Washington State, USA. Vet Pathol. 2019 Jan;56(1):118-132.

492. Han S, Mansfield KG. Severe hoof disease in free-ranging Roosevelt elk (Cervus elaphus roosevelti) in southwestern Washington, USA. J Wildl Dis. 2014 Apr;50(2):259-270.

493. Müller-Schwarze D, Quay WB, Brundin A. The caudal gland in reindeer (Rangifer tarandus L.) : Its behavioral role, histology, and chemistry. J Chem Ecol. 1977 Sep;3(5):591-601.

494. Bubenik GA. Morphological investigations of the winter coat in white-tailed deer: Differences in skin, glands and hair structure of various body regions. Acta Theriol. 1996;41(1):73-82.

495. Ovcharenko ND, Kuchina EA. Influence of environmental factors of on the structural and functional state of its specific skin gland of Red deer (Cervus elaphus sidiricus Severtzov, 1872). Ukr J Ecol. 2018;8(4):469-475.

496. Odend'hal S, Miller KV, Hoffmann DM. Preputial glands in the white-tailed deer (Odocoileus virginianus). J Mammal. 1992 May 26;73(2):299-302.

497. Hibler CP, Wilson KL, Spraker TR et al. Field validation and assessment of an enzyme-linked immunosorbent assay for detecting chronic wasting disease in mule deer (Odocoileus hemionus), white-tailed deer (Odocoileus virginianus), and Rocky Mountain elk (Cervus elaphus nelsoni). J Vet Diagn Invest. 2003 Jul;15(4):311–319.

498. Fraser JR. Infectivity in extraneural tissues following intraocular scrapie infection. J Gen Virol. 1996 Oct;77 (Pt 10):2663-8.

499. Gushue D, Herbst A, Sim V, et al. 14-3-3 and enolase abundances in the CSF of Prion diseased rats. Prion. 2018;12(3-4):253-260.

500. Payne AP. The harderian gland: a tercentennial review. J Anat. 1994 Aug;185 (Pt 1)(Pt 1):1-49.

501. O'Rourke KI, Baszler TV, Besser TE, et al. Preclinical diagnosis of scrapie by immunohistochemistry of third eyelid lymphoid tissue. J Clin Microbiol. 2000 Sep;38(9):3254-9.

502. O'Rourke KI, Duncan JV, Logan JR, et al. Active surveillance for scrapie by third eyelid biopsy and genetic susceptibility testing of flocks of sheep in Wyoming. Clin Diagn Lab Immunol. 2002 Sep;9(5):966-71.

503. Vascellari M, Aufiero GM, Nonno R, et al. Diagnosis and PrP genotype target of scrapie in clinically healthy sheep of Massese breed in the framework of a scrapie eradication programme. Arch Virol. 2005 Oct;150(10):1959-76.

504. Monleón E, Garza MC, Sarasa R, et al.An assessment of the efficiency of PrP^{sc} detection in rectal mucosa and third-eyelid biopsies from animals infected with scrapie. Vet Microbiol. 2011 Jan 27;147(3-4):237-43.

505. Cooper SK, Hoover CE, Henderson DM, et al. Detection of CWD in cervids by RT-QuIC assay of third eyelids. PLoS One. 2019 Aug 28;14(8):e0221654.

506. Pangerl A, Pangerl B, Buzzell GR, et al. Characterization of β-adrenoceptors in the syrian hamster Harderian gland: sexual differences and effects of either castration or superior cervical ganglionectomy. J Neurosci Res. 1989 Apr;22(4):456-460.

507. Huhtala A, Huikuri K, Palkama A, et al. Innervation of the rat harderian gland by adrenergic and cholinergic nerve fibres. Anat Rec. 1977 Jun;188(2):263-271.

508. Butler JM, Ruskell GL, Cole DF, et al. Effects of VIIth (facial) nerve degeneration on vasoactive intestinal polypeptide and substance P levels in ocular and orbital tissues of the rabbit. Exp Eye Res. 1984 Oct;39(4):523-532.

509. Nilsson SF. Nitric oxide as a mediator of parasympathetic vasodilation in ocular and extraocular tissues in the rabbit. Invest Ophthalmol Vis Sci. 1996 Sep;37(10):2110-9.

510. Nilsson SF, Linder J, Bill A. Characteristics of uveal vasodilation produced by facial nerve stimulation in monkeys, cats and rabbits. Exp Eye Res. 1985 Jun;40(6):841-52.

511. Sakai T. Comparative anatomy of mammalian harderian glands. In: Webb SM, Hoffman RA, Puig-Domingo ML, et al., editors. Harderian Glands. Heidelberg (Germany): Springer Berlin; 1992. p.7-23.

512. Nieto-Diaz M, Pita-Thomas DW, Munoz-Galdeano Teresa, et al. Deer antler innervation and regeneration. Front Biosci (Landmark Ed). 2012 Jan 1;17(4):1389-401.

513. Wang F-B, Cheng P-M, Chi H-C, et al. Axons of passage and inputs to superior cervical ganglion in rat. Anat Rec (Hoboken). 2018 Nov;301(11):1906-1916.

514. Rando TA, Bowers CW, Zigmond RE. Localization of neurons in the rat spinal cord which project to the superior cervical ganglion. J Comp Neurol. 1981 Feb 10;196(1):73-83.

515. Spraker TR, Gidlewski T, Powers JG, et al. Progressive accumulation of the abnormal conformer of the prion protein and spongiform encephalopathy in the obex of nonsymptomatic and symptomatic Rocky Mountain elk (Cervus elaphus nelsoni) with chronic wasting disease. J Vet Diagn Invest. 2015 Jul;27(4):431-41.

516. Spraker TR, Balachandran A, Zhuang D, et al. Variable patterns of distribution of PrP(CWD) in the obex and cranial lymphoid tissues of Rocky Mountain elk (Cervus elaphus nelsoni) with subclinical chronic wasting disease. Vet Rec. 2004 Sep 4;155(10):295-302.

517. Johnson CJ, Herbst A, Duque-Velásquez C, et al. Prion protein polymorphisms affect chronic wasting disease progression. PLoS One. 2011 Mar 18;6(3):e17450.

518. Kreeger TJ, Montgomery DL, Jewell JE, et al. Oral transmission of chronic wasting disease in captive Shira's moose. J Wildl Dis. 2006 Jul;42(3):640-645.

519. Sigurdson CJ, Spraker TR, Miller MW, et al. PrP(CWD) in the myenteric plexus, vagosympathetic trunk and endocrine glands of deer with chronic wasting disease. J Gen Virol. 2001 Oct;82(Pt 10):2327-2334.

520. Russo D, Fantaguzzi CM, Di Guardo G, et al. Characterization of sheep (Ovis aries) palatine tonsil innervation. Neuroscience. 2009 Jul 7;161(3):813-826.

521. Cancedda MG, Di Guardo G, Chiocchetti R, et al. Role of palatine tonsils as a prion entry site in classical and atypical experimental sheep scrapie. J Virol. 2014 Jan;88(2):1065-1070.

522. González L, Pitarch JL, Martin S, et al. Identical pathogenesis and neuropathological phenotype of scrapie in valine, arginine, glutamine/valine, arginine, glutamine sheep infected experimentally by the oral and conjunctival routes. J Comp Pathol. 2014 Jan;150(1):47-56.

523. González L, Pitarch JL, Martin S, et al. Influence of polymorphisms in the prion protein gene on the pathogenesis and neuropathological phenotype of sheep scrapie after oral infection. J Comp Pathol. 2014 Jan;150(1):57-70.

524. Contreras-Aguilar MD, Gómez-García F. Salivary glands' anatomy and physiology. In: Tvarijonaviciute A, Martínez-Subiela S, López-Jornet P, et al., editors. Saliva in health and disease. Cham (Switzerland): Springer Nature Switzerland AG; 2020. p. 3-21.

525. Rezek O, Boldogkoi Z, Tombácz D, et al. Location of parotid preganglionic neurons in the inferior salivatory nucleus and their relation to the superior salivatory nucleus of rat. Neurosci Lett. 2008 Aug 8;440(3):265-269.

526. Schultz T, Soinila J, Tolonen R, et al. The sympathetic and parasympathetic nature of neuropeptide Y-immunoreactive nerve fibres in the major salivary glands of the rat. Histochem J. 1994 Jul;26(7):563-570.

527. Barrell GK, Simpson-Morgan MW. Major lymph nodes of the head of the fallow deer (Dama dama) and lymphatic drainage of antlers. Aust Vet J. 1990 Nov;67(11):406-407.

528. Schummer A, Wilkins H, Vollmerhaus B, et al. The anatomy of the domestic animals. Vol. 3, The circulatory system, the skin, and the cutaneous organs of the domestic mammals. Berlin (Germany): Springer-Verlag Berlin Heidelberg GmbH; 1981.

529. Ashton EH, Oxnard CE. Variation in the maxillary nerve of certain animals. Proc Zool Soc Lond. 1958 Dec;131(4):607-625.

530. DeJoia C, Moreaux B, O'Connell K, et al. Prion infection of oral and nasal mucosa. J Virol. 2006 May;80(9):4546-4556.

531. Bessen RA, Martinka S, Kelly J, et al. Role of the lymphoreticular system in prion neuroinvasion from the oral and nasal mucosa. J Virol. 2009 Jul;83(13):6435-6445.

532. Sbriccoli M,Cardone F, Valanzano A, et al. Neuroinvasion of the 263K scrapie strain after intranasal administration occurs through olfactory-unrelated pathways. Acta Neuropathol. 2009 Feb;117(2):175-184.

533. Denkers ND. Oral and nasal mucosal pathways of prion infection in chronic wasting disease [dissertation]. Fort Collins (CO): Colorado State University; 2010.

534. Holcomb KM, Galloway NL, Mathiason CK, et al. Intra-host mathematical model of chronic wasting disease dynamics in deer (Odocoileus). Prion. 2016 Sep 2;10(5):377-390.

535. Bland KP, Cottrell DF. The nervous control of intraluminal pressure in the vomeronasal organ of the domestic ram. Q J Exp Physiol. 1989 Nov;74(6):813-824.

536. Eccles R. Autonomic innervation of the vomeronasal organ of the cat. Physiol Behav. 1982 Jun;28(6):1011-1015.

537. Melese-d'Hospital PY, Hart BL. Vomeronasal organ cannulation in male goats: evidence for transport of fluid from oral cavity to vomeronasal organ during flehmen. Physiol Behav. 1985 Dec;35(6):941-944.

538. Bessen RA, Shearin H, Martinka S, et al. Prion shedding from olfactory neurons into nasal secretions. PLoS Pathog. 2010 Apr 15;6(4):e1000837.

539. Spraker TR, O'Rourke KI, Balachandran A, et al. Validation of monoclonal antibody F99/97.6.1 for immunohistochemical staining of brain and tonsil in mule deer (Odocoileus hemionus) with chronic wasting disease. J Vet Diagn Invest. 2002 Jan;14(1):3-7.

540. McCotter RE. The connection of the vomeronasal nerves with the accessory olfactory bulb in the opossum and other mammals. Anat Rec. 1912 Aug;6(8):299-318.

541. Kratzing J. The structure of the vomeronasal organ in the sheep. J Anat. 1971 Feb;108(Pt 2):247-260.

542. Salazar I, Quinteiro PS, Cifuentes JM. The soft-tissue components of the vomeronasal organ in pigs, cows and horses. Anat Histol Embryol. 1997 Sep;26(3):179-186.

543. Salazar I, Quinteiro PS, Alemañ N. Diversity of the vomeronasal system in mammals: the singularities of the sheep model. Microsc Res Tech. 2007 Aug;70(8):752-62.

544. Salazar I, Brennan PA. Retrograde labelling of mitral/tufted cells in the mouse accessory olfactory bulb following local injections of the lipophilic tracer DiI into the vomeronasal amygdala. Brain Res. 2001 Mar 30;896(1-2):198-203.

545. Meisami E, Bhatnagar KP. Structure and diversity in mammalian accessory olfactory bulb. Microsc Res Tech. 1998 Dec 15;43(6):476-499.

546. Salazar I, Sánchez-Quinteiro P, Alemañ N, et al. Anatomical, immnunohistochemical and physiological characteristics of the vomeronasal vessels in cows and their possible role in vomeronasal reception. J Anat. 2008 May;212(5):686-96.

547. Silverman JD, Kruger L. Calcitonin-gene-related-peptide-immunoreactive innervation of the rat head with emphasis on specialized sensory structures. J Comp Neurol. 1989 Feb 8;280(2):303-330.

548. Gartiolet LP. Recherches sur l'organe de Jacobson [dissertation]. Paris (France): Faculté de Médecine de Paris; 1845.

549. Lohrberg M, Wilting J. The lymphatic vascular system of the mouse head. Cell Tissue Res. 2016 Dec;366(3):667-677.

550. Eltony SA, Elgayar SA. Morphology of the non-sensory tissue components in rat aging vomeronasal organ. Anat Histol Embryol. 2011 Aug;40(4):263-277.

551. Salazar I, Sánchez Quinteiro P. Supporting tissue and vasculature of the mammalian vomeronasal organ: the rat as a model. Microsc Res Tech. 1998 Jun 15;41(6):492-505.

552. Taniguchi K, Mikami S. Fine structure of the epithelia of the vomeronasal organ of horse and cattle. A comparative study. Cell Tissue Res. 1985;240(1):41-r8.

553. Kondoh D, Nakamura KG, Ono YS, et al. Histological features of the vomeronasal organ in the giraffe, Giraffa camelopardalis. Microsc Res Tech. 2017 Jun;80(6):652-656.

554. Arnautovic I, Abdalla O, Fahmy MF.Anatomical study of the vomeronasal organ and the nasopalatine duct of the one-humped camel. Acta Anat (Basel). 1970;77(1):144-154.

555. Ibrahim D. Histochemical analysis of the vomeronasal organ of the one-humped camel (Camelus dromedarius) [dissertation]. Morioka (Japan): Iwate University; 2014.

556. Ghoshal NG, Getty R. Innervation of the forearm and foot in the ox (Bos taurus), sheep (Ovis aries) and goat (Capra hircus). Iowa State Univ. Vet. 1967;29(1):19-29.

557. Ghoshal NG. A comparative morphological study of the somatic innervation of the antebrachium and manus, crus and pes of the domestic animals (Bovidae, Ovidae, Capridae, Suidae, Equidae) [dissertation]. Ames (IA): Iowa State University; 1966.

558. Baum H. Die lymphgefäße der gelenke der schulter- und beckengliedmaße der haustiere (hund, rind, pferd und schwein). Zschr Anat Entw. 1927;84:192–202. German.

559. Heath T, Brandon R. Lymphatic and blood vessels of the popliteal node in sheep. Anat Rec. 1983 Nov;207(3):461-472.

560. Tsopelas C, Bellon M, Bevington E, et al. Lymphatic mapping with 99mTc-Evans Blue dye in sheep. Ann Nucl Med. 2008 Nov;22(9):777-785.

561. van Keulen LJM, Vromans MEW, van Zijderveld FG. Early and late pathogenesis of natural scrapie infection in sheep. APMIS. 2002 Jan;110(1):23-32.

562. Glatzel M, Heppner FL, Albers KM, Aguzzi A. Sympathetic innervation of lymphoreticular organs is rate limiting for prion neuroinvasion. Neuron. 2001 Jul 19;31(1):25-34.

563. Kimberlin RH, Walker CA. Pathogenesis of mouse scrapie: evidence for neural spread of infection to the CNS. J Gen Virol. 1980 Nov;51(Pt 1):183-7.

564. Giron LT, Crutcher KA, Davis JN. Lymph nodes--a possible site for sympathetic neuronal regulation of immune responses. Ann Neurol. 1980 Nov;8(5):520-525.

565. Llewellyn-Smith IJ. Sympathetic preganglionic neurons. In: Llewellyn-Smith IJ, Verberne AJM, editors. Central regulation of autonomic functions. 2nd ed. Oxford University Press; 2011. p. 98-119.

566. Ronzon F, Bencsik A, Lezmi S, et al. BSE inoculation to prion diseases-resistant sheep reveals tricky silent carriers. Biochem Biophys Res Commun. 2006 Dec 1;350(4):872-877.

567. Buijs RM, van der Vliet J, Garidou M-L, et al. Spleen vagal denervation inhibits the production of antibodies to circulating antigens. PLoS One. 2008 Sep 5;3(9):e3152.

568. Denkers ND, Telling GC, Hoover EA. Minor oral lesions facilitate transmission of chronic wasting disease. J Virol. 2011 Feb;85(3):1396-9.

569. Alarcon P, Marco-Jimenez F, Horigan V, et al. A review of cleaning and disinfection guidelines and recommendations following an outbreak of classical scrapie. Prev Vet Med. 2021 Aug;193:105388.

570. Hawkins SA, Simmons HA, Gough KC, et al. Persistence of ovine scrapie infectivity in a farm environment following cleaning and decontamination. Vet Rec. 2015 Jan 24;176(4):99.

571. Gough KC, Baker CA, Simmons HA, et al. Circulation of prions within dust on a scrapie affected farm. Vet Res. 2015 Apr 16;46:40.

572. Gough KC, Baker CA, Hawkins S, et al. Rapid recontamination of a farm building occurs after attempted prion removal. Vet Rec. 2019 Jan 19;184(3):97.

573. Kim TY, Shon HJ, Joo YS, et al. Additional cases of Chronic Wasting Disease in imported deer in Korea. J Vet Med Sci. 2005 Aug;67(8):753-9.

574. Wyckoff AC, Lockwood KL, Meyerett-Reid C, et al. Estimating prion adsorption capacity of soil by BioAssay of Subtracted Infectivity from Complex Solutions (BASICS). PLoS One. 2013;8(3):e58630.

575. Sohn HJ, Park KJ, Roh IS, et al. Sodium hydroxide treatment effectively inhibits PrP. Prion. 2019 01;13(1):137-140.

576. Saunders SE, Bartz JC, Vercauteren KC, et al. An enzymatic treatment of soil-bound prions effectively inhibits replication. Appl Environ Microbiol. 2011 Jul;77(13):4313-7.

577. Booth CJ, Lichtenberg SS, Chappell RJ, et al. Chemical Inactivation of Prions Is Altered by Binding to the Soil Mineral Montmorillonite. ACS Infect Dis. 2021 04 09;7(4):859-870.

578. Maddison BC, Owen JP, Bishop K, et al. The interaction of ruminant PrP(Sc) with soils is influenced by prion source and soil type. Environ Sci Technol. 2010 Nov 15;44(22):8503-8.

579. Kuznetsova A, McKenzie D, Cullingham C, et al. Long-Term Incubation PrP. Pathogens. 2020 Apr 23;9(4).

580. Maddison BC, Baker CA, Terry LA, et al. Environmental sources of scrapie prions. J Virol. 2010 Nov;84(21):11560-2.

581. Hughson AG, Race B, Kraus A, et al. Inactivation of Prions and Amyloid Seeds with Hypochlorous Acid. PLoS Pathog. 2016 Sep;12(9):e1005914.

582. Gough KC, Baker CA, Maddison BC. An in vitro model for assessing effective scrapie decontamination. Vet Microbiol. 2017 Aug;207:138-142.

583. Eraña H, Pérez-Castro M, García-Martínez S, et al. A Novel, Reliable and Highly Versatile Method to Evaluate Different Prion Decontamination Procedures. Front Bioeng Biotechnol. 2020;8:589182.

584. Saunders SE, Bartz JC, Vercauteren KC, et al. Enzymatic digestion of chronic wasting disease prions bound to soil. Environ Sci Technol. 2010 Jun 01;44(11):4129-35.

585. Pilon JL, Nash PB, Arver T, et al. Feasibility of infectious prion digestion using mild conditions and commercial subtilisin. J Virol Methods. 2009 Oct;161(1):168-72.

586. Janoš P. Separation methods in the chemistry of humic substances. J Chromatogr A. 2003 Jan 03;983(1-2):1-18.

587. Peña-Méndez EM, Havel J, Patočka J. Humic substances - compounds of still unknown structure: applications in agriculture, industry, environment, and biomedicine. J Appl Biomed. 2005;3(1):13-24.

588. Cheshire MV, Cranwell PA, Falshaw CP, et al. Humic acid—II : Structure of humic acids. Tetrahedron. 1967;23(4):1669-1682.

589. Thorn KA, Folan DW, MacCarthy P. Characterization of the International Humic Substances Society standard reference fulvic and humic acids by solution state carbon-13 (^{13}C) and hydrogen-1 (^{1}H) nuclear magnetic resonance spectrometry. Denver (CO): U.S. Geological Survey;1989. (Water Resources Investigation Report; 89-4196).

590. Stenson AC, Marshall AG, Cooper WT. Exact masses and chemical formulas of individual Suwannee River fulvic acids from ultrahigh resolution electrospray ionization Fourier transform ion cyclotron resonance mass spectra. Anal Chem. 2003 Mar 15;75(6):1275-84.

591. Ikeya K, Sleighter RL, Hatcher PG. Characterization of the chemical composition of soil humic acids using Fourier transform ion cyclotron resonance mass spectrometry. Geochim Cosmochim Ac. 2015 Mar 15;153:169-182.

592. Kuznetsova A, Cullingham C, McKenzie D, et al. Soil humic acids degrade CWD prions and reduce infectivity. PLoS Pathog. 2018 11;14(11):e1007414.

593. Smith CB, Booth CJ, Wadzinski TJ, et al. Humic substances interfere with detection of pathogenic prion protein. Soil Biol Biochem. 2014;68:309-316.

594. Davenport KA, Hoover CE, Bian J, et al. PrPC expression and prion seeding activity in the alimentary tract and lymphoid tissue of deer. PLoS One. 2017;12(9):e0183927.

595. Rees EE, Merrill EH, Bollinger TK, et al. Targeting the detection of chronic wasting disease using the hunter harvest during early phases of an outbreak in Saskatchewan, Canada. Prev Vet Med. 2012 Apr 01;104(1-2):149-59.

596. Castle AR, Daude N, Gilch S, et al. Application of high-throughput, capillary-based Western analysis to modulated cleavage of the cellular prion protein. J Biol Chem. 2019 Feb 22;294(8):2642-2650.

597. Otero A, Bolea R, Hedman C, et al. An Amino Acid Substitution Found in Animals with Low Susceptibility to Prion Diseases Confers a Protective Dominant-Negative Effect in Prion-Infected Transgenic Mice. Mol Neurobiol. 2018 Jul;55(7):6182-6192.

598. Wishart, WD. Hybrids of white-tailed and mule deer in Alberta. J Mammal. 1980;61(4):716-720.

599. Mahrt JL, Colwell DD. Sarcocystis in wild ungulates in Alberta. J Wildl Dis. 1980 Oct;16(4):571-6.

601. Ghaemmaghami S, Phuan PW, Perkins B, et al. Cell division modulates prion accumulation in cultured cells. Proc Natl Acad Sci U S A. 2007 Nov 13;104(46):17971-6.

602. Tennant JM, Li M, Henderson DM, et al. Shedding and stability of CWD prion seeding activity in cervid feces. PLoS One. 2020;15(3):e0227094.

603. Henderson DM, Manca M, Haley NJ, et al. Rapid antemortem detection of CWD prions in deer saliva. PLoS One. 2013;8(9):e74377.

604. Ness A, Jacob A, Saboraki K, et al. Cellular prion protein distribution in the vomeronasal organ, parotid, and scent glands of white-tailed deer and mule deer. Prion. 2022 Dec;16(1):40-57.

605. Wood WF, Shaffer TB, Kubo A. Volatile ketones from interdigital glands of black-tailed deer,Odocileus hemionus columbianus. J Chem Ecol. 1995 Oct;21(10):1401-8.

606. Gassett JW, Wiesler DP, Baker AG, et al. Volatile compounds from interdigital gland of male white-tailed deer (Odocoileus virginianus). J Chem Ecol. 1996 Sep;22(9):1689-96.

607. LaFauci G, Carp RI, Meeker HC, et al. Passage of chronic wasting disease prion into transgenic mice expressing Rocky Mountain elk (Cervus elaphus nelsoni) PrPC. J Gen Virol. 2006 Dec;87(Pt 12):3773-3780.

608. Otero A, Duque Velásquez C, Aiken J, et al. White-tailed deer S96 prion protein does not support stable in vitro propagation of most common CWD strains. Sci Rep. 2021 May 27;11:11193.

609. Castilla J, Saá P, Morales R, et al. Protein misfolding cyclic amplification for diagnosis and prion propagation studies. Methods Enzymol. 2006;412:3-21.

610. Saá P, Castilla J, Soto C. Ultra-efficient replication of infectious prions by automated protein misfolding cyclic amplification. J Biol Chem. 2006 Nov 17;281(46):35245-52.

611. Johnson CJ, Aiken JM, McKenzie D, et al. Highly efficient amplification of chronic wasting disease agent by protein misfolding cyclic amplification with beads (PMCAb). PLoS One. 2012;7(4):e35383.

612. John TR, Schätzl HM, Gilch S. Early detection of chronic wasting disease prions in urine of pre-symptomatic deer by real-time quaking-induced conversion assay. Prion. 2013 2013 May-Jun;7(3):253-8.

613. Hannaoui S, Amidian S, Cheng YC, et al. Destabilizing polymorphism in cervid prion protein hydrophobic core determines prion conformation and conversion efficiency. PLoS Pathog. 2017 Aug;13(8):e1006553.

614. Alberta Agriculture, Food and Rural Development. Agricultural Land Resource Atlas of Alberta, 2nd Edition. Edmonton (AB): Alberta Agriculture, Food and Rural Development, Resource Management and Irrigation Division, Conservation and Development Branch; 2005.

615. Pinkus H. Notes on the anatomy and pathology of the skin appendages: I. The wall of the intra-epidermal part of the sweat duct. J Invest Dermatol. 1939;2(4):175-186.

616. Christophers E, Plewig G. Formation of the acrosyringium. Arch Dermatol. 1973 Mar;107(3):378-82.

617. Brayton KA, O'Rourke KI, Lyda AK, et al. A processed pseudogene contributes to apparent mule deer prion gene heterogeneity. Gene. 2004 Feb 04;326:167-73.

618. Aguzzi A, Heikenwalder M. Pathogenesis of prion diseases: current status and future outlook. Nat Rev Microbiol. 2006 Oct;4(10):765-75.

619. Heikenwalder M, Zeller N, Seeger H, et al. Chronic lymphocytic inflammation specifies the organ tropism of prions. Science. 2005 Feb 18;307(5712):1107-10.

620. Hamir AN, Kunkle RA, Miller JM, et al. Abnormal prion protein in ectopic lymphoid tissue in a kidney of an asymptomatic white-tailed deer experimentally inoculated with the agent of chronic wasting disease. Vet Pathol. 2006 May;43(3):367-9.

621. Davenport R, Heawood C, Sessford K, et al. Differential expression of Toll-like receptors and inflammatory cytokines in ovine interdigital dermatitis and footrot. Vet Immunol Immunopathol. 2014 Sep 15;161(1-2):90-8.

622. Agbaje M, Rutland CS, Maboni G, et al. Novel inflammatory cell infiltration scoring system to investigate healthy and footrot affected ovine interdigital skin. PeerJ. 2018;6:e5097.

623. Cunningham AA, Kirkwood JK, Dawson M, et al. Bovine spongiform encephalopathy infectivity in greater kudu (Tragelaphus strepsiceros). Emerg Infect Dis. 2004 Jun;10(6):1044-9.

624. Notari S, Moleres FJ, Hunter SB, et al. Multiorgan detection and characterization of protease-resistant prion protein in a case of variant CJD examined in the United States. PLoS One. 2010 Jan 19;5(1):e8765.

625. Orrú CD, Yuan J, Appleby BS, et al. Prion seeding activity and infectivity in skin samples from patients with sporadic Creutzfeldt-Jakob disease. Sci Transl Med. 2017 Nov 22;9(417).

626. Wang Z, Manca M, Foutz A, et al. Early preclinical detection of prions in the skin of prion-infected animals. Nat Commun. 2019 01 16;10(1):247.

627. Wenborn A, Terry C, Gros N, et al. A novel and rapid method for obtaining high titre intact prion strains from mammalian brain. Sci Rep. 2015 May 07;5:10062.

628. Curtis AS, Forrester JV, McInnes C, et al. Adhesion of cells to polystyrene surfaces. J Cell Biol. 1983 Nov;97(5 Pt 1):1500-6.

629. Maroudas NG. Sulphonated polystyrene as an optimal substratum for the adhesion and spreading of mesenchymal cells in monovalent and divalent saline solutions. J Cell Biol. 1977 Mar;90(3):511-520.

630. Maroudas NG. Adhesion and spreading of cells on charged surfaces. J Theor Biol. 1975;49(1):417-424.

631. Kučera F, Jančář J. Homogeneous and heterogeneous sulfonation of polymers: A review. Polym Eng Sci. 1998 May; 38(5):783-792.

632. Coughlin JE, Reisch A, Markarian MZ, Schlenoff JB. Sulfonation of polystyrene: toward the “ideal” polyelectrolyte. J Polym Sci, Part A: Polym Chem. 2013 Jun;51(11):2416-2424.

633. Baigorri R, Fuentes M, González-Gaitano G, et al. Complementary multianalytical approach to study the distinctive structural features of the main humic fractions in solution: gray humic acid, brown humic acid, and fulvic acid. J Agric Food Chem. 2009 Apr 22;57(8):3266-72.

634. Tomaszewski JE, Schwarzenbach RP, Sander M. Protein encapsulation by humic substances. Environ Sci Technol. 2011 Jul 15;45(14):6003-10.

635. Hsu P, Hatcher PG. Covalent coupling of peptides to humic acids: Structural effects investigated using 2D NMR spectroscopy. Org Geochem. 2006 Dec; 37(12):1694-1704.

636. Pucci A, Russo F, Rao MA, et al. Location and stability of a recombinant ovine prion protein in synthetic humic-like mineral complexes [Article]. Biology and Fertility of Soils. 2012 May 2012;48(4):443-451.

637. Wadsworth JD, Powell C, Beck JA, et al. Molecular diagnosis of human prion disease. Methods Mol Biol. 2008;459:197-227.

638. D'Castro L, Wenborn A, Gros N, et al. Isolation of proteinase K-sensitive prions using pronase E and phosphotungstic acid. PLoS One. 2010 Dec 20;5(12):e15679.

639. Fang C, Imberdis T, Garza MC, et al. A Neuronal Culture System to Detect Prion Synaptotoxicity. PLoS Pathog. 2016 05;12(5):e1005623.

640. Andréoletti O, Lacroux C, Chabert A, et al. PrP(Sc) accumulation in placentas of ewes exposed to natural scrapie: influence of foetal PrP genotype and effect on ewe-to-lamb transmission. J Gen Virol. 2002 Oct;83(Pt 10):2607-2616.

641. Levine DJ, Stöhr J, Falese LE, et al. Mechanism of scrapie prion precipitation with phosphotungstate anions. ACS Chem Biol. 2015 May 15;10(5):1269-77.

642. Meyer RK, Oesch B, Fatzer R, et al. Detection of bovine spongiform encephalopathy-specific PrP(Sc) by treatment with heat and guanidine thiocyanate. J Virol. 1999 Nov;73(11):9386-92.

643. McCutcheon S, Hunter N, Houston F. Use of a new immunoassay to measure PrP Sc levels in scrapie-infected sheep brains reveals PrP genotype-specific differences. J Immunol Methods. 2005 Mar;298(1-2):119-28.

644. Hnasko R, Lin A, McGarvey J, et al. Enhanced detection of infectious prions by direct ELISA from the brains of asymptomatic animals using DRM2-118 monoclonal antibody and Gdn-HCl. J Immunol Methods. 2018 05;456:38-43.

645. Vrentas CE, Greenlee JJ, Tatum TL, et al. Relationships between PrPSc stability and incubation time for United States scrapie isolates in a natural host system. PLoS One. 2012;7(8):e43060.

646. Safar J, Wille H, Itri V, et al. Eight prion strains have PrP(Sc) molecules with different conformations. Nat Med. 1998 Oct;4(10):1157-65.

647. Duque Velásquez C, Kim C, Haldiman T, et al. Chronic wasting disease (CWD) prion strains evolve via adaptive diversification of conformers in hosts expressing prion protein polymorphisms. J Biol Chem. 2020 04 10;295(15):4985-5001.

648. Saunders SE, Bartz JC, Telling GC, et al. Environmentally-relevant forms of the prion protein. Environ Sci Technol. 2008 Sep 01;42(17):6573-9.

649. Hayashi H, Takata M, Iwamaru Y, et al. Effect of tissue deterioration on postmortem BSE diagnosis by immunobiochemical detection of an abnormal isoform of prion protein. J Vet Med Sci. 2004 May;66(5):515-20.

650. Buschmann A, Kuczius T, Bodemer W, et al. Cellular prion proteins of mammalian species display an intrinsic partial proteinase K resistance. Biochem Biophys Res Commun. 1998 Dec 30;253(3):693-702.

651. Walter DW, Walsh DP, Farnsworth ML, et al. Soil clay content underlies prion infection odds. Nat Commun. 2011 Feb 15;2:200.

652. Kuznetsova A, McKenzie D, Banser P, et al. Potential role of soil properties in the spread of CWD in western Canada. Prion. 2014 Jan-Feb;8(1):92-99.

653. Gabizon R, Meiner Z, Halimi M, et al. Heparin-like molecules bind differentially to prion-proteins and change their intracellular metabolic fate. J Cell Physiol. 1993 Nov;157(2):319-25.

654. Caughey B, Brown K, Raymond GJ, et al. Binding of the protease-sensitive form of PrP (prion protein) to sulfated glycosaminoglycan and congo red [corrected]. J Virol. 1994 Apr;68(4):2135-41.

655. Shyng SL, Lehmann S, Moulder KL, et al. Sulfated glycans stimulate endocytosis of the cellular isoform of the prion protein, PrPC, in cultured cells. J Biol Chem. 1995 Dec 15;270(50):30221-9.

656. Brimacombe DB, Bennett AD, Wusteman FS, et al. Characterization and polyanion-binding properties of purified recombinant prion protein. Biochem J. 1999 Sep 15;342 Pt 3:605-13.

657. Pan T, Wong BS, Liu T, et al. Cell-surface prion protein interacts with glycosaminoglycans. Biochem J. 2002 Nov 15;368(Pt 1):81-90.

658. Warner RG, Hundt C, Weiss S, et al. Identification of the heparan sulfate binding sites in the cellular prion protein. J Biol Chem. 2002 May 24;277(21):18421-30.

659. Lane A, Stanley CJ, Dealler S, Wilson SM. Polymeric ligands with specificity for aggregated prion proteins. Clin Chem. 2003 Oct; 49(10):1774.

660. Horonchik L, Tzaban S, Ben-Zaken O, et al. Heparan sulfate is a cellular receptor for purified infectious prions. J Biol Chem. 2005 Apr 29;280(17):17062-7.

661. Imamura M, Tabeta N, Kato N, et al. Heparan Sulfate and Heparin Promote Faithful Prion Replication in Vitro by Binding to Normal and Abnormal Prion Proteins in Protein Misfolding Cyclic Amplification. J Biol Chem. 2016 Dec 16;291(51):26478-26486.

662. Lane AR, Stanley CJ, Wilson SM, inventor; Microsens Biophage Limited, assignee. Binding of pathological forms of prion proteins. United States patent US 7.659,076 B2. 2010 Feb 9.

663. Estey LA, Toomik R, inventor; IDEXX Laboratories, Inc., assignee. Transmissible spongiformencephalopathy test reagents and methods. United States patent US 7.659,076 B2. 2010 Feb 9.

664. Vázquez-Fernández E, Vos MR, Afanasyev P, et al. The Structural Architecture of an Infectious Mammalian Prion Using Electron Cryomicroscopy. PLoS Pathog. 2016 09;12(9):e1005835.

665. Kraus A, Hoyt F, Schwartz CL, et al. High-resolution structure and strain comparison of infectious mammalian prions. Mol Cell. 2021 11 04;81(21):4540-4551.e6.

666. Lisle E. Observations in Husbandry. Lisle T, (editor). London (UK): J. Hughs; 1757.

667. Parry HB. Scrapie disease in sheep : historical, clinical, epidemiological, pathological and practical aspects of the natural disease. Oppenheimer DR, editor. London: Academic Press; 1983.

668. Thaer S. Ueber die Traberkrankheit in Frankenfelde. Möglinsche Annalen der Landwirthschaft 1st ed. 1826;17:35-78. German.

669. Stockman S. Scrapie: an obscure disease of sheep. J Comp Pathol Ther. 1931; 26:317-327.

670. Michaelis JD. Arabische Grammatik, nebst einer Arabischen Chrestomathie. Gottingen: Victorinus Boßiegel; 1781. German. P. 96.

671. Lane EW. Arab-English lexicon. Book 1. Part 3. London (England): Williams and Norgate; 1867. P. 1036-1037.

Appendix 1. On the discovery of prions - presence of scrapie in England before 1800

Information and historical research in this chapter has been included in a manuscript to be submitted to Prion as: Ness, Anthony; Aiken, Judd; McKenzie, Debbie (2022). Presence of sheep scrapie and deer rabies in England prior to 1800.

A1.1 Sheep scrapie

Scrapie in sheep and goats is the first described transmissible spongiform encephalopathy (TSE). TSEs are fatal neurodegenerative disorders caused by prions – disease-associated misfolded proteins that replicate their isoforms using a template-like mechanism [1-3]. Scrapie and chronic wasting disease (CWD) affecting cervids are contagious among susceptible animals [4-6]. Two major classifications of scrapie are recognized: classical scrapie and atypical (Nor98) scrapie. Classical scrapie presents with hind limb ataxia and/or weakness, head tremors, behavioural changes, abnormal posture and gait, weight loss, and pruritus (skin itching) which leads to sheep rubbing against objects and losing their wool [7,p.60-71, 8-11]. Atypical scrapie is usually detected prior to onset of clinical disease by prion surveillance programs; clinical signs are typically characterized by ataxia (often in the hind limbs), behavioural changes, and weight loss, in the absence pruritus, [6, 12-13].

A1.2 First reports of sheep scrapie

Despite millennia of domestication of sheep and goats, scrapie appeared to emerge suddenly in the 18th century. Parry attributed the sudden appearance and establishment of scrapie in England and the Electorate of Saxony to trends of extreme inbreeding which may have genetically predisposed sheep to developing the disease [7,p.8-11]. He also noted that agricultural writings

in both countries flourished at this time, increasing documented reports of disease. Leopoldt of the Lordship of Sorau (then part of the Electorate of Saxony, now in western Poland) is credited with documentation of classical scrapie in continental Europe in a 1750 agricultural guide [14-15,p.348].

Although 1750 has been often listed as the earliest recorded description of sheep scrapie, the disease was likely recognized much earlier. A 1772 letter by Thomas Comber (1722-1778) [16] is frequently cited as dating scrapie in England to approximately 1732 - based on a secondhand anecdote claiming that the disease had been present for 40 years [17]. Scrapie was initially referred to a number of different names in England including '*shaking*', '*rickets*', '*goggles*' (all referring to the unsteady gait), and '*rubbers*' (referring to pruritic rubbing) [7,p.34-43, 14, 18,p.1-3]. An earlier description was made by Edward Lisle (**Figure A1.1**) who referred to the disease in England as the '*shaking*':

> Some years the sheep will be apt to be taken with a disease they call the shaking; some farms are more subject to it than others: it is a weakness which seizes their hindquarters, so that they cannot rise up when they are down: I know no cure for it.
>
> This shaking, as I observed is incident to some farms, insomuch as some years an hundred of a flock have died of it: neither Mr. Oxenbridge, Nat. Ryalls, nor Mr. Bishop's shepherd knew of any cure for it. – But they said that horses going with sheep are apt to cause it, and so are briery hedgerows growing out in the ground; but that milchkine [dairy cows] and goats going with the sheep were good against it …[19,p.339].

Figure A1.1. Portrait of the agriculturist Edward Lisle (b. abt. 1666-1722) on the frontispiece of 'Observations in Husbandry' (1757) - his posthumously compiled works. Illustrated by S. F. Ravent Sculp. Attribution: image asset no. 1546030001 from The British Museum. © The Trustees of the British Museum.

It is difficult to pinpoint when Lisle first observed *shaking* in sheep as his agricultural notes were compiled after his death, in 1722, by his son, Thomas Lisle. The timeframe of Edward Lisle's

observations and notes on *shaking* is narrowed by Thomas Lisle's foreword that states his father's agricultural interest and study began in approximately 1693. As for location, Edward Lisle's notes on agriculture were based on observations of farming on his various estates as well as on his travels. Lisle's estates were in Hampshire or Wiltshire, Oxenbridge (from the above quote) farmed in Wiltshire while Ryalls and Bishop were from Dorsetshire. In a separate note regarding bloodletting for preventing a disease in sheep called red-water (babesiosis), Lisle briefly mentions that the *shaking* affects sheep in Leicestershire, the East Midlands:

> [Sir Ambrose Phillipps' shepherd] prefers bleeding in the tail to the eye-vein, both for [preventing] the red-water, and the shaking, which his sheep are subject to.[19,p.341]

The sheep affected by *shaking* in Leicestershire affected those of Lisle's father-in-law, Sir Ambrose Phillipps of Garenton (b. Abt. 1637-1706) [20-21,p.76-78], dating *shaking* in Leicestershire to 1693-1706, based on Sir Phillipps' death. The brief mention of *shaking* in Leicestershire suggests that Lisle had first observed disease in Wiltshire and Dorsetshire. The existence of *shaking* occurring on multiple farms in Wiltshire and Dorsetshire suggest a more established presence of scrapie in those southern counties.

Interestingly, pruritus – causing the scratching, scraping, or rubbing of wool in classical scrapie – is not described by Lisle. By 1783, Wiltshire sheep affected by scrapie (then termed *goggles*) were described as having hind limb weakness with no mention of pruritus [22]. In the 20th and 21st centuries, pruritus is not always the dominant clinical sign and hind limb ataxia is negatively correlated with pruritus [8-10, 23]. M'Gowan and Parry's historical reviews of scrapie included non-pruritic scrapie being predominant in the South of England before 1800 [7,p.34-35, 18,p.3-4]. One explanation is that the Wilkshire and Dorsetshire cases represent a strain of scrapie resembling atypical Nor98 where pruritus is absent and hind limb ataxia can be present (although

hind limb ataxia can also be present in classical scrapie) [10, 13]. Nor98 is, however, poorly transmitted [6, 13, 24], whereas Lisle noted outbreaks. Apparent outbreaks of a Nor98-like disease could be explained by the extreme inbreeding of the Wiltshire Horn and Dorset Horn sheep conferring a high degree of genetic susceptibility to scrapie [7,p.8-11, 10, 13]. A non-pruritic form of classical scrapie is more consistent with the reported spread of *shaking* and *goggles* in the South of England. Lisle also lists the *shaking* as a disorder distinct from diseases that could be symptomatically conflated with scrapie – notably *gid* or *giddiness* (coenurosis), and the *staggers* (hypomagnesemia) [19,p.338-339]. The symptoms described are not consistent with a differential diagnosis of rabies in sheep (a possibility at the time) which typically manifests, in sheep, as the furious form of rabies with headbutting, aggression, drooling, head and muzzle tremors, and finally paralysis with rapid death occurring within days of onset of clinical signs [25-28]. Scrapie was sufficiently predominant in Dorsetshire and Wiltshire such that, in the second half of the 18th century, it was referred to as the '*Wiltshire disorder*' [22, 29-30,p.26-27]. The decline in popularity and near extinction of the Wiltshire Horn breed of sheep has been partly attributed to their reputation for developing scrapie [30,p.26-27, 31].

Several more cases of scrapie were reported in England prior to 1800 (**Figure A1.2**). The emergence of scrapie threatened the reputations and incomes of those involved. In 1754, Lincolnshire sheep breeders and feeders conveyed their concerns to legislators on the spread of scrapie in the area by breeders and jobbers [intermediary sellers] with the hopes of future regulations being implemented [32]. Despite a lack of described symptoms, the report includes several temporal reference points:

Mr. *Nicholas Wildman*, of *Sutton*, Grasier, said, That there has been a Distemper amongst the Sheep in *Lincolnshire*, about Ten Years, called the Rickets, or Shaking; which, he believes, is spread to other Counties; and when once a Sheep has contracted this Distemper, it never recovers:

That, in the Spring 1753, the Witness bought an Hundred Sheep of a Jobber, of different sorts; and, in Two of the Sorts, there were several Sheep which were distempered… [32].

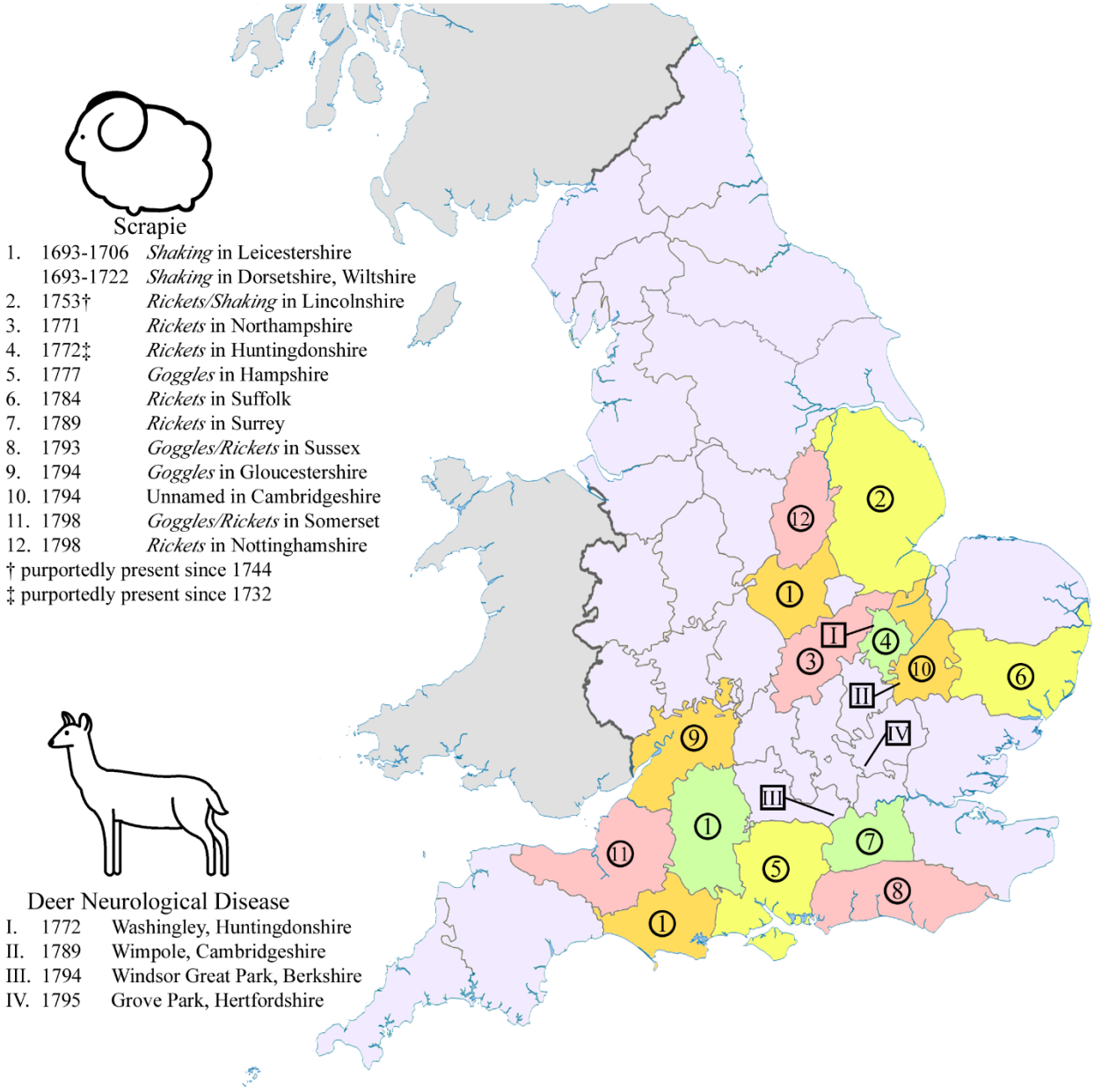

Figure A1.2. First known presence of scrapie and deer rabies outbreaks in English counties prior to 1800.

Farmers accused of selling sheep infected with the *rickets* (Northamptonshire, 1771) and *goggles* (Hampshire, 1777) took out newspaper advertisements defending the quality of their livestock [33-34]. One Northamptonshire farmer won a defamation suit in 1785 against a shepherd who had claimed the farmer's rams were infected with *rickets*/*rubbers* [35].

Pruritic classical scrapie in England was described by rector Thomas Comber writing from Huntingdonshire, England in 1772:

> The principal Symptom of the first Stage of this Distemper, is a Kind of Light-Headedness, which makes the affected Sheep appear much wilder than usual, when his Master or Shepherd as well as a Stranger, approaches him. He bounces up suddenly from his Laire, and runs to a Distance, as though he were pursued by Dogs, &c [et cetera]. These Actions seem to indicate that his Sight is affected: and I dare say, if his Eye-Balls were examined, they would appear inflamed.
>
> In the second Stage of the Distemper, the principal Symptom of the Sheep is his rubbing himself against Trees, Posts, &c. with such Fury as to pull off his Wool and tear away his Flesh.
>
> The distressed Animal has now a violent Itching in his Skin, the Effect of an highly inflamed Blood: but it does not appear that there is ever any cutaneous Eruption, or salutary critical Discharge. In short, from all Circumstances the Fever appears now to be at its Height.
>
> The third and last Stage of this dreadful Malady seems to be only the Progress of Dissolution, after an unfavourable Crisis. The poor Animal, as condemned by Nature, appears stupid, separates from the Flock, *walks irregularly*, (whence probably the Name of this Disease, *Rickets*) generally lies, and eats little. These Symptoms increase in Degree till Death, which follows a general Consumption, which appears upon Dissection of the Carcase; the Juices and even Solids having suffered a general Dissolution, insomuch that the Solids have no longer any of the good Properties of Flesh, nor the Blood of its usual Colour, &c. [17]

Comber reported clinical signs consistent with classical scrapie and, based on local anecdotes, suggests that *rickets* had been in England for perhaps 40 years – i.e., 1732 which had been, before the acknowledgement of Edward Lisle's observations, suggested to be the earliest date for scrapie. References to scrapie appear between 1784 and 1798 under names of *rickets*, *goggles*,

shaking, and *rubbers* in the counties of Cambridgeshire, Gloucestershire, Hampshire, Leicestershire, Somerset, Suffolk, Surrey, Sussex, and the counties previously reporting the disease [30,p.26-27, 36-40, 41,p.27, 42-45]. The county of Norfolk in the East of England likely had scrapie prior to 1800. *Rickets* was established in multiple farms in Norfolk by 1804 with the one location being affected as early as 1800 [46]. John Claridge judged in 1793 that *shaking*, *rickets*, and *goggles* were all the same disease and in 1809 John Lawrence, an agricultural writer, wrote that Lisle's description of *shaking* is the same disease as *goggles* [30,p.26-27, 47].

Two distinct geographical foci of scrapie existed in England prior to 1800 (**Figure A1.2**), one spanning the South West and the South East regions of England and a second encompassing the East Midlands and the East of England regions. Parry recognized these foci as Wessex and East Anglia [7,p.34-39]. Although clinical descriptions of disease are rare, sheep in Wiltshire and Dorsetshire did not display pruritus [19,p.339, 22] while those in the east often, but not always, presented with pruritus [17, 36, 38, 40, 44]. The geographic separation of scrapie signs during 18th century England (before prolonged and extensive trade of sheep between regions) is supportive of two independent outbreaks of scrapie – atypical scrapie or non-pruritic classical scrapie in the South of England, and classical pruritic scrapie in the East Midlands and East of England. Different breeds were affected in the two foci with disease in the East Midlands and the East of England involving the Norfolk Horn and Old Hampshire breeds while scrapie predominantly affected the Wiltshire Horn and Dorset Horn breeds in the South East and South West foci [7,p.16-24, 30,p.26-27, 37, 39-40, 41,p.27]. The geographical separation of sheep breeds could also explain the absence of pruritus in the South of England. As speculated earlier, the extreme inbreeding of the Wiltshire Horn and Dorset Horn sheep may have influenced the predominant symptoms of scrapie in the breeds. For comparison, continental European outbreaks

of classical scrapie prior to 1800 were largely restricted to descendants of imported Spanish Merino breeds [7,p.32-34]. The Old Hampshire breed is now extinct and the Norfolk Horn barely survived extinction [48-49]. The modern Wiltshire Horn and Dorset Horn are among the breeds with highest incidence of scrapie [50]. The modern Norfolk Horn population has a high frequency of the ARR (scrapie-resistant) prion protein genotype while the Wiltshire Horn has a more mixed genotype frequency [51]. These two breeds have, however, experienced population bottleneck effects due to the near extinction of the breeds suggesting that modern prion protein genotype frequencies may not be representative of their historical populations.

A1.3 Presence of deer rabies in England before 1800

Concurrent with the establishment of scrapie in England, there were reports of a disease in deer with scrapie-like symptoms. Comber, who reported the pruritic symptoms of scrapie, documented the disease in deer as follows:

> I will conclude, Sir, this long Letter, by observing that there is acknowledged a strong Analogy betwixt Sheep and Deer. I am assured by several Persons of Credit, that a Distemper exactly the same as *Rickets* in Sheep is found to have arisen of late Years among Deer in some Parks (Particularly in that of – Apprice, Esq; at *Washingley*, in this County). How desirable is it, that the Masters of Parks should instruct their Keepers to observe all the Symptoms of Deer thus dying, and compare them with those of Sheep! [17]

Comber's suggestion that there might be a link between sheep *rickets* and the deer disease leads to the question as to whether this deer disease is an unrecorded outbreak of CWD in the English countryside (**Figure A1.2**), nearly 200 years prior to the disease being described in North America [52]. The possibility of a scrapie-initiated CWD epidemic in Georgian era England is remotely possible. Sheep scrapie is transmissible to elk and white-tailed deer by intracerebral inoculation and the clinical signs of CWD are visually similar to scrapie [4, 53-54]. Given the

independent emergence of CWD in Colorado and Fennoscandia [52, 55], CWD may not be restricted to a disease of the 20th and 21st centuries. In 1794, Charles Vancouver (1756-1815?) [56] reports neurological disease in deer at nearby Wimpole (Wimple) park, Cambridgeshire:

> Wimple park, contains about four hundred acres, and is at present, depastured by deer, sheep, and cow cattle; amongst the former, a disease does, and has prevailed for some years past, which in some degree, may be compared, from its resemblance with the very extraordinary one, observed amongst the sheep, in the neighbourhood of Ashley. The first symptom of the disorder, observable in the deer, is similar to that amongst the sheep; which is an apparent uneasiness in the head, and the rubbing of its horns against the trees, (this action however is common to deer, at particular seasons, in all countries, whether in a perfectly wild, or more domesticated state) but the most extraordinary effect of this disease is, that the animal appears to labour under a sort of madness, in pursuing the herd, which now flee before him, and endeavour to forsake him; trying to bite, or otherwise annoy them, with all his strength and power, which soon being exhausted, he becomes sequestered from the rest of the herd, and in that deplorable state of the disease, breaks his antlers against the trees, gnaws large collops of flesh, from off his sides, and hind quarters, appears convulsed for a short time, and soon expires.
>
> The greater part of the flock of deer, which were very numerous in this park, have been carried off by this dreadful disorder, in the course of the last three years. In the months of July, August, and September, and when in full pasture, they are more subject to its fatal influence, than at other times, though it prevails to a certain degree throughout the year [57]

Both Comber and Vancouver commented on the similarity of the deer disease with scrapie, suggesting they were referring to the same deer disease. The deer of the Windsor Great Park were reported as infected circa 1794, with the outbreak lasting until at least 1798 [58,p.275-276, 59]. With the disease affecting the deer in a Royal Park, King George III sought out information about the Wimpole outbreak. A 1794 letter from Philipe York, 3rd Earl of Hardwicke, the owner of the Wimpole estate, to King George III of England provides more details about the Wimpole deer disease:

> It began in the summer of 1789, and principally affected the old bucks and does, the greater part of which were destroyed by it in the course of that year. Those that were attacked by the disorder, separated themselves from the herd, and ran with great violence against trees or whatever was in their way. Before the summer of 1790, upwards of 200 deer had died of the disorder out of 300 that formed the original stock… about 150 new deer were introduced into the Park in the course of that & the following year. From the year 1790, the disorder has never raged in so violent a manner; but from ten to thirty of different ages, & of the new deer as well as the old, have died ever[y] year since that time… I forgot to mention that the disorder has affected fawns of 3 or 4 days old & of the new stock: they appear to lose the use of their hind limbs, & died in a few hours… [58,p.275-276].

The described symptoms differ from CWD in the 20th and 21st centuries– notably the biting of other deer and pruritus which are both absent in clinical CWD [4]. A writer in 1799 responded to Vancouver's report and suggested that the disease at Wimpole was caused by the *staggers* (hypomagnesemia) despite pruritus and biting also not being a symptom of the latter [60,p.229-237, 61-62]. CWD can be transmitted vertically, but is not immediately lethal to fawns [63-64]. Further outbreaks of the unknown deer disease would continue to periodically appear in deer parks into the 19th century. The most thorough investigation into the disease outbreaks was published in 1888. Cope and Horsely published a combined report on the 1886 outbreak in Richmond Park. Cope investigated the case history while Horsely studied the disease experimentally. Cope's report provides evidence of deer disease outbreaks with the same symptoms in Grove Park, Hertfordshire in 1795, the Windsor Great Park outbreak mentioned earlier, and cases on other estates in 1872 and 1880 [28, 59]. The investigators were not aware of the older Washingley and Wimpole cases. One of the earliest symptoms noted in the Cope report is infected deer holding their noses up to the air - a symptom reminiscent to the raised head and fixed stare of scrapie-infected sheep [7,p.61, 59]. Symptoms in all of the outbreaks were nearly identical to those reported at Wimpole – excessive rubbing of vegetation (sometimes so extreme that the bone of the forehead was exposed), aggressive behaviour, chasing and biting other deer,

and biting of their own sides. Like Wimpole, a fawn from Richmond Park became symptomatic and rapidly died.

Affected, penned deer displayed extreme aggression (including attempts at biting) towards handlers, hind limb ataxia progressing to paralysis, and death within 2-8 days of onset of clinical signs [59]. The short clinical phase of disease (within 8 days) excludes CWD prions as the causative agent. The disease persisted when Cope moved the deer to new pastures. Based on clinical signs and case history, Cope and a veterinary inspector, Lupton began to suspect rabies. Rabies is an encephalitic disease caused by the neurotropic viruses of the *Lyssavirus* genus which is most commonly transmitted through saliva from bites by infected animals [65-66]. Symptomatic animals typically present with one of two forms - aggressive (furious) or dumb (paralytic) rabies [65-67]. Cervid rabies in the modern world is, generally speaking, rare and self-limiting [68-73].

Although deer were known, on rare occasions, to be bitten and infected by rabid dogs, neither veterinarians nor the extant literature had knowledge of rabies outbreaks in deer herds. Deer were generally believed to be dead-end hosts of rabies. The feasibility of rabies transmission between cervids via biting was regarded as doubtful as deer have a dental pad instead of upper incisors. Print news reports of a possible herd of rabies-infected deer at Stainborough Park in 1856 initiated an investigation by a medical officer who, controversially, declared that the disease was rabies. Subsequent veterinarian inquirers and physicians remained unconvinced of the Stainborough outbreak being caused by rabies [74-75]. Cope did not refer to the 1856 outbreak in his historical background [59].

Cope and Horsley did, however, investigate rabies as a possible cause of the Richmond Park epizootic [59]. To understand disease transmission, an uninfected deer and a clinically affected deer from Richmond Park were co-housed in a single pen. The infected deer immediately attacked the other, biting about the ears and neck. The naïve animal developed clinical signs 19 days later and died shortly thereafter. Careful observation of Richmond Park deer determined that biting by infected deer did not cause lacerating open wounds, but the attacked deer were exposed to residual saliva when subsequently licking the bitten areas.

Cope sent infected deer to Horsley in London to experimentally test for rabies. An infected buck sent to London was too violent to approach for 2 days until it fell unconscious, dying following a high fever on the third day. Spinal cord tissue from multiple infected deer and medullary tissue from a fawn that died of clinical disease were intracerebrally inoculated into rabbits which all developed and died of 'typical' rabies. Spinal cord tissue from the fawn was inoculated into a dog which also developed and died of rabies. The cause of the outbreaks in deer was, therefore, conclusively confirmed.

Similar to scrapie, rabies outbreaks in deer were unknown prior to the 18th century despite deer parks existing since medieval times. While extreme inbreeding of sheep may have created the genetic predisposition for certain breeds of sheep to develop scrapie, what could have allowed for rabies, an ancient disease, to suddenly become epizootic in deer? Rabies has been recorded in Britain since the High Medieval Period, but the disease did not become widely entrenched in England (almost exclusively in dogs) until the 1770's [67]. The presence of rabies in England does not by itself explain why rabies outbreaks in deer occurred during this time period. The multiple rabies outbreaks in English deer beginning in the late 18th century may have been influenced by two changes to deer parks. Beginning in the 18th century, typical English deer

parks were transformed from vast royal forests into smaller estate enclosures with paddocks and pastures [76]. The density of trees decreased to provide the landed gentry with views of their land and ornamental herds [77]. The widespread establishment of rabies in dogs combined with the smaller enclosures and the reduced tree cover of 18th and 19th century deer parks may have fostered the conditions for rabies outbreaks in deer parks. The cessation of rabies outbreaks in deer can then be attributed to policies in the 1880s and 1890s aimed aggressively at eradicating rabies in dogs, with the elimination of rabies in England by 1902 [28, 67].

Two neurological diseases of animals emerged in 18th century England. The first recorded appearance of the scrapie prion disease in sheep can be dated to between 1693-1722 in the Southwest of England and between 1693-1706 in the East Midlands. Thomas Comber's letter on scrapie was published in 1772 with the concluding intrigue of an existing, unknown scrapie-like disease in deer. Precisely 250 years since the deer disease was first noted we have come to a confident answer on the causative agent - rabies. The reports of diseased deer in 18th Century England by Comber and Vancouver (cases unknown to Cope and Horsley) can now be attributed not to a prion, but to a virus.

A1.4 Figure Attribution

Attribution of Figure A1.2 is a derivative of "English counties 1851" by Dr Greg, Wikimedia Commons, used under CC BY-SA 3.0.

A1.5 Appendix 1 literature cited

1. Prusiner SB. The prion diseases. Brain Pathol. 1998 Jul;8(3):499-513.

2. Jarrett JT, Lansbury PT. Seeding "one-dimensional crystallization" of amyloid: a pathogenic mechanism in Alzheimer's disease and scrapie? Cell. 1993 Jun 18;73(6):1055-8.

3. Colby DW, Prusiner SB. Prions. Cold Spring Harb Perspect Biol. 2011 Jan 01;3(1):a006833.

4. Williams ES. Chronic wasting disease. Vet Pathol. 2005 Sep;42(5):530-49.

5. Mathiason CK. Scrapie, CWD, and Transmissible Mink Encephalopathy. Prog Mol Biol Transl Sci. 2017;150:267-292.

6. Greenlee JJ. Review: Update on Classical and Atypical Scrapie in Sheep and Goats. Vet Pathol. 2019 Jan;56(1):6-16.

7. Parry HB. Scrapie disease in sheep : historical, clinical, epidemiological, pathological and practical aspects of the natural disease. Oppenheimer DR, editor. London: Academic Press; 1983.

8. Healy AM, Weavers E, McElroy M, et al. The clinical neurology of scrapie in Irish sheep. J Vet Intern Med. 2003 2003 Nov-Dec;17(6):908-16.

9. Cockcroft PD, Clark AM. The Shetland Islands scrapie monitoring and control programme: analysis of the clinical data collected from 772 scrapie suspects 1985-1997. Res Vet Sci. 2006 Feb;80(1):33-44.

10. Ulvund MJ. Ovine Scrapie disease: Do we have to live with it? Small Ruminant Res. 2008;76(1-2):131-140.

11. Vargas F, Bolea R, Monleón E, et al. Clinical characterisation of natural scrapie in a native Spanish breed of sheep. Vet Rec. 2005 Mar 05;156(10):318-20.

12. Benestad SL, Sarradin P, Thu B, et al. Cases of scrapie with unusual features in Norway and designation of a new type, Nor98. Vet Rec. 2003 Aug 16;153(7):202-8.

13. Benestad SL, Arsac JN, Goldmann W, et al. Atypical/Nor98 scrapie: properties of the agent, genetics, and epidemiology. Vet Res. 2008 Jul-Aug;39(4):19.

14. Schneider K, Fangerau H, Michaelsen B, et al. The early history of the transmissible spongiform encephalopathies exemplified by scrapie. Brain Res Bull. 2008 Dec 16;77(6):343-55.

15. Leopoldt JG. Nützliche und auf die Erfahrung gegründete Einleitung zu der Land-Wirthschafft [Useful and experience-based introduction to agriculture]. Sorau: Johann Gottlieb Rothen; 1750. German.

16. Nichols J. Literary anecdotes of the eighteenth century; comprizing biographical memoirs of William Bowyer, printer, F. S. A., and many of his learned friends. Vol. 8. London (England): Nichols, son, and Bentley; 1814. Rev. Dr. Thomas Comber, Dean of Durham; p. 423-424.

17. Comber T. A letter to Dr. Hunter, physician in York. Concerning the rickets in sheep. In: Real Improvements in Agriculture. London (England): W. Nicoll; 1772. p. 73-83.

18. M'Gowan JP. Investigation into the disease of sheep called "scrapie" (traberkrankheit; la tremblante): with especial reference to its association with sarcosporidiosis. Edinburgh (UK): William Blackwood and Sons; 1914.

19. Lisle E. Observations in Husbandry. Lisle T, (editor). London (UK): J. Hughs; 1757.

20. Girouard M. Ambrose Phillipps of Garendon. Archit Hist. 1965;8:25-38.

21. Everard JB. Charnwood forest. Leicester (UK): Edward Shardlow, The Chromo Press; 1907.

22. Anonymous. On the disease called goggles in sheep. Letters and Papers on Agriculture, Planting, &c. 2nd ed. Vol. 1. Bath (UK): R. Cruttwell; 1783:46-47.

23. Konold T, Phelan LJ, Donnachie BR, et al. Codon 141 polymorphisms of the ovine prion protein gene affect the phenotype of classical scrapie transmitted from goats to sheep. BMC Vet Res. 2017 May 04;13(1):122.

24. Simmons MM, Moore SJ, Konold T, et al. Experimental oral transmission of atypical scrapie to sheep. Emerg Infect Dis. 2011 May;17(5):848-54.

25. Hudson LC, Weinstock D, Jordan T, et al. Clinical features of experimentally induced rabies in cattle and sheep. Zentralbl Veterinarmed B. 1996 Apr;43(2):85-95.

26. Brookes SM, Klopfleisch R, Müller T, et al. Susceptibility of sheep to European bat lyssavirus type-1 and -2 infection: a clinical pathogenesis study. Vet Microbiol. 2007 Dec 15;125(3-4):210-23.

27. Zhu Y, Zhang G, Shao M, et al. An outbreak of sheep rabies in Shanxi province, China. Epidemiol Infect. 2011 Oct;139(10):1453-6.

28. Worboys M. Mad Cows, French Foxes and Other Rabid Animals in Britain, 1800 to the Present. Vet Hist. 2017 Feb 01;18(4):543-567.

29. Young A. A farming tour in the south and west of England, 1796. In: Young A, editor. Annals of agriculture and other useful arts. Vol. 28. Bury St. Edmunds (England): Arthur Young; 1797. p. 460-487, 620-640.

30. Claridge J. General view of the agriculture in the county of Dorset: with observations on the means of its improvement. London (England): W. Smith; 1793.

31. Copus AK. Changing Markets and the Development of Sheep Breeds in Southern England 1750–1900. Agr Hist Rev. 1989;37(1):36-51.

32. The report from the committee, to whom the petition of several gentlemen, farmers, and other persons, breeders and feeders of sheep, in the county of Lincoln, was referred. London (England): 1755.

33. Advertisement and Notices. Sheep. Northampton Mercury. 1771 October 7;52(30):117.

34. Advertisement and Notices. Hampshire Chronicle. 1777 August 18;5(261):1.

35. News. Northampton Mercury 1785 July 11;66(19):3.

36. Young A. A five days tour to Woodbridge, &c. In: Young A, editor. Annals of agriculture and other useful arts. Vol. 2. London (England): Arthur Young; 1784. p. 105-168.

37. Young A. A tour in Sussex. In: Young A, editor. Annals of agriculture and other useful arts. Vol. 11. Bury St. Edmund's (England): Arthur Young; 1789. p. 170-304.

38. Young A. Some notes concerning the drill husbandry. In: Young A, editor. Annals of agriculture and other useful arts. Vol. 18. Bury St. Edmund's (England): Arthur Young; 1792. p. 308-320.

39. Young A. Some farming notes in Essex, Kent, and Sussex. In: Young A, editor. Annals of agriculture and other useful arts. Vol. 20. Bury St. Edmund's (England): Arthur Young; 1793. p. 220-297.

40. Vancouver C. General view of the agriculture of the county of Cambridge: with observations on the means of its improvement. London (England): W. Smith; 1794. Ashley and Silvery; p. 11-13.

41. Turner G. General view of the agriculture of the county of Gloucester: with observations on the means of its improvement. London (England): J. Smeeton; 1794.

42. Billingsly J. General view of the agriculture of the county of Somerset: with observations on the means of its improvement. 3rd ed. London (England): Richard Phillips; 1798. Chapter 8, Live stock; p.142-151.

43. Lowe R. General view of the agriculture of the county of Nottingham: with observations on the means of its improvement. London (England): W. Smith; 1798. Chapter 8, Live stock; p. 123-134.

44. Parkinson R. The experienced farmer: an entire new work, in which the whole system of agriculture, husbandry, and breeding of cattle, is explained and copiously enlarged upon; and the best methods, with the most recent improvements, pointed out. Vol. 1. London (England): G. G. and J. Robinson; 1798. Section 34, Disorders incident to sheep; with the methods of cure; p. 177-194.

45. Fleet T. Restorative for the rot in sheep, discovered by Tho. Fleet, of Moundsmere. In: Robbins W (editor). The annual Hampshire repository: or, historical, economical, and literary miscellany; a provincial work, of entirely original materials, comprising all matters relative to the county, including the Isle of Wight, &c. Vol. 1. Winchester (England): Robbins; 1799. p. 84-87.

46. Young A. General View of the Agriculture of the County of Norfolk. London (England): G. and W. Nicol;1804. Chapter 12, Live stock; p. 444-478.

47. Lawrence J. A general treatise on cattle, the ox, the sheep, and the swine. 2nd ed. London (England): Sherwood, Neely & Jones; 1809. Sheep and lambs; p. 514-537.

48. Ryder ML. The history of sheep breeds in Britain. Agric Hist Rev. 1964;12(1):1-12.

49. Ryder ML. The history of sheep breeds in Britain (continued). Agric Hist Rev. 1964;12(2):65-82.

50. Del Rio Vilas VJ, Gutian J, Pfeiffer DU et al. Analysis of data from the passive surveillance of scrapie in Great Britain between 1993 and 2002. Vet Record. 2006 Dec 9;159:799-804.

51. Townsend SJ, Warner R, Dawson M. PrP genotypes of rare breeds of sheep in Great Britain. Vet Rec. 2005 Jan 29;156(5):131-134.

52. Williams ES, Young S. Chronic wasting disease of captive mule deer: a spongiform encephalopathy. J Wildl Dis. 1980 Jan;16(1):89-98.

53. Hamir AN, Miller JM, Cutlip RC, et al. Transmission of sheep scrapie to elk (Cervus elaphus nelsoni) by intracerebral inoculation: final outcome of the experiment. J Vet Diagn Invest. 2004 Jul;16(4):316-21.

54. Greenlee JJ, Smith JD, Kunkle RA. White-tailed deer are susceptible to the agent of sheep scrapie by intracerebral inoculation. Vet Res. 2011 Oct 11;42:107.

55. Benestad SL, Mitchell G, Simmons M, et al. First case of chronic wasting disease in Europe in a Norwegian free-ranging reindeer. Vet Res. 2016 09 15;47(1):88.

56. Fox HSA. Vancouver, Charles (bap. 1756, d. 1815?), agricultural improver and writer. Oxford University Press; 2004.

57. Vancouver C. General view of the agriculture of the county of Cambridge: with observations on the means of its improvement. London (England): W. Smith; 1794. Wimpole; p. 93-95.

58. Aspinall A, editor. The later correspondence of George III. Vol. 2, February 1793 to December 1797. London (UK). Cambridge University Press; 1963.

59. Cope AC, Horsley V. Reports on the outbreak of rabies among deer in Richmond park during the years 1886-7. London (UK): Committee of Council for Agriculture; 1888.

60. Anderson J. Recreations in agriculture, natural-history, arts, and miscellaneous literature. Vol. 1. London (England): T. Bensley; 1799.

61. Mayland HF. Grass tetany. In: Church DC, editor. The Ruminant Animal, Digestive Physiology and Nutrition. Englewood Cliffs (NJ): Prentice Hall; 1988. p. 511-531.

62. Underwood WJ, Blauwiekel R, Delano ML, et al. Biology and Diseases of Ruminants (Sheep, Goats, and Cattle). In: Fox JG, Anderson LC, Otto GM, et al., editors. Laboratory Animal Medicine. 3rd ed. San Diego (CA): Elsevier Academic Press; 2015. p. 623-694.

63. Sigurdson CJ, Williams ES, Miller MW, et al. Oral transmission and early lymphoid tropism of chronic wasting disease PrPres in mule deer fawns (Odocoileus hemionus). J Gen Virol. 1999 Oct;80 (Pt 10):2757-2764.

64. Nalls AV, McNulty E, Powers J, et al. Mother to offspring transmission of chronic wasting disease in reeves' muntjac deer. PLoS One. 2013;8(8):e71844.

65. Fooks AR, Cliquet F, Finke S, et al. Rabies. Nat Rev Dis Primers. 2017 Nov 30;3:17091.

66. Scott TP, Nel LH. Lyssaviruses and the fatal encephalitic disease rabies. Front Immunol. 2021 Dec 2;12:786953.

67. Steele JH, Fernandez PJ. History of rabies and global aspects. In: Baer GM, editor. The natural history of rabies. 2nd ed. Boca Raton (FL): CRC Press, Inc.; 1991. p. 1-24.

68. Chalmers AW, Scott GR. Ecology of rabies. Trop Anim Health Prod. 1969;1:33-55.

69. Blancou J, Aubert MFA, Artois M. Fox rabies. In: Baer GM, editor. The natural history of rabies. 2nd ed. Boca Raton (FL): CRC Press, Inc.; 1991. p. 257-290.

70. Prestrud P, Krogsrud J, Gjertz I. The occurrence of rabies in the Svalbard Islands of Norway. J Wildl Dis. 1992;28(1):57-63.

71. Kim J-H, Hwang E-K, Sohn H-J, et al.. Epidemiological characteristics of rabies in South Korea from 1993 to 2001. Vet Rec. 2005 Jul 9;157;53-56.

72. Petersen BW, Tack DM, Longenberger A, et al. Rabies in captive deer, Pennsylvania, USA, 2007–2010. Emerg Infect Dis. 2012 Jan;18(1):138-141.

73. Ørpetveit I, Reiten MR, Benestad SL, et al. Rabies in arctic fox (Vulpes lagopus) and reindeer (Rangifer tarandus platyrhynchus) during an outbreak on Svalbard Norway, 2011-2012. J Wildl Dis. 2022 Jun 6;10.7589/JWD-D-21-00112.

74. Cartledge. The Veterinarian. 1856;29(4):341-342.

75. Payne H. The alleged rabies in Stainborough Park. Assoc Med J. 1856;4(173):350.

76. Fletcher J. Gardens of Earthly Delight: The History of Deer Parks. Oxford (UK): Oxbow Books; 2011. Chapter 15, The Restoration and Landscape: from ashes to avenues; purgatory to Paradise; p. 176-187.

77. Belin Md. From the Deer to the Fox : The Hunting Transition and the Landscape, 1600–1850. Hatfield (UK): University Of Hertfordshire Press; 2013. Chapter 3, The landscape of deer hunting; p. 23-56.

Appendix 2. Methods for imaging deer hair

A2.1 Field Emission scanning electron microscopy

Surface structures of deer hairs was examined by field emission scanning electron microscopy. Mule deer and white-tailed deer tarsal gland hairs and shoulder hairs were mounted onto scanning electron microscope sample stubs using conductive double sided adhesive carbon tabs. Conductive gold coating of mounted samples was applied using a Leica EM SCD005 cool sputter coater (Leica Microsystems, Germany). Sample surface architecture was examined using a ZEISS Sigma 300 VP field emission scanning electron microscope (Carl Zeiss AG, Germany).

A2.2 Confocal fluorescence microscopy using glutaraldehyde-induced fluorescence

A novel method of examining hair internal and external structures was investigated. Surface and internal structures of deer tarsal gland and shoulder hairs was examined by confocal fluorescence microscopy. Glutaraldehyde fixation can induce fluorescent properties in molecules through the introduction of double bonds [1]. Fluorescence of hair structures was induced by submersion of the hairs in a solution of 0.8% (v/v) glutaraldehyde in 50mM phosphate buffered saline (pH 8.25) for 30 minutes at 37˚C. Internal and surface hair structures were visualized using a Zeiss LSM 700 laser scanning confocal microscope (Carl Zeiss AG, Germany). Glutaraldehyde-induced fluorescence was imaged with fluorescent excitation by a 405nm diode laser. Images were processed using ImageJ software to make Z-stack composites (**Figure A2.1**). Glutaraldehyde-induced fluorescence may provide some utility for hair analysis where scanning electron microscopy or simple light microscopy do not suffice.

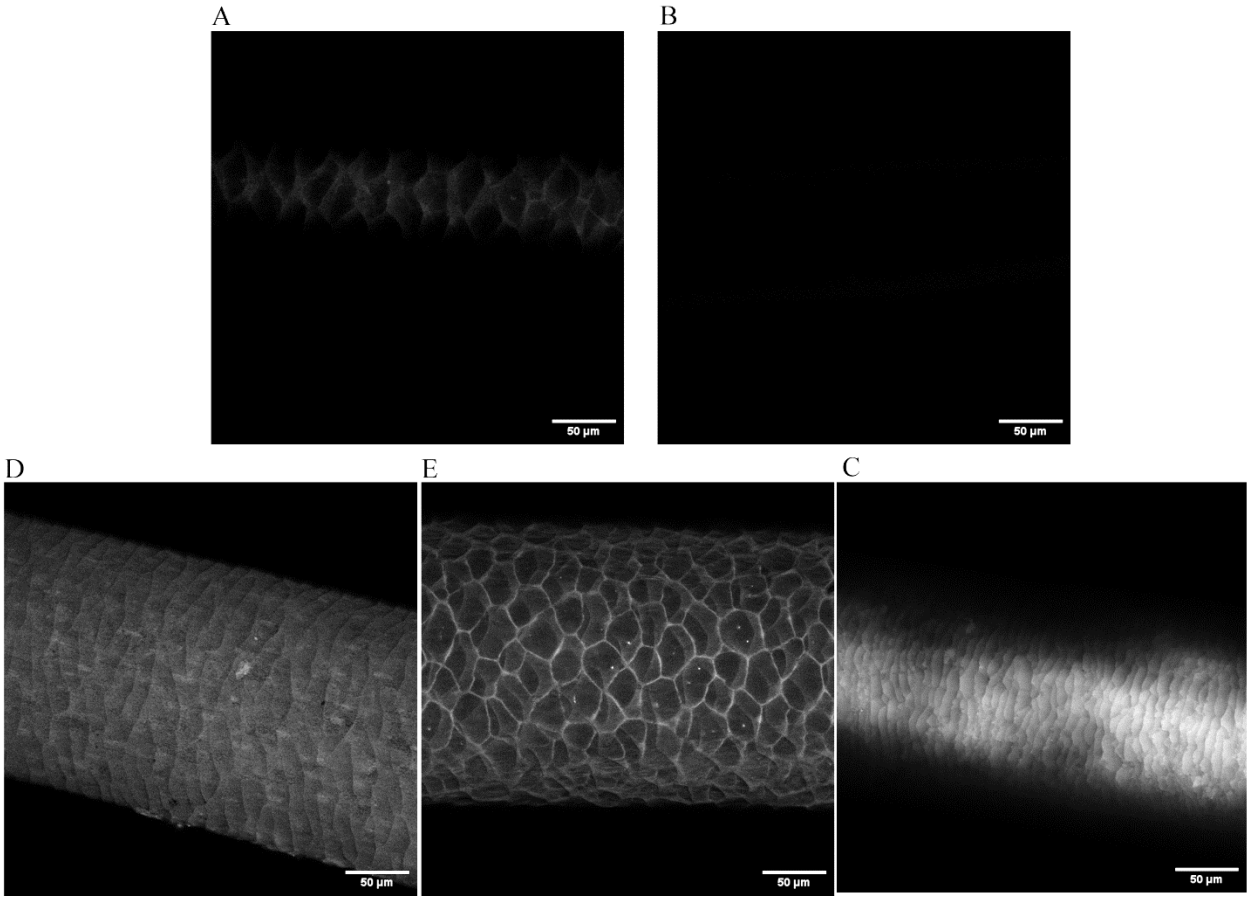

Figure A2.1. Induction of deer hair fluorescence by glutaraldehyde fixation. Male white-tailed deer guard hair still images A) with and B) without fluorescence induction by 30 minutes of 0.8% glutaraldehyde fixation at 37°C in PBS, pH 8.25. Z-stack projections of the same hair near the C) hair tip, and near the D) hair base. E) Mule deer male tarsal gland osmetrichia cuticular scale surface architecture. Induced fluorescence was imaged by fluorescent confocal microscopy following excitation by a 405nm diode laser.

A2.3 Appendix 2 literature cited

1. Collins JS, Goldsmith TH. Spectral properties of fluorescence induced by glutaraldehyde fixation. J Histochem Cytochem. 1981 Mar;29(3):411-414.

Appendix 3. Conformational stability immunoassay

A3.1 Conformational stability immunoassay of enriched prions

High-binding 96 well flat-bottomed strip microplates (Greiner Bio-One International, GmbH, Austria) were coated with 300ng (hamster) or 500ng (deer) prion-enriched preparations (section 5.3.1) in 50mM sodium carbonate-bicarbonate coating buffer (pH 9.60). A reference standard curve was included for deer CSA experiments by coating wells with a dilution series of recombinant full-length wildtype deer PrP. Coated plates were allowed to adsorb antigen by incubation at room temperature for 2 hours, then overnight at 4°C. Humic acid (MilliporeSigma, USA) was prepared in HyClone™ Molecular Biology Grade water (Cytiva, USA). Wells coated with PrP^{Sc} or PrP^{CWD} enriched preparations were exposed to 200µL of 0-6M concentrations of either guanidine hydrochloride (GdnHCl) or 0-6M of urea in PBS for 10 minutes at room temperature with shaking. Wells were blocked with 200µL of 3% (w/v) bovine serum albumin (VWR International, LLC., USA) in PBS for 2 hours at room temperature. Samples were probed with 1:5,000 anti-PrP SHA31 (Cayman Chemical, USA) overnight at 4°C, washed and then probed with 1:5,000 goat anti-mouse IgG HRP conjugate (Bio-Rad Laboratories, Inc., USA) secondary antibody for 2 hours at room temperature, washed 5 times with TBS-T, then developed with BioFX® TMB One Component HRP Microwell Substrate (Surmodics, Inc., USA) chromagen. Samples 650nm absorbance was measured. The reaction was stopped with the addition of 50µL of 2N sulfuric acid, then 450nm absorbance was measured (**Figure 4.1C**).

Apparent fractional change (F_{app}) was calculated from 450nm absorbance values or quantified PrP^{CWD} mass values to generate CSA curves using Equation 6.1, where V_C is the value of the given chaotropic agent concentration, V_N is the value for the native protein conformation (0M chaotropic agent concentration), and V_{Max} is the value for the unfolded protein conformation

(maximum chaotropic agent concentration used) [1-2]. Replicates were compared with two-way ANOVA multiple comparisons tests with the Bonferroni correction (* $p < 0.05$, ** $p < 0.01$, *** $p < 0.001$).

Equation 4.1 $$F_{app} = \frac{V_C - V_N}{V_{Max} - V_N}$$

A3.2 CSA results

The utility of PE-PTA-Filter prion enrichments (Chapter 4) for use in conformation stability assay (CSA) [1-2] was assessed. Prion enrichments from deer CWD and hamster prion strains (Hyper, Drowsy, and 263K) were adsorbed to microplates and denatured by of either of the two chaotropic agents guanidine hydrochloride or urea. Exposed PrP epitopes were detected by the central-region recognizing SHA31 antibody. Multiple samples were able to be assayed on the same microplate simultaneously. The experiments reported are intended to determine conditions for using adsorbed PK and PE prion enrichments in CSA.

The results best resembling typical CSA experiments [2] was obtained from PK-digested hamster prion preparations exposed with guanidine hydrochloride (**Figure A3.1A, C**). No significant differences between the apparent fractional change of unfolding (F_{app}) between the three hamster prion strains were found for any chaotropic agent concentration when PK enriched samples are denatured with guanidine hydrochloride (**Figure A3.1C**). Use of detection antibodies recognizing alternative epitopes may reveal strain-specific differences in structural stability. Urea up to a concentration of 6M was unable to appropriately expose the PrP^{Sc} epitopes relative to no-chaotrope controls as indicated by no appreciable increase in 450nm absorbance (**Figure A3.1B**). The calculated F_{app} results of hamster prion strain urea-treated CSA are

interpreted to have no meaningful value. PE-digested prion preparations exposed with either guanidine hydrochloride or urea had a different problem. Despite an equivalent amount of protein coated per well as the PK-digested preparations, the PE-digested preparations demonstrated high PrP^{Sc} detection with or /without chaotropic exposure (**Figure A3.2A-B**). The higher relative PrP^{Sc} detection of PE-digested preparations could be a result of epitope exposure during enzyme digestion – possibly by digestion of extraneously proteins bound to prion fibrils – or a higher proportion of PrP^{Sc} contributing to total protein adsorbed to wells. Calculated F_{app} of PE-digested hamster prion preparations is also considered to have no meaningful value (**Figure A3.2C-D**).

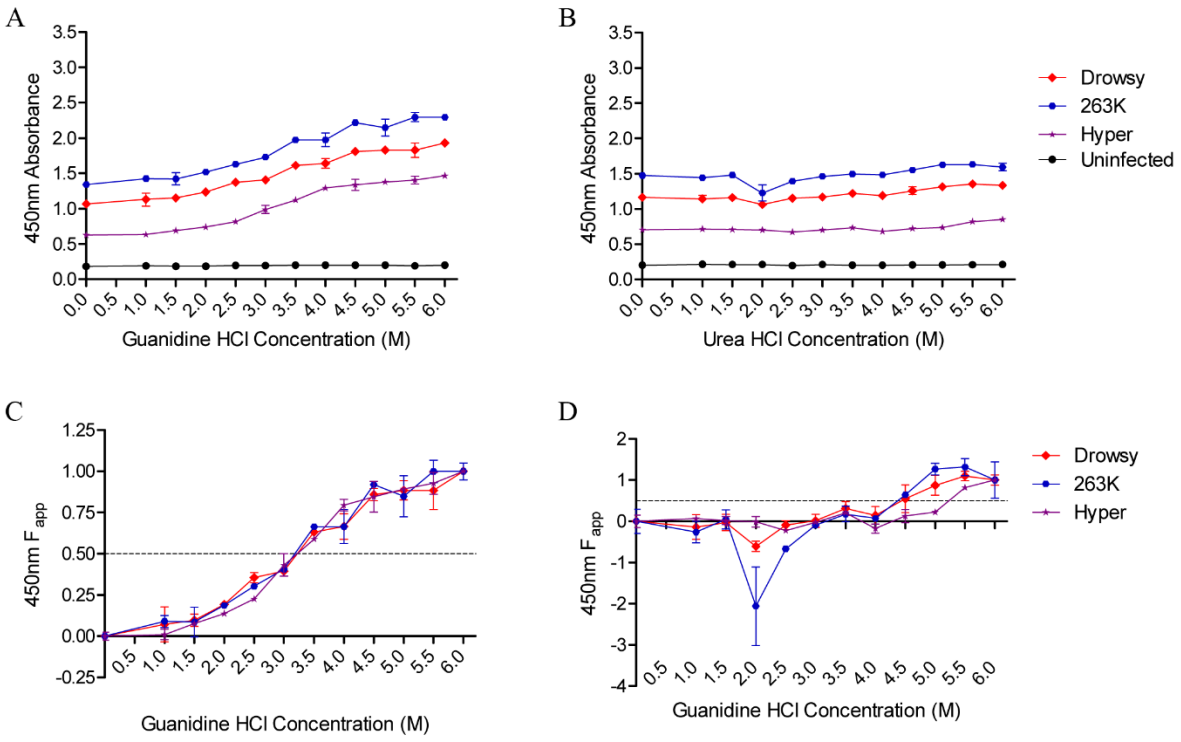

Figure A3.1. Conformational stability assay of proteinase K-enriched hamster prions. Preparations from brain homogenates enriched for prions by proteinase K (PK), PTA precipitation, and 0.45µm filtration were adsorbed to a solid support. Epitope exposure by increasing concentrations of A, C) guanidine hydrochloride and B, D) urea for 10 minutes at room temperature allowed for enhanced detection of total PrP. A-B) 450nm absorbance and C-D) the apparent fractional change (F_{app}) of unfolding as determined by anti-PrP SHA31 (1:5,000). Error bars represent standard error of the mean.

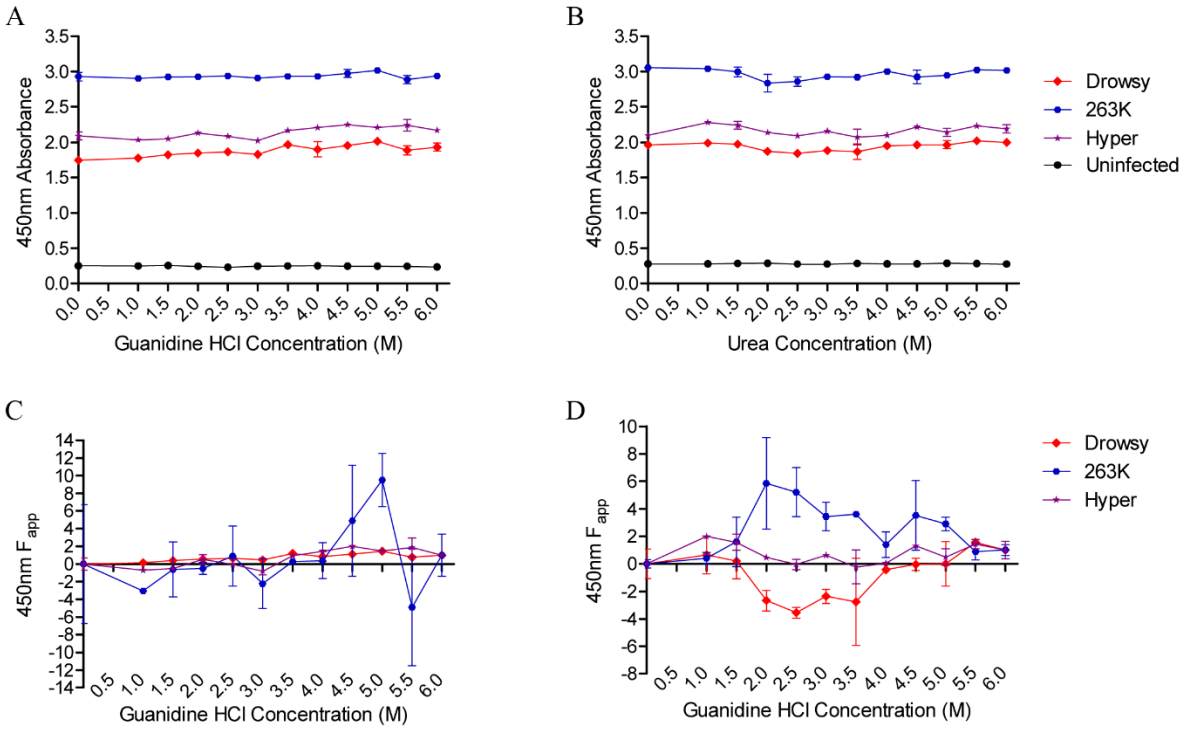

Figure A3.2. Conformational stability assay of pronase E-enriched hamster prions. Preparations from brain homogenates enriched for prions by pronase E (PE), PTA precipitation, and 0.45µm filtration were adsorbed to a solid support. Epitope exposure by increasing concentrations of A, C) guanidine hydrochloride and B, D) urea for 10 minutes at room temperature allowed for enhanced detection of total PrP. A-B) 450nm absorbance and C-D) the apparent fractional change (F_{app}) of unfolding as determined by anti-PrP SHA31(1:5,000). Error bars represent standard error of the mean.

CSA using PE-digested preparations was more successful with CWD-infected deer isolates. With the deer isolates, we were calculated the F_{app} using the 450nm absorbance values and, separately, using the calculated PrP^{CWD} mass detected as determined from a full-length deer recPrP standard curve. Three CWD-infected deer isolates were examined for prion conformational stability differences by CSA on one microplate (**Figure A3.3**, **Figure A3.4**). Both guanidine hydrochloride (**Figure A3.3C**) and urea (**Figure A3.3D**) were sufficient chaotropic agents to expose PrP^{CWD} epitopes to produce typical CSA curves. No significant differences were observed between the F_{app} (450nm absorbance or quantified PrP^{CWD} mass

detected) of the mule deer isolates 102565 [3] and 62439 for either guanidine hydrochloride or urea epitope exposure (**Figure A3.4**). Significant differences between chaotropic agent-induced conformational changes were observed between the 107459 isolate and the other two isolates (**Table A3.1**). Caution must be taken when interpreting the results of this particular data set when considering that the sample isolates have not been characterised as separate prion strains through bioassay studies.

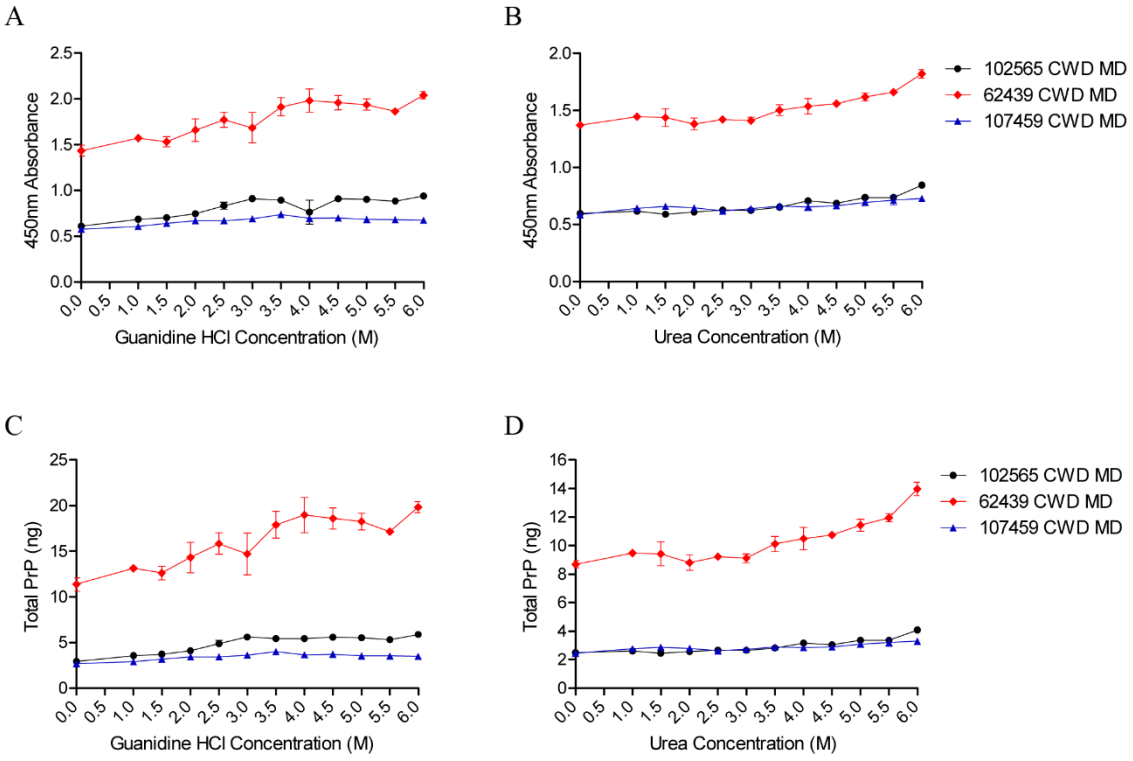

Figure A3.2. Conformational stability assay of prion-enriched CWD-infected mule deer isolates. Preparations from brain homogenates enriched for prions by pronase E, PTA precipitation, and 0.45µm filtration were adsorbed to a solid support. Epitope exposure by increasing concentrations of A, C) guanidine hydrochloride and B, D) urea for 10 minutes at room temperature allowed for enhanced detection of total PrP. A-B) 450nm absorbance, C-D) quantified total PrP^{CWD} detected as determined by recombinant PrP standard curve. PrP^{CWD} was detected by anti-PrP SHA31. (1:5,000) Error bars represent standard error of the mean.

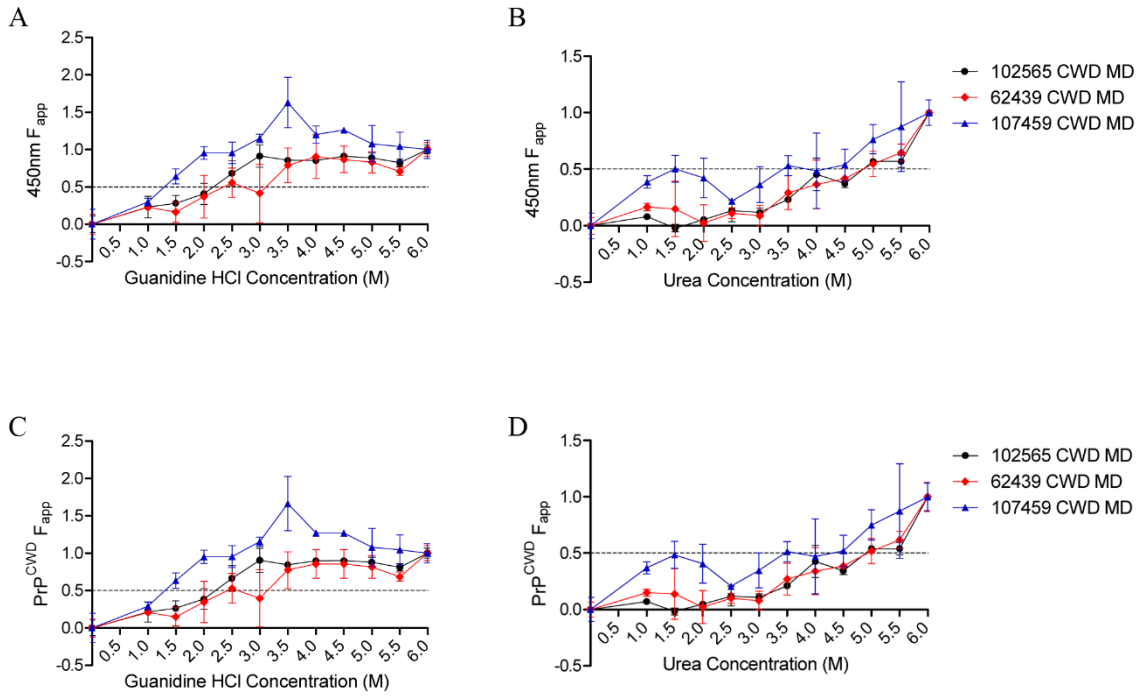

Figure A3.3. Conformational stability assay calculated F_{app} of prion-enriched CWD-infected mule deer isolates. Preparations from brain homogenates enriched for prions by pronase E, PTA precipitation, and 0.45µm filtration were adsorbed to a solid support. Epitope exposure by increasing concentrations of A, C) guanidine hydrochloride and B, D) urea for 10 minutes at room temperature allowed for enhanced detection of total PrP. The apparent fractional change (F_{app}) of unfolding as determined by anti-PrP SHA31 (1:5,000) was calculated from the values of Figure 4-20. A-B) F_{app} calculated from 450nm absorbance values. C-D) F_{app} calculated from PrP^{CWD} mases detected as determined by a deer recPrP standard curve. Error bars represent standard error of the mean.

Table A3.1. Conformational stability assay 2-way ANOVA statistical results for CWD-infected isolates (Figure 4-24C, D).

	Chaotrope (M)	0	1.0	1.5	2.0	2.5	3.0	3.5	4.0	4.5	5.0	5.5	6.0
107459 vs 102565	Urea	n.s.	n.s.	* $p < 0.05$	n.s.	n.s.	n.s.	n.s.	n.s.	n.s.	n.s.	n.s.	n.s.
	Guanidine HCl	n.s.	n.s.	n.s.	* $p < 0.05$	n.s.	n.s.	** $p < 0.01$	n.s.	n.s.	n.s.	n.s.	n.s.
107459 vs 62439	Urea	n.s.	n.s.	n.s.	n.s.	n.s.	n.s.	n.s.	n.s.	n.s.	n.s.	n.s.	n.s.
	Guanidine HCl	n.s.	n.s.	n.s.	* $p < 0.05$	n.s.	** $p < 0.01$	*** $p < 0.001$	n.s.	n.s.	n.s.	n.s.	n.s.

Samples assayed in duplicate. PrP^{CWD} epitopes exposed by 10 minute with the chaotropic agent concentration, then detected by SHA31 (1:5,000).

A3.3 Discussion

Elementary investigations into the use of PE or PK-digested, PTA-precipitated, and 0.45µm filtered prion enrichments for CSA were promising. Interestingly, overt species differences were observed between the CSA results of hamster prion strains and CWD-infected deer isolates. Three hamster prion strain PE-digested enrichments were not suitable for CSA regardless of whether guanidine hydrochloride or urea was used as a chaotropic agent (**Figure A3.2**). Consistently high detection results with all concentrations of chaotropic agent (**Figure A3.2A-B**) suggest that the epitope recognized by SHA31 is almost entirely exposed in all three hamster strains following the enrichment using PE digestion. PE may have sufficiently digested extraneous proteins bound to the prion fibrils to fully expose the PrP^{Sc} epitope recognized by the SHA31 antibody [4-5]. Epitope exposure of the CWD-infected isolates by guanidine hydrochloride and urea, however, produced more traditional CSA results (**Figure A3.4**). Use of a recombinant deer PrP standard curve allowed for quantification of detected PrP^{CWD} following epitope exposure (**Figure A3.3**) and subsequently derived mass-related F_{app} (**Figure A3.4C-D**). CWD isolate 107459 was determined to have statistically significant differences in chaotrope conformational stability relative to two other isolates (**Table A3.1**). The CSA data indicate that CWD isolate 107459 could be a different strain then the other substrates that has yet to be investigated. The results of the PE-digested hamster and mule deer prion enrichments demonstrate the enrichment methodology's potential for prion strain differentiation by CSA for CWD, but not hamster prion strains.

A3.4 References

1. Safar J, Wille H, Itri V, et al. Eight prion strains have PrP(Sc) molecules with different conformations. Nat Med. 1998 Oct;4(10):1157-65.

2. Duque Velásquez C, Kim C, Haldiman T, et al. Chronic wasting disease (CWD) prion strains evolve via adaptive diversification of conformers in hosts expressing prion protein polymorphisms. J Biol Chem. 2020 04 10;295(15):4985-5001.

3. Otero A, Duque Velásquez C, Aiken J, et al. White-tailed deer S96 prion protein does not support stable in vitro propagation of most common CWD strains. Sci Rep. 2021 May 27;11:11193.

4. Wenborn A, Terry C, Gros N, et al. A novel and rapid method for obtaining high titre intact prion strains from mammalian brain. Sci Rep. 2015 May 07;5:10062.

5. Petrakis S, Malinowska A, Dadlez M, et al. Identification of proteins co-purifying with scrapie infectivity. J Proteomics. 2009 May 02;72(4):690-4.